

**REMEDICATION OF RAINFALL INDUCED
LANDSLIDE IN HILLS OF BANGLADESH USING
VEGETATION AND NAILING**

by

SHAMONTEE AZIZ

**MASTER OF SCIENCE IN CIVIL AND GEOTECHNICAL
ENGINEERING**



**DEPARTMENT OF CIVIL ENGINEERING
BANGLADESH UNIVERSITY OF ENGINEERING AND
TECHNOLOGY
DHAKA, BANGLADESH**

November 2020

REMEDICATION OF RAINFALL INDUCED LANDSLIDE IN HILLS OF BANGLADESH USING VEGETATION AND NAILING

by

SHAMONTEE AZIZ

A thesis submitted to the Department of Civil Engineering,
Bangladesh University of Engineering and Technology, Dhaka, in partial
fulfillment of the degree of
Master of Science in Civil and Geotechnical Engineering




DEPARTMENT OF CIVIL ENGINEERING

BANGLADESH UNIVERSITY OF ENGINEERING AND
TECHNOLOGY

November 2020

The thesis titled "Remediation of Rainfall Induced Landslide in Hills of Bangladesh Using Vegetation and Nailing", submitted by Shamontec Aziz, Student Number-1017042121P (Session October-2017) has been accepted as satisfactory in partial fulfillment of the requirement for the degree of Master of Science in Civil and Geotechnical Engineering on November 28, 2020.

BOARD OF EXAMINERS



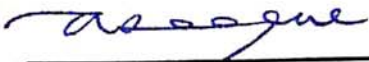
Dr. Mohammad Shariful Islam
Professor
Department of Civil Engineering
BUET, Dhaka-1000

Chairman
(Supervisor)



Dr. Md. Delwar Hossain
Professor and Head
Department of Civil Engineering
BUET, Dhaka-1000

Member
(Ex-Officio)



Dr. Abu Siddique
Professor
Department of Civil Engineering
BUET, Dhaka-1000

Member



Dr. Sharif Moniruzzaman Shirazi, CEng
Professor and Head
Department of Civil Engineering
World University of Bangladesh
Dhaka-1205

Member
(External)

DECLARATION

It is thereby declared that except for the contents where specific references have been made to the work of others, the study contained in this thesis is the result of investigations carried out by the author under the supervision of Dr. Mohammad Shariful Islam, Professor, Department of Civil Engineering, Bangladesh University of Engineering and Technology.

No part of this thesis has been submitted to any other university or educational establishment for a degree, diploma or other qualification (except for publication).



28.11.2020

Shamontee Aziz

ACKNOWLEDGEMENT

All praises to Allah the most beneficial and merciful. By the grace and proper guidance of Almighty Allah the author has been able to complete the thesis work after a journey of nearly three years.

The author would like to express her utmost gratitude towards Dr. Mohammad Shariful Islam, Professor, Department of Civil Engineering, BUET for his earnest supervision, prudent guidance, inclusive and important comments, timely and efficient discussion sessions. It was my honor and pleasure to work under his constant guidance. I shall always be indebted to him for making me familiar with an environment conducive to research. It would not have been possible for me to complete the thesis within this amount of time except his encouragement. His devotion towards research has always galvanized me to strive for better outcomes. His expertise and valuable knowledge sharing throughout the research work have provided immense assistance to me.

The author would like to express her heartfelt thanks to Dr. Md. Delwar Hossain, Professor and Head, Department of Civil Engineering, BUET, for the valuable time he has provided as member of the board of examiners. The author is indebted to Dr. Abu Siddique, Professor, Department of Civil Engineering, BUET, for sharing his knowledge and experience and thus enlightening me. The author would also like to take the opportunity to express genuine admiration towards Dr. Sharif Moniruzzaman Shirazi, Professor and Head, Department of Civil Engineering, World University of Bangladesh for his kind consent to be the member of my advisory committee. His co-operation and essential suggestions helped me to understand the importance of research. I am thankful towards Soil Resource Development Institute (SRDI) for their help in determination of chemical property and nutrient content of the soil samples.

I thank my husband for the inspiration and support all through the research work. I also express my gratitude towards my family members for their unconditional support, love and blessing. Their selfless encouragement has increased my devotion towards the research work.

ABSTRACT

In recent times, the rainfall induced landslides have been prominent in the Chattogram Hill Districts of Bangladesh. Excessive rainfall, deforestation and indiscriminate hill cutting have made Chattogram extremely vulnerable to topsoil erosion, slope instability, and thus to landslides.

The existing topography of the hills of Chattogram City was studied and soil samples were collected from two hills of the city. Their physical and chemical properties were determined through laboratory and field tests. One of the soils has been characterized as sandy silt and the other as silty sand. Both the soil samples have very low to low total nitrogen, potassium and phosphorous, thus were nutrient deficient. These were used to make six small scale glass models. One of these was bare and vetiver grass (*Vetiveria zizanoides*) was planted in other five to study its growth. The prepared physical models were tested under artificially simulated rainfall to determine the effectiveness of vetiver grass in rain-cut erosion reduction. Finite Element Modeling via Plaxis 2D was also conducted with the obtained soil properties to determine the factor of safety, thus the stability of bare, vegetated and nailed hill slopes in natural and terraced condition.

The average root length for vegetated models were 55 cm and average number of tillers increased from 3 to 23 in 12 months. Thus, the growth of vetiver has been satisfactory even in the nutrient deficit hilly soils. The bare soil generated a sediment yield of 11.7 kg whereas it varied between 0.10-0.63 kg (94.6%-99% reduction in erosion) for the other five vegetated models. Hence, vetiver is effective in reduction of rainfall induced erosion and will eventually ensure slope stability. The numerical analysis show that an increase in slope angle decreases the factor of safety. At maximum stable angles, where factor of safety is greater than 1.0 in natural condition, incorporation of vetiver increased the factor of safety up to 16% with the increase of root zone depth and the factor of safety varied between 1.064 to 1.171 for vegetated condition. However, the reinforcing effect of vetiver was inhibited when the slope angles exceed the threshold angle which is $46.33 \pm 3.50^\circ$ and $33.33 \pm 1.97^\circ$ for sandy silt and silty sand.

For stabilizing steeper slopes, terracing it with smaller slope heights has been observed as a suitable option. The positive reinforcing effect of vetiver was more pronounced here, than the natural slope and it increased the factor of safety up to 60%. Terracing also increased the range of threshold angles for both the soil types. This higher range facilitates restoration of slope with lower amount of earthwork than compared to that of natural slope. The stability of natural slopes, where only vegetation is not sufficient, can also be ensured by using nailing. The increase in factor of safety due to nailing was more prominent for sandy silt than silty sand. Overall, the study suggests eco-friendly and feasible solutions for the reduction of soil erosion and safeguarding slope stability. This shall propose a direction to the decision making authorities of Chattogram City about sustainable measures for restoration of dangerous hills and mitigating the risks of landslide.

TABLE OF CONTENTS

DECLARATION	I
ACKNOWLEDGEMENT	II
ABSTRACT	III
LIST OF TABLES	X
LIST OF FIGURES	XI
NOTATIONS AND ABBREVIATIONS	XV
CHAPTER 1: INTRODUCTION	1
1.1 General	1
1.2 Background	2
1.3 Objectives of Research	4
1.4 Organization of the Thesis	4
CHAPTER 2: LITERATURE REVIEW	6
2.1 Introduction	6
2.2 Study Area	6
2.3 Salient Physical and Natural Features of Chattogram Hill Tracts	7
2.3.1 Topography	7
2.3.2 Physiography	9
2.3.3 Geomorphology	9
2.3.4 Geology	9
2.4 Climate and Rainfall Pattern of Chattogram Hill Tracts	13
2.5 Nutrient Condition of Soil and Vegetation Growth	18
2.6 Vegetation of Chattogram Hill Tracts	18
2.7 Landslides in Chattogram Hill Tracts	18
2.7.1 Natural causes of landslide	19
2.7.2 Man-made causes of landslide	19

2.7.3	Previous landslides	20
2.8	Type of landslides	26
2.9	Mechanism of Rainfall Induced Landslide	27
2.10	Previous Studies on Rainfall Induced Landslides and Simulation	29
2.11	Possible Remediation Measures	30
2.11.1	Structural measures	30
2.11.2	Non-structural measures	31
2.11.3	Bioengineering Measures	33
2.12	Slope Stability Analysis	33
2.12.1	Limit equilibrium method	34
2.12.2	Finite element analysis	35
2.13	Application of Vegetation in Soil Bioengineering	36
2.13.1	Application of vetiver in slope stability and its characteristics	37
2.14	Soil Reinforcement by Roots	41
2.14.1	Tensile strength of roots	41
2.14.2	Root area ratio and shear strength of roots	43
2.14.3	Root behavior modeling	43
2.15	Effect of Vegetation on Erosion Reduction	45
2.15.1	Mechanism of soil erosion	45
2.15.2	Agents of soil erosion	46
2.15.3	Estimation of soil erodibility	47
2.15.4	Reduction of soil erosion	47
2.16	Soil Nailing for Slope Stability	48
2.16.1	Elements of soil nailing	49
2.16.2	Effect of different nail parameters on slope stability	50
2.16.2.1	Nail length	50

2.16.2.2 Diameter of nail	51
2.16.2.3 Nail spacing	51
2.16.2.4 Nail inclination	51
2.16.2.5 Grout and soil properties	51
2.17 Summary	52
CHAPTER 3: EXPERIMENTAL PROGRAM	53
3.1 Introduction	53
3.2 Soil Sample Collection	53
3.3 Determination of Soil Properties	53
3.3.1 Sieve analysis and hydrometer analysis of soil	53
3.3.2 Field density test	54
3.3.3 Direct shear test	54
3.3.4 Permeability test	54
3.4 Experimental Setup for Model Study	57
3.4.1 Small scale glass model preparation	57
3.4.2 Soil placement in the models	57
3.4.3 Types of models	59
3.4.4 Artificial rainfall simulator	62
3.4.5 Calibration of rainfall simulator	62
3.4.6 Determining required rainfall intensity	64
3.4.7 Setup for experiment	64
3.4.7.1 Setup of rainfall simulator	64
3.4.7.2 Arrangement for collection of runoff rater and eroded soil	66
3.5 Determination of Soil Erodibility	66
3.6 Numerical Modeling and Analysis	68

3.6.1	Model geometry	68
3.6.2	Finite Element Model	70
3.6.3	Mesh and fixities	70
3.6.4	Modeling soil properties	70
3.6.4.1	Elements	70
3.6.4.2	Material model	71
3.6.4.3	Drainage type	71
3.6.4.4	Strength and stiffness parameters	71
3.6.4.5	Interface element	72
3.6.5	Modeling root properties	72
3.6.1	Safety calculation (ϕ -c Reduction)	75
3.6.2	Nailing modeling	77
3.7	Summary	79
CHAPTER 4: RESULTS AND DISCUSSIONS		80
4.1	Introduction	80
4.2	Properties of Soil Samples	80
4.2.1	Grain size analysis of soil	80
4.2.2	In-situ and dry density of soil	81
4.2.3	Effective shear strength parameters	81
4.2.4	Coefficient of vertical permeability	81
4.3	Chemical Properties and Nutrient Content	81
4.4	Growth Study of Vetiver	86
4.5	Reduction of Soil Erosion by Vetiver	90
4.5.1	Comparison between sediment yield generated from bare and vegetated soil of S-1	90
4.5.2	Effect of arrangement of vetiver on erosion control	94

4.5.2.1	Effect of number of tillers per point	94
4.5.2.2	Effect of spacing between vetiver tillers	94
4.5.3	Effect of jute geo-textile along with vegetation in erosion reduction	96
4.5.4	Effect of vetiver on erosion reduction of different soil type	96
4.6	Effect of Vegetation on Infiltration and Runoff	97
4.6.1	Comparison between vegetated and bare models for same soil type	97
4.6.2	Comparison between vegetated models of different soil type	97
4.7	Change of Slope Angle due to Erosion	98
4.8	Effect of Slope Angle on Soil Erosion	101
4.9	Results from Numerical Analysis	101
4.9.1	Stable angle for bare slope	102
4.9.2	Effect of vetiver on slope stability of natural slope	102
4.9.2.1	Effect of spatial distribution	102
4.9.2.2	Effect of root zone depth	104
4.9.3	Threshold angles for stable natural slope with vetiver	107
4.9.4	Stability analysis of terraced slopes	108
4.9.5	Safe angles for different step heights of terraced slope	108
4.9.6	Effect of vetiver on terraced slope	108
4.9.7	Threshold angle for stable terraced slopes with vetiver	112
4.9.8	Parametric study	112
4.9.8.1	Relation between factor of safety and root zone depth	112
4.9.8.2	Relationship between factor of safety and slope angle	113
4.9.8.3	Relation between factor of safety and height of slope for terraced slope	113
4.9.9	Effect of nailing in slope stability	115
4.9.9.1	Effect of nail length	115

4.9.9.2	Effect of nailing on terraced slope	117
4.10	Findings of the Study	118
CHAPTER 5: CONCLUSIONS AND RECOMMENDATIONS		119
5.1	Introduction	119
5.2	Conclusions	119
5.3	Recommendations	121
5.4	Summary	122
REFERENCES		123
APEENDIX A: TOTAL DISPACEMENT OF BARE, ROOTED AND NAILED SOIL		140

LIST OF TABLES

Table 2.1: Stratigraphic formation and geotechnical features of Chattogram city and surrounding area	15
Table 2.2: Details of major landslide events in Chattogram District, Bangladesh	24
Table 2.3: General physical effects of vegetation on slope stability	37
Table 2.4: Physiological, morphological and ecological characteristics of vetiver	39
Table 2.5: Maximum root length of vetiver in different soil	39
Table 2.6: Shoot length and root diameter of vetiver	40
Table 3.1: Summary of the performed laboratory and field tests	56
Table 3.2: Summary of all six models	60
Table 3.3: Values of Soil erodibility factor for different soils	67
Table 3.4: Values of slope length and steepness factor for different slope angles	67
Table 3.5: Added cohesion for different depth of soil layer	74
Table 3.6: Nail properties	79
Table 4.1: Properties of soil samples	85
Table 4.2: Chemical properties and nutrient contents of S-1 and S-2	85
Table 4.3: Different parameters of vetiver grass in different models with different soil types	88
Table 4.4: Factor of safety of rooted soil	103
Table 4.5: Factor of safety at different root zone depths	105
Table 4.6: Threshold angle for natural slope with H=15m	107
Table 4.7: Factor of safety at different root zone depth for terraced slope for S-1	110
Table 4.8: Factor of safety at different root zone depth for terraced slope for S-2	110
Table 4.9: Threshold angle for stable terraced slopes with vetiver for S-1 and S-2	112
Table 4.10: Factor of safety for different nail lengths at different slope angles for S-1	116
Table 4.11: Factor of safety for different nail lengths at different slope angles for S-2	116

LIST OF FIGURES

Figure 2.1: Location map of (a) Chattogram Hill Districts, (b) Chattogram Metropolitan Area (CMA) and Chattogram City Corporation (CCC)	8
Figure 2.2: (a) Elevation map of Chattogram Metropolitan Area; (b) Slope map of Chattogram Metropolitan Area	10
Figure 2.3: Land cover map of Chattogram Metropolitan Area	11
Figure 2.4: Geomorphological map of Chattogram City Corporation and surrounding area	12
Figure 2.5: Geological map of Chattogram City Corporation and surrounding area	14
Figure 2.6: Annual rainfall pattern of Chattogram city from 1960 to 2010	17
Figure 2.7: Precipitation map of CMA	17
Figure 2.8: Casualties due to landslide in Bangladesh	21
Figure 2.9: Number of landslides in different districts of the Chattogram Hill Tracts (2001-2007)	21
Figure 2.10: Location of landslides from 2001 to 2017 in different areas of Chattogram hilly area	22
Figure 2.11: Location of landslides in Chattogram Metropolitan Area	23
Figure 2.12: Probable slide location and damaged house in Rangamati	23
Figure 2.13: Mechanism of rainfall induced landslide; (a) Start of rainfall; (b) Generation of failure surface; (c) Flow of soil and debris	28
Figure 2.14: Vetiver system along Ho Chi Minh Highway, Vietnam	38
Figure 2.15: Relation between tensile strength and diameter of vetiver grass root	42
Figure 2.16: Relationship between root area ratio and depth of soil layer	45
Figure 2.17: (a) Schematic diagram of soil reinforcement by root; (b) Root reinforcement model	46
Figure 3.1: (a) Location of Chattogram District; (b) Location of soil sample collection	55
Figure 3.2: Natural condition of hills (a) Tiger Pass hill; (b) Berma Haji hill	56
Figure 3.3: Contour map of Bangabandhu hill of Chattogram	58
Figure 3.4: Schematic diagram of glass model	59

Figure 3.5: (a) Bare model after soil placement; (b) Vetiver grass with three tillers; (c) Initial root condition of vetiver grass; (d) M-2 after plantation of vetiver	61
Figure 3.6: Schematic diagram of rainfall simulator tray	63
Figure 3.7: Plan view of the perforated steel tray : used as rainfall simulator	63
Figure 3.8: Plan view of set up for rainfall tray calibration	65
Figure 3.9: (a) Complete setup including rainfall tray, supports and rain gauges; (b) Positioning of rain gauges	65
Figure 3.10: (a) Rainfall tray setup above the model; (b) M-6 with covered trench for collection of runoff and eroded soil; (c) Collected soil and water	67
Figure 3.11: Schematic diagram of natural slope (H=15m)	68
Figure 3.12: Schematic diagram of model in FEM where H_T = height of each step of terraced slope, (a) $H_T=7.5m$; (b) $H_T=5m$; (c) $H_T=3m$	69
Figure 3.13: Summary of the analysis steps for vegetation	76
Figure 3.14: Summary of different cases with variations of parameters for nailing	78
Figure 4.1: Grain size distribution curve for S-1 and S-2	80
Figure 4.2: (a) Change of shear stress with shear displacement for S-1; (b) Mohr-Coulomb failure envelope of S-1	82
Figure 4.3: (a) Change of shear stress with shear displacement for S-2; (b) Mohr-Coulomb failure envelope of S-2	83
Figure 4.4: Coefficient of vertical permeability (k) of S-1 at different void ratios	84
Figure 4.5: Coefficient of vertical permeability (k) of S-2 at different void ratios	84
Figure 4.6: Schematic diagram (plan view) of vetiver grass plantation in glass models; (a) M-1, M-2, M-4, M-5; (b) M-3	87
Figure 4.7: Measurement of growth of vetiver grass in different models with different soil; (a) Model condition before rainfall test, (b) Shoot length measurement, (c) Vetiver tillers with long roots, (d) Root distribution of vetiver grass, (e) Clump diameter measurement	89
Figure 4.8: Average root and shoot length of vetiver for 5 different models	90
Figure 4.9: Canopy provided by vetiver tillers	92
Figure 4.10: Soil accumulation around vetiver plants in M-1	92
Figure 4.11: (a) Eroded soil with runoff; (b) Eroded surface after rainfall of M-6	93

Figure 4.12: Rainfall test on M-1 generating low sediment yield	93
Figure 4.13: Area of canopy covers (m ²) for different models	95
Figure 4.14: Sediment yield (kg) produced by different models after 30 minutes of rainfall with an intensity of 500mm/hr	95
Figure 4.15: Variation of volume of infiltration (m ³) with time (minutes) for M-1 and M-6	99
Figure 4.16: Cumulative runoff (m ³) of M-1, M-3, M-4, M-5 and M-6 with time (minutes)	99
Figure 4.17: Variation of volume of infiltration (m ³) with time (minutes) for M-1 and M-2	100
Figure 4.18: Cumulative runoff (m ³) of M-1 and M-2 with time (minutes)	100
Figure 4.19: Slope angles (degree) for different models before and after rainfall	101
Figure 4.20: Change of factor of safety with slope angle (degree) for natural slope (H=15m)	103
Figure 4.21: Change of factor of safety with root zone depth (m) for S-1 and S-2	105
Figure 4.22: Percent increase in factor of safety at different root zone depths (m)	106
Figure 4.23: (a) Total displacement at bare condition for S-1	106
Figure 4.24: Total displacement at rooted condition (h _r =2m) for S-1	107
Figure 4.25: Factor of safety for different slope height (m) and slope angles (degree) for terraced slope	109
Figure 4.26: Change of factor of safety with increasing root zone depth (m) for terraced slope	110
Figure 4.27: Percent increase of factor of safety with varying root zone depth (m) for terraced slope for S-1	111
Figure 4.28: Percent increase of factor of safety with varying root zone depth (m) for terraced slope for S-2	111
Figure 4.29: Relationship between factor of safety and root zone depth (m) at different step heights	113
Figure 4.30: Relationship between factor of safety and slope angle (degree) at different slope heights	114

Figure 4.31: Relationship between factor of safety and slope height (m) for terraced slope at different slope angles	114
Figure 4.32: Percent increase in factor of safety for different nail length (m) at different slope angle (degree) for S-1	116
Figure 4.33: Percent increase in factor of safety for different nail length at different slope angle (degree) for S-2	117
Figure 4.34: Percent increase in factor of safety for natural and terraced slope at different slope angle (degree)	118
Figure A.1: Potential failure surface and total displacement (cm) of soil S-1 for terraced slope ($H_T=7.5$ m, $\beta=46^\circ$); (a) Bare condition; (b)-(d) Rooted condition where h_r is respectively 1.0 m, 2.0 m, 3.0 m	144
Figure A.2: Potential failure surface and total displacement (cm) of soil S-1 for terraced slope ($H_T=5$ m, $\beta=55^\circ$); (a)-(d) Rooted condition where h_r is respectively 0.5 m, 1.5 m, 2.5 m, 3.0 m	148
Figure A.3: Potential failure surface and total displacement (cm) of soil S-2 for terraced slope ($H_T=7.5$ m, $\beta=31^\circ$) in rooted condition where h_r is 1.5 m	149
Figure A.4: Potential failure surface and total displacement (cm) of soil S-2 for terraced slope ($H_T=5$ m, $\beta=32^\circ$); (a) Rooted condition where h_r is 0.5 m; (b) Rooted condition where h_r is 3.0 m	151
Figure A.5: Potential failure surface and total displacement (cm) of soil S-2 for terraced slope ($H_T=3$ m, $\beta=45^\circ$); (a) Rooted condition where h_r is 1.0 m; (b) Rooted condition where h_r is 1.5.m	153
Figure A.6: Potential failure surface and total displacement (cm) of soil S-1 for natural slope ($H=15$ m, $\beta=38^\circ$); (a) Bare condition; (b) Nailed condition where nail length (l) is 10.5 m (0.7H)	155
Figure A.7: Potential failure surface and total displacement (m) of soil S-1 for terraced slope ($H_T=7.5$ m, $\beta=38^\circ$); (a) Bare condition; (b) Nailed condition where nail length (l) is 6.75 m (0.9 H_T)	157
Figure A.8: Potential failure surface and total displacement (cm) of soil S-2 for natural slope ($H=15$ m, $\beta=38^\circ$); (a) Bare condition; (b) Nailed condition where nail length (l) is 10.5 m (0.7H)	159

NOTATIONS AND ABBREVIATIONS

Symbol	Description
c_r	Added apparent cohesion
RAR	Root area ratio
D	Root diameter
Tr	Root tensile strength
h_r	Root zone depth
G_s	Specific gravity
k	Coefficient of vertical permeability
ϕ	Angle of internal friction
ϕ'	Effective angle of internal friction
c	Cohesion
c'	Effective cohesion
E	Young's modulus
ν	Poisson ratio
V:H	Vertical: Horizontal
ψ	Dilatancy angle
β	Slope angle
β_{lim}	Threshold angle
H	Slope height of single slope
H _r	Slope height/ step height of terraced slope
l	Nail length
θ	Angle of shear distortion in the shear zone
t_r	Total mobilized tensile stress of root fibers per unit area of soil
σ'	Effective normal stress on shear plane
σ	Normal stress on shear plane
s	Shear strength of soil
γ_w	Unit weight of water
γ_{insitu}	In-situ unit weight of soil
γ_{dry}	Dry unit weight of soil
γ_{sat}	Saturated unit weight of soil
EA	Axial stiffness
EI	Flexural rigidity

ω_n	Natural moisture content
e	Void ratio
F_{max}	Maximum force required to cause tensile failure
2D	Two dimensional
BMD	Bangladesh Meteorological department
BNBC	Bangladesh National Building Code
CCC	Chattogram City Corporation
CHD	Chattogram Hill Districts
CHT	Chattogram Hill Tracts
CMA	Chattogram Metropolitan Area
EWS	Early Warning System
FE	Finite element
FEM	Finite element modeling
FS	Factor of Safety
GSB	Geological Survey of Bangladesh
JGT	Jute geo-textile
OM	Organic matter
RCC	Reinforced Cement Concrete
SM	Silty sand
TN	Total nitrogen
USCS	Unified soil classification system
USGS	United States Geological Survey
USLE	Universal soil loss equation

CHAPTER 1

INTRODUCTION

1.1 General

Bangladesh is a small country located in South Asia. It is a country which has been frequented by disasters. Bangladesh has a total land of 147,570 km² including 17,342 km² hilly areas (Hossain et al., 2014). Mostly disasters are caused by nature. However, human interventions have largely contributed to landslides. Landslide incidence is a response of changes in land cover and land use (Rubel and Ahmed, 2013). Weak sub-soil conditions along with high intensities of rainfall increase the risk of landslides in steep hilly areas.

Though once rare, landslides are becoming increasing common in hilly regions of Bangladesh. This disaster is most alarming in the Chattogram Hill Tracts. From 1999 to 2018, total 631 people have lost their lives due to landslides in CHT. The most recent landslide on June 13, 2017 killed 159 and injured 88 people (Ahmed, 2017).

The Chattogram Hill Tracts were formed during the Tertiary period of geological scale. The hills are mainly composed of sandstones, siltstones and shales, together with minor beds of conglomerates which are unconsolidated or semi-consolidated (Khan et al., 2012). The subsoil is composed of heavy silt loam or silty clay which is resulted from shales. During heavy rainfall, these soils absorb the rainfall and cannot hold the extra weight added by the water. Thus slope stability is compromised, and landslides occur.

Bangladesh receives almost 80% of its rainfall during the monsoon season. Monsoon arrives between May and early June. The monsoon is less intense in the west where it is around 1500-1600mm per year. The intensity increases towards the east in Chattogram and may reach up-to 2900 mm per year. More to the south, rainfall reaches 3,500 mm per year in Cox's Bazar, and up to 4,000 mm in the more southern city of Teknaf (Chowdhury, 2012). The intensity of rainfall has increased in Chattogram Metropolitan Area in last five decades and the heavy rainfall intensity has been considered as triggering factor of most of the landslides which have occurred in recent times. About 80% of landslide which occurred between 2000 to 2009 occurred in between May and September during the peak rainfall months in the wet period of the

year when the rainfall was greater than 200 mm and about 30% of the total landslides occurred in the month of June (with average monthly rainfall >600 mm) (Khan et al., 2012).

Besides, these natural factors, rapid urbanization has turned the hilly areas into reclaimed built-up lands in Chattogram City. Along with this, the indiscriminate hill cutting, *jhoom* cultivation and deforestation have changed the land cover and increased the steepness of hills. As a result, when all these factors, namely steep slopes, high intensity rainfall and weak soil structures, are integrated, the risk of landslide is increase by many folds.

This thesis tries to explore the effectiveness of vegetation as a cost effective and sustainable solution, alongside the role of nailing as a structural measure for minimizing the landslide vulnerability of the hills located in Chattogram City by conducting small scale tests and numerical modeling.

1.2 Background

In Bangladesh, landslide is caused due to natural phenomenon and human activities which is accentuated by climate change. Like other tropical mountainous region of Southeast Asia, rainfall induced landslides are common in CHT (Brand et al., 1984) including Chattogram City. Slope saturation by water is the primary natural cause of the landslide (Highland and Bobowsky, 2008). Egeli and Pulat (2011) found that shallow landslides in nearly saturated non cohesive or slightly cohesive soil is caused by high intensity, short duration rainfall which infiltrates into soil and changes inter granular friction and effective stresses. For the slope of loose sand with high water content, pore water pressure can increase substantially during failure and can decrease shear strength of soil (Moriwaki et al., 2004). It has been reported that 100 mm of rainfall in 3 hours or 200 mm rainfall in 24 hours or 350 mm rainfall in 3 days can trigger landslides in the vicinity of Chattogram and Cox's Bazar (Ahmed, 2017).

A natural hill is a stable surface. But as urbanization is increasing, the foot hill regions of most hills in Chattogram city are being cut. This increases the steepness of the slope. Hills are moderately vulnerable at a slope angle of 20-30 degrees and highly vulnerable at slope angles of 40-60 degrees. On the other hand, the hill slopes of Chattogram are cut even at slopes angle as steep as 70 degree. These make the slopes extremely

unstable. Field studies suggest that failure patterns of some landslides are transitional, and others are rotational (Islam, 2018).

Different initiatives have been taken by the government to mitigate the risks of this disaster. Ministry of Disaster Management and Relief under the Comprehensive Disaster Management Programme-II (2012) have performed a detail landslide inventory survey, rainfall threshold analysis and developed Early Warning System for Cox's Bazar District in 2012. An Early Warning System for Chattogram Metropolitan Area was also developed in 2014. Along with these, international organizations have tried to raise awareness and tried to apply different control measures. Most common measures to stabilize the hill slopes is construction of reinforced concrete retaining wall and masonry toe wall which are expensive in the context of Bangladesh. However, for the measures to be fully effective, it has been emphasized that they need to be sustainable and most likely indigenous. And so, the application of hard engineering solutions may not provide the best and complete solution. In this scenario, vegetation may work as a promising method for erosion control and slope stabilization.

Roots of plants and vegetation are believed to play an essential role in slope stabilization and erosion control (Gray, 1974, 1978; Waldron and Dakessian, 1981; Coutts, 1983; Wu, 1976; Abe and Ziemer, 1991; Gyssels et al., 2005; De Baets et al., 2007). The main effect of vegetation on slope stability is considered because of the mechanical stabilization due to the response of roots (Voottipruex et al., 2008). To understand the interaction between the vegetation and hill slope stability, interconnected experimental and modeled approaches are required (Temgoua et al., 2017). Mathematical models and numerical simulation of the root-soil interaction has been studied. However, vegetation are mostly effective for shallow slope failures.

Another widely used approach for slope stabilization is soil nailing. Among the various available techniques for slope restoration such as retaining wall, conventional soil nail, rock bolting, anchors; soil nailing has proved to be an effective and successful solution for landslide mitigation (Yang and Drumm, 2000; Geoguide, 2008; Soga et al., 2016; Talukdar et al., 2018). It requires minimum amount of earthwork and reduces risk during construction. Numerical analysis of slope stability by nailing have been carried out by finite element and limit equilibrium method (Singh and Babu, 2010; Alsubal et

al., 2017; Sharma et al., 2019). Design and efficiency of nailing depends on various factors such as nail length, nail inclination, soil types and bond strength of grout.

To understand the extent of the risk of landslide; a fair understanding of the geometry of the hilly terrains of Chattogram Hill Tracts and sub-soil characteristics of the hill soil is essential. This will lead to the understanding about the feasibility and effectiveness of different measures to mitigate the risk. Different methods may prove to be suitable for different soil and topographic condition. The present study focuses on the effectiveness of two such measures e.g. vegetation and nailing. These insights will be useful for comprehensive strategic planning and development of landslide protection schemes for the hills of Bangladesh.

1.3 Objectives of Research

The objectives of this study are:

- (i) To examine the topography of selected hills and their sub-soil characteristics as well as the nutrient contents of the soil of those hills.
- (ii) To investigate the effectiveness of bioengineering (vegetation) and nailing as remedial measures for mitigation of rainfall induced landslide.
- (iii) To make a comparative assessment of the effectiveness of different measures (vegetation and soil nailing) for remediating landslides in natural hill slopes and terraced slopes by numerical simulation using Plaxis 2D.

1.4 Organization of the Thesis

The whole study has been divided into five chapters. These have been arranged to represent the sequential development of the study.

Chapter One includes the introduction, present state of the problem, background of this study and the organization of the thesis.

Chapter Two documents the literature review. This includes the study area profile, the topographic and sub-surface condition of Chattogram Hill Tracts and specifically the area under Chattogram City Corporation Area. The rainfall patterns and associated landslide risks have also been presented. It contains details of previous landslides and the characteristics of those. The previous studies on effectiveness of vegetation e.g.

vetiver grass (*Vetiveria zizanioides*) in reducing erosion and increasing slope stability have been summarized here. Later the chapter discusses about the application of nailing in slope stability in universal as well as in Bangladesh context. Previous numerical slope stability analysis using vetiver and nailing have also been mentioned in this Chapter.

The experimental setup and methodology of numerical analysis have been outlined in Chapter Three. This includes the methods followed for the experiment on small scale models and quantification of the eroded soil. This chapter also discusses the details of the finite element analysis. It summarizes the different parameters used in this study. Description of elements for modeling the root behavior as well as soil nailing for both natural and terraced slopes are also included in this chapter.

The nutrient condition and the index properties of the soil are presented in Chapter Four. The results obtained from different small scale models are also presented here. The factor of safety obtained for natural and terraced slope under different conditions e.g. bare, rooted and nailed have also been presented and discussed.

Lastly, Chapter Five outlines the major conclusions drawn from this study. Some recommendations have also been provided to enhance the research on this topic in the future.

CHAPTER 2

LITERATURE REVIEW

2.1 Introduction

The chapter aims to present the previous literary researches which have been conducted regarding the rainfall induced landslides and slope stability. As this research investigates the effectiveness of measures e.g. vegetation and nailing in remediation of landslides', this chapter tries to provide a summary of the theoretical aspects and the applications of these measures which have been conducted in the past. This chapter also encapsulates the behavior of rooted soil and its potential in erosion control.

In hilly environment, one of the most damaging and significant natural disaster, which has also been recognized as the third most important natural hazard induced disaster is landslides (Alcántara-Ayala et al., 2006; Van et al., 2010). Asian countries, especially Nepal, China, Japan and India have been most vulnerable to landslides (Kirschbaum et al., 2010; Wu, 2017; Shrestha et al., 2017) and Bangladesh has recently been added to the list (Rabby and Li, 2020). The hill tracts of Chattogram, especially Chattogram city is highly vulnerable to landslide risks (Ahmed and Dewan 2017; Islam et al., 2017; Islam, 2018; Ahmed et al., 2018; Aziz et al., 2020). In recent years, the rate of urbanization in the city has increased rapidly. This has also been accompanied by high intensities of rain which has resulted in landslides. A landslide can be defined as the movement of a mass of rock, earth or debris down a slope (Cruden, 1991). Hence, different structural measures are employed to stabilize the slopes. In recent times, the application of vegetation as an environment friendly and sustainable solution has been gaining popularity in increasing slope stability. Considering the above stated facts, the topography and rainfall patterns of Chattogram city, their implications on landslides and the effectiveness of different measures have been studied.

2.2 Study Area

Mountains of Bangladesh are in the southern, eastern and northern part of the country including the Chattogram Hill Tracts and Chattogram Region; Mymensingh, Jamalpur; and Sylhet Region (Sarker, 2013). Chattogram Hill Tracts (CHT) are the only extensive hilly area in Bangladesh that lies in southeastern part of the country

bordering Myanmar on the southeast, the Indian state of Tripura on the north, Mizoram on the east and Chattogram district on the west. The area of the Chattogram Hill Tracts is 13, 184 km², which is approximately one-tenth of the total area of Bangladesh. In this region, some hills are also located in the main city of Chattogram (Chowdhury, 2012).

Chattogram is the main seaport of Bangladesh. The city is comprised of small hills and narrow valleys, bounded by the Karnaphuli River to the south-east, the Bay of Bengal to the west, and Halda River to the north-east (Ahmed, 2014).

Chattogram has been divided into different administrative boundaries such as Chattogram Metropolitan Area (CMA), Chattogram City Corporation (CCC) and Chattogram Statistical Metropolitan Area (Ahmed, 2014). Figure 2.1 shows their locations. Two hills, locally known as Tiger Pass Hill and Berma Haji Hill, located in the boundary of Chattogram City Corporation area, are chosen for this study.

2.3 Salient Physical and Natural Features of Chattogram Hill Tracts

2.3.1 Topography

Chattogram is vastly different in terms of topography, with the exception of Sylhet and northern Dinajpur, from the rest of Bangladesh, being a part of the hilly regions that branch off from the Himalayas (Emran et al., 2018). This eastern off shoot of the Himalayas, turning south and southeast, passes through Assam and Tripura State and enters Chattogram across the river Feni (Sarker, 2013).

The range loses height as it approaches Chattogram town and breaks up into 6 small hillocks scattered all over the town. This range appears again on the southern bank of the Karnaphuli River and extends from one end of the district to the other. Chandranath or Sitakunda is the highest peak in the district, with an altitude of 351 meters above mean sea level (Osmany, 2014).

The Chattogram Hills rise steeply to narrow ridge lines, generally no wider than 36 meters, with altitudes from 600 to 900 meters above sea level (Rahman, 2012).

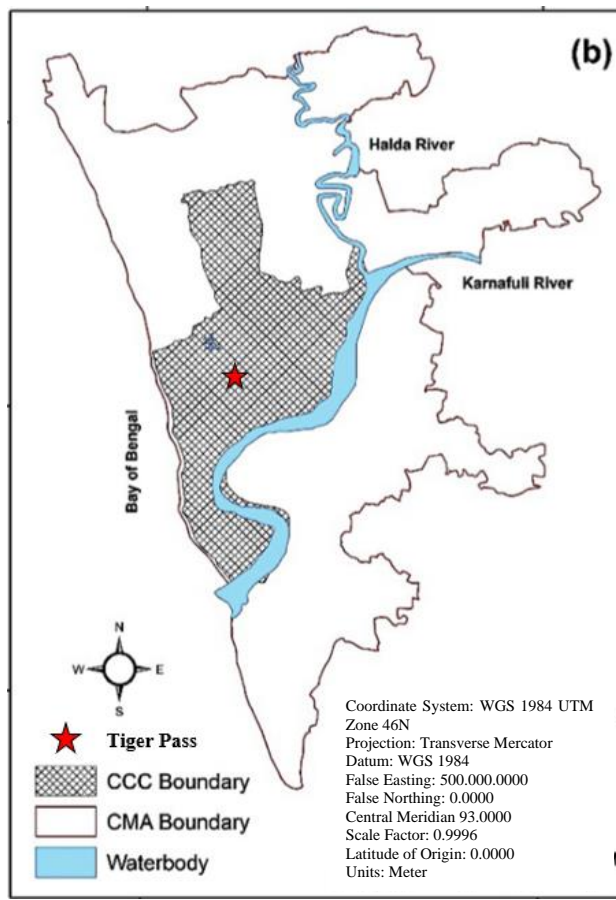
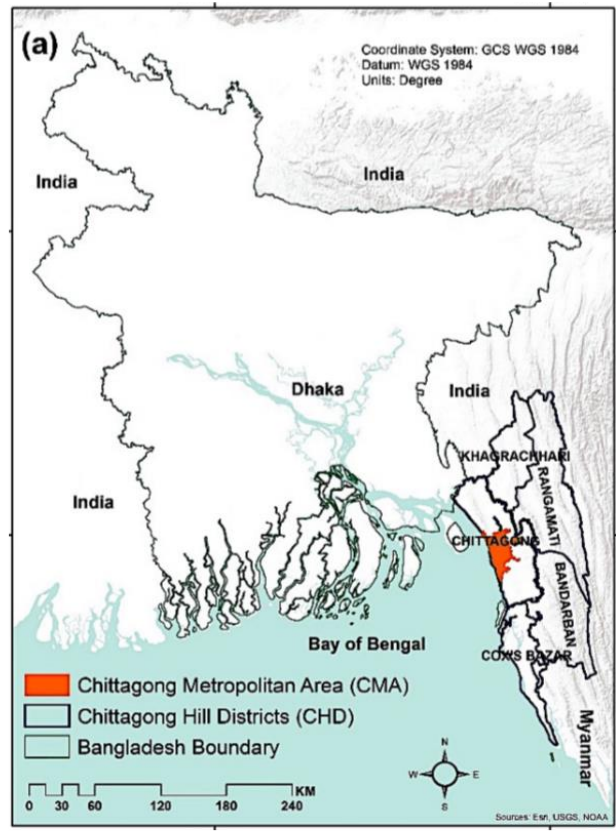


Figure 2.1: Location map of (a) Chattogram Hill Districts, (b) Chattogram Metropolitan Area (CMA) and Chattogram City Corporation (CCC) (Ahmed et al., 2018)

Figure 2.2 (a) represents the elevation difference that can be observed in CMA. The slope also varies from 0 to 34.63 degrees as can be seen in Figure 2.2(b). From the study it is seen that there are almost 14 types of land cover in CHT. When the area of CMA is considered, there are five classes e.g. urban, semi-urban, vegetation, bare soil and water (Ahmed, 2014). Figure 2.3 shows the land cover of CMA. Here the two hills of our study fall within the urban area. So, the effect of landslide in these built up areas are extremely dangerous.

2.3.2 Physiography

According to the physiography of Bangladesh, the CHT falls under the Northern and Eastern Hill unit and the High Hill or Mountain Ranges sub-unit (Osmany, 2014). At present, all the mountain ranges of the Chattogram Hill Tracts are almost hogback ridges. They rise steeply, thus looking far more impressive than their height would imply. Most of the ranges have scarps in the west, with cliffs and waterfalls. The region is characterized by a huge network of trellis and dendritic drainage consisting of some major rivers draining into the Bay of Bengal (Chowdhury, 2012).

2.3.3 Geomorphology

Based on landforms, its genesis, evolution and morpho-dynamics, Chattogram City can be divided into three broad distinct geomorphological divisions: (1) hilly area, (2) fluvio-tidal plain and (3) tidal plain (GSB, 2013). The hilly part of the city is characterized by different types of erosional processes, and therefore landforms have distinctive erosional features, whereas Fluvio-tidal and tidal landforms are depositional landforms that has distinctive accretion features. Each type of landform is again divided into the number of geomorphic units. Figure 2.4 shows the three major divisions along with their subdivisions (GSB, 2013).

2.3.4 Geology

The salient geotechnical features are dependent on the geology of an area. The susceptibility of CHT to landslides is influenced by its geological features. The Indian plate was initially a part of the ancient continent of Gondwanaland. After the break-up of Gondwanaland, Indo-Australian plate together moved towards south-easterly of about 1750 km at a drift rate of 6 cm/yr (Sarker, 2013).

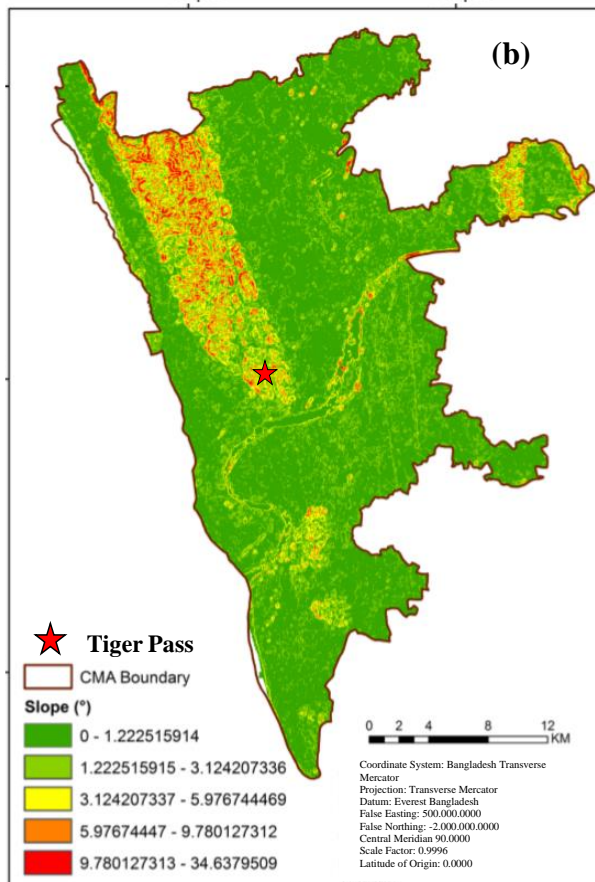
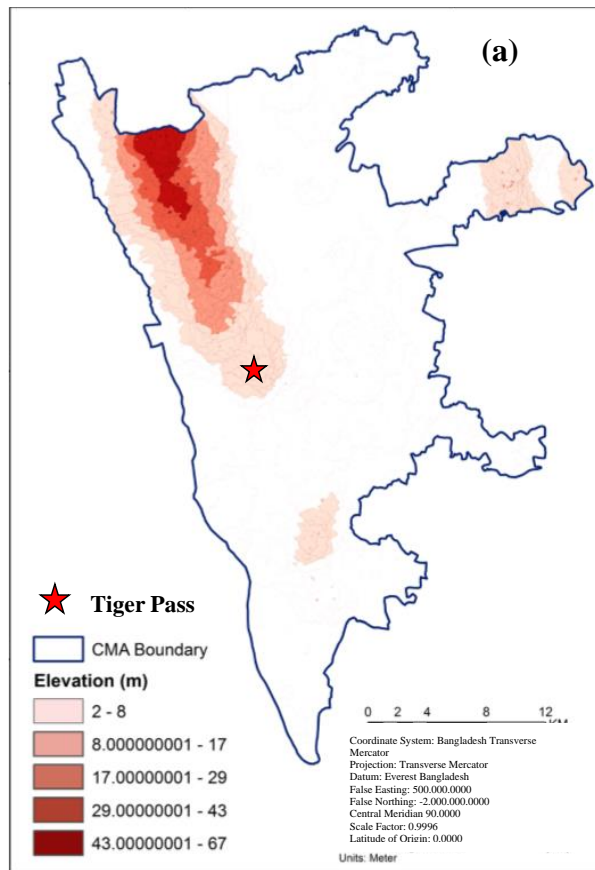


Figure 2.2: (a) Elevation map of Chattogram Metropolitan Area; (b) Slope map of Chattogram Metropolitan Area (Ahmed, 2014)

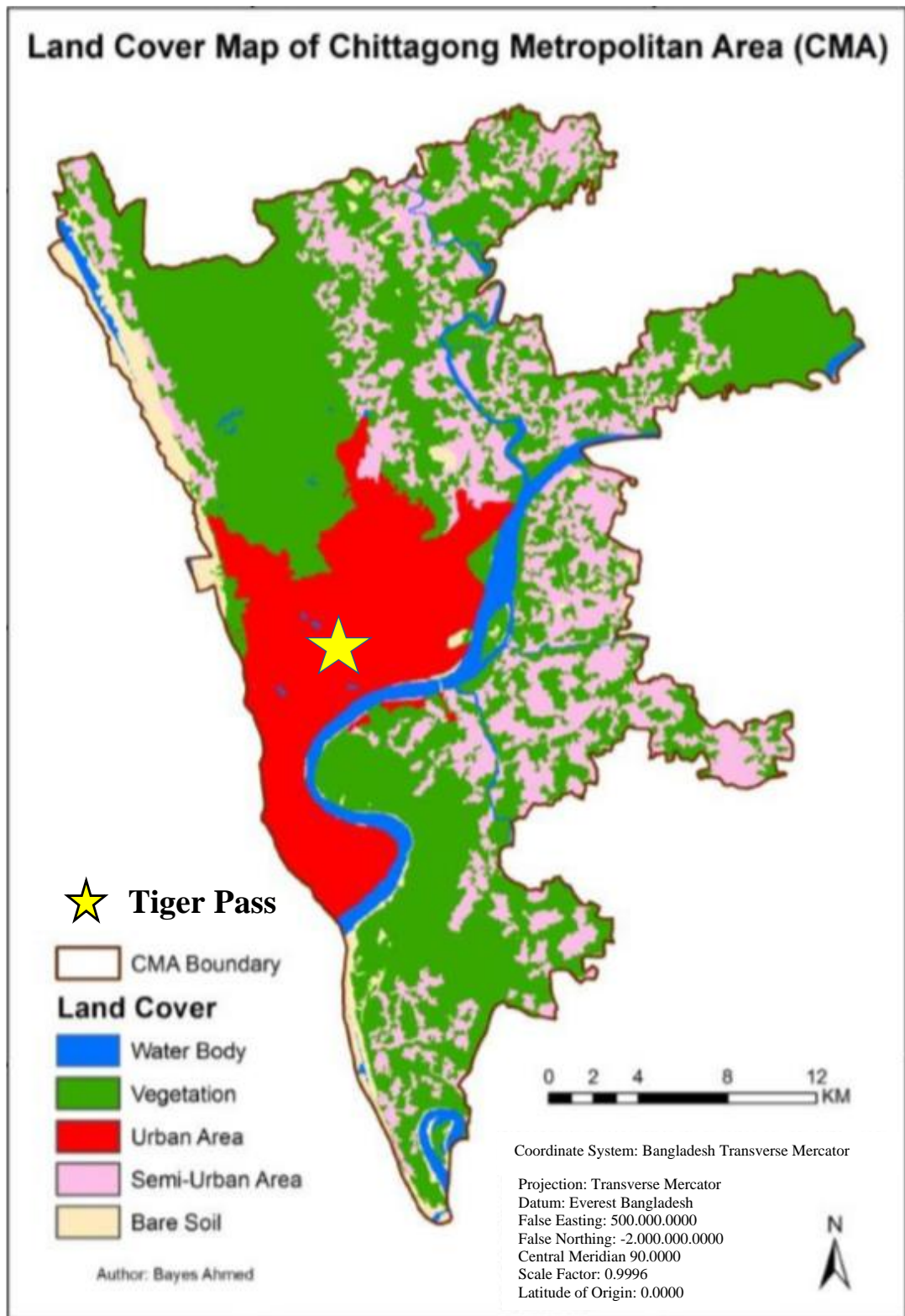


Figure 2.3: Land cover map of Chattogram Metropolitan Area (Ahmed, 2014)

Later India broke apart from Australia and started to drift north-easterly. That is the time when the history began for the Chattogram Hill Tracts Hilly area of Bangladesh and it developed in tertiary age (Osmany, 2014).

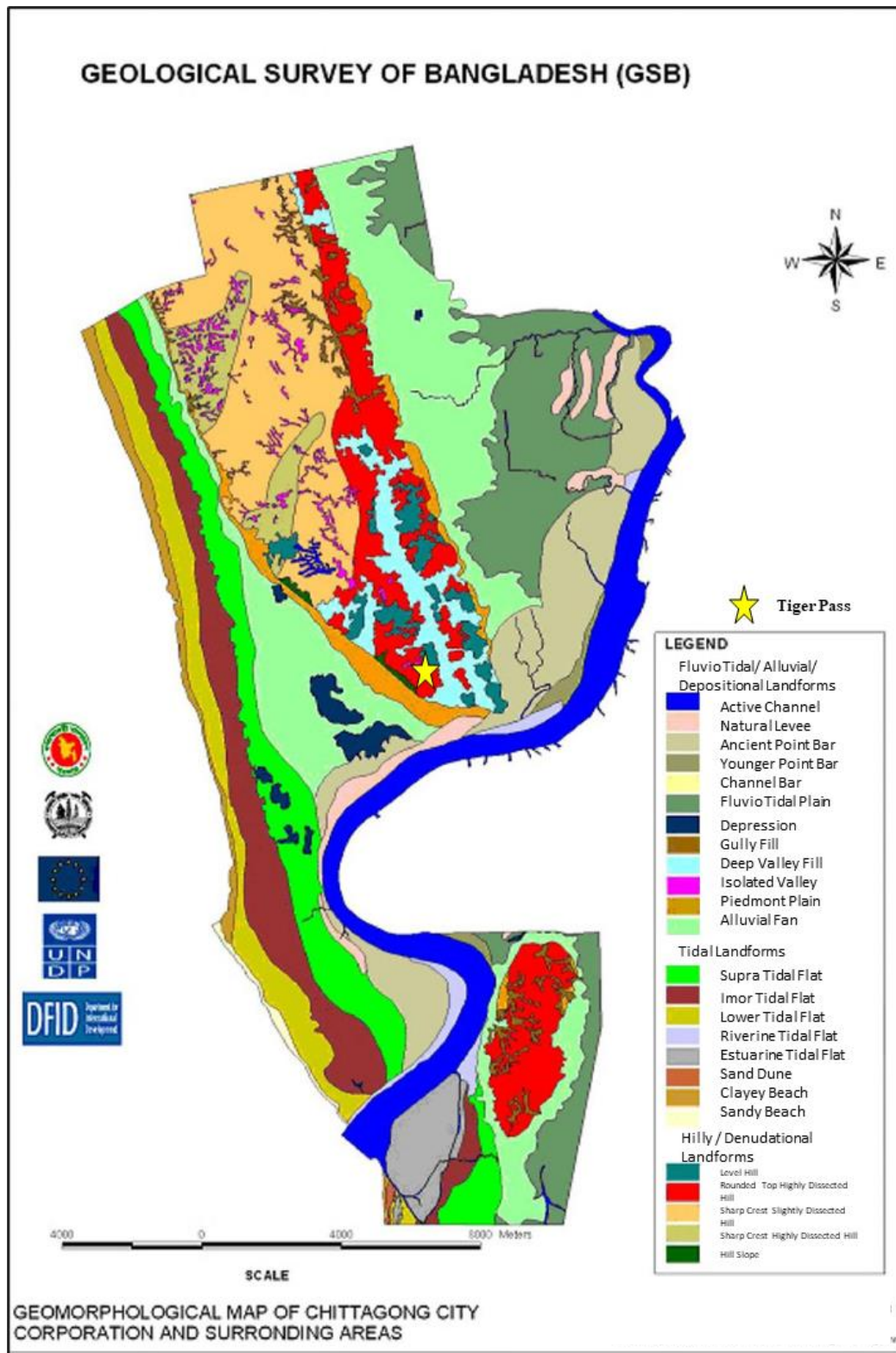


Figure 2.4: Geomorphological map of Chattogram City Corporation and surrounding area (GSB, 2013)

Chattogram City lies in the southern plunging part of the Sitakund Anticline. The anticline is asymmetrical and is characterized by a steeper western (faulted) flank and a gently sloping eastern flank. In the plunge area around the city, the folded sediments

are highly twisted and distorted (Muminullah, 1978; Hasan, 1981). Around Chattogram City, from east to west, exposed geological formations are Dihing Formation, Dupi Tila Formation, Tipam Sandstone and Boka Bil Formation (Alam et al., 1990). Under varying environments, these formations, as shown in Figure 2.5, were deposited during Mio-Pliocene time (25–2 Ma). The detailed properties of all these deposits have been presented in Table 2.1. From Table 2.1 it can be observed that, their rock types as well as their geotechnical properties are non-identical.

Moreover, since its deposition, the rocks have undergone different climatic conditions as well as tectonic activities which eventually influenced the geotechnical properties of the rocks. The presence of ripple marks and the frequent alternation of sand and silt of the Boka Bil Formation reveal that the sedimentation took place in strong current at times (Karim et al., 1990).

The change of facies from argillaceous to arenaceous points out that the environmental condition gradually changed. The presence of clay galls and lignite suggests that the rocks of Tipam Formation display arenaceous in the northern part and argillaceous in the south. This change of lithofacies in the formation reveals that the gradual regression of sea started in the northern part earlier than the south. The environmental condition was later reduced to estuarine. The sediments of Dupi Tila Formation were deposited in this environment and continued to occur towards the close of Pliocene. The occurrence of shale and sandstone pebbles, iron incrustations and silicified wood establishes the fact that the sediments of Dihing Formation were derived mostly from older formations in a fluvial environment (Krishnan, 1982).

2.4 Climate and Rainfall Pattern of Chattogram Hill Tracts

The weather of CHT is characterized by tropical monsoon climate with mean annual rainfall nearly 2,540 mm in the north-east and 2,540 to 3,810 mm in the south-west (Ahmed et al., 2018). The dry and cool season is from November to March, pre-monsoon season is April to May which is very hot and sunny and monsoon season is from June to October, which is warm, cloudy, and wet (Chowdhury, 2012).

Moreover, due to climate change, Chattogram Metropolitan Area is experiencing higher intensity of rainfall in recent years which is making the landslide situation worse (Mangiza, 2011). A gradual upward shift in precipitation is noted in the last five

decades (1960–2010), with an abrupt fluctuation in the mean annual precipitation levels which can be seen from Figure 2.6 (BMD, 2013).

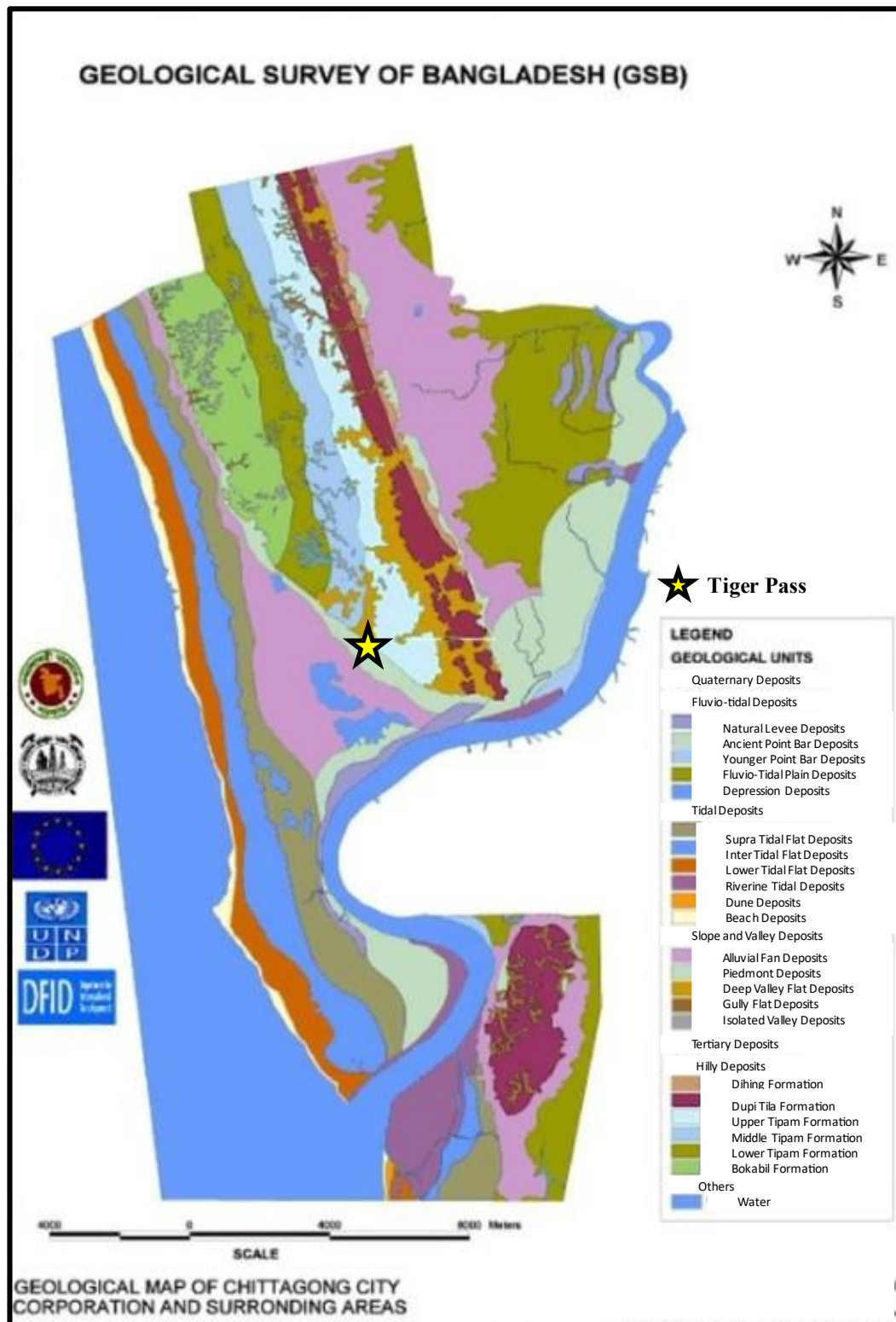


Figure 2.5: Geological map of Chattogram City Corporation and surrounding area (GSB, 2013)

From the data obtained from Geological Survey of Bangladesh and USGS website average annual precipitation map was prepared (Persits et al., 2001) as shown in Figure 2.7.

Table 2.1: Stratigraphic formation and geotechnical features of Chattogram city and surrounding area (Karim et al., 1990)

Name of the formation/ age	Soil/rock type		Geotechnical and geological characteristics
Dihing Formation/ Pliocene (13–1 Ma)	Reddish brown to brick red, massive, highly ferruginous, weathered sandy to clayey silt, clay and pebbly sandstone at places, oxidized iron incrustation. On top weathered residual soils.		Very soft (981-2943 kPa) to soft (2943-9810 kPa) in hardness*, low-to-medium relative strength, uniaxial compressive strength of 98.1-196 kPa
Dupi Tila Formation/ Mio-Pliocene (15–5 Ma)	Sandstone and alternation of silty sand and silty shale. Sandstone massive and medium to fine grained, silty sand beds are grayish to yellowish brown, thickly laminated to bedded. Silty shale is light gray to gray, very thinly laminated, fissile. Presence of iron incrustation.		Longitudinal joints present dipping almost parallel to the bedding, spacing varies from closed to 1.5 cm, filled with ferruginous band with coarse sand. Soft (2943-9810 kPa) in hardness. Low-to-medium relative strength.
Tipam Sandstone Formation/ Mid Miocene (25–13 Ma)	Upper Tipam	Sandstone, siltstone and occasional shale, Sandstone cross-bedded and local unconformity at the base	Soft in hardness (2943-9810 kPa), moderately weathered, faulted, conjugate (planar) joints are present with vertical and dipping orientation, spacing <1 cm, uniaxial compressive strength $>54 \times 10^3$ kPa

Table 2.1: Contd. (Karim et al., 1990)

Name of the formation/ age		Soil/rock type	Geotechnical and geological characteristics
Tipam Sandstone Formation/ Mid Miocene (25–13 Ma)	Middle Tipam	Silty shale and shale, bedded, shale relatively hard, at places calcareous.	Moderate (9810-24525 kPa) to hard (24525-68670 kPa; 250-700 kg/cm ²) in hardness, faulted, uniaxial compressive strength varies from 54×10 ³ - 100×10 ³ kPa
	Lower Tipam	Massive sandstone, yellowish brown to brown, medium to coarse grained, loose to dense, cross-bedded.	Moderate (9810-24525 kPa), at places hard (24525-68670 kPa) in hardness, slightly to highly weathered, faulted, planar and conjugate joints are seen with vertical and dipping orientation, spacing <1 cm, ferruginous and argillaceous filling, medium to low relative strength, uniaxial compressive strength varies from 27×10 ³ kPa to 73.5×10 ³ kPa
Boka Bil Formation/ Early Miocene (34–25 Ma)	Silty shale, siltstone, sandstone and alternation of sand and siltstone. Cross bedding, cross lamination, ripple marks and load casts are present.	Moderate (9810-24525 kPa) to hard (24525-68670 kPa) in hardness, faulted, planar diagonal to conjugate joints present, closed spacing, filled with mainly parent material, uniaxial compressive strength varies from 24525-68670 kPa	
* Harness scale varies as very soft, soft, moderate and hard			

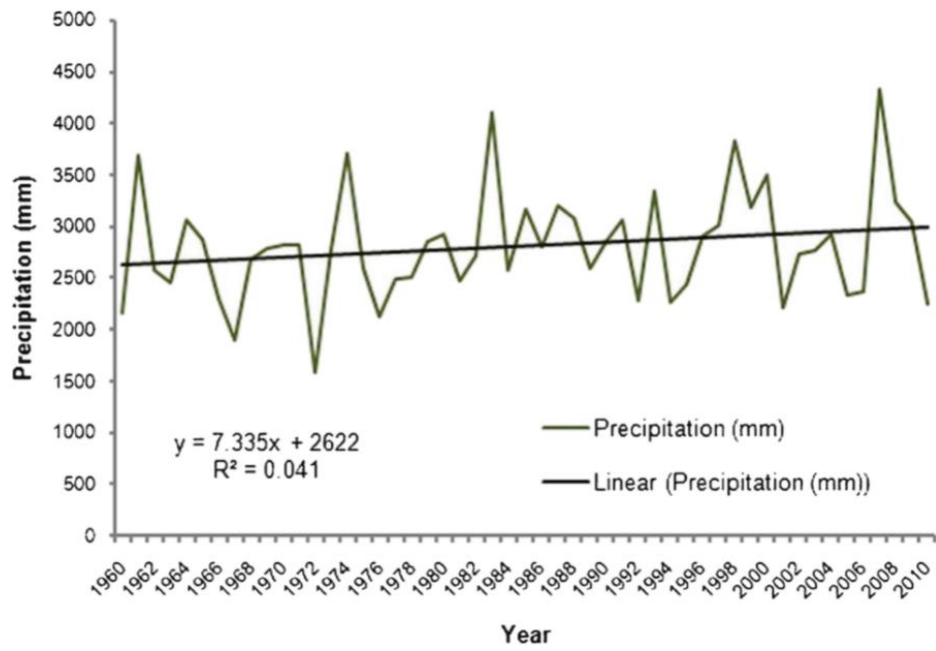


Figure 2.6: Annual rainfall pattern of Chattogram city from 1960 to 2010 (BMD, 2013)

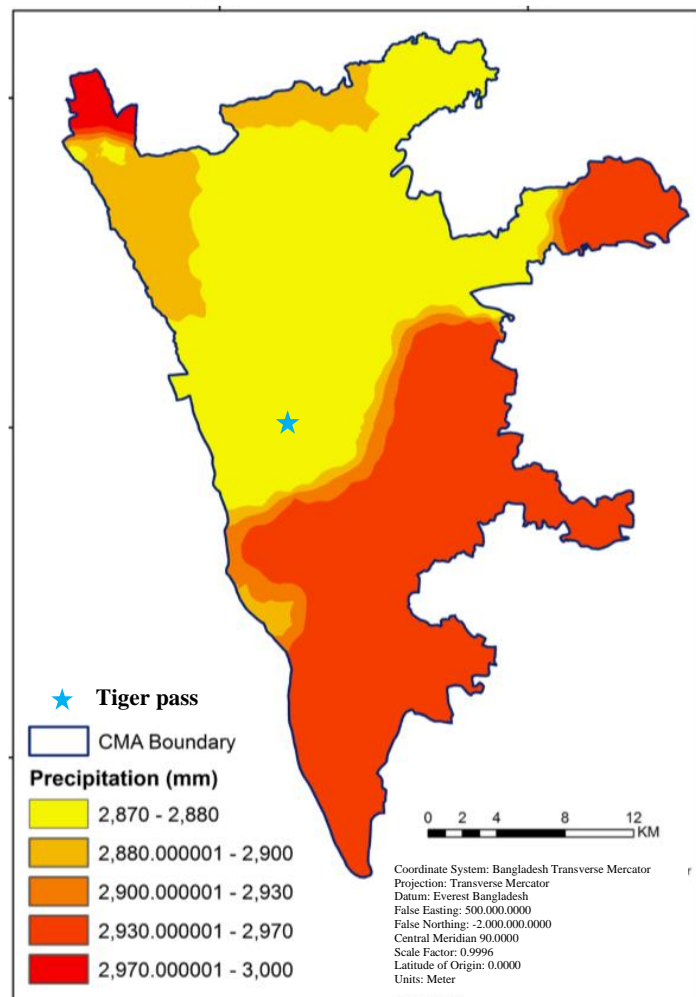


Figure 2.7: Precipitation map of CMA (Persits et al., 2001)

2.5 Nutrient Condition of Soil and Vegetation Growth

Fertility is the potential nutrient status of a soil to produce crops. The general soil of hills of Chattogram is also low in organic content and in nutrient (Hassan et al., 2017). Other limitations including very steep slopes, heavy monsoon rainfall, erodibility of most soils, difficulty of making terrace, generally low and rapid permeability make the hills unsuitable for cultivation. Hills are mainly under natural and planted forests. Shifting cultivation is practiced in some places. The shifting cultivation includes land clearing and burning. This, when followed by excessive rainfall, causes erosion of the top soil along with nutrient contents (Gafur et al., 2000). In this condition the vegetation which do not require nutrient rich soil can be considered for plantation along the hill slopes of CHT.

2.6 Vegetation of Chattogram Hill Tracts

The hills of Chattogram Hill Tracts are not very suitable for cultivation but there are wide range of natural vegetation (Hassan et al., 2017). Among the total area of CHT, about 75% is covered with forest area and they are ecologically classified as Tropical wet-evergreen, Tropical semievergreen, Tropical moist-deciduous, Tropical open deciduous and Savannah forests (Das, 1990). The vegetation is characterized by semi-evergreen (deciduous) to tropical evergreen and are dominated by tall trees belonging to dipterocarpaceae, euphorbiaceae, lauraceae, leguminosea and rubiaceae (Osamny, 2014). Dipterocarpaceae are mainly woody trees with taped branched and deep root. Euphorbiaceae consists of annual and perennial herbs and woody shrubs or trees. Rubiaceae are mostly shrubs with some herbs and trees. It also has branched tap root system. A portion of the forest is also characterized as grassland (Das, 1990).

2.7 Landslides in Chattogram Hill Tracts

When rock, soil or debris move downward under the influence of gravity, the event is termed as landslide (Guzzetti et al., 2012). Though Bangladesh has been frequented by disasters, landslide was not one of those in the past. Landslides are mostly caused by natural factors such as rainfall and earthquakes. Chattogram hill tracts is in zone II ($Z=0.28$) according to the seismic zonation map of Bangladesh (BNBC, 2020) and rainfall intensity in this region is also high. In recent years due to the combined effect

of human activities and climate change, landslides have become frequent in Chattogram hill tracts.

2.7.1 Natural causes of landslide

Landslides can be caused for different natural phenomena including intense rainfall, earthquake, rapid snow melt, volcanic activity. In our context, the following are responsible for landslides:

- a) The hill tracts of Chattogram are mainly composed of weather able feldspar. It gets eroded by agents like water and air. The landslide is closely related to shear strength of the soil. When the induced shear stress is greater than the shear strength of the soil the slope fails thus landslides occur. Shear strength is controlled by several variables such as friction, which itself is proportional to the normal force, as well as many other variables such as the roughness, cohesion, and dryness of the material (Biswas et al., 2017).
- b) High intensities of rainfall increase the probability of slope saturation which is the primary cause of the landslide. Saturation can also occur due to changes in ground-water levels and surface-water level. Once the pore spaces are saturated the mass of the soil increases. Gravity exerts a force downward proportional to the increased mass. This increases the induced shear force on the soil and thus chances of landslide increase (Islam, 2018).
- c) Earthquake reduces the shear strength of soil particles. Earthquakes in steep landslide-prone areas greatly increase the likelihood that landslides will occur. The rapid infiltration is facilitated by the ground shaking, liquefaction of susceptible sediments, or shaking-caused dilation of soil materials. Thus the slope gets saturated at an accelerated pace (Biswas et al., 2017; Ali et al., 2018).
- d) Absence of vertical vegetation due to natural events (i.e. wild fire) decreases the bondage of soil particles and stability of soil (Islam, 2018).

Among all the natural causes the earthquake and high intensity rainfall can be regarded as the primary triggering factor of landslide.

2.7.2 Man-made causes of landslide

Along with the natural causes, some activities conducted by humans increase the risk of landslide. Indiscriminate hill cutting, deforestation, rapid growth of urban areas and

thus illegal human settlement on hill slopes have played roles in causing landslides. The followings keep contributing to the risk of landslide of CMA (Ahmed 2014; Ahmed, 2017; Ali et al., 2018):

- a) The city of Chattogram is attracting many rural-urban migrants and thus the population is increasing. For this, most open spaces are turned into built up areas and certain hilly areas into settlement. For establishing the dwellings at the foothill region, hill cutting is continued, and the risk of landslide is increasing.
- b) Tress planted along the slope of hills hold the soil and reduces the probability of landslide. But for establishing the houses at the slopes and foot of hills deforestation is done. Along with this, a vicious circle of selling the trees continue. This again poses the threat of landslide. In addition, some of the afforestation practices are also responsible for the destabilization of soil particles if the local soil characteristics are not considered.
- c) Industries, roads etc. are being constructed due to rapid urbanization. However, these activities along the hilly slopes need special consideration. Without proper considerations the earthworks involved in these activities alter the shape of a slope along with imposing new loads on an existing slope.

2.7.3 Previous landslides

Among the different disasters the world is facing, landslide has been recognized as the third most important type (Van et al., 2010). It has influenced Bangladesh in recent years. Among the different hill districts causalities have been reported in Chattogram, Rangamati, Bandarban, Cox's Bazar and Sylhet (Ahmed et al., 2018). Figure 2.8 presents the percentage of casualties which different areas have faced (Rahman, 2012). From this we can see that most of the causalities have occurred in CHT and the maximum percentage of casualties have occurred in Chattogram. During the last five decades, Chattogram suffered through 12 landslides. By the devastation of this disaster 17 people died in 1999, 13 in 2000, 54 in 2010 and 17 causalities occurred in 2011 in Bangladesh (Sarker, 2013).

Considering the number of landslides that has occurred in CHT, we can see that Chattogram has faced the maximum, 208 landslides from 2001 to 2017 followed by

Rangamati. Figure 2.9 shows the number of landslides in different districts of Chattogram Hill Area (Rabby and Li, 2020). Khagrachari has the lowest number of landslides which is 87. Figure 2.10 shows the spatial distribution of the landslides in different districts of Chattogram hilly area (Rabby and Li, 2020). Chattogram Hill Tracts face a great threat of rainfall induced landslide. The human settlement on the slopes of hills are the most vulnerable. Two such examples are the landslide of 2007 and 2017. The landslide of 2007 took place in Chattogram Metropolitan Area on 11 June, taking the life of 128 people (Islam, 2018).

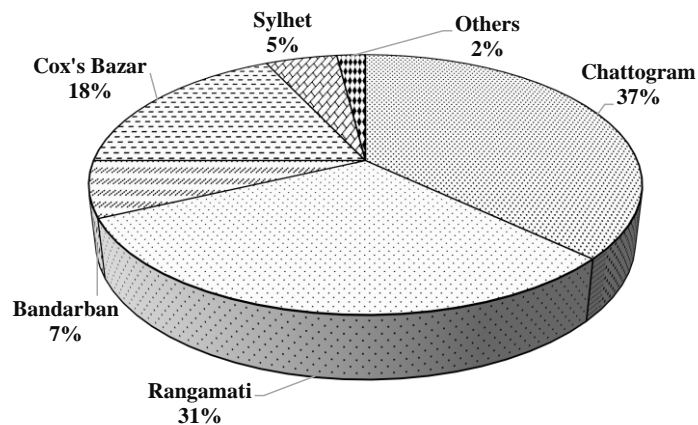


Figure 2.8: Casualties due to landslide in Bangladesh (Reproduced from Rahman, 2012)

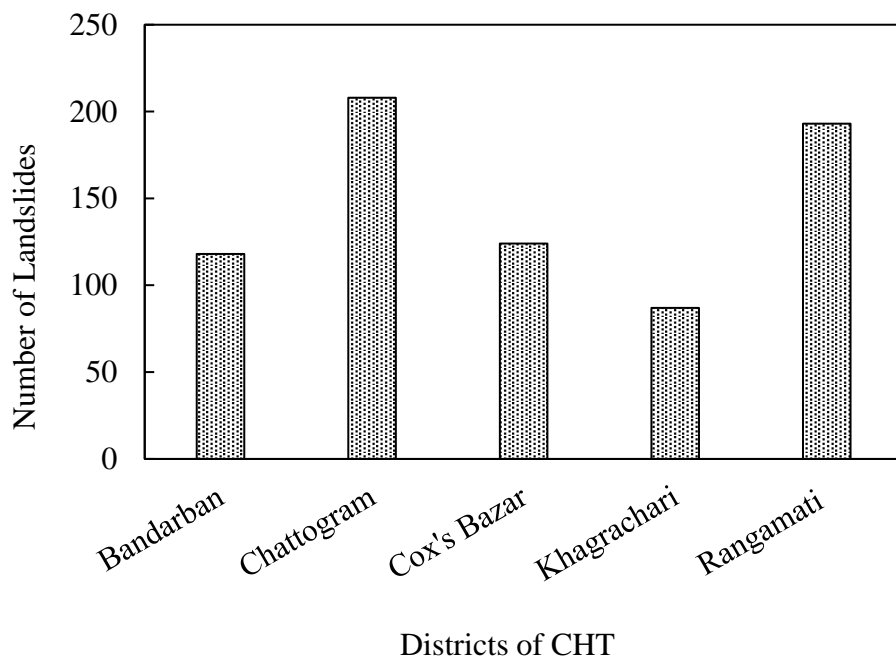


Figure 2.9: Number of landslides in different districts of the Chattogram Hill Tracts (2001-2007) (Based on data obtained from Rabby and Li, 2020)

The biggest landslide disaster of Bangladesh is the one of June 2017 which was triggered by rainfall and killed 168 people in Chattogram, Bandarban and Rangamati. More than 40 thousand houses were damaged (Ahmed et al., 2018). Despite these, the rapid urbanization continues in Chattogram Metropolitan Area which has made the situation more critical. Ahmed (2014) had conducted field visits and 20 locations of landslide have been identified by him until 2013. Figure 2.11 shows the location of these landslides. Most of these are shallow in nature. The rainfall intensity and their duration have played particularly important role in producing these shallow landslides (Khan et al., 2012).

Figure 2.12 shows a real scenario of Rangamati during the landslide of June 2017. The two major landslides of 2007 and 2017 were also triggered by 610mm of heavy rainfall over eight consecutive days (Ahmed et al., 2018).

Table 2.2 presents the landslides that has occurred in Chattogram Hill District since 1999 to 2018 (Local newspapers and Ahmed, 2017). It also states the cumulative rainfall associated with each of the event.

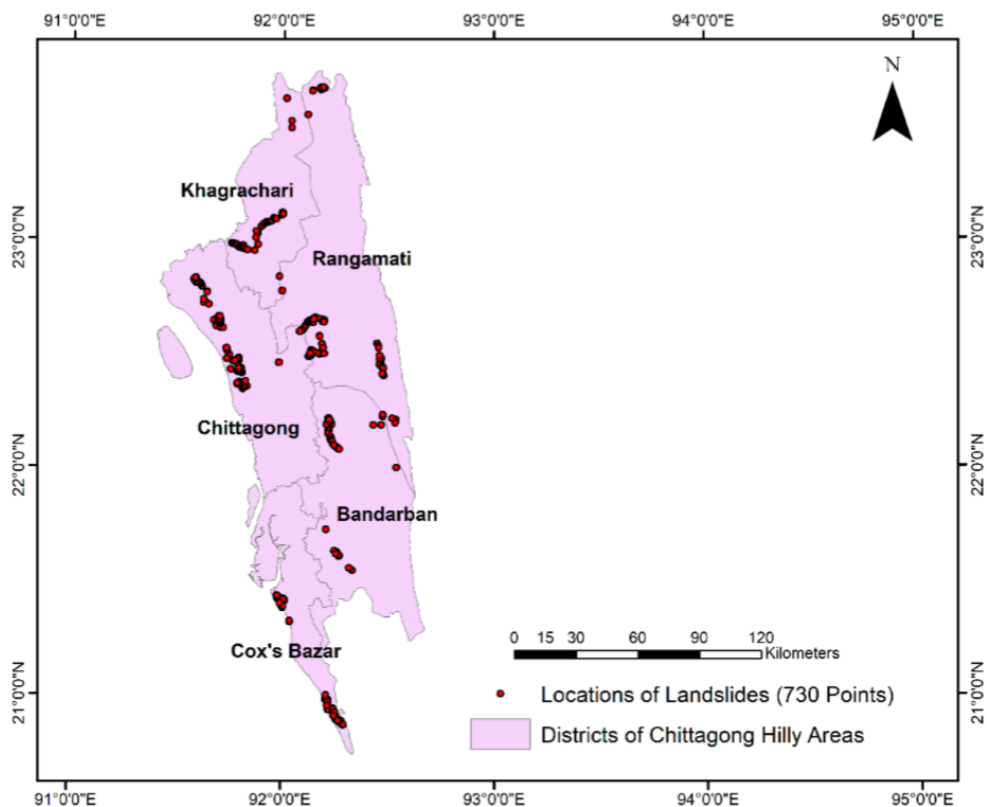


Figure 2.10: Location of landslides from 2001 to 2017 in different areas of Chattogram hilly area (Rabby and Li, 2020)

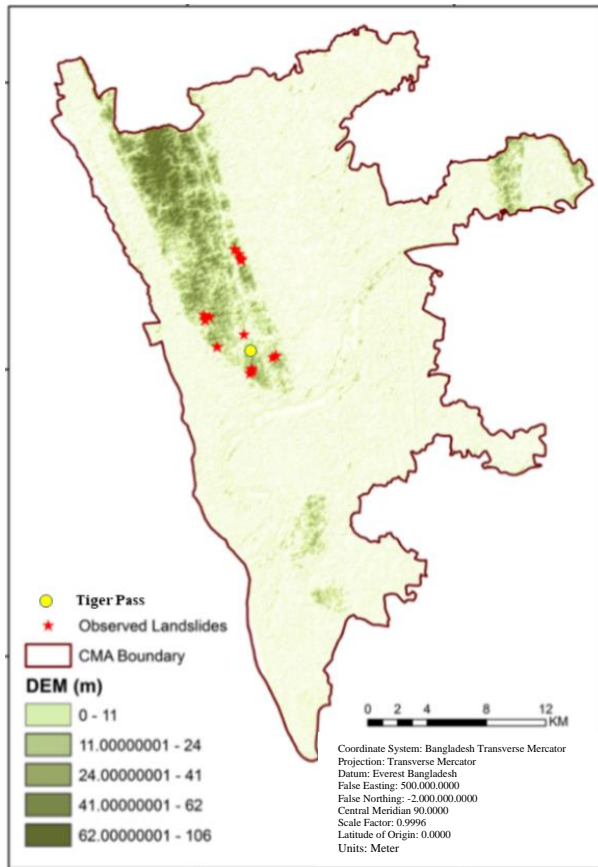


Figure 2.11: Location of landslides in Chattogram Metropolitan Area (Ahmed, 2014)



Figure 2.12: Probable slide location and damaged house in Rangamati (Source: The Daily Star, June 19, 2017)

Table 2.2: Details of major landslide events in Chattogram District, Bangladesh (Source: Local newspapers and Ahmed, 2017)

Date	Location	Rainfall Sequence	Consequences
13/08/1999	Different locations of Chattogram District	435 mm 12 days, 2–13 Aug 1999	17 fatalities 350 houses damaged
29/06/2003	Patiya, Chattogram	658 mm 10 days, 20–29 June 2003	4 fatalities
10/07/2006	Satkania, Chattogram	231 mm 6 days, 4–9 July 2006	2 fatalities
11/06/2007	Different locations of Chattogram District	610 mm 8 days, 4–11 June 2007	128 people died 100 injured
10/09/2007	Nabi Nagar, Chattogram	452 mm 7 days, 4–10 Sept 2007	2 fatalities
18/08/2008	Matijharna, Chattogram City	454 mm 11 days, 8–18 Aug 2008	11 fatalities 25 injured
01/07/2011	Batali Hill, Chattogram	200 mm 6 days, 25–30 June 2011	19 people died many injured
26/06/2012	Lebubagan and Foys lake surroundings, Chattogram	889 mm 8 days, 19–26 June 2012	90 fatalities 150 injured

Table 2.2: Contd. (Source: Local newspapers and Ahmed, 2017)

Date	Location	Rainfall Sequence	Consequences
28/07/2013	Lalkhan Bazar, Chattogram	148 mm 2 days, 26–27 July 2013	2 fatalities
21/06/2014	Pachlaish, Chattogram	2 days continuous heavy rainfall	1 fatality, 2 injured
23/06/2015	DT Road Rail Gate, Chattogram	Wall collapse due to 2 days of heavy rainfall	2 fatalities
19/07/2015	Motijharna and Tankir Pahar, Chattogram	205 mm 5 days, 15–19 July 2015	6 fatalities
13/06/2017	All five hill districts	Several days of continuous rainfall	159 fatalities 88 injured
21/07/2017	Sitakunda, Chattogram	Several days of continuous rainfall	5 fatalities
14/10/2018	Akbar Shah area's Firoz Shah Colony, and Panchlaish	464 mm 5 days, 9–13 October 2018	4 fatalities

2.8 Type of landslides

Landslide describes a variety of process that generally result in downward movement of slope forming materials. According to Varnes (1978), the slope movements that cause landslides can be classified into five types: falls, topples, slides, lateral spreads and flows.

The movement of mass where a distinct zone of weakness separates the slide material from more stable underlying material is termed as slides. The two major types of slides are rotational slides and translational slides. If sliding is on a predominantly planar slip surface, then the slide is called a translational slide. If movement is on a curved slip surface, then the slide is called a rotational slide. A lot of rotational slide end up as a mudflow leaving a gaping hole in the ground where the slide began (Varnes, 1978).

When the movement involves deformation of the soil mass and then downslope flow of a viscous fluid, it is termed as “Flow”. There are mainly five types of flow (USGS, 2004): (i) Debris flow, (ii) Debris avalanche, (iii) Earth flow, (iv) Mudflow and (v) Creep (Cruden, 1991).

According to United States Geological Survey, a debris flow is a form of rapid mass movement in which a combination of loose soil, rock, organic matter, air, and water mobilize as a slurry that flows downslope. Debris flows also commonly mobilize from other types of landslides that occur on steep slopes, are nearly saturated, and consist of a large proportion of silt- and sand-sized material. Earthflow is closely related to debris flow. Here the material is earth. It occurs in moderate to steep slope. It occurs when the top soil or the over burden soil seasonally becomes saturated by heavy rains. The material slumps away the upper part of the slope leaving a scarp and flows down to form a bulge at the toe. Earthflows range from small to the very big, involving hundreds of tons of material blocking or destroying roads, damming rivers and destroying houses. Earth flows mainly occur in fine-grained materials or clay bearing rocks. However, dry flows of granular material are also possible.

In rock, usually falls and translational slides (involving one or more planes of weakness) will occur. Since soil is more homogenous and lacks a visible plane of weakness, rotational slides or flows occur (Cruden and Varnes, 1996).

Based on the classification of Cruden and Varnes (1996) if the movement is of soil is rapid, the water content is wet, the material is soil (earth) and type of movement is slide then the landslide is termed as “earth slide”. Most of the landslides that have occurred in CHT contained 80% sand and finer particles. Most of them are also triggered by heavy rainfall and the soil was wet. The landslides were shallow in nature (Khan et al., 2012). So, the landslides in CHT are classified as earth slides.

2.9 Mechanism of Rainfall Induced Landslide

Almost every landslide has multiple causes. Slope movement occurs when forces acting down-slope (mainly due to gravity) exceed the strength of the earth materials that compose the slope (Biswas et al., 2017). Causes include factors that increase the effects of down-slope forces and factors that contribute to low or reduced strength. In case of rainfall induced landslides, two of the factors may contribute to the landslide: (i) Pore water pressure and (ii) Added weight of water (Ali et al., 2018).

Pore water pressure is highly responsible for the rainfall induced landslides. Most of the hill slopes remain barren and during dry season tension cracks may be formed. During rainfall, the water easily infiltrates into the barren soil and increases the pore water pressure. Due to this increased pressure, vertical crown cracks are formed at the convex part of the hill slopes. These cracks make it easy for the rainwater, to infiltrate into the soil rapidly. This accumulated water generates horizontal stresses on the sliding mass and reduces the stability.

The pore water pressure generally generates in the convex part and when it exceeds the shear resistance, the soil starts to move. The initial slide of soil, with a larger amount of water, starts from this convex part which rolls over the concave part of the slope and reaches a regular part. As the soil is mostly non-cohesive in nature, the slide terminates as a dry flow in case of Chattogram Hill Tracts. Figure 2.13 shows schematic diagram this mechanism (Ali et al., 2018).

Again, due to the infiltrated rainwater, the weight of the soil increases. Under the action of gravity, this added weight may exceed the resisting forces. Thus, landslide is triggered.

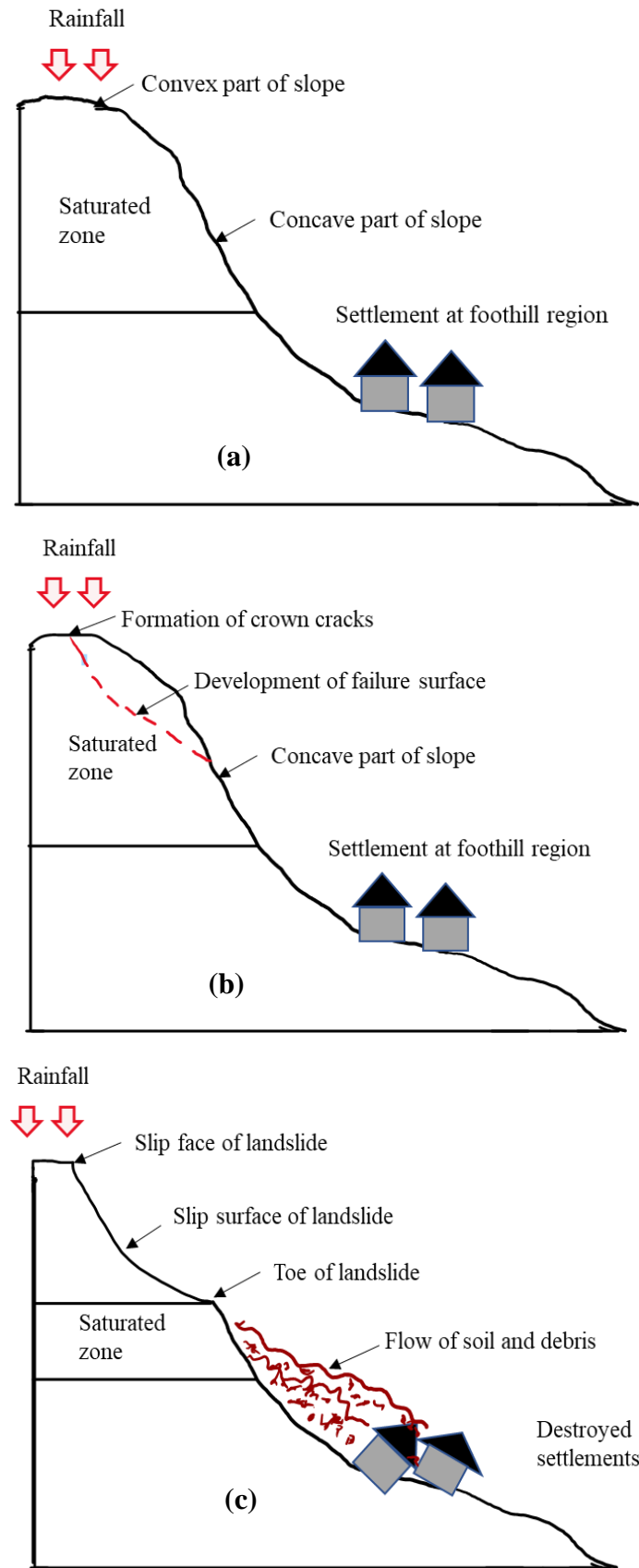


Figure 2.13: Mechanism of rainfall induced landslide; (a) Start of rainfall; (b) Generation of failure surface; (c) Flow of soil and debris (Reproduced from Ali et al., 2018)

2.10 Previous Studies on Rainfall Induced Landslides and Simulation

In the last few years, landslide has emerged as a disaster of major concern for the southeastern part of Bangladesh, Particularly in Chattogram city with the increasing trend of damage and frequency. Most of the landslides that occurred in CHT are caused due to rainfall. Very few studies (Khan and Chang 2006, 2008) related to the landslide problems of this area have been undertaken, but only some of those consider the effects of rainfall intensity and duration. Khan et al., (2012) studies the critical antecedent rainfall condition for the shallow landslides in Chattogram city by using Gumbel's distribution. A landslide inventory for the CMA was prepared by Ahmed et al., (2014) including various factors like rainfall intensity, landslide location, potential causes, damages etc. Also, Ahmed et al., (2018) studied the rainfall threshold values for landslides in CMA and has associated a hazard class with each landslide. An early warning system has also been developed.

Studies of landslides relating to rainfalls, Onodera et al., (1974) for example, found that the slope failures increased abruptly after rainfall exceeded 150–200 mm with the rainfall intensity more than 20–30 mm per hour in Japan. An approximate rainfall value of 250 mm is a likely threshold for the occurrences of landslides in San Benito County, California (Oberste-Lehn, 1976) and in Alameda County, California (Nilsen et al., 1976). According to Guidicini and Iwasa (1977), landslides can occur in southeast Brazil when precipitations exceed 8–17% of the mean annual precipitation and the catastrophic event may occur with rainfall of more than 20% of the annual mean. Ng and Shi (1998) suggest that short-duration rainfalls with high intensity can trigger landslides in Hong Kong.

An evaluation of shallow landslides induced by a particular rainfall event was done with a time–space based approach and Geographic Information System (Xie et al., 2004). Chang et al., (2008) proposed a landslide model using a quantitative precipitation during typhoon that could be used to compute probabilistic landslide occurrence for a real-time monitoring system. Guzzetti et al., (2004) described the rainfall triggered landslides with cumulative and continuous rainfall data combined with other information collected from the landslide occurrences. Again, Guzzetti et al., (2008) investigated the rainfall intensity–duration for initiation of shallow landslide and proposed a global intensity–duration for shallow landslide occurrences. Marques

et al., (2008) studied the role of rainfall in landslides on the regional scale for Portugal and found that the landslides were related both to short-duration precipitation events (1–3 days) with high average intensity (between 78 and 144 mm/day) and long-lasting rainfall episodes (1–5 months) with a lower intensity (between 9 and 22 mm/day).

A number of different approaches were also devised to incorporate the rain infiltration in terms of pore water pressure distribution inside the slope for shallow landslide (Haneberg, 1991). Generally, these approaches use models of infinite slope stability analysis to find the critical pore pressure distribution at failure. Gabet et al., (2004) developed a slope stability model where they used 3 years of daily rainfall and sediment transport data to define the relation between monsoonal rainfall and landslides in the Annapurna region of Nepal and suggested that the two distinct threshold values, seasonal accumulation and daily amount, were critical for landslide to occur.

2.11 Possible Remediation Measures

There are two types of solutions which may be applied in case of remediation of landslides. One is the hard solution which are the structural measures. Another one is soft engineering which indicate the non-structural measures. The applicability of these depend on various factors such as possible consequences, construction difficulties, environmental condition, cost etc.

2.11.1 Structural measures

Among different available structural measures, the application of retaining walls is quite common in Bangladesh. Specially the application of Reinforced Cement Concrete (RCC) retaining walls are observed. However, the construction cost is high for these. Relatively large space is also required for the wall and it is not possible to build retaining walls to all dangerous slopes along the hill sides.

From the study of Islam (2018) it has been observed that general and existing slopes can also be modified by

- (i) Reduction of the slope angle: This method improves the stability by reducing the driving force. However, it is suitable only for cuts into deep soil where

rotational landslides may occur. A complete solution involves additional modification of the land.

- (ii) Addition of light-weight materials: This method replaces the in-situ material with a light weight one. However, it requires large amount of earthwork and it is costly.

To increase the slope stability, the internal slope can be reinforced. It may be done by application of anchors, soil nails, geotextiles and geogrids (Elahi, 2018). Anchors can be applied by linking at the surface to each other by a beam frame which is generally made of reinforced concrete. It involves high cost of installation thus might not be suitable for Bangladesh. Geotextiles can be layered in compacted fill embankments to engender additional shear strength and it greatly enhances the stability when the space is limited. Soil nail can reduce the chances of landslide by increasing the in-situ stability of slopes. Steel reinforcement bars are inserted into the soil and they are anchored to the soil strata. This can be applied in irregular shapes and is ideal for tight spaces. The facing height is not restricted. Also, limited shoring is required for the installation process (Elahi, 2018). Thus, soil nailing is suitable for Bangladesh. In this study, the effectiveness of soil nailing has been studied in detail. Structural measures are effective in reducing the risk of landslides, but we need to think about more cost effective and sustainable solutions.

2.11.2 Non-structural measures

- a) Landslide Inventory: To apply any measure to reduce the risk of landslide, first its location needs to be identified. The locations which have experienced landslide previously can be more vulnerable to landslides in future too. It is difficult to get the data set as the old events may not have been documented or not remembered. Using the geomorphological signatures of soil, the occurrence of landslide can be identified. Also, by going through newspapers, reports and digital archives the location, intensity, causality etc. of landslides can be determined. This will help to build a landslide inventory and help the authorities to prioritize among various locations for application of structural measures (Ahmed, 2014, Ahmed, 2017).
- b) Awareness and Community Based Approach: The foot hill region of the hills includes settlements among which mostly belong to the underprivileged population. They need to be made aware about the potential risks about these

illegal settlements. Along with the awareness raising, they need to be prepared about the course of action they need to follow pre, during and post a landslide occurrence. The community should be equipped properly with available resources for risk reduction and emergency response and should be trained for effective response. This may reduce the impact of landslide and reduce casualties (Ahmed, 2014, Ahmed, 2017).

- c) **Modern Techniques for Landslide Prediction and Early Warning System:** Early Warning Systems (EWS) are essential, especially if the structural mitigation measures fail or are absent (Kelman and Glantz, 2014, Kelman et al., 2018). This early warning system is an essential tool for landslide disaster risk reduction and can be made operational at local scale. In Bangladesh, the Ministry of Disaster Management and Relief under the Comprehensive Disaster Management Program-II (2012) has developed a community-based landslide EWS for the Cox's Bazar district. They conducted detailed landslide inventory surveying, rainfall threshold analysis and a series of community-based participatory activities. Also, a "Dynamic Web-GIS Based Landslide Early Warning System" for the Chattogram Metropolitan Area by Ahmed et al., (2018). Several advanced methods such as probabilistic approach for landslide susceptibility analysis, runout modeling using volume based method, in situ ground based monitoring techniques, remote sensing techniques etc. are being developed and critically examined for prediction of landslides thus slope stability (Chae et al., 2017). Very recently an Acoustic Emission based early warning system has been developed by Dixon et al., (2018). This sensor measures accelerating deformation behavior and can be used to issue signals once the deformations exceed prescribed levels. The effectiveness of these EWS also depends on the participation and response of the local people. But, through this, the risk of landslide can be predicted beforehand, and the risk can be mitigated.
- d) **Regulating Illegal Hill Cutting and Settlement:** Most of the hills in Bangladesh, along with Chattogram are susceptible to landslides as illegal hill cutting are performed (Islam, 2018). These actions cause instability of slopes. To stabilize the hills in existing conditions, before application of structural measures, the hill cutting needs to be controlled. A national hill management policy preparation is in process to ban on setting up brick kilns and reducing cutting hill for settlements

and other purposes. The illegal settlements need to be controlled too. In order to do this, the vulnerable people staying in these settlements need to be relocated.

2.11.3 Bioengineering Measures

Bioengineering measures (Islam and Arifuzzaman, 2010; Islam et al., 2013; Islam and Hossain, 2013; Islam et al., 2014; Islam et al., 2016; Islam et al., 2017; Islam et al., 2020) are sustainable and environment friendly for slope stabilization. Mostly applied hard solutions are both costly and are not sustainable. Now, these are being supplanted by vegetated composite soil-structure bodies. This process has come to be known as biotechnical slope protection. Biotechnical slope protection system consists of two parts. First one is biotechnical stabilization. In this process mechanical (structural) elements are used along with living elements to control erosion and slope failure. Here both the mechanical and biological elements work together to stabilize the slope. Another one can be called a subset of this biotechnical stabilization which is called soil bioengineering stabilization. Here the living elements e.g. roots, stems, branches etc. work as the reinforcement to increase the stability of the slope (Islam et al., 2016; Islam et al., 2017).

Though the stabilization of slope is studied by geotechnical engineers, the effectiveness of bioengineering measures largely depends on the characteristics of the vegetation which is better understood by plant scientists. As a result, this application needs collaborative knowledge exchange between plant scientists, hydrologists, foresters and geotechnical engineers.

2.12 Slope Stability Analysis

Slope stability has been a long-standing problem in geotechnical practice. It is an important and challenging issue of geotechnical engineering. Natural and landscape slopes may lose their stability. It may happen due to sliding of soil mass along a slip surface or detachment. When the shear stresses developed on a slope exceeds the shear strength of the slope its termed as failure of slope. The collapse may be developed due to excavation activities and rainfall infiltrating. So, it is an important parameter that which circumstances will make the slope unstable and the properties of soil related to this instability. The slope stability analysis consists determining the soil mechanical properties along with the shape and the position of the possible failure surface. For

analyzing the stability of slopes in situ site investigation and accurate laboratory tests of soil are needed.

The slope stability analysis can be divided into two major categories. One is the conventional method which includes the kinematic and limit equilibrium analysis. Another one is the numerical method which are preferred over the conventional ones. Numerical analysis includes, finite element, finite difference and boundary element which falls within continuum modeling which cannot be performed in the conventional method (Islam, 2018; Elahi, 2018; Elahi et al., 2018, Elahi et al., 2019). Numerical analysis also includes discontinuous modeling. However, the limitations of analysis methods should not be ignored.

2.12.1 Limit equilibrium method

Limit Equilibrium is widely used in geotechnical field and it follows some assumptions. Firstly, the soil behaves as a Mohr-Coulomb material. The Factor of Safety (FS) of the cohesive component of strength and the frictional component of strength are equal for all soils involved. Each block within the slip surface has the same factor of safety. Inter-slice forces are assumed; to deem the problem determinate (Griffiths and Lane, 1999; Cheng and Lau, 2014; Aryal, 2008). The limit equilibrium method utilizes the method of vertical slices, where the entire sliding mass is divided into a reasonable number of slices and the inter-slice forces are computed based on an assumed inter-slice force functional relationship (Aryal, 2008). Slip surfaces are assumed and the static equilibrium equations are used to calculate the stresses and factor of safety on each slice (Cheng and Lau, 2014).

For determination of stability of the slope the limit equilibrium method compares the resisting forces and the forces causing the failure. The equation of static equilibrium is applied throughout the safety calculation process. The static equilibrium conditions are:

- (i) Equilibrium of forces in the vertical direction,
- (ii) Equilibrium of forces in the horizontal direction, and
- (iii) Equilibrium of moments about any point (Duncan and Wright, 2005)

2.12.2 Finite element analysis

The Finite Element (FE) method involves transferring the slopes geometry and soils properties into a mesh with a finite number of elements and nodes. Approximations are made for the continuity of displacements, the stresses between elements and the connectivity of the elements through theoretical analysis and mathematical formulations namely finite difference technique (Huat and Mohammed, 2006) which involves differential equation which is transformed into matrix equation for each element. The main concepts in the FE modeling are:

- (i) Discretization of the region being analyzed into finite elements. These discrete elements are assumed to be interconnected only at the joints which are called nodes.
- (ii) The use of interpolating polynomials to describe the variation of a field variable within an element.

Each node again needs to satisfy the following equations and relations (Huat and Mohammed, 2006):

- (i) The equations of equilibrium
- (ii) The compatibility of displacements
- (iii) The material constitutive relationships

The basic idea of this method is replacing the continuum having an unlimited or infinite number of unknowns by a mathematical model which has a limited or finite number of unknowns at certain chosen discrete points called the "nodes".

The finite element analysis can provide a very good prediction of the behavior of soil structure interaction problems if the different construction stages and the material behavior are simulated correctly and accurately in the analysis (Janbu, 1957; Gupta et al., 2016)). With the advancement of technology there has been a large increase in the use of the FEM specifically in slope stability analysis. The FEM have the following benefits (Hammouri et al., 2008):

- (i) The analysis can run relatively quickly.
- (ii) The Finite Difference method is a simple approach.
- (iii) Able to monitor progressive failure of the soil up to and including the FS.

- (iv) Can accommodate a wide range of slope geometries and problems.
- (v) The failure occurs within the slope where the resisting forces are outweighed by the driving forces. That is no assumptions are required regarding the location and direction of the slip surface models.
- (vi) Can calculate deformation, stresses and pore pressures within the slope.

Many problems in soil mechanics are concerned with stress and deformations in the soil due to boundary and body, forces; therefore, the FEM is used for the evaluating of displacement, forces and strain or stress field starting from initial boundary force or displacement field (Maula and Zhang, 2011). Although many believe the FE and Finite Difference methods overcome the limit equilibrium method's deficiencies, it has its limitations, including:

- (i) Calculated factor of safety can be dependent of the relative conditions chosen.
- (ii) An inexperienced user may not be aware of meshing errors, boundary conditions or time restrictions involved in the analyses.
- (iii) The Finite Difference technique can run analysis slower than the Finite Element method, particularly for linear problems.
- (iv) The Finite Element and Finite Difference method are considered more complex compared to the Limit Equilibrium method.

2.13 Application of Vegetation in Soil Bioengineering

Vegetation has proven to be effective in increasing the stability of slopes. However, the nature of its root and mechanism of slope stability is quite complex. The architecture of roots varies between species which as a result varies the tensile strength of roots. However, the selection of correct vegetation is crucial. Deep rooted, woody vegetation provide stability against shallow mass failures. On the other hand, dense cover of grass or herbaceous vegetation provides protection against erosion (Truong et al., 2008).

Table 2.3 shows the general effects of the vegetation on slope stability (Truong et al., 2008). Vetiver is a promising plant which reduces the erosion and has contributed in mitigation of shallow landslides (Islam et al., 2017, Islam 2018, Islam et al., 2020). It is a perennial grass belonging to the poacca family. These species grow fast and in dense clumps.

The roots may grow up to 3-4 m in the first year (Truong et al., 1995) which helps to reinforce the soil and increases slope stability. In the context of Bangladesh, vetiver is the most appropriate vegetation for stabilization of hill slopes (Islam et al., 2014; Islam et al., 2017).

Table 2.3: General physical effects of vegetation on slope stability (Truong et al., 2008)

Physical Characteristics		Beneficial Effects
(i) Root aeration	(ii) Root distribution and morphology (iii) Root tensile strength (iv) Spacing, diameter and embedment of trees (v) Shear strength of soils	Root reinforcement, soil arching, buttressing, anchorage, arresting the roll of loose boulders
(i) Moisture content of soil		
(ii) Level of ground water, Pore pressure/soil suction		
(i) Net rainfall on slope		
(i) Manning's coefficient		
(i) Root area ration, distribution and morphology		Root wedging of near-surface rocks and boulders and uprooting in typhoon
(i) Mean weight of vegetation		Surcharging the slope by large (heavy) trees (sometimes beneficial depending on actual situations)
(i) Design wind speed for required return period	(ii) Mean mature tree height for groups of trees	Can tackle the wind loading

2.13.1 Application of vetiver in slope stability and its characteristics

The application of vetiver grass (*Vetiveria zizanoides*) has been studied by the World Bank for soil and water conservation in India in the 1980s. Important researches have been conducted since then and it has been understood in last 15 years that the field of

application of vetiver is very wide (Lavania, 2003). Due to its unique morphological, physiological and ecological characteristics, it can survive and adapt to wide range of climatic and soil conditions (Truong, 2002). Vetiver is being applied in erosion and sediment control of steep slopes around the world including Africa, Asia, Australia, Central and South America. Figure 2.14 shows the application of vetiver system along the slope of the Ho Chi Minh Highway in Vietnam which has been proved to be effective in protecting the slope (Xuan, 2014).

When planted in single rows vetiver plants will form a hedge which is very effective in slowing and spreading run off water, reducing soil erosion, conserving soil moisture and trapping sediment and farm chemicals on site. Although any hedges can do that, vetiver grass, due to its extraordinary and unique morphological and physiological characteristics, can do it better than all other systems tested (Truong et al., 2008). Moreover, because of its dense and massive root system underground, it offers better shear strength increase per unit fiber concentration in the soil than for tree roots. The clump diameter can be about 300 mm and the height can vary from 500 mm to 1500 mm (Voottipruex et al., 2008). The characteristics of vetiver are stated in Table 2.4. The maximum root lengths observed from various studies have been summarize in Table 2.53.



Figure 2.14: Vetiver system along Ho Chi Minh Highway, Vietnam (Source: Xuan, 2014)

Table 2.4: Physiological, morphological and ecological characteristics of vetiver (Truong et al., 1995; Truong, 2002; Truong et al., 2008)

Parameters		Characteristics
Growth	Morphological character	<ul style="list-style-type: none"> (i) Dense hedge is formed when planted close together (ii) New shoots develop from the underground crown making vetiver resistant to fire, frosts, traffic and heavy grazing pressure (iii) Does not have stolon and short rhizomes with a massive finely structured root system grows extremely fast, in some applications rooting depth can reach 3-4m in the first year.
	Physiological character	<ul style="list-style-type: none"> (i) Ability to regrow even after being affected by droughts, frosts and salinity (ii) Grow in soil with a pH range between 3.3 to 12.5 without providing any soil amendment (iii) Efficient in absorbing dissolved nutrients e.g. N and P (iv) Highly resistance to pests, diseases and fire (v) Intolerant to heavy shade and this reduces the growth greatly
Tolerance to climatic variation		<ul style="list-style-type: none"> (i) Adaptable to dry and tropical climate (ii) Tolerant to prolonged drought, flood, submergence (iii) Stiff and erect stems can stand up to relatively deep-water flow (iv) Grows rapidly under rainfall ranging from 300mm to 6000mm per annum
Tolerance to soil condition		<ul style="list-style-type: none"> (i) Highly tolerant of growing medium high in acidity, alkalinity, salinity, and magnesium
Tolerance to heavy metal		<ul style="list-style-type: none"> (i) Tolerant of As, Cd, Cr, Ni, Pb, Hg, Se and Zn in the soils; also absorbs Al and Mn (ii) Efficient in absorbing heavy metals in polluted water.

Other parameters e.g. shoot length, root diameter have also been studied and are shown in Table 2.6.

In case of the study of Arif (2017), the shoot length in sandy soil can be as high as 115 cm in 1 month, whereas for red clay (Parshi, 2015) the growth of shoot was only 19 cm. Also, due to different site location and their weather, variability in growth has been observed.

Table 2.5: Maximum root length of vetiver in different soil

Time (months)	Maximum Root Length (cm)	Soil Type	Reference
3	13.5	Dredged Sand	Islam et al., 2013, Islam et al., 2016, Islam et al., 2017, Islam, 2018
	18	Low Plastic Silt	
	96	Sand	
6	50	Clayey silt	
	25.4	Sandy Silt	
	21.5	Low Plastic Silt	
	16.5	Dredged Sand	
	11.5	Low Plastic Clay	
12	24.5	Low Plastic Silt	
	20	Dredged Sand	
	16	Low Plastic Clay	
13	50	Sandy Silt	

Table 2.6: Shoot length and root diameter of vetiver (Islam, 2018)

Time (months)	Maximum shoot length (cm)			Average root diameter (cm)
	Arif (2017)	Islam (2013)	Parshi (2015)	Arif (2017)
1	115	25	19	0.11
2	121	50	40	0.12
3	125	75	60	0.13
4	142	100	110	0.13

2.14 Soil Reinforcement by Roots

Roots physically reinforce soils, resist erosion, and increase infiltration of water into the soil. Roots form physical pathways (little tunnels) that help water infiltrate the soil. Deep, woody roots lock the soil layers together, and lateral roots connect many plants into an interlocking grid. Fine feeder roots form a network through the upper soil layer, preventing surface erosion. Groundcovers and grasses have relatively shallow roots and low biomass, so they prevent surface erosion only, and do not stabilize deep soil. Trees possess deeper roots than shrubs and are essential for slope plantings. Puget Sound bluff soils often feature porous sandy, gravelly soil overtopping dense, clayey glacial till. Rainfall saturates the upper soils and then seeps laterally over the glacial till, causing slides. Deep tree roots penetrate into the compacted layer and help tie the layers together, preventing slides. Tree roots occurring at the crest and toe of a slope help to prevent wasting in these susceptible areas where larger slides often start (Nasrin, 2013).

Most of the vegetation that are found in CHT are tress, herbs and shrub with branched tap root system. Some part of it is characterized as grassland (Das, 1990). However, most grass has fibrous roots which spread out from the underground part of the culms and hold the soil in a horizontal pattern. The roots that penetrate vertically into the soil are not deep. In contrast, the roots system of vetiver grass does not expand horizontally but penetrates vertically deep into the soil, whether it to be the main roots, secondary roots or fibrous roots (Chaipattana Foundation, 1996). Thus, these roots can reinforce shallow soil slopes.

2.14.1 Tensile strength of roots

For slope stability, the mechanical reinforcement provided by roots is the main factor. Rooted soil works as a matrix which has shear strength higher than the soil or the root separately. This is because the roots are strong in tension and weak in compression whereas, the soil is weak in tension and strong in compression (Voottipreux et al., 2008).

Vetiver has tensile strength between 40-180 MPa for ranges of root diameter 0.2-2.2mm (Truong, 2004). The tensile strength T_R can be obtained from Equation 2.1.

$$T_R = \frac{F_{max}}{\frac{\pi D^2}{4}} \quad (2.1)$$

Here, F_{max} is the maximum force (N) required to cause tensile failure and D is the average root diameter (mm). T_R is inversely related to root diameter. Figure 2.15 shows the correlation between root diameter and tensile strength obtained by different researchers. Voottipreux et al., (2008) found a relation between root diameter and tensile strength for vetiver grass for diameters ranging from 0.2mm-1.3mm as shown in Equation 2.2. Teerawattanasuk et al., (2014) found a similar equation for diameters ranging between 0.25mm-2.9mm as shown in Equation 2.3. Again, Islam and Badhon (2020) found a relation where $T_R = 18.878 * D^{-1.12}$ which has a R^2 value of 0.614.

$$T_R = 16.95 \cdot D^{-0.60} \quad (2.2)$$

$$T_R = 15.239 \cdot D^{-0.893} \quad (2.3)$$

Equation 2.2 has a R^2 value of 0.755 and Equation 2.3 has a R^2 value of 0.806. As Equation 2.3 has a better correlation value and is obtained for a wider range of diameters we have used this in this study.

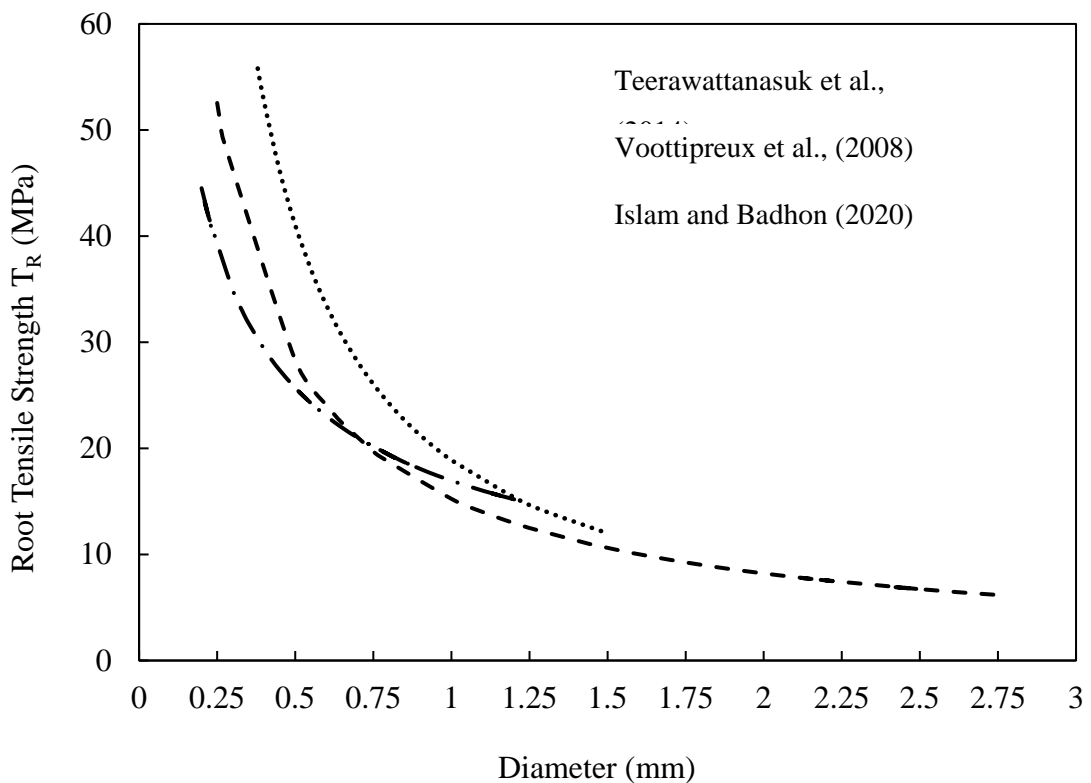


Figure 2.15: Relation between tensile strength and diameter of vetiver grass root

2.14.2 Root area ratio and shear strength of roots

As roots are included in the soil, they bind the soil mass together and thus increases the shear strength. The contribution of roots to the shear strength is considered to have the characteristics of added cohesion or adhesion (Wu et al., 1979). Root cohesion proportionately increases the soil-root shear strength.

Root area ratio (RAR) or biomass concentration is another factor which effects the root contribution to soil strength. According to Gray and Leiser (1982), RAR is defined as the fraction of the soil cross-sectional area occupied by roots per unit area. RAR can also be determined based on Root Length Density and root diameter. For grasses, RAR at different soil depth classes (every 0.10 m), can be calculated using the following Equation 2.4 (De Baets et al., 2008).

$$RAR = \frac{\frac{RL}{P} a_i}{A} \quad (2.4)$$

Here RL is the total length of roots per class of soil depth (m); a_i is the mean cross-sectional area of the root section of a representative plant (m^2); P is the class of soil depth used (0.10 m); and A is the reference area (m^2), calculated by the vertical projection of the plant's aerial biomass.

From the study of Machado et al., (2015) it was found that, the density of vetiver roots decreases of an average by 82.76% between 0-0.1m to 0.4-0.5m. It also shows that RAR has a strong negative correlation with depth. A best fit regression analysis was conducted which yields a R^2 value of 0.9717. The plot of RAR vs Depth (m) is shown in Figure 2.16. The maximum RAR for various grasses were found near the top and becomes less than 0.5% at a depth of 0.5m (De Baets et al., 2008). The mean percentage of RAR for vetiver grass was found to be 1.66% for the 0-0.10 m layer (Machado et al., 2015). This is quite high when compared to other grasses. This can be accounted due to extremely dense and fibrous root system of vetiver grass. The RAR up to a depth of 0.5m was obtained using this relationship for this study.

2.14.3 Root behavior modeling

The effect of roots on soil fixation has been reported by several authors. From a mechanical point, rooted soil behavior can be simulated by using different root

reinforcement models. Some of them are based on traditional limit equilibrium approaches (Greenwood, 2006), other are based on more advanced numerical analysis (Bourrier et al., 2013).

The most common mechanical root reinforcement models are the perpendicular and inclined root reinforcement model (Wu et al., 1979), the fiber bundle model (Pollen and Simon, 2005; Schwarz et al., 2010) the energy approach model (Ekanayake et al., 1997) and a number of limit equilibrium, finite element and finite difference numerical methods integrating the above models (Briggs, 2010; Mickovski et al., 2011; Bourrier et al., 2013). All the approaches consider a composite material comprising soil matrix and roots and, therefore, must include two different mechanical behaviors in the analysis. Although attempts have been made in the past to account for this (Lin et al., 2010; Bourrier et al., 2013), the modelled root system and soil properties were either assumed or simplified to suit the particular model, otherwise it was difficult to apply those in practical scenarios.

Among the various models, the model of Wu et al., (1979) allows for simple and quick calculation of soil reinforcement by roots using tensile strength and root distribution information. It assumes that the roots are oriented perpendicular to the shear plane and tension is transferred to the roots when the soil is sheared. The increased shear strength in the form of added cohesion can be stated as Equation 2.5.

$$s = c_s + c_r \quad (2.5)$$

Here, s is soil shear strength (kPa), c_s (kPa) is the shear strength of the soil reinforced by roots and c_r (kPa) is the increase in shear strength due to the presence of roots. When shear forces occur, the root fiber deforms. The tension developed in the roots is resolved with a tangential component resisting shear and a normal component increasing the confining pressure on the shear plane. The most critical assumption of this model implies that all roots attain ultimate tensile strength simultaneously during soil shearing (Simon et al., 2006). The predicted shear strength increase from a full mobilization of root tensile strength is given by:

$$c_r = t_r (\cos \theta \tan \phi' + \sin \alpha) \quad (2.6)$$

Here θ is the angle of shear distortion in the shear zone, ϕ' is the soil friction angle ($^\circ$) and t_r is the total mobilized tensile stress of root fibers per unit area of soil. Figure 2.17

shows the mechanism of soil reinforcement by roots where X is the deformation of roots with respect to the vertical line (Gray and Lieser, 1982). Wu et al., (1979) found that the value of the bracket term is relatively insensitive to normal variation in θ and ϕ ($40\text{--}90^\circ$ and $25\text{--}40^\circ$ respectively) with values ranging from 1.0 to 1.3. In most studies this term is set to an average value of 1.2. So now, for the added cohesion, tensile strength and the fraction of soil cross-section occupied by the roots e.g. RAR is needed (Gray and Barker, 2004). The effect of reinforcement can be modeled in the numerical simulation by addition of this extra cohesion to the soil properties. On the other hand, the roots can also be modeled as beam elements. In both cases the roots increase the shear strength of the soil (Islam et al., 2010; Islam and Hossain, 2013).

2.15 Effect of Vegetation on Erosion Reduction

2.15.1 Mechanism of soil erosion

Soil erosion is a natural phenomenon which is a twofold process. It includes particle detachment and its transportation. Erosion is caused by drag or tractive forces which are the function of velocity, discharge, shape of particles and roughness of particles. On the other hand, erosion is resisted by inertial, friction and cohesive forces which are the function of basic soil properties, soil structure and physicochemical interactions (Islam, 2018).

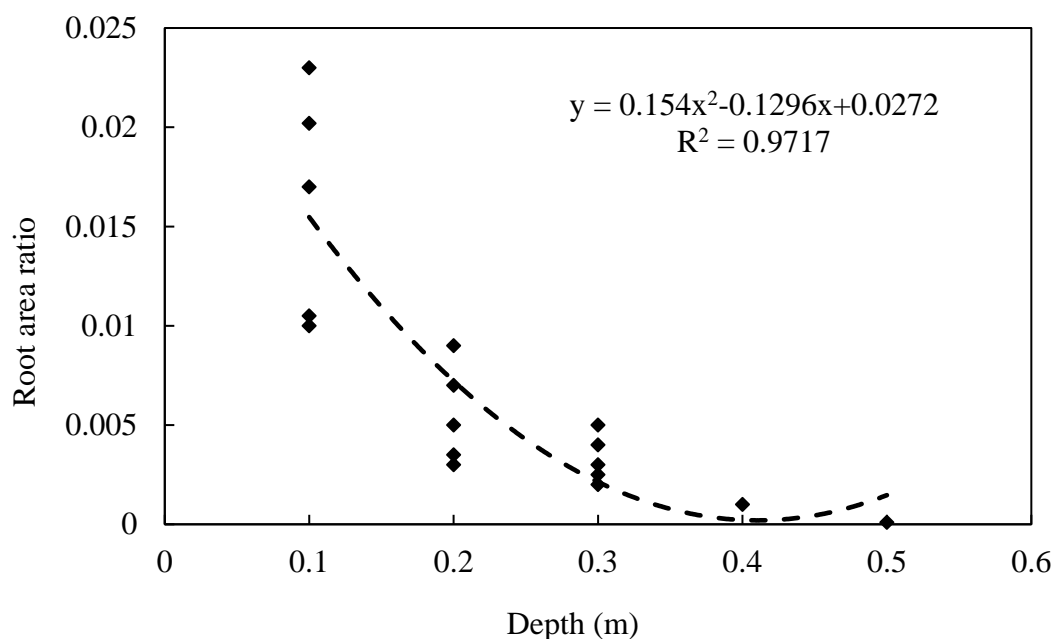
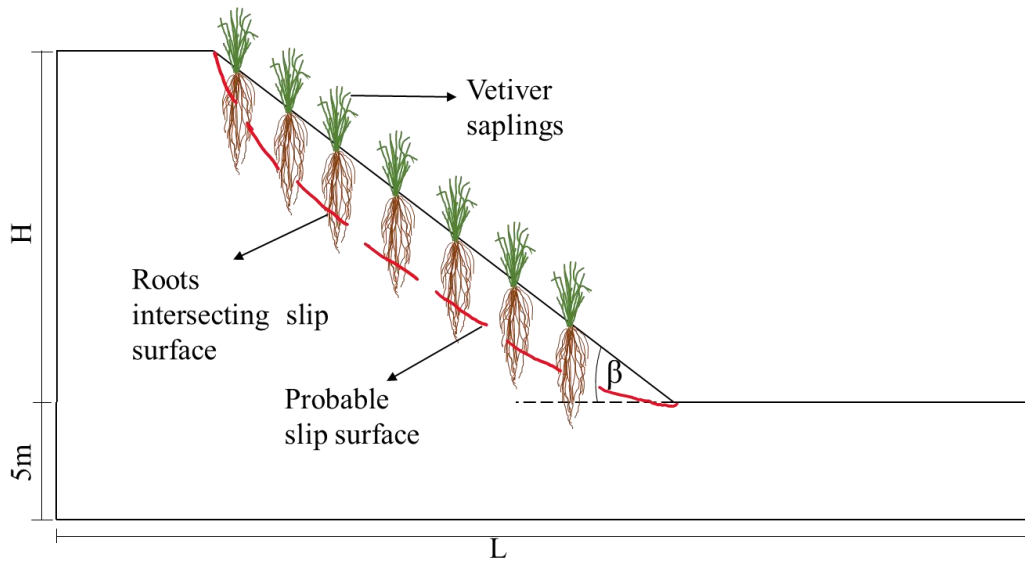
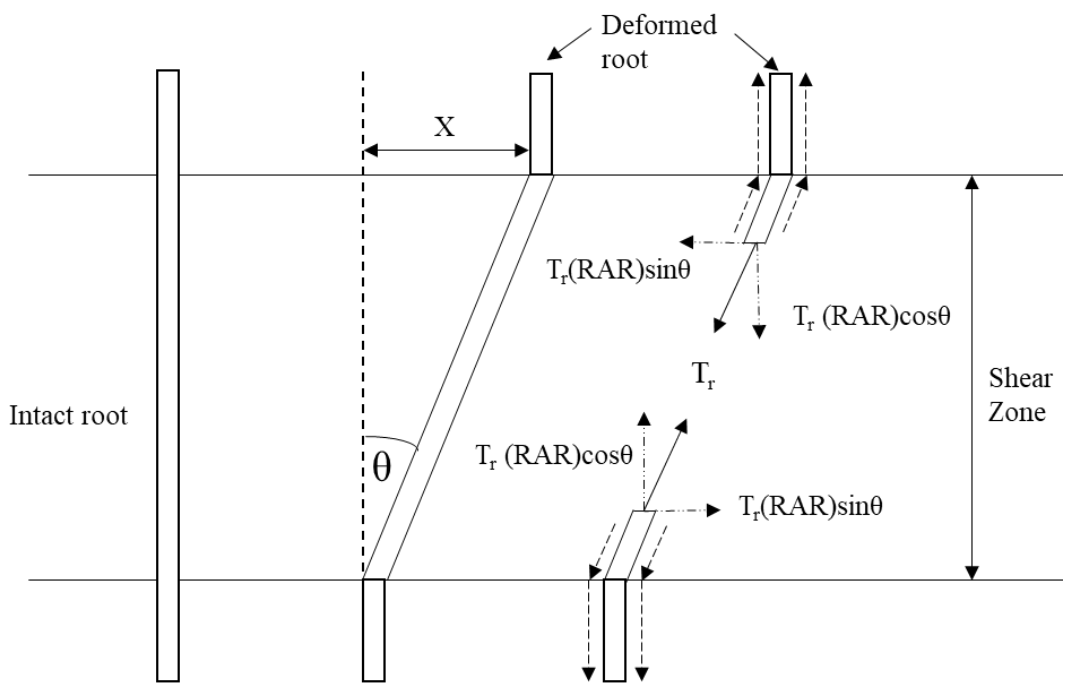


Figure 2.16: Relationship between root area ratio and depth of soil layer (Reproduced from Machado et al., 2015)



(a)



(b)

Figure 2.17: (a) Schematic diagram of soil reinforcement by root; (b) Root reinforcement model (Reproduced from Gray and Lieser, 1982)

2.15.2 Agents of soil erosion

Erosion is caused mainly by two agents: (i) rainfall and (ii) wind. The extent of erosion by rainfall is dependent upon soil type, climate, topography and vegetative cover. The

intensity and duration of rainfall play vital role in soil erosion. On the other hand, only relatively dry soils are susceptible to wind erosion.

While considering the erosion triggered by rainfall, the mechanism involves two steps. As the raindrops hit the soil particles, their bond strength becomes weak and thus they become vulnerable to detachment. When the rainfall continues over a long period and the intensity exceeds the infiltration capacity of soil, runoff starts. The loosened soil mass is then subjected to an additional hydraulic push induced by the surface runoff. The runoff carries the soil downwards and induces a failure surface (Nasrin, 2013; Nasin and Islam, 2018).

2.15.3 Estimation of soil erodibility

Various models have been developed and used for determination of the eroded soil amount as well as erodibility of soil. However, the dominant model applied worldwide to soil loss prediction is the Universal Soil Loss Equation (USLE), because of its convenience in application (Prasannakumar et al., 2012). This equation as shown in Equation 2.7 is a function of five input factors: rainfall erosivity; soil erodibility; slope length and steepness; cover management; and support practice (Goldman et al., 1986). These factors vary over space and time and depend on other input variables.

$$A = R \times K \times LS \times C \times P \quad (2.7)$$

Here R is the rainfall erosion index ($\text{MJ mm ha}^{-1} \text{h}^{-1} \text{y}^{-1}$), K is the soil erodibility factor ($\text{t ha h ha}^{-1} \text{MJ}^{-1} \text{mm}^{-1}$), LS is the slope length and steepness factor (dimensionless), C is vegetative cover factor (dimensionless) and P is the erosion control practice factor (dimensionless).

2.15.4 Reduction of soil erosion

To protect the soil from eroding the following need to be ensured (Nasrin, 2013):

- (i) The velocity of the water flowing over the surface needs to be reduced so that the drag or tractive forces working on the soil is reduced
- (ii) The soil needs to be protected or reinforced by suitable cover or the bond strength between soil particles needs to be increased so that they may resist erosion.

Topsoil erosion of natural slopes become more vulnerable in bare soil where top surface is not covered with significant vegetation since vegetation acts as a natural reinforcement of soil. The vegetation, if planted on contours, forms a protective barrier across the slope. This reduces the impact energy of the rainfall. Thus, the soil detachment is reduced. Again, it slows the runoff water as it impedes the downward flow. So, the vegetative cover effectively performs both the tasks which are needed to protect the soil erosion. Ideally, species to be used as barrier for erosion and sediment control should have the following characteristics (Smith and Srivastava 1989):

- (i) Form an erect, stiff and uniformly dense hedge so it can offer high resistance to overland water flow and have extensive and deep roots, which bind soil to prevent riling and scouring near the barrier.
- (ii) Ability to survive moisture and nutrient stress and to re-establish top growth quickly after rain.

Vetiver has dense root system that binds the soil particles together up to a depth of 3m and also reduces erosion (Nasrin and Islam, 2018). The runoff carrying sediments gets slowed down when crossing this hedge. This root system filters the runoff and the sediment free runoff continues to flow downward in a reduced speed (Carlin et al., 2003). The sediments get deposited and a terrace is formed which continues to conserve the eroded soil.

Soil erosion can also be controlled with the use of Jute Geotextile (JGT) which can reduce erosion up to 10 ton per hector per year. A study conducted by Molla (2014) evaluates the performance of JGT for soil erosion control. It was found that soil loss for 500 gram per square meter (gsm) jute mat is higher than for 700 gsm jute mat. For both JGT, soil loss decreases significantly compared to the controlled bare slope. JGT is hygroscopic in nature due to the intrinsic properties of jute fiber and its flexibility increases due to absorption of water. JGT creates a moist environment around the soil surface which is conducive to rapid growth of vegetation. So, use of both Jute Geotextile and vegetation together can reduce the erosion effectively.

2.16 Soil Nailing for Slope Stability

Soil nailing is an in-situ soil reinforcement technique used for enhancing the stability of slopes, retaining walls and excavations. The technique involves installation of

closely spaced, relatively slender structural elements, i.e., soil nails, into the ground to stabilize the soil mass (Babu and Singh, 2009). The technique of soil nailing has been increasing in popularity because it offers cost-effective retaining system for a variety of ground conditions such as the side slopes of canals, temporary vertical cuts for constructing basements, and permanent excavation near roads. In analyzing the effect of nailing on slope stabilization Jayanandan (2015) found that lateral deformation is reduced by about 41% and factor of safety increases almost 1.2 times than that of slope without nailing.

The basic concept of nailing relies upon the transfer of resisting tensile forces generated in the nails into the ground through friction or adhesion mobilized at the interfaces. As the ground exerts the driving forces, i.e. lateral earth pressure, on the wall or weight of a potentially sliding soil mass, so it provides the nail bond resistance. This friction interaction between the ground and the nail restrains the ground movement (Fan and Luo, 2008).

Several numerical studies related to soil nailing and its effect on slope stability has been performed previously. Apart from the overall stability analysis of slopes, many research works have been carried out to find out the effect of different nail parameters like length, diameter and spacing in stabilizing the slopes. Researchers have also verified the result obtained from FEM with LEM and real field data and found quite satisfactory results (Hammouri et al., 2008; Tschuchnigg et al., 2015; Neves et al., 2016; Chakrabarti et al., 2017).

2.16.1 Elements of soil nailing

Basically, four elements are essential in soil nailing (Fan and Luo, 2008; Samiezadeh et al., 2014; Elahi, 2018):

- a) Nails: It is mainly composed of steel which are the reinforcing bars. At first holes are drilled and the nails are inserted into the holes. The nails are placed by maintaining a horizontal and vertical spacing. Tensile stress is applied passively to the nails, in response to the deformation of the retaining materials. After then the holes are filled with grout.
- b) Grout: When the holes are drilled before placing the nails, these holes are filled with grout. Grout is a mixture of neat cement and they are placed after placing

the nails. It transfers the stresses from the ground to the nails. It also serves as a protective cover for nails. The grout strength is an important factor and usually a 28-day unconfined compressive strength of 21 MPa is specified for grout.

- c) Nail head: A soil-nail head typically comprises a reinforced concrete pad, a steel bearing plate and nuts. Its primary function is to provide a reaction for individual nails to mobilize tensile forces.
- d) Sloping face: Slope facing can be soft or hard. It provides the slope with surface protection. Soft facings such as vegetation cover are usually non-structural, whereas hard and flexible facings e.g. sprayed concrete, reinforced concrete and stone pitching, can be either structural or non-structural. A structural slope facing can enhance the stability of a soil-nailed system by the transfer of loads from the free surface in between the soil-nail heads to the soil nails and redistribution of forces between soil nails.

2.16.2 Effect of different nail parameters on slope stability

Different nail characteristics, such as length, diameter, inclination etc. influence the slope stability and the factor of safety of soil mass.

2.16.2.1 Nail length

The nail lengths situated in the lower one-third of the slope is more important for slope stability (Fan and Luo, 2008). From the study of Tang and Jiang (2015) it has been found that nail lengths have effect on factor of safety and the increase of factor of safety becomes slow when the length of the nails become same as the height of the slope. Gunawan et al., (2017) in their study related length and diameter ratio of nail with FS for 20m height of sand slope for different angle of friction, ϕ and slope angle, β and found that with the increase of length of nail, factor of safety increases. However, longer nails need larger movement to mobilize the full capacity of the soil nails than the shorter one. This results in large deformations are generated when the ground is comprised of loose material or disturbance is created during drilling. So, nails longer than 20m need to be used carefully. Length of nail has also significant effect for deep seated slip surface and has less effect with shallow slip surface (Alsubal et al., 2017).

2.16.2.2 Diameter of nail

Usually nails with diameter of 25 mm, 32 mm and 40 mm are used which are made of high yielding deformed steel bars (Tang and Jing, 2015). For a slope made of sand with a height of 20 m, different angle of friction and different slope angle, it has been observed that with the increase in diameter the factor of safety increases (Gunawan et al., 2017). Nails with smaller diameters should be used with caution, especially when the nail length is long, as these generate excessive bending during installation.

2.16.2.3 Nail spacing

The soil nails need to be placed at optimum spacing to ensure reinforcement. If they are placed far apart then the grout and the nails will not work as an integral unit. Tang and Jiang (2015) also found that with the increase of soil nail spacing factor of safety gradually decreases. Horizontal rows of soil nails should be staggered to improve the integral action between the soil nails and the ground. Whereas, it has been suggested that if the number of nails are kept unchanged, the vertical spacing of nails are not too significant (Fan and Luo, 2008). Again, placing the nails too close will cause difficulty in nail insertion and will not be cost effective. Soil nails are commonly installed at a spacing of 1.5 m to 2.0 m (Neves et al., 2016).

2.16.2.4 Nail inclination

For practical purposes, the inclination of nails in a construction is kept uniform. As the grouting is done under low pressure or the action of gravity, to facilitate proper grouting, the nails are inserted downward with inclination angle varying between 5° to 20° . Theoretically, if the nails are aligned with the direction of maximum tensile strain of the soil, its effect will be maximized. According to Tang and Jiang (2015), highest factor of safety was found when inclination of nail was 15° with the horizontal.

2.16.2.5 Grout and soil properties

The mobilized shear strength, e.g. the bond strength of grout is important for slope stability. It is affected by the soil condition surrounding the nail and the grouting process along with nail increment.

For drilled and grouted nails in cohesion less soil, the magnitude of the overburden pressure and the nature of the granular soil affect the soil friction angle, which in turn affects the bond strength. Nailing is not effective in soft clays as it is difficult to

establish good bond strength (Cheng et al., 2013). Effectiveness of nailing varies with soil properties. Impact of nailing is huge for the soils with higher angle of friction. With the increase of angle of friction factor of safety increases.

2.17 Summary

Landslide has been addressed as a major problem in CHT. The topographic features and geology of Chattogram City, effect of the increased intensity of rainfall and high urban growth have been studied by many and the studies show that the features compound the landslide risks. However, the studies previously conducted in Chattogram region focuses mainly on the planning aspects, causes of the landslide and landslide mapping. Even though the literature establishes the fact that the vegetation is effective in reducing the erosion and increasing the slope stability, the growth of vegetation in Chattogram and the effect of nutrient contents of soil on this growth has been studied in an extremely limited extent. To address this and promote the application of sustainable solution, this study particularly focuses on the application of vegetation e.g. *Vetiveria zizanioides* in increasing the slope stability of selected hills of Chattogram city. It also aims to quantify the soil erosion under similar rainfall conditions which prevail during the landslides in CHT by model study.

Finite element analysis for slope stability by using a sustainable solution as vetiver, has been done on a limited scale. Previously Elahi et al., (2019) and Islam et al., (2020) have studied the effect of varying root depth of vetiver in four different slope angles, nonetheless, no attempt has been made to investigate the slope angle at which the natural hills can be safe and which spatial distribution will yield the maximum safety. Again, the variation of threshold angles, along with varying slope geometry e.g. natural slope and terraced slope, for achieving safety by use of vetiver needs to be investigated. This study aims to find a suitable and applicable slope geometry to maximize the effect of vegetation by looking at the relation of slope angle, slope height and root zone depth of vetiver with factor of safety (FS). Also a comparative study with hard solutions, e.g. soil nailing, will reveal the difference between the efficiency of vetiver and the conventional solution. This experimental along with the numerical study will pave a way to think about the protection measures that can be taken by the development authorities of Chattogram and other urban built up hilly areas to reduce the risk of landslides.

CHAPTER 3

EXPERIMENTAL PROGRAM

3.1 Introduction

Research has been conducted on landslides and techniques for its remediation. However, there are few studies regarding the sustainable remedial measures of rainfall induced landslides, especially in the context of the hilly terrain of Bangladesh. This chapter discusses the experimental setup for the model study and describes the process of numerical modeling and analysis.

3.2 Soil Sample Collection

Two soil samples were collected from two hills of Chattogram locally known as Tiger Pass Hill (Latitude 22°20'38.1" N, Longitude 91° 49'00.6" E) and Berma Haji Hill (Latitude 22°21'30.8" N, Longitude 91°49'10.6" E). These are denoted as S-1 and S-2 throughout this study. Both the hills are located within the boundary of Chattogram City Corporation Area. It was not possible to collect the samples from different depth due to physical limitations faced in hills. Thus, only disturbed samples from the top layer were collected.

Figure 3.1 shows the location of Chattogram along with the location of the two hills from where samples have been collected. Figure 3.2 shows the natural condition of these hills.

3.3 Determination of Soil Properties

The collected samples were tested in the Geotechnical Engineering Laboratory of Department of Civil Engineering, Bangladesh University of Engineering and Technology. Table 3.1 shows the summary of the performed tests. Along with these, the nutrient contents were also tested from Soil Resource Development Institute (SRDI).

3.3.1 Sieve analysis and hydrometer analysis of soil

The distribution of different grain sizes effect the engineering properties of the soil. Sieve analysis was done to determine the gradation of the soil samples. Following

ASTM D422, the oven dried sample was first passed through #200 sieve. The retained soil was oven dried and sieved for ten minutes using a mechanical sieve shaker. The retained weight of soil in each sieve was measured and gradation curve was obtained.

For S-1, as greater percentage of soil (more than 12%) passed through #200 sieve, hydrometer analysis was done. 50gm of soil passing #200 sieve was mixed with the solution of dispersing agent and water. Readings were taken at 2, 4, 8, 15, 30 minutes; 1, 2, 4, 8 hours and 1, 2, 3, 4 days from the starting of the test. Combining the results of sieve analysis and hydrometer analysis, the combined gradation curve for S-1 has been obtained.

3.3.2 Field density test

To determine the in-situ and dry density of the soil, field density test following ASTM D1556 (sand cone method) was performed in Tiger Pass and Berma Haji hill. Two tests were performed at each hill site. The ground was first made leveled and a metal frame was placed. A 15 cm deep hole was dug, and the removed soil was weighed. The hole was later filled with the Ottawa sand and its weight was measured. The natural moisture content (ω_n) of the soil samples was determined from this test. Following the formula $\gamma_{\text{insitu}} = \gamma_{\text{dry}}(1 + \omega)$, dry density of soil was determined. Again, the in-situ void ratio was determined using the formula $e = \frac{G_s \gamma_w}{\gamma_{\text{dry}}} - 1$.

3.3.3 Direct shear test

In the laboratory, direct shear test under consolidated drained condition was performed following ASTM D3080. Reconstituted samples were prepared keeping the moisture content of the soil close to the natural one. The test was performed under the normal stresses (σ') of 93 kPa, 186 kPa and 372 kPa. From the graph of shear stress (kPa) and shear displacement (mm) peak shear stresses for each normal stress was determined. These peak values were plotted against normal stresses and a straight-line approximation of the Mohr-Coulomb failure envelope curve was drawn.

3.3.4 Permeability test

Permeability is an important property of soil that determines how easily water can flow through the soil volume. To determine the coefficient of vertical permeability, Falling

head permeability test following ASTM D5084 was performed. Over dried soil sample was placed in the lower chamber of the permeameter. A tamping rod was used to compact the soil in three layers. The sample length was measured, and the top of the chamber was secured with screws. The sample was made saturated by letting water flow through the prepared sample. Then the elapsed time, for fall of head of 50 cm, was recorded for three times. The same procedure was repeated for two other densities of soil and thus coefficient of vertical permeability was determined.

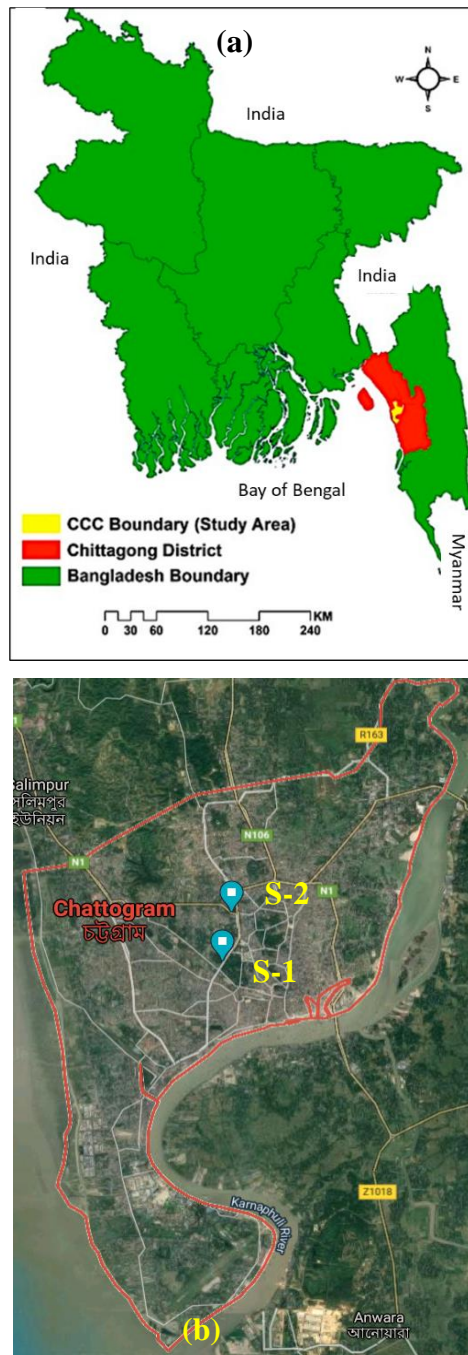


Figure 3.1: (a) Location of Chattogram District; (b) Location of soil sample collection

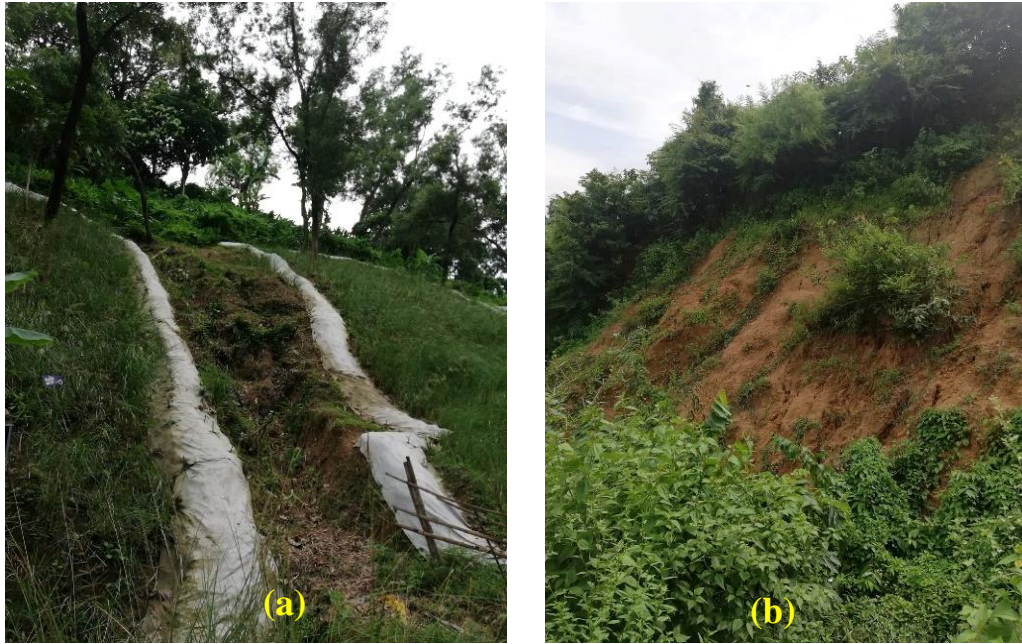


Figure 3.2: Natural condition of hills (a) Tiger Pass hill; (b) Berma Haji hill

Table 3.1: Summary of the performed laboratory and field tests

Properties	Test Name	ASTM Reference	Sample ID on which tests were performed	Determined Parameters
Index Properties	Sieve Analysis	ASTM D422	S-1, S-2	Gradation curve, Coefficient of curvature, Coefficient of uniformity
	Hydrometer Analysis		S-1	
	Natural Moisture Content	ASTM D2974	S-1, S-2	Natural moisture content
	Specific Gravity	ASTM D854	S-1, S-2	Specific gravity
Physical Property	Field Density Test	ASTM D1556	S-1, S-2	In-situ density and dry density
Engineering Properties	Direct Shear Test (CD)	ASTM D3080	S-1, S-2	Effective shear strength parameters (c' and ϕ')
	Falling Head Permeability Test	ASTM D5084	S-1, S-2	Coefficient of vertical permeability (k)

3.4 Experimental Setup for Model Study

The erosion potential of bare soil and vegetated soils have been studied in this research. The study at the field level is extensive and difficult to conduct. Hence, we prepared small scale models to study the effect of vegetation in reducing the erosion of the hilly soil of Chattogram during rainfall and thus reduce vulnerabilities to landslide.

3.4.1 Small scale glass model preparation

Trapezoidal glass models were prepared to represent typical slope of Chattogram hill tracts. With this we have studied the erosion potential of the hills of CHT. These models were prepared following the dimensions which were used by Islam (2018). By examining the slope angles from the hill contours, collected from Chattogram City Corporation, as shown in Figure 3.3, it has been found that at some parts, the slope is as steep as 50° and at others it is as mild as 20° . Again, parts with slope angles ranging between 36° - 40° are also observed. In the models the slope was maintained as 1V:1.33H which yields a slope angle of 37° . This lies in between the aforementioned range and thus the model represented the field condition to some extent. The length, width and height of the glass models was 900 mm, 600 mm and 600 mm respectively. The scaling factor was 1:15. Circular holes with a diameter of 2.54cm were created at the base of the glass models so that the infiltrated water did not get stagnant at the bottom of the model. A schematic diagram of the glass model is shown in Figure 3.4.

3.4.2 Soil placement in the models

The S-1 soil was very stiff in dry condition and it was difficult to place the soil into the model and achieve a similar density to the in-situ one. So, for S-1, at first the collected soil samples were made uniform by using a hammer. A 15 cm sand bed was made to be the base for the models. It was done in order to accelerate the infiltration from the model to the soil. Before the models were placed, the sand bed was made even. The in-situ density was known though performing in-situ field density test. We tried to place the soil samples maintaining a uniform density. As the density obtained by us and Islam (2018) was close, we followed the method suggested by them. We placed a certain weight of soil and compacted it in every layer of 7.5 cm by using a hammer of 2.5 kg where the drop height was 304.8 mm

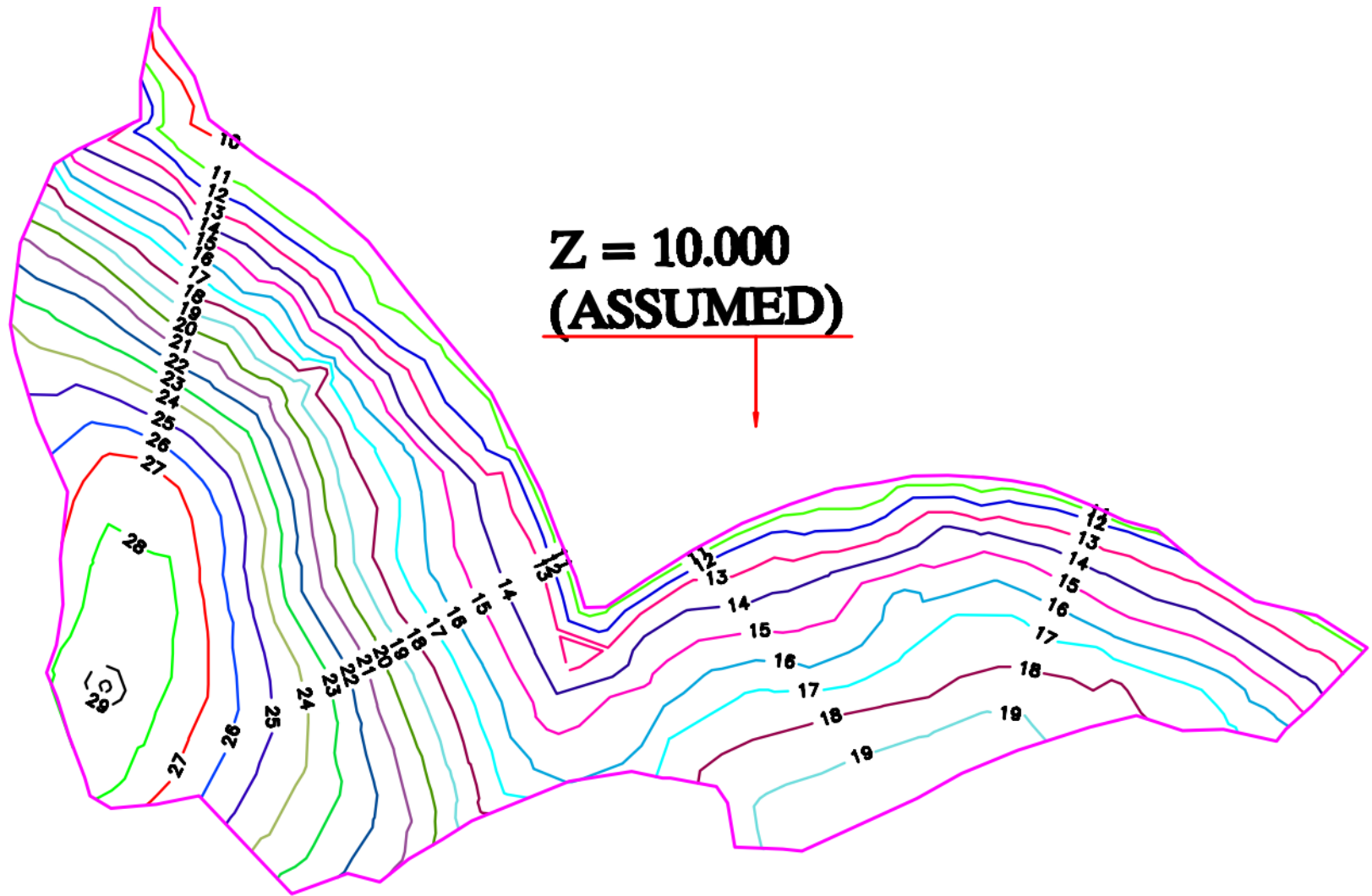


Figure 3.3: Contour map of Bangabandhu hill of Chattogram (Source: Chattogram City Corporation)

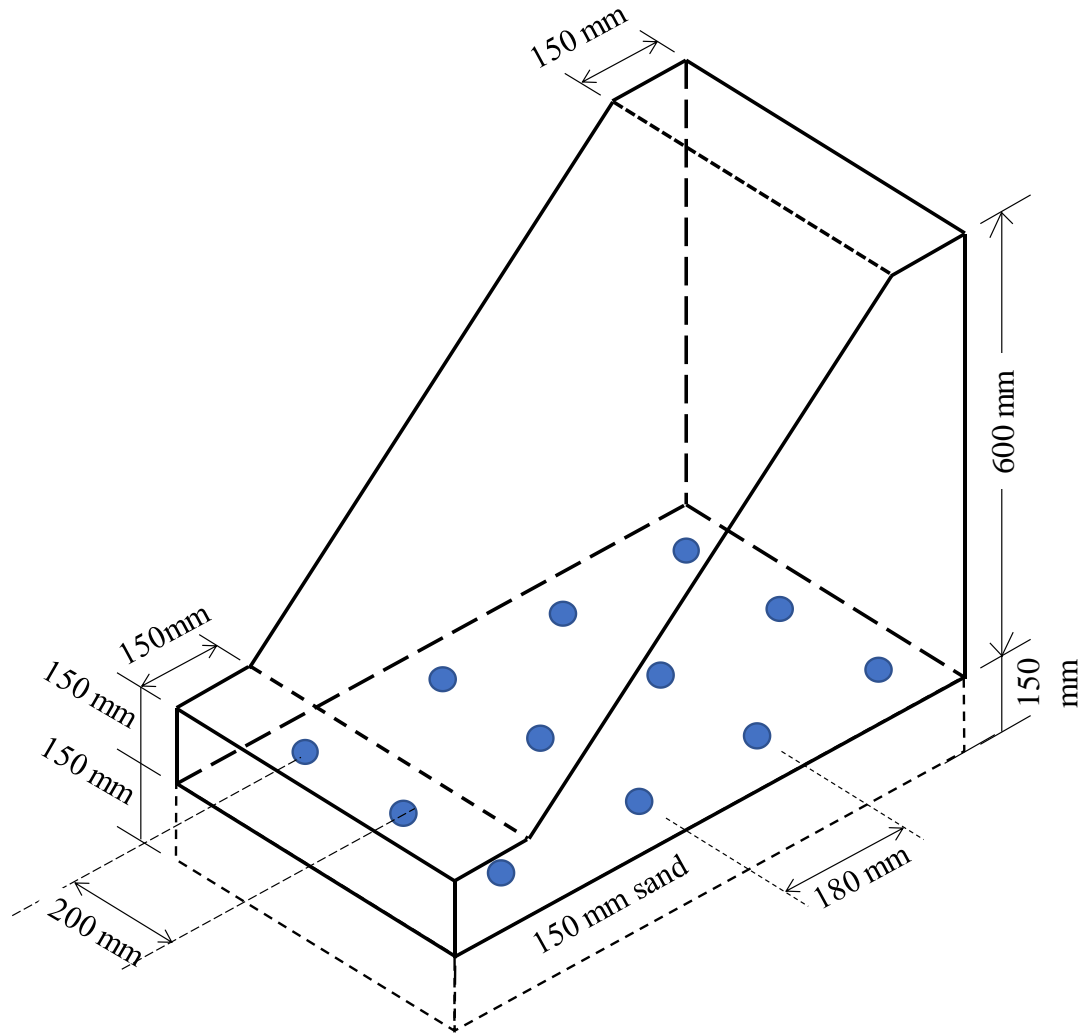


Figure 3.4: Schematic diagram of glass model

3.4.3 Types of models

Total six models were prepared with variations in soil type, vegetation plantation pattern and number of tillers per point. Models were prepared using two types of sample as discussed earlier. To prepare the models, at first the models were leveled by using a spirit level. Then soil was placed into the models as stated in Article 3.4.2. After soil placement, vetiver plantation was done in five models among the six models. The initial shoot length of the vetiver samplings was 20 cm and the diameter of the clump was 1.30 cm. No plantation was done in M-6 to measure the erosion of bare soil during rainfall. In M-5, vetiver plantation was done after placing a sheet of Geo-jute of 500 gsm above the top layer. Table 3.2 shows the summary of the models along with the varying features. Figure 3.5 shows the steps of model preparation. All the models were prepared on November 18, 2018. Before conducting the experiment and

exposing the models to artificial rainfall the models were nurtured for one year. The vegetation was regularly watered. Their growth was recorded after 12 months of plantation, after performing the tests though artificially simulated rainfall. During this time they went through a complete weather cycle consisting of summer, rainy season and winter.

Table 3.2: Summary of all six models

Model No.	Soil Type	Spacing between two tiller plantation point (cm)	No. of tillers per point	Layout of vetiver plantation (Row × Column)	Plantation pattern and other features
M-1	S-1	15	3	5×4	Vetiver grass was planted in square pattern
M-2	S-2	15	3	5×4	Vetiver grass was planted in square pattern
M-3	S-1	23	3	4×3	Vetiver grass was planted in square pattern
M-4	S-1	15	5	5×4	Vetiver grass was planted in square pattern
M-5	S-1	15	3	5×4	Vetiver grass was planted in square pattern along with single layer of Geo-jute
M-6	S-1	-----	-----	-----	No vetiver grass was planted



(a)



(b)



(c)



(d)

Figure 3.5: (a) Bare model after soil placement; (b) Vetiver grass with three tillers; (c) Initial root condition of vetiver grass; (d) Model-2 after plantation of vetiver

3.4.4 Artificial rainfall simulator

Artificial rainfall was simulated by using a perforated steel tray rainfall simulator. This test aimed to quantify the rainfall induced erosion. The rainfall simulator was designed by Chowdhury et al., (2017). A rectangular tray made of mild steel was used to make the simulator. It has an area of 1.11 m^2 ($1.22\text{m} \times 0.91\text{m}$).

As it can simulate rainfall on an area of 1.11 m^2 which is equal to the projected area of the prepared glass models, it was used in this study. Due to having the same projected area, most of the rainfall generated by the simulator fell directly above the glass models and minimum water loss was ensured. Figure 3.6 shows the schematic diagram of the rainfall simulator tray and Figure 3.7 shows the perforated steel tray which was used as the rainfall simulator. It has an empty space of 0.152m in all side for accidental purposes. A 50 mm high boundary was used on all sides to maintain a constant depth of water on the tray. The rainfall simulator works on a pipe based water supply. 2 mm pore opening was used in the tray having a center to center spacing of 25 mm.

On a rectangular grid of $1.07 \text{ m} \times 0.762 \text{ m}$, 1305 pore openings were created using a hand drill machine having 2 mm drills. In both the inner and outer side of the tray, equal pore diameter was maintained. When the fall height was kept as 3.0 m from ground, the simulator performs satisfactorily in terms of rain drop size distribution (D_{50}), spatial variability (according to Christiansen's Uniformity Coefficient), drop velocity rainfall accumulation rate (Chowdhury et al., 2017). Drop size distribution was estimated using Flour Pellet Method (Miguntanna, 2009; Egodawatta, 2007; Navas et. al. 1990; Clarke and Walsh, 2007; Bentley, 1904). The mean diameter of the rain drops (D_{50}) is 4.18 mm which is greater than that of D_{50} of natural rainfall (3.25 mm). This is on the conservative side because the greater the drop size of the rainfall, the greater the velocity gain due to gravitational force (Laws and Parsons, 1943) which causes comparatively more erosion. Being at a height of 3m from the ground, the rain drops attain 46.67% terminal velocity of the natural rainfall.

3.4.5 Calibration of rainfall simulator

The rainfall simulator which has been described in Article 3.4.4 was calibrated to produce required amount of rainfall intensity. To calibrate it, we set the rainfall tray on a frame made of bamboo. The height of the tray from ground level was 3.0 m. This

height was chosen as Chowdhury et al. (2017) had used this height for determination of different parameters of the rain tray which are stated in Article 3.4.4. Five rain gauges of 12.7 cm diameter were used. The rain gauges came with calibrated 100 ml plastic cylinders which contained the water. The rain gauges were placed under the rainfall tray. Figure 3.8 shows the plan view of the arrangement of the rain gauges along with the rainfall tray and Figure 3.9 shows the setup in the field. Before starting the water supply, it was ensured, with the help of spirit level, that the rainfall tray was completely horizontal. Otherwise the rainfall distribution would not have been uniform at all sides.

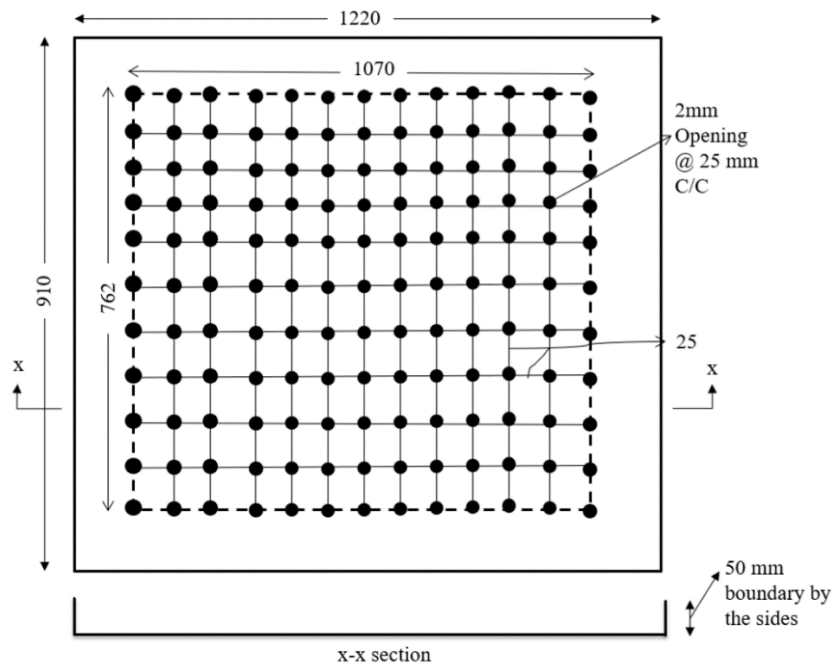


Figure 3.6: Schematic diagram of rainfall simulator tray (Chowdhury et al., 2017)

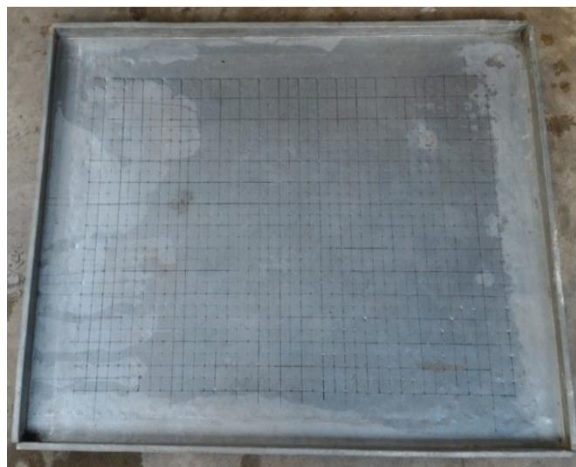


Figure 3.7: Plan view of the perforated steel tray: used as rainfall simulator

Four trials were given and each time the flowrate was varied and gradually decreased. For determining the rainfall intensity, the Thiessen Polygon method was adopted. Each rain gauge worked as a station of point rainfall. Polygons were constructed and each polygon contained one rain gauge. At each trial, the rainfall intensity was measured. From the obtained data a graph of flowrate (m^3/s) vs intensity (mm/hr) was plotted. A regression equation, $\text{Flowrate} (\text{m}^3/\text{s}) = 3 \times 10^{-7} - 5 \times 10^{-5} \times \text{Rainfall Intensity} (\text{mm}/\text{hr})$, was developed which presented a R^2 value of 0.9861. From this equation, we decided the flowrate which was required for generating the desired rainfall intensity for this study.

3.4.6 Determining required rainfall intensity

For this study we needed to produce a rainfall intensity which can generate a rainfall intensity high enough to trigger landslides. In a study conducted by Ahmed et al. (2018), 5-days consecutive rainfall was considered for rainfall threshold analysis. The rainfall threshold, for triggering landslides, was estimated ranging from 70–250 mm, which is a conservative method and helps to avoid any unavoidable errors. Moreover, in areas most susceptible to landslide, the rainfall is estimated to be >250 mm. So, to trigger the condition of landslide we needed to generate 250 mm rainfall within our experiment period. Duration of rainfall for this experiment was 30 minutes, so we set our desired rainfall intensity to be 500 mm/hr. From equation obtained from regression analysis the required flowrate to generate a rainfall intensity of 500 mm/hr is found to be $0.0001 \text{ m}^3/\text{s}$.

3.4.7 Setup for experiment

3.4.7.1 Setup of rainfall simulator

For conducting the experiment, at first, a frame was made using bamboo and wooden planks. The rainfall tray was set on the horizontal wooden planks. The height of the rainfall tray from ground level was 3.0 m to match the height of fall with the one used in the calibration process. The rainfall tray was set exactly above the models and their alignment was verified by hanging a plumb bob from the rainfall tray. It was done to ensure that all the rainfall directly falls on the model and not elsewhere. Pipe based water supply was used to simulate the rainfall. A flow rate of around $0.0001 \text{ m}^3/\text{s}$ was maintained and rainfall was continued for thirty minutes.

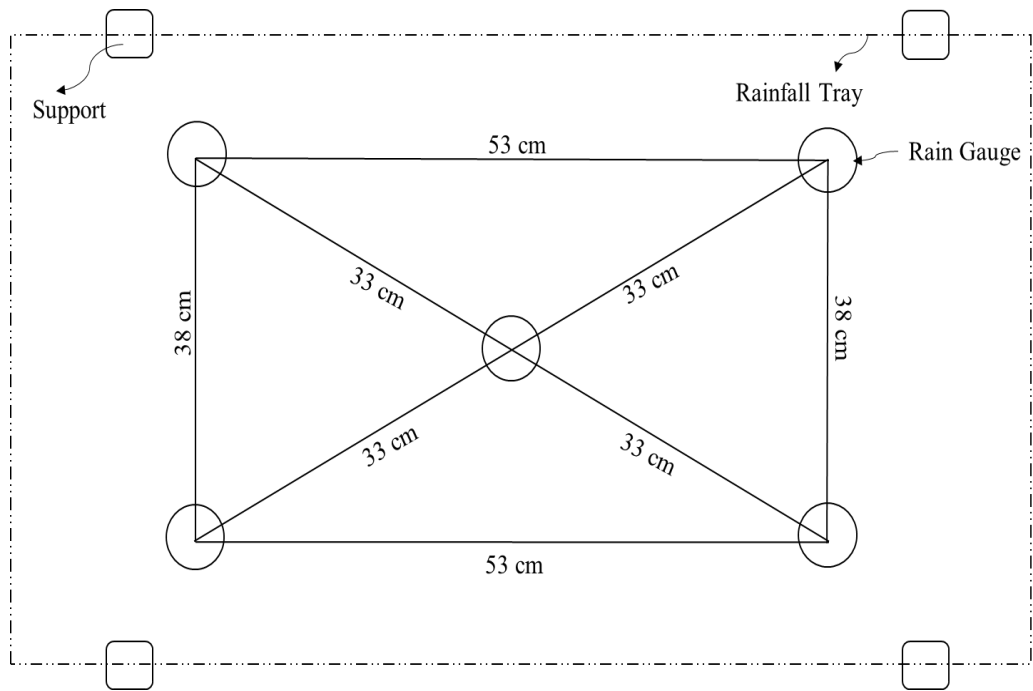


Figure 3.8: Plan view of set up for rainfall tray calibration



(a)



(b)

Figure 3.9: (a) Complete setup including rainfall tray, supports and rain gauges; (b) Positioning of rain gauges

3.4.7.2 Arrangement for collection of runoff water and eroded soil

When the models were exposed to the artificial rainfall, a part of the rainfall infiltrated into the soil. After a while, runoff started along with erosion of soil particles. To retain both the runoff water and the soil a trench was made along the edge of the front side of the model. Water proof hard boards were attached at the opposing edges of the models and the trench was covered with a plastic cloth to ensure minimum loss of soil and runoff water. Figure 3.10 shows the setup of the model and the collection mechanism of the runoff and eroded soil.

The runoff water and the soil were then transferred to large buckets. They were kept aside for 3-4 days so that the soil particles, which came with the runoff water, could settle down. Then the water was separated, and its volume was measured. The eroded wet soil was oven dried at a temperature of $110\pm 5^{\circ}\text{C}$ for 24 hours and its dry weight was measured.

3.5 Determination of Soil Erodibility

Universal soil loss equation was used to determine the erodibility of the soil S-1 and S-2 in bare condition and at two slope angles. Once the slope was taken equal to the model slope which was 1V:1.33H. Another slope angle was taken as 3V:1H as such steep slopes are present in the studied hills. In this process suitable values for five different parameters had been selected.

The value of R was calculated using Equation 3.1 (Tirkey et al., 2013). This is valid for an annual rainfall intensity range of 340mm to 3500mm. The annual rainfall intensity r for CHD is 3378mm, which falls within the range.

$$R = 81.5 + 0.375 \times r \quad 340 \leq r \leq 3500\text{mm} \quad (3.1)$$

As the soil loss was calculated for bare condition with no vegetation cover factor, C was taken as 1. It was considered that the slope had irregular cuts and thus the erosion control practice factor P was taken as 0.9. Other two factors, K (depends on soil type) and LS (depends on slope height and length) were determined following the guidelines provided by Goldeman et al., 1986. The obtained values for these factors are presented Table 3.3 and Table 3.4.

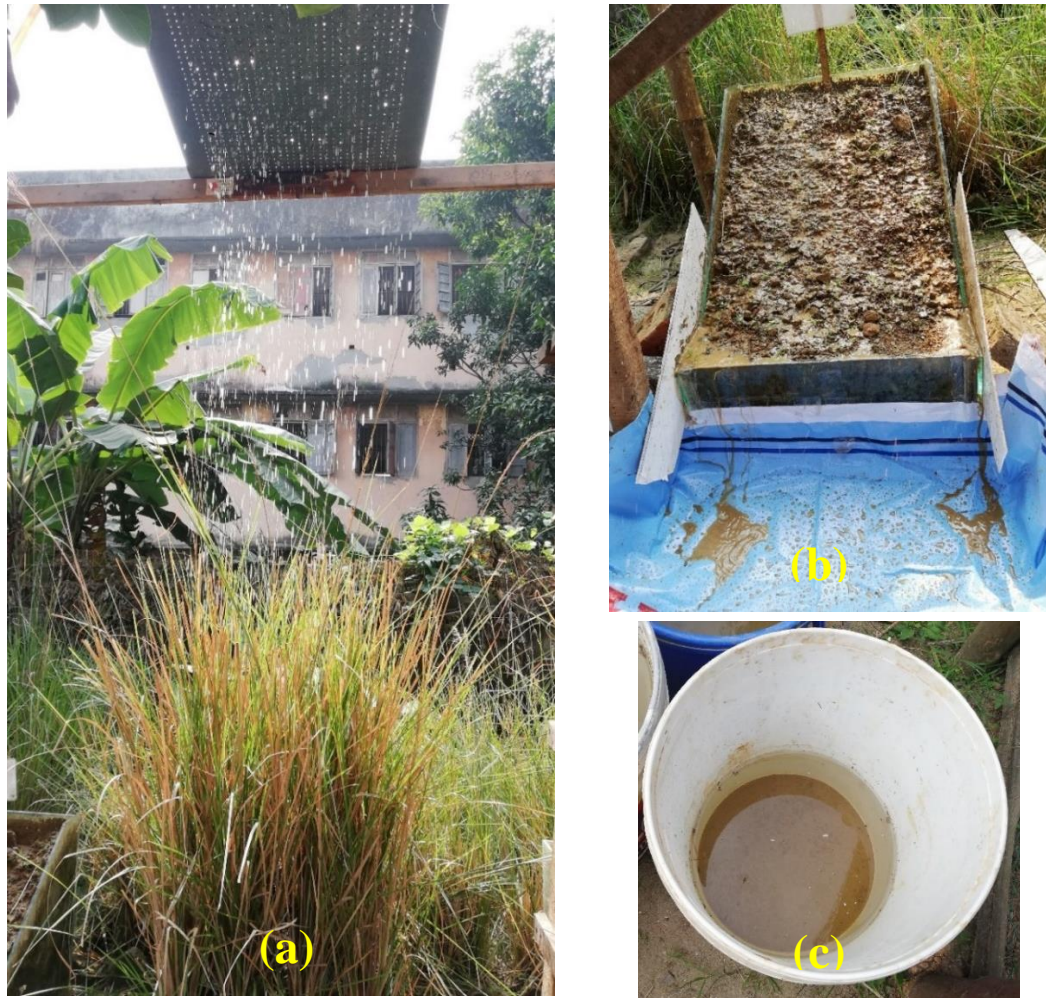


Figure 3.10: (a) Rainfall tray setup above the model; (b) M-6 with covered trench for collection of runoff and eroded soil; (c) Collected soil and water

Table 3.3: Values of soil erodibility factor for different soils

Soil Type	Soil Erodibility Factor K ($t\ ha\ h\ ha^{-1}\ MJ^{-1}\ mm^{-1}$)
S-1	0.071
S-2	0.029

Table 3.4: Values of slope length and steepness factor for different slope angles

Slope	Slope length and Steepness Factor LS
1V:1.33H	28.03
3V:1H	53.82

3.6 Numerical Modeling and Analysis

Numerical modeling was done by Plaxis 2D which performs finite element analysis. Different soil conditions for natural slope e.g. bare and vegetated slope were modeled for two types of soil. Their stability was analyzed by finding the Factor of Safety. Besides vegetation, slopes with nailing were modeled and analyzed by varying nailing parameters and their arrangements. Stability analysis of terraced slope was also simulated numerically.

3.6.1 Model geometry

Two type of geometry was studied in this study. 2D models were generated keeping the dimensions of the hills of Chattogram City Corporation Area in mind. First a model with a single, rectilinear slope was defined. Height of the complete model was considered as 20 m. The height of the slope (H) was taken as 15 m. The slope angles (β) had been varied and the length of the slope varied as a function of β . Figure 3.11 shows the typical geometry of this model. Another model was defined with terraced slope. The number of steps had been varied as two (each step having height $H_T=7.5\text{m}$), three (each step having height $H_T=5\text{m}$) and five (each step having height $H_T=3\text{m}$), while keeping the whole slope height as 15m. The slope angles of each step were kept same. Figure 3.12 shows the schematic diagram of the terraced model. In the schematic diagrams, L is the length of the slope, β = slope angle and $\alpha+\beta=90^\circ$.

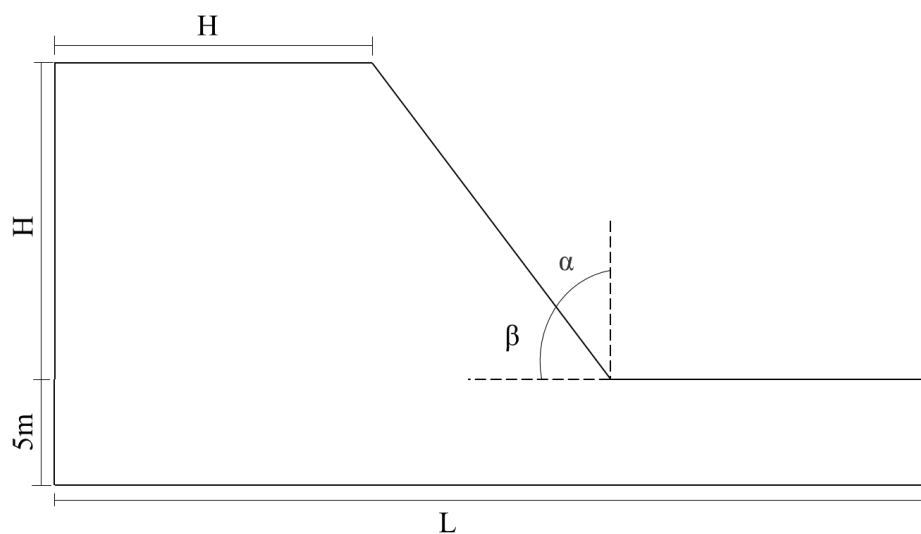
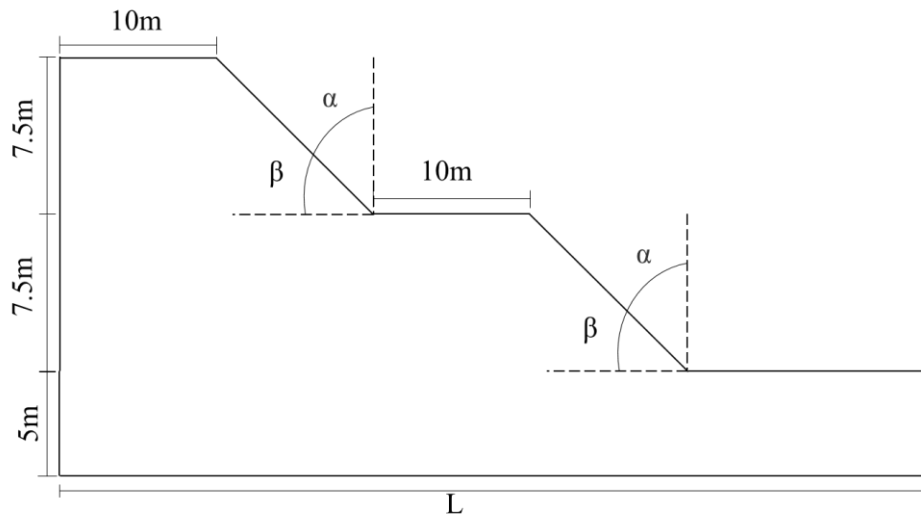
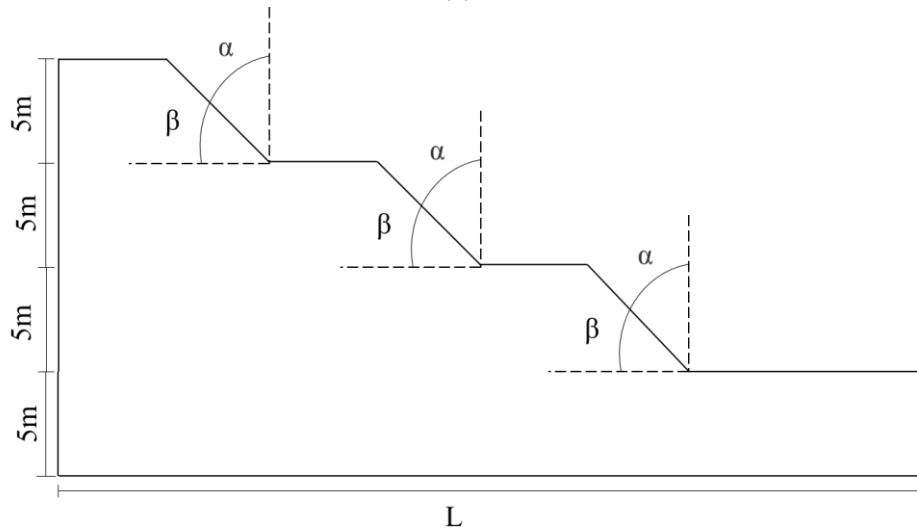


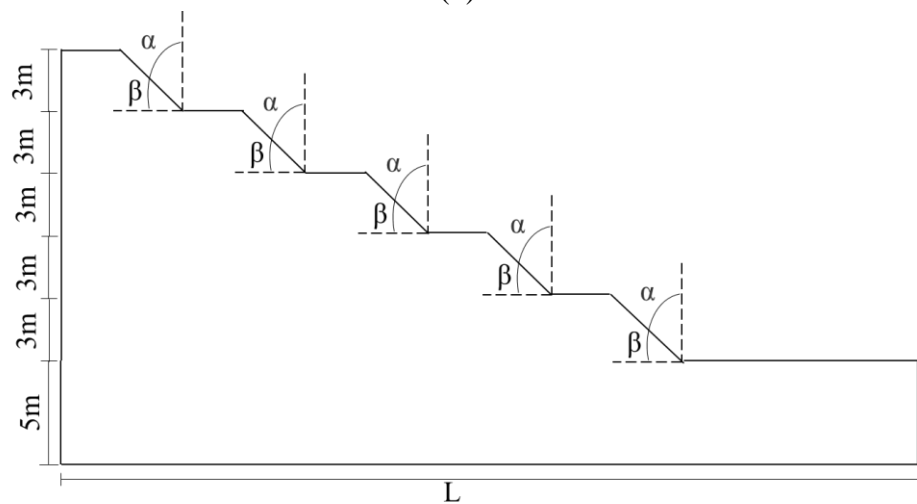
Figure 3.11: Schematic diagram of natural slope (H=15m) where H= slope height; L= slope length, β = slope angle; $\alpha+\beta=90^\circ$



(a)



(b)



(c)

Figure 3.12: Schematic diagram of model in FEM where H_T = height of each step of terraced slope, (a) $H_T=7.5\text{m}$; (b) $H_T=5\text{m}$; (c) $H_T=3\text{m}$

3.6.2 Finite Element Model

Plaxis 2D does the FEM analysis based on two types of models. One is Plane Strain Model and the other one is Axisymmetric model. In this study, Plane Strain Model was used. This model is used for geometries with more or less uniform cross section and corresponding stress state and loading scheme over a certain length perpendicular to the cross section (Z direction). Where-as, Axisymmetric model is used for circular cross sections (Plaxis 2D Reference Manual CONNECT Edition V20). We were considering slope stability analysis, where the soil continues in longitudinal direction and so plane strain model was applicable here.

3.6.3 Mesh and fixities

After defining the geometry and assigning the properties of different elements the model needs to be divided into finite elements. These finite elements are called mesh. In this study a medium mesh was used. This was used as using a fine mesh takes longer time for analysis and coarse meshes may not always provide accurate numerical results. So to obtain correct numerical results by keeping the calculation time minimal, a sufficient mesh size was selected.

For the fixities, boundary conditions were selected depending on the behavior of the physical slope. The sides of the models could only accommodate vertical movement and had been restrained in horizontal direction. The movement of the soil mass was restrained in both x and y direction at the bottom which means the prescribed displacement in both of these directions were zero.

3.6.4 Modeling soil properties

3.6.4.1 Elements

For modeling soil layers there are two types of elements available in Plaxis 2D: 6-node triangle and 15 node triangles. In this study, 15 node triangle elements had been used. Though this is more suitable for axisymmetric models, 6 noded triangle elements overestimate the failure loads or factor of safety. So, during safety analysis or bearing capacity analysis by phi-c reduction use of 15 noded elements are preferred. This element provides fourth order interpolation for displacement and the numerical integration involves twelve stress points.

3.6.4.2 Material model

Plaxis supports different models to accommodate the non-linear behavior of soil. Among them after linear elastic model (which is too limited for simulating soil behavior) the Mohr- Coulomb model (MC) is relatively fast and provides first estimation of deformations. In this study, MC model had been used to obtain the first approximation of soil behavior and first analysis of the stability problem. This is a linearly elastic perfectly plastic model that considers a constant average stiffness for the soil layer. As we considered the soil as homogenous, the stiffness should also remain the same over the depth of soil layer.

3.6.4.3 Drainage type

The values of strength and stiffness parameters depend on the type of drainage used. We are considering the situation when the soil gets saturated after rainfall and thus is vulnerable to landslides. So, the factor of safety needed to simulate a similar condition. In undrained analysis, pore pressures are generated assuming very low compressibility of pore fluids and are valid for saturated soils. For this in this study the Undrained behavior was used.

Among the undrained condition Undrained A had been used. It enables modeling undrained behavior using effective parameters for stiffness and strength. It generates pore water pressure which is more accurate than Undrained B. It also performs consolidation analysis which affect the shear strength thus represent a true scenario.

3.6.4.4 Strength and stiffness parameters

For Mohr-Coulomb model, five soil parameters are required. Two stiffness parameters are Young's modulus (E) and Poisson ratio (ν). Other three include strength parameters cohesion (c), friction angle (ϕ) and angle of dilatancy (ψ).

The effective cohesion c' and effective friction angle ϕ' were obtained from Consolidated Drained (CD) Direct Shear test which was performed on reconstituted samples. Here a moisture content close to the in-situ condition was maintained.

The angle of dilatancy is the change of volume observed in granular materials while subjected to shear. For cohesive soil this angle is very low, mostly near to zero. For cohesionless soil, it depends on friction angle. For soils with $\phi > 30^\circ$, $\psi = \phi - 30^\circ$. In our

study, the non-cohesive soils have friction angles slightly greater than 30°. However, use of a positive dilatancy angle results in very high and unrealistic tensile pore stresses. So, ψ' was taken as zero.

Soil Young's modulus (E), commonly referred to as soil elastic modulus, is an elastic soil parameter and a measure of soil stiffness. It is defined as the ratio of the stress along an axis over the strain along that axis in the range of elastic soil behavior. In this study, modulus of elasticity of respective soil and Poisson ratio was determined according to literature (Bowles, 2012).

3.6.4.5 Interface element

To model the interface of soil and root, the interface element was used. The properties of interface elements are related to soil model parameters of surrounding soil. In Mohr-Coulomb model the main interface parameter is R_{inter} which is the strength reduction factor. In this study $R_{inter} = 1.0$ was used. The value signifies that the interface had the same strength properties as the surrounding soil.

3.6.5 Modeling root properties

In this study the effect of vegetation on the stability of slope had been studied. Here the roots of *Vetiveria zizanoides* were considered to provide reinforcement to the soil. It increases the shear strength of the soil as the roots bind the soil together. The contribution of root reinforcement to shear strength is considered to have the characteristics of added cohesion or adhesion (Wu et al., 1979). Here the effect of roots had been considered by addition of cohesion to soil layers.

Generally, Mohr-Coulomb failure criterion model is applied to determine the effect of root-soil reinforcement on the shear strength of soil. It is assumed in the model that the roots are cylindrical, elastic and perpendicular to the shearing plane. Thus, the tension is transferred to the roots when the soil is under shear. The root's contribution, e.g. the apparent added cohesion is accommodated in the total shear strength as shown in Equation 3.1.

$$s = c_s + c_r + \sigma \tan \varphi \quad (3.2)$$

Here, c_s is the cohesion parameter of soil, c_r is the added cohesion, σ is the normal stress on the shear plane and φ is the friction angle. When the roots, perpendicular to

shear zone, are displaced laterally by an amount X , and distorted by angle of shear, θ , the mobilization of tensile resistance in the fibers in the soil can be translated into a tangential component ($\cos\theta \cdot \tan\phi'$) and a normal component ($t_r \sin\theta$). Expressed as a reinforcement strength per unit area of soil, the root, c_r , cohesion is:

$$c_r = t_r (\cos\theta \tan\phi' + \sin\theta) \quad (3.3)$$

t_r is the total tensile root strength per unit area of soil (Voottipruex et al., 2008). t_r is the product of two parameters, average tensile strength of the root (T_r) and the Root Area Ratio (RAR) as shown in Equation 3.4.

$$t_r = T_r \times \text{RAR} \quad (3.4)$$

Sensitivity analysis indicates that the values of ($\cos\theta \tan\phi' + \sin\theta$) can be approximated as 1.2 for $25^\circ < \phi' < 40^\circ$ (Wu, 1976; Wu et al., 1979). Hence, Equation 3.3 can be written as Equation 3.5.

$$c_r = 1.2 \times T_r \times \text{RAR} \quad (3.5)$$

The tensile strength of vetiver roots was obtained from laboratory tests performed by Teerawattanasuk et al. (2014) where the root diameter varied between 0.25 mm to 2.90 mm. The tensile strength has a good correlation with diameter ($R^2=0.806$). Equation 3.6 shows the relationship.

$$T_r = 15.239 \times D^{-0.893} \quad (3.6)$$

T_r is in MPa and D is the diameter of root in mm. The root diameter obtained from the models fall within the range stated above so this was used in this study. Root area ratio (RAR) is the fraction of soil occupied by the root as shown in Equation 3.7.

$$\text{RAR} = \frac{A_r}{A} \quad (3.7)$$

A_r is the cross section of root and A is the area of the soil occupied by the root. It varies with the depth of soil layer. According to the study of Machado et al., (2015), a strong negative relationship, as shown in Equation 3.8, exists between RAR and soil depth ($R^2=0.9717$) which has been used in this research.

$$\text{RAR} = 0.154x^2 - 0.1296x + 0.0272 \quad (3.8)$$

Table 3.5 shows how the added cohesion is calculated based on RAR value. According to this procedure described, at the age of 12 months, considering the diameter as 2.8 mm, the added cohesion at 0.5m depth was calculated as 6.36 kPa which was within the range suggested by Chok et al., (2015).

Most field studies conclude that predominantly the biomass of roots is found at the top 0.5m of the soil where roots provide the maximum reinforcement and stabilizes shallow slope (De Baets et al., 2007; Leung et al., 2013). Even vetiver has large clumps near the soil. But as depth increases, the root diameter becomes smaller and this results in higher tensile strength which may counterbalance the reduction of RAR with depth and overall increase their product viz. the added cohesion. Again, concentrated increase in RAR at depths for various species have been observed due to increased nutrient availability (Weaver and Clements, 1938) and moisture content (Manschadi et al., 1998). Moreover, at steep slopes, higher root densities at greater depths have been reported (De Baets et al., 2007). These may increase the added cohesion at larger depths which as a result increases the root reinforcement effect (Kokutse et al., 2016, Tsige et al., 2020). So, by assuming the added cohesion as constant, the mechanical reinforcement of vetiver roots was taken on a conservative side.

Table 3.5: Added cohesion for different depth of soil layer

Age (months)	Diameter (mm)	Tensile strength of root, T_r (MPa) [Eqn. 3.6]	Depth of Layer h (m)	Root Area Ratio [Eqn. 3.8]	Added apparent cohesion, c_r (kPa) [Eqn. 3.5]
12	2.8 (maximum diameter obtained from model study)	5.89	0	0.0272	192.2496
			0.15	0.011225	79.3383
			0.30	0.00218	15.40824
			0.50	0.0009	6.3612

At first, for the natural slope (H=15m) the factor of safety was calculated at barren condition and the maximum stable angle was determined. How vegetation will effect the slope stability at that angle was then analyzed by varying the depth of root zone (h_r). Later it was observed until which slope angle can vetiver effectively provide stability to the slope. This angle has been termed as threshold angle β_{lim} . For the terraced slope geometry, it was observed if this provides any increase to the maximum stable slope angle for three different configuration of step size as mentioned earlier. As vetiver roots can grow up to 3.0 m, its effect was also considered at six different h_r , varying from 0.5 m to 3.0 m at 0.5 m interval. The threshold angles for vegetated terraced slopes were also determined to find suitable step height for protecting vertical cuts in hill slopes. Finally parametric studies were conducted to determine relationships of factor of safety with root zone depth, slope angle and slope height. The summary of different cases is stated in Figure 3.13.

3.6.1 Safety calculation (phi-c Reduction)

This study aims to determine the global safety factor of the slopes which were modeled. The factor of safety is given by,

$$FS = \frac{\text{available strength}}{\text{strength at failure}} \quad (3.9)$$

The available strength is the input parameters. The strength at failure is calculated in Plaxis by reducing the strength parameters of soil. This process is called phi-c reduction method. The shear strength parameters $\tan\phi$ and c are successively reduced until failure of the slope occurs. The safety factor is calculated by Load advancement number of step procedure. The incremental multiplier M_{sf} is used to specify the increment of the strength reduction of the first calculation step. The increment was by default set to 0.1, which is generally found to be a good starting value.

At a given stage, the value of the soil strength parameters is defined by the total multiplier ΣM_{sf} . ΣM_{sf} is defined as the input strength parameters by the reduced strength parameter.

$$\Sigma M_{sf} = \frac{\tan\phi_{input}}{\tan\phi_{reduced}} = \frac{c_{input}}{c_{reduced}} \quad (3.10)$$

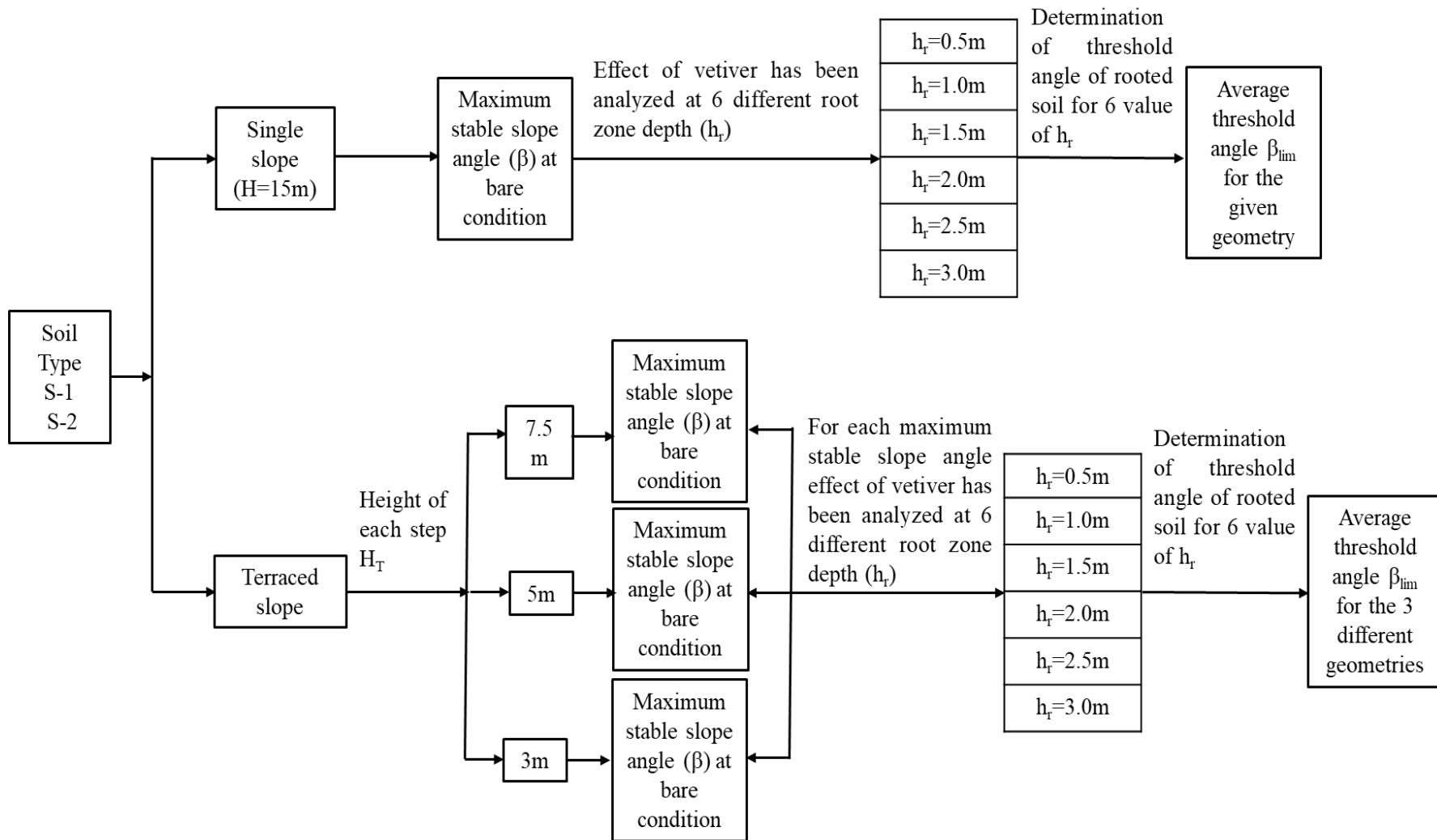


Figure 3.13: Summary of the analysis steps for vegetation

ΣMsf is set to 1.0 at the start of a calculation to set all material strength to their input values. The factor of safety is the value of ΣMsf at failure. The safety reduction method which was adopted here gives similar safety factors as obtained from conventional stability analysis based on Limit Equilibrium Method and slip circle analysis (Plaxis 2D Reference Manual CONNECT Edition V20).

3.6.2 Nailing modeling

Nailing had been used as reinforcement and its effect in slope stability was analyzed in this study. To model the nails, plate elements were used. Plate elements are basically beam elements which can be used to model slender structures in the ground with significant rigidity (bending or stiffness) and normal stiffness. For modeling nails, axial stiffness and bending stiffness play important role (Shiu and Chang, 2006; Fan and Luo, 2008) which can be addressed by using a plate element.

In this study, plate elements of circular cross section were used. A hole of 10 cm diameter was considered. An equivalent modulus of elasticity (E_{eq}) was obtained according to Equation 3.11 (Babu and Singh, 2009). For this, an equivalent axial stiffness (EA) and equivalent bending stiffness (EI) was calculated by Equation 3.12 and 3.13.

$$E_{eq} = E_n \frac{A_{nail}}{A} + E_g \frac{A_{grout}}{A} \quad (3.11)$$

$$EA = \frac{E_n}{S_h} \frac{\pi}{4} d_n^2 \quad (3.12)$$

$$EI = \frac{E_n}{S_h} \frac{\pi}{64} d_n^4 \quad (3.13)$$

Here, #9 bars were used as nails with a cross sectional area $A_{nail} = 6.5 \text{ cm}^2$. A_{grout} is the area of grout and A is the area of nail plus area of grout. Young's modulus of steel nail, E_n was 200 GPA and Young's modulus of concrete grout, E_g was 22 GPA. S_h is the horizontal spacing of the nails which was taken as 1.0m. With these values an equivalent diameter (d_{eq}) was calculated by Plaxis using Equation 3.14. Figure 3.14 shows the summary of the variation of parameters for analysis using nailings.

$$d_{eq} = \sqrt{12 \frac{EI}{EA}} \quad (3.14)$$

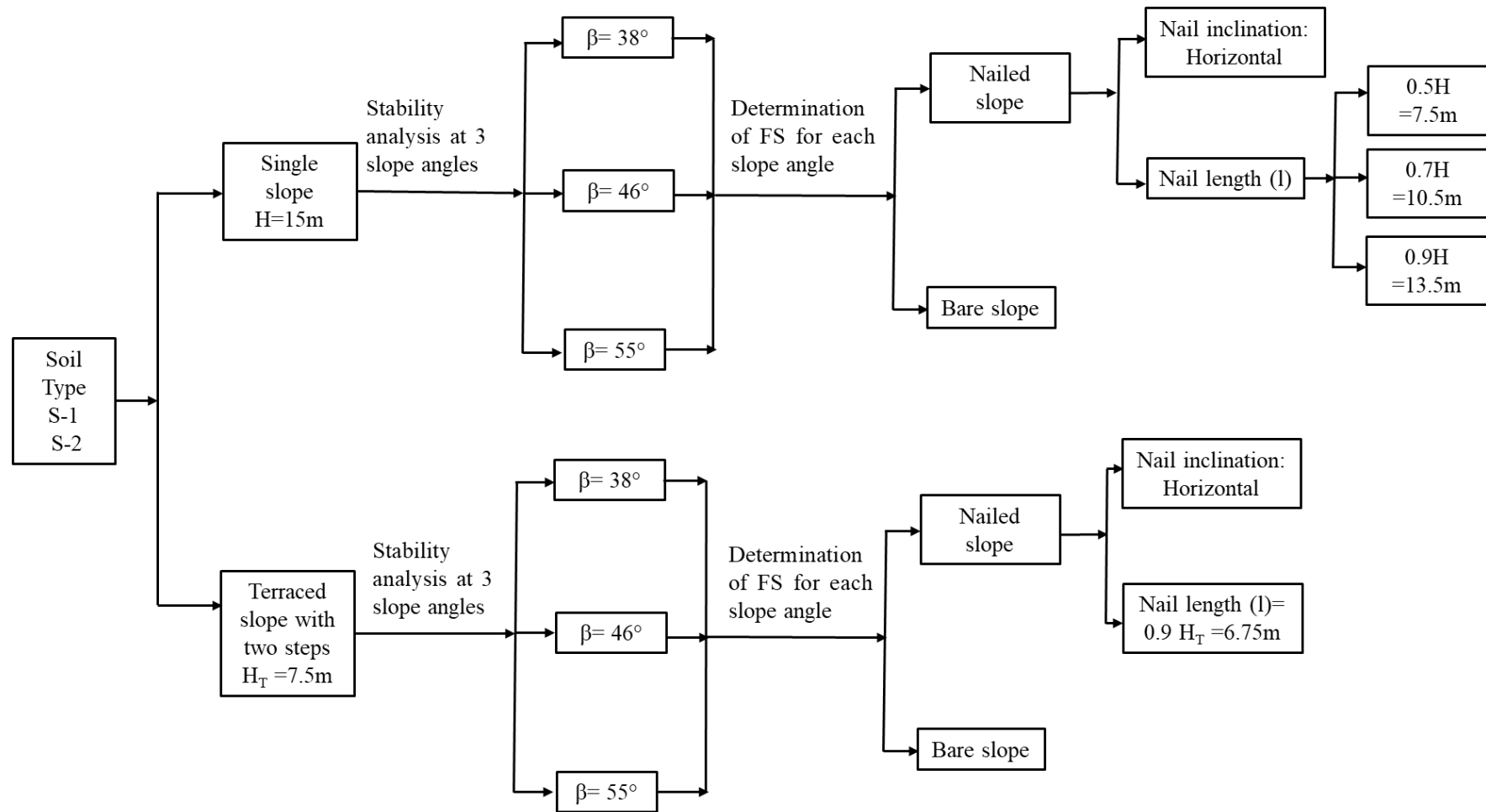


Figure 3.14: Summary of different cases with variations of parameters for nailing

For the interface, the strength reduction coefficient R_{inter} was assigned. The value can vary in between 0.95 to 1.07 (Chu and Yin, 2005). In this study R_{inter} was taken equal to 1.0. A virtual thickness was assigned to define the material property of the interface. The higher the value, the more is the elastic deformation. In general, the interface element is supposed to generate very little elastic deformation. It is calculated by multiplying the virtual thickness factor to the global element size. This factor was taken as 0.1 which was a default value. Table 3.6 shows the properties of the nails.

For both natural and terraced slope, the slope stability at three slope angles ($\beta= 38^\circ$, 46° and 55°) were analyzed with and without nails. All studies were performed for two types of soil S-1 and S-2. For natural slopes, the nail length was varied. It was taken as a function of slope height. For the natural slope of $H=15m$, nail lengths (l) were considered as $0.5H$, $0.7H$ and $0.9H$. The effect of horizontal nails were studied.

For terraced slope, one case was considered where the entire slope was divided into 2 steps, each having $H_T=7.5m$. Here the nail length (l) was taken as $0.9H_T$ thus $6.75m$. The nail inclination was kept the same as the previous cases.

Table 3.6: Nail properties

Parameters	Value
Axial Stiffness EA (kN/m)	2.90×10^5
Flexural Rigidity, EI (kN.m ² /m)	181.4
Poisson ratio, ν	0.3

3.7 Summary

This chapter describes the detailed methods of all the experimental steps starting from soil sample collection, index property determination, model preparation till erosion test under artificial rainfall condition. It also delineates the specifications of parameters for finite element analysis along with various processes and thus provides a summarized, but wholesome picture of the topics covered in the numerical study.

CHAPTER 4

RESULTS AND DISCUSSIONS

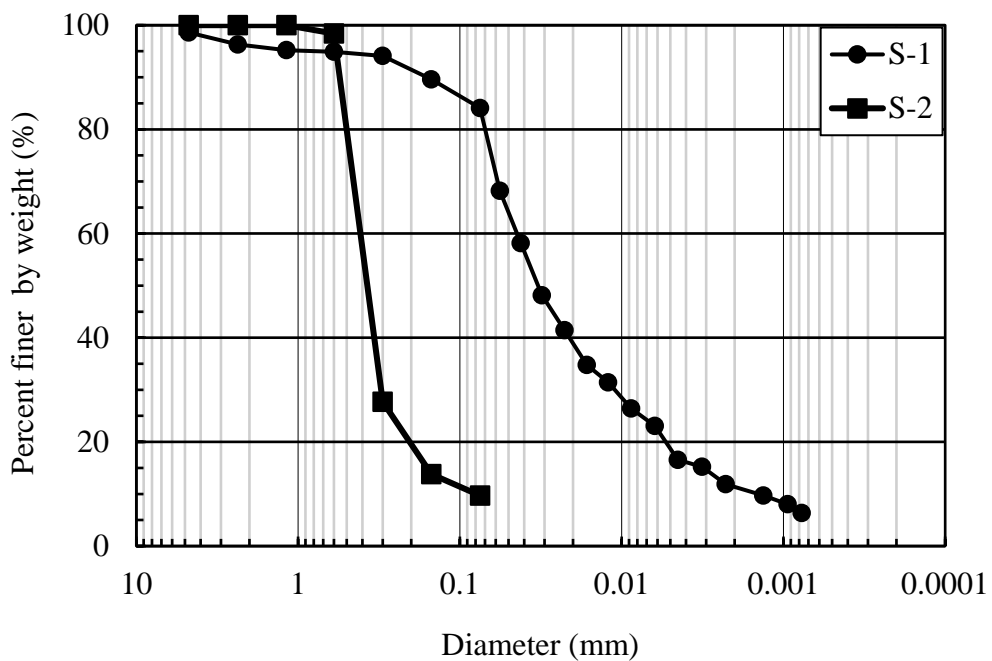
4.1 Introduction

This chapter presents the results of this study along with their respective discussions. This discusses the soil properties, nutrient contents and the growth of vetiver in small glass models. The test results obtained through rainfall test on models and their interpretations are delineated here. Further, the results obtained from the Finite Element analysis are presented and discussed in detail.

4.2 Properties of Soil Samples

4.2.1 Grain size analysis of soil

Two types of soil were collected from Tiger pass (S-1) and Berma Haji (S-2), and their grain size analysis was done by sieve analysis and hydrometer analysis. Percent finer than #200 sieve (by weight) for S-1 is 84.1% and for S-2 it is 9.7%. Figure 4.1 presents the gradation curve for both the soils. Also, the soil are found to be non-plastic. From these results and according to Unified Soil Classification System (USCS), S-1 is classified as sandy silt and S-2 is classified as silty sand (SM).



4.2.2 In-situ and dry density of soil

From the field density test, the in-situ density (γ) is obtained as 17.65 kN/m³ for S-1 and 18.63 kN/m³ for S-2. From the difference of weight the moist and oven dry soil, the natural moisture content (ω_n) was determined, and it is 21.7% and 10.23% for S-1 and S-2, respectively. Following the relationship of three phase diagram of soil, the dry density (γ_{dry}) was calculated for S-1 and S-2 as 14.42 kN/m³ and 17.17 kN/m³ respectively.

4.2.3 Effective shear strength parameters

Figure 4.2 and Figure 4.3 shows the results of the Consolidated Drained (CD) Direct Shear test (CD) of S-1 and S-2. The dry density after consolidation varied between 13.48 kN/m³ to 14.34 kN/m³ for S-1 and for S-2 it varied between 17.06 kN/m³ to 18.35 kN/m³. From the Mohr-Coulomb failure envelope, we can see that both soil samples have zero effective cohesion, thus are cohesionless. S-1 has a higher angle of effective internal friction of 39°, whereas for S-2 it is 33°.

4.2.4 Coefficient of vertical permeability

Coefficient of vertical permeability was obtained for three different void ratios. Figure 4.4 and Figure 4.5 present the relationship between void ratio and coefficient of vertical permeability obtained from the laboratory test. Coefficient of vertical permeability of sandy silt is found to be within the range of 4.61×10^{-7} m/s to 1.56×10^{-6} m/s. For silty sand, the value of coefficient of vertical permeability varied from 3.71×10^{-5} m/s to 5.30×10^{-5} m/s. For numerical analysis, the value of coefficient of vertical permeability was taken as 4.61×10^{-7} m/s and for S-2 it was taken as 3.71×10^{-5} m/s as at these two values of the void ratio (0.86 and 0.73, respectively) were closest to that of the in-situ void ratio. Table 4.1 summarizes the soil properties.

4.3 Chemical Properties and Nutrient Content

The nutrient properties, pH and organic content of S-1 and S-2 were tested with help of Soil Resource Development Institute (SRDI). The soil samples were collected from top surface (15 cm) as during rainfall induced erosion, nutrients of this surface get washed off. Thus, it was necessary to determine the existing quality of the top soil.

Among the nutrients, the amount of total Nitrogen (TN), Potassium (K), Phosphorous (P), Sulfur (S), Boron (B) and Zinc (Zn) were determined.

Table 4.2 shows the results obtained from the test. The soil of Chattogram hill tracts is moderately to strongly acidic in nature (Chowdhury, 2012). From the pH we can see that it varies within 6.2 to 6.4 which is slightly acidic. Vetiver is adaptive to a wide range of soil types (pH 3.0 to 10.5) (Truong and Baker, 1998). So, the pH is within the tolerance limit of vetiver grass.

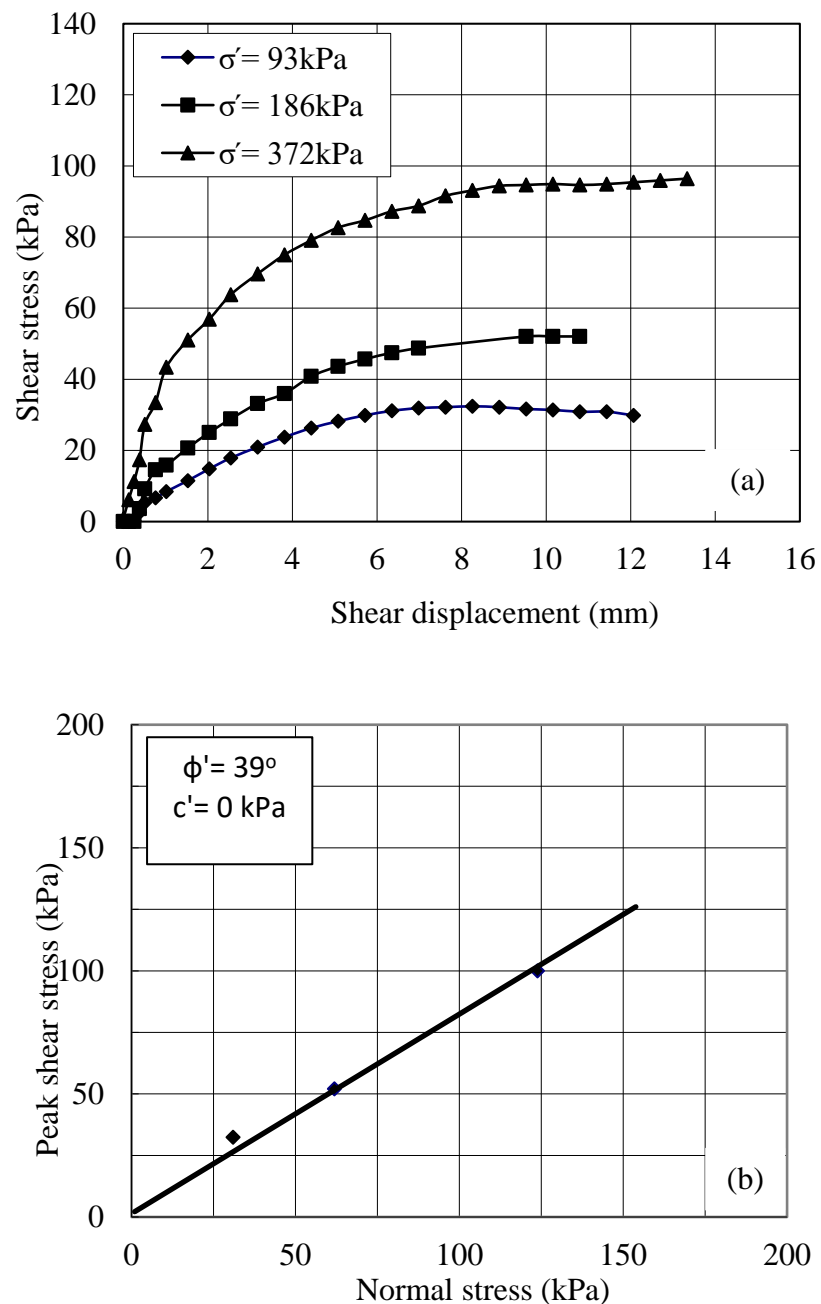


Figure 4.2: (a) Change of shear stress with shear displacement for S-1; (b) Mohr-Coulomb failure envelope of S-1

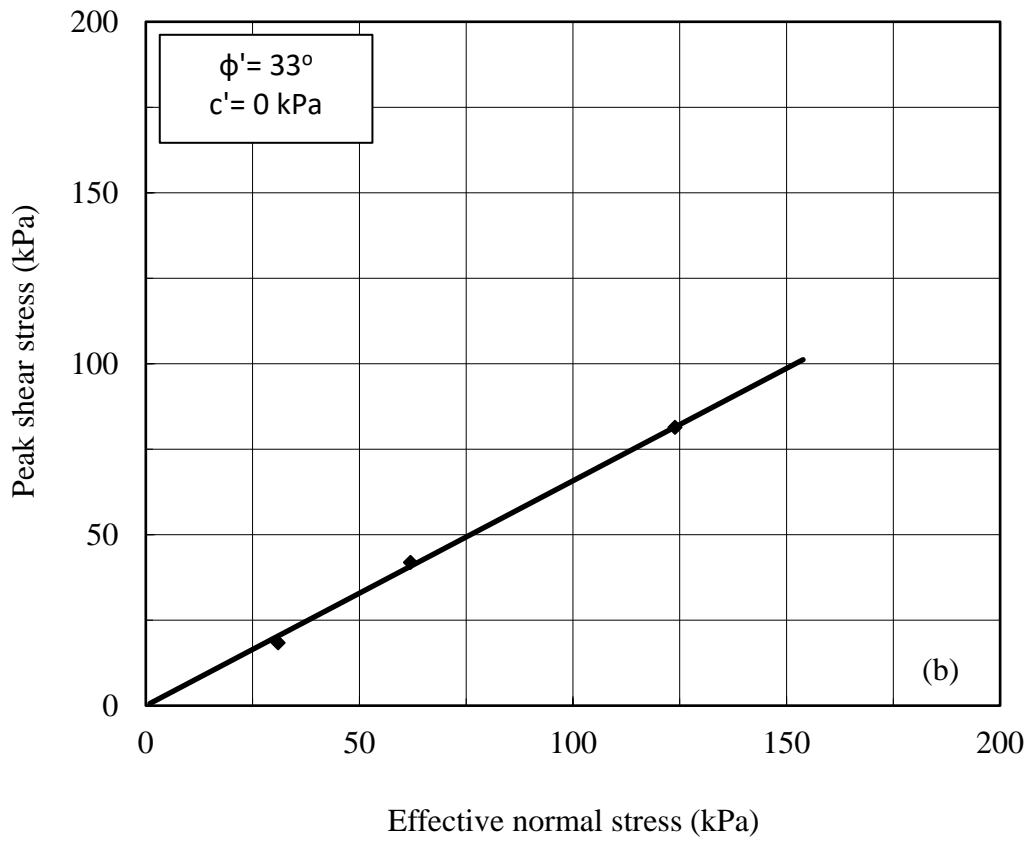
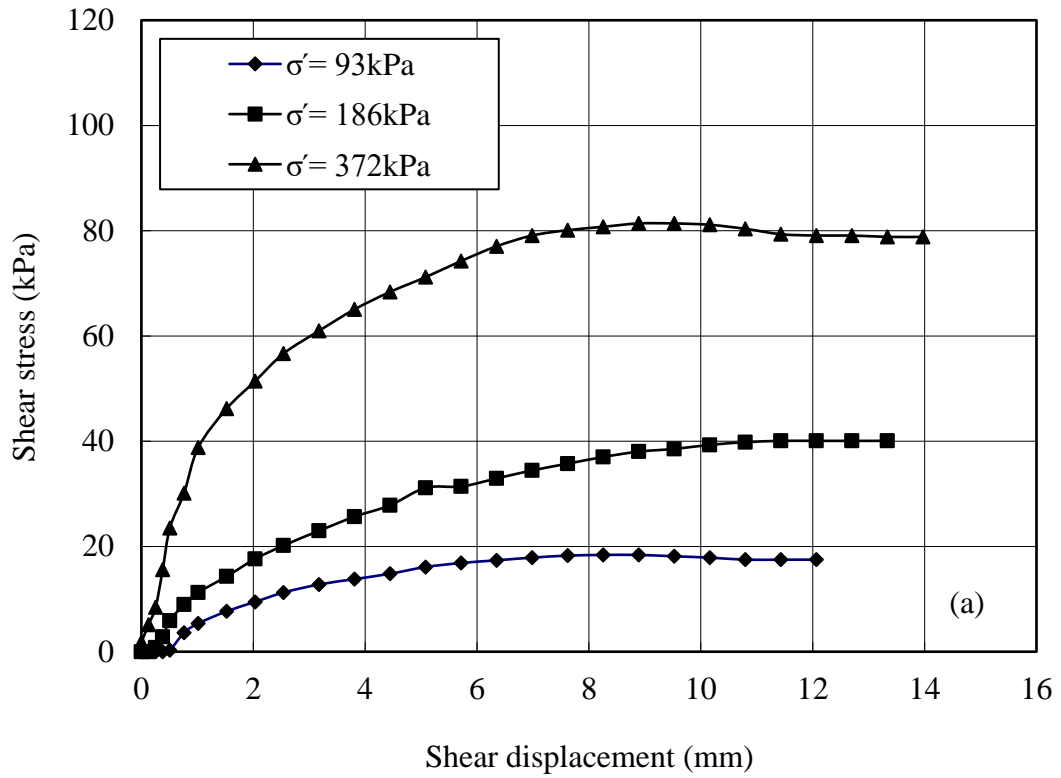


Figure 4.3: (a) Change of shear stress with shear displacement for S-2; (b) Mohr-Coulomb failure envelope of S-2

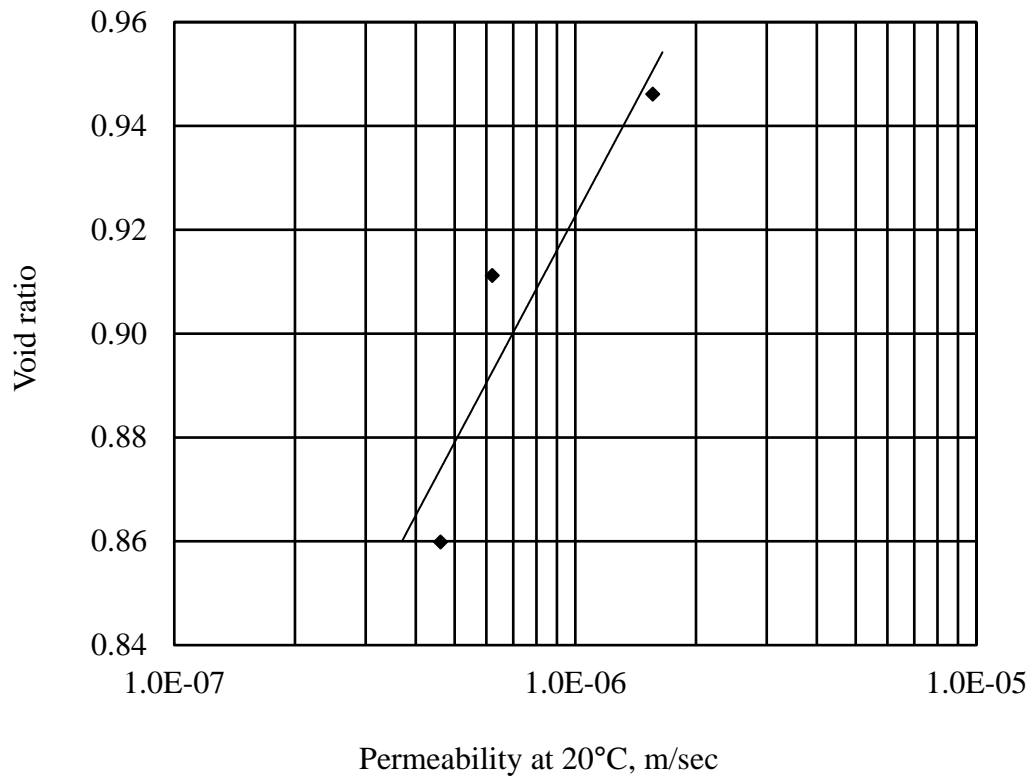


Figure 4.4: Coefficient of vertical permeability (k) of S-1 at different void ratios

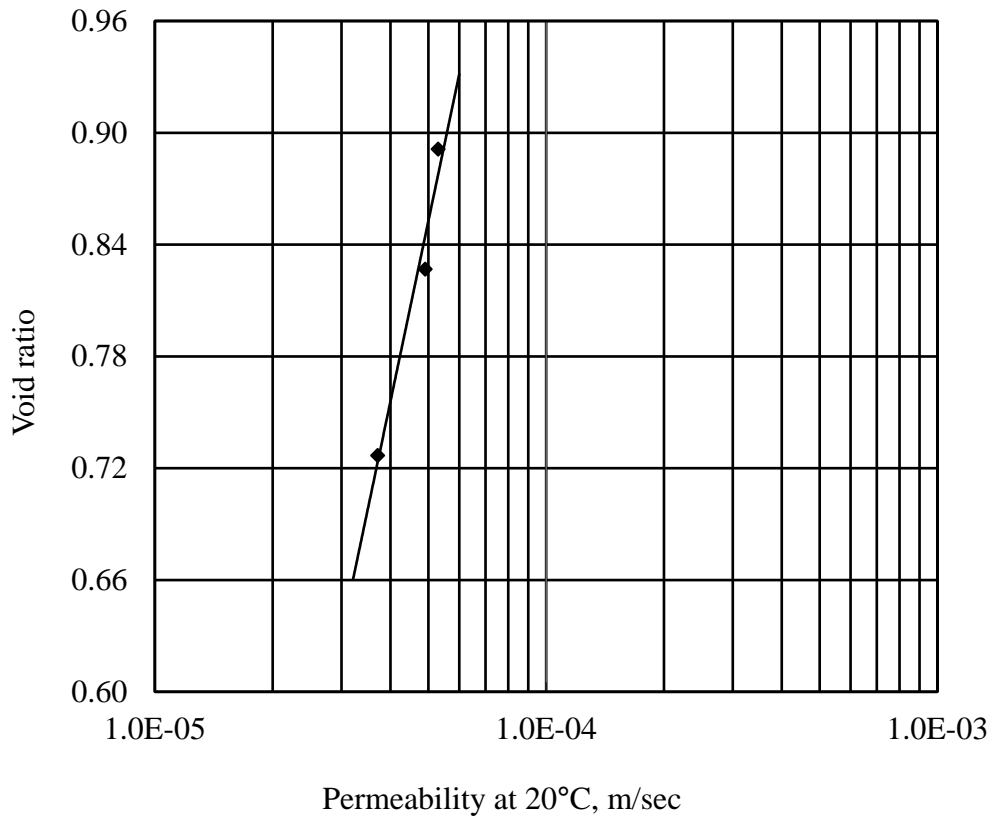


Figure 4.5: Coefficient of vertical permeability (k) of S-2 at different void ratios

Table 4.1: Properties of soil samples

Physical Properties	S-1	S-2
In-situ density, γ (kN/m ³)	17.65	18.63
Dry density, γ_{dry} (kN/m ³)	14.42	17.17
Saturated density, γ_{sat} (kN/m ³)	18.82	20.6
Index Properties	S-1	S-2
Natural moisture content, ω_n (%)	21.7	10.23
Specific Gravity, (G_s)	2.67	2.65
Atterberg Limits	Non-plastic	Non-plastic
Soil Type	Sandy Silt	Silty Sand (SM)
Engineering Properties	S-1	S-2
Angle of internal friction, ϕ' (°)	39	33
Cohesion, c' (kPa)	0	0
Co-efficient of permeability, k (m/s)	4.61×10^{-7} - 1.56×10^{-6}	3.71×10^{-5} - 5.30×10^{-5}
In-situ void ratio, e	0.82	0.51

Table 4.2: Chemical properties and nutrient contents of S-1 and S-2

Soil	pH	Organic Matter (%)	Total Nitrogen (%)	Potassium (K) meq/100 gm	Phosphorus (P) ppm	Sulfur (S) ppm	Boron (B) ppm	Zinc (Zn) ppm
S-1	6.4	0.40	0.020	0.11	2.01	61.35	0.46	0.67
S-2	6.2	0.06	0.003	0.09	1.03	10.30	0.13	0.80

Bangladesh's soils are generally low in organic matter content; most soils having less than 1.5 % organic matter in surface 0-15 cm (BARC, 2005). For both S-1 and S-2, the organic content is very low according to the classification of BARC.

Most terrestrial ecosystems are considered nitrogen (N) and/or phosphorus (P) limited (Aerts and Chapin, 1999). Following the trend of OM, the TN is also low in most of the land of Bangladesh. In both the soil samples TN is found to be very low. Phosphorus is also very low in both the samples. K in S-1 was low and in S-2, it is very low. However, Nitrogen, P and K are called primary nutrients because of their large requirement and Ca, Mg and S are called secondary nutrients (BARC, 2005). So, there is deficiency of all three primary nutrients in both the soil samples. The soil condition is not suitable for growth for plants which cannot tolerate nutrient deficiency. Vetiver has the ability to survive moisture and nutrient stresses and reestablish top growth quickly after rain (Smith and Srivastava, 1989). From this, we can say that vetiver is suitable for plantation in the existing soil condition.

Usually the tribal people practice shifting cultivation in the slopes of the hills. Studies showed impact of erosion, which is influenced by shifting cultivation (*Jhum*) at steep and continuous sloping sites, on nutrient contents. It shows, loss of organic carbon, nitrogen, phosphorus, potassium, calcium and magnesium was more pronounced in the eroded than in the non-eroded or partially eroded sites (Farid et al., 1992). Vetiver's strong and massive root system along with its unique ecological characteristics provide a bio-engineering tool for soil erosion control. As a secondary effect of reduced erosion, the nutrient condition will not deteriorate. The ability of vetiver to survive in unfavorable conditions and acting as a pioneer plant creates micro-climates which permits other indigenous plants to prosper (Truong and Loch, 2004). So vetiver will also facilitate the growth of natural plants which will reduce the erosion and subsequently reduce the risk of landslide.

4.4 Growth Study of Vetiver

Since plantation, all the models were nurtured on a regular basis. The initial plantation was done in November, 2018 when the temperature was around 27°C. As it was winter and the weather was dry with average monthly humidity of 70%, the grass had been irrigated using potable water twice a week. During the rainy season, no additional water was provided. The maximum average rainfall was recorded in August, 2019 and was close to 350 mm (BMD, 2019). After 12 months of plantation and conducting the rainfall test on all the models, measurements of maximum shoot length, maximum root length, clump diameter and root diameter were taken. The average increase of the

number of tillers per point was also recorded. The schematic diagram of a model with vetiver grass is presented in Figure 4.6. The results of measurements have been presented in Table 4.3. Figure 4.7 shows the conditions of the models before rainfall tests and the different steps of measurement recording. It can be observed that the average root length varies between 66.7 cm to 41.5 cm. The average shoot length is in the range between 210.8 cm to 160.9 cm. The average clump diameter is between 10.1 cm to 15.90 cm. The root diameter varies between 1.6 mm to 2.5 mm. The growth is also satisfactory in terms of number of tillers as they increased from 3 to 23 on an average.

From Figure 4.8, it is observed that the maximum root and shoot length have been obtained in M-2 which contained soil S-2 and are respectively 66.7 cm and 210.8 cm on average. However, the root diameter in this model is only 1.6 mm. The maximum average root diameter is obtained for soil S-1 in model 1, which is 2.5 mm. From Article 4.3, we have concluded that the nutrient content of the soil of the hills, both S-1 and S-2, is quite low, still the growth of vetiver in these soils is quite satisfactory. Though the nutrient content of S-1 is slightly better than S-2, the greater permeability of S-2 may facilitate more infiltration and percolation. Thus the roots can avail more water which enhances the growth. Also, from previous literature (Islam et al., 2013, 2016, 2017), better growth has been observed in case of sandy soil.

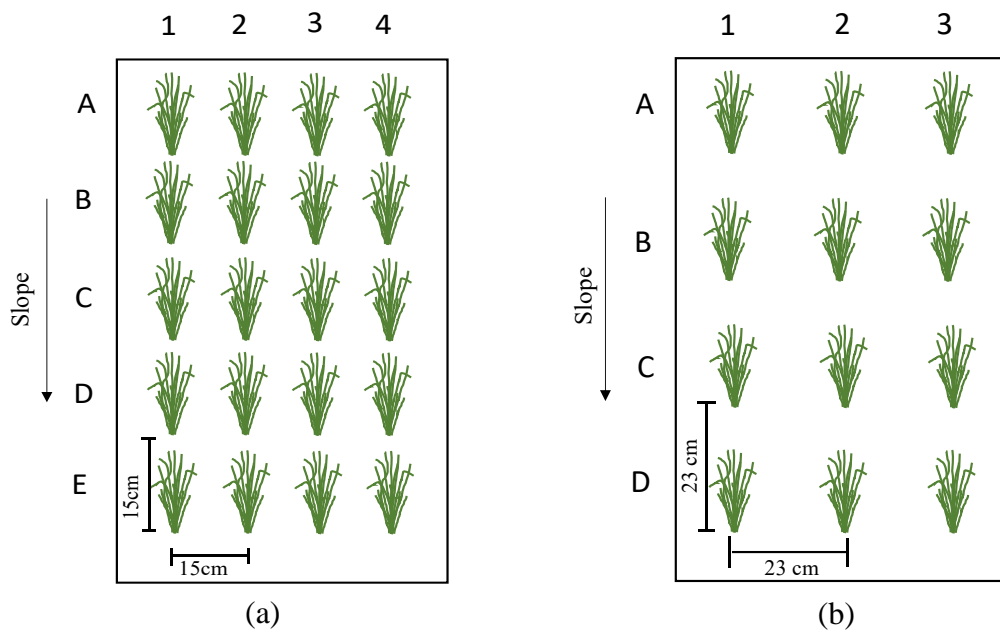


Figure 4.6: Schematic diagram (plan view) of vetiver grass plantation in glass models; (a) M-1, M-2, M-4, M-5; (b) M-3

Table 4.3: Different parameters of vetiver grass in different models with different soil types

Soil Type	Model Number	Row and Column	Maximum Shoot Length (cm)	Number of tillers	Maximum Root Length (cm)	Clump Diameter (cm)	Root Diameter (mm)
S-1	M-1	A1	162.5	13	66	12.7	2.6
		B2	205.7	14	51	12.7	1.7
		C3	213.4	17	45.7	15.2	2.8
		D4	--	--	71.1	17.8	2.8
	Average		193.9	15	58.5	14.6	2.5
	M-3	A1	223.4	37	35.6	7.6	2.5
		B2	205.7	31	53.3	15.2	1.6
		C3	173.7	25	35.6	7.6	1.4
	Average		200.9	31	41.5	10.1	1.8
	M-4	A1	223.4	31	66	25.4	1.1
		B2	190.5	25	61	17.8	2.8
		C3	180.1	32	45.7	15.2	2.8
		D4	--	--	35.6	5.1	2
	Average		198	29	52.1	15.9	2.2
	M-5	A1	213.4	21	76.2	17.8	2.5
B2		134.7	19	61	7.6	1.4	
C3		134.7	13	53.3	10.2	1.9	
D4		--	--	40.6	12.7	2.8	
Average		160.9	18	57.8	12.1	2.2	
S-2	M-2	A1	221	26	86.4	15.2	2
		B2	251.5	30	68.6	7.6	2.1
		C3	160	12	68.6	12.7	1.2
		D4	--	--	43.2	7.6	1.1
	Average		210.8	23	66.7	10.8	1.6



(a)



(b)



(c)



(d)



(e)

Figure 4.7: Measurement of growth of vetiver grass in different models with different soil; (a) Model condition before rainfall test, (b) Shoot length measurement, (c) Vetiver tillers with long roots, (d) Root distribution of vetiver grass, (e) Clump diameter measurement

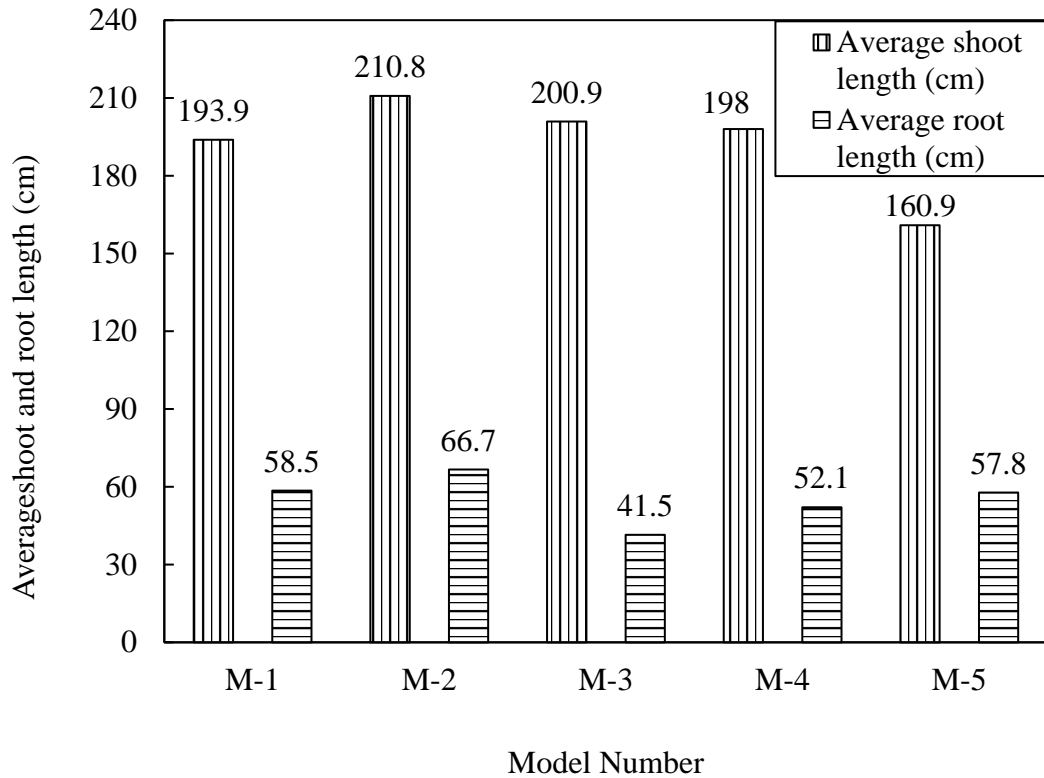


Figure 4.8: Average root and shoot length of vetiver for 5 different models

The previous study of Islam (2018) reported a maximum average root length of 35.6 cm in 3 months for clayey silty sand (SM-SC). In this study, in a growth period of one year, the roots reached almost 70 cm which is almost twice than the previous one. So, it can be inferred that, the roots may further grow and reach depths of 3-4 m as supported by literature. The average root diameter is also higher than that obtained by Islam (2018) which was 1.23 mm.

These observations also support the claim that vetiver can thrive even under nutrient stresses. Hence, considering the unbecoming soil condition of the hills of Chattogram, vetiver can be a viable option for increasing the slope stability of these hills along with erosion reduction as well as for soil quality conservation.

4.5 Reduction of Soil Erosion by Vetiver

4.5.1 Comparison between sediment yield generated from bare and vegetated soil of S-1

M-1 and M-6 were subjected to the same artificial rainfall having an intensity of 500mm/hr for 30 minutes after one year of plantation. These models consisted of sandy

silt. The eroded soil was collected, and oven dry weight was recorded. From this, we obtained that M-6 generated an erosion load of 11.7 kg in this duration. Whereas M-1 generated a load of just 0.63 kg in the same time span. So, the bare soil generated almost 18.5 times more eroded soil than model no. 1. Similarly, M-1, M-3 and M-5 which have vetiver grass with different plantation patterns, generate 0.54 kg, 0.59 kg and 0.30 kg of eroded soil respectively. According to the previous study of Islam (2018), the bare soil generated ten times more eroded soil than the vegetated soil for clayey silty sand under a much lower intensity of rainfall, 188 mm/hr. Thus, in case of sandy silt, the effect of vetiver grass in erosion reduction is found to be more pronounced than clayey silty sand. The better growth of vetiver grass in sandy silt may be responsible for such phenomenon.

The soil of Tiger pass is non-plastic sandy silt. The vetiver roots penetrate deep into the soil and the roots can grow up to 52 cm in sandy silt (Islam et al., 2013). In our study, we obtained the average root length to be 58.5 cm for M-1. This root structure of vetiver plays an important function in retaining the soil even under this high intensity rainfall. Vetiver (*Vetiveria zizanoides*) roots can have tensile strength as high as 60 MPa (Teerawattanasuk et al., 2014). The roots matrix of such high tensile strength increases the confining stress in the soil mass. The complex root structure tightly binds the soil mass and increases the shear strength. This phenomenon is completely absent in case of bare soil. Also there is no inherent cohesion. As a result, the soil erosion is much higher in M- 6 than in M-1.

Apart from the contribution of roots, the canopy provided by the vegetation also impacts the erosion process. When rainfall is the agent of erosion, the impact of raindrops weakens the bond between soil particles. When the infiltration capacity is exceeded, runoff starts, and the loose soil particles starts to flow with the runoff. However, the canopies work as a barrier between the rain drops and the soil. Figure 4.9 shows the arrangement of vetiver tillers in M-1 in one row, there are total 5 horizontal rows like this. These tillers keeps the elliptical projected area safe from rain fall by providing canopy. Thus, the impact energy is reduced and soil erosion decreases. From the experiment, it is also observed that the dense, stiff hedge of vetiver plants provide resistance to the runoff carrying the sediment. In Figure 4.10, we can see that the eroded soil gets stuck around the hedge of vetiver grass in M-1.

Hence, only the runoff water continues to flow downward. If this process continues, the sediments get deposited and a terrace is formed which continues to conserve the eroded soil (Carlin et al., 2003). On the other hand, in M-6, there is no resistance to the flow of sediment and so the eroded soil flows down with the runoff water. This results in a scoured surface which is shown in Figure 4.11 (a). It can also be observed that the amount of runoff is quite high for M-6 and the soil erosion started within 3 minutes of rainfall. Whereas, in Figure 4.12, condition of M-1 is shown. Here for the first five minutes of the rainfall test, almost no soil was eroded.

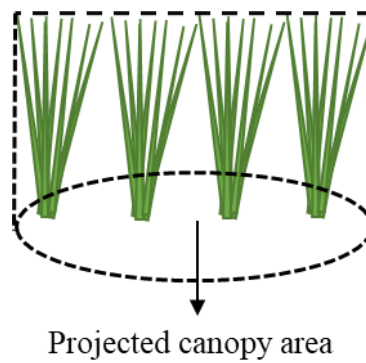


Figure 4.9: Canopy provided by vetiver tillers

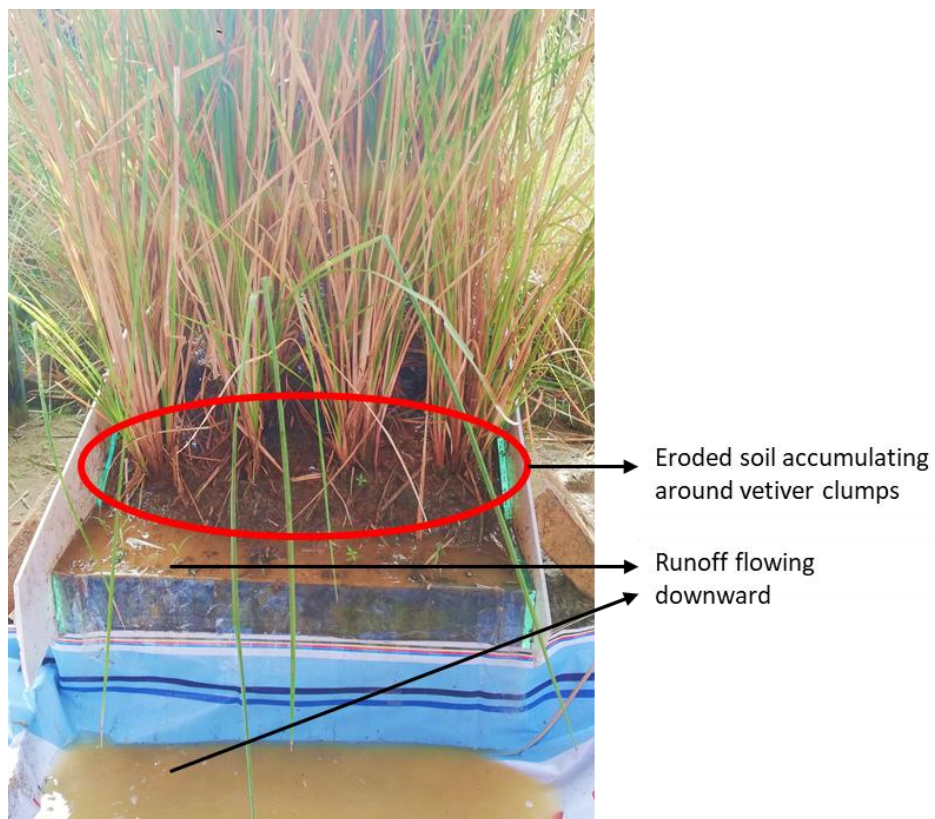


Figure 4.10: Soil accumulation around vetiver plants in M-1



Figure 4.11: (a) Eroded soil with runoff; (b) Eroded surface after rainfall of M-6



Small amount of eroded soil with low runoff

Figure 4.12: Rainfall test on M-1 generating low sediment yield

4.5.2 Effect of arrangement of vetiver on erosion control

4.5.2.1 Effect of number of tillers per point

M-4 generated a sediment yield of 0.59 kg, which is 6.3% less than M-1. Both the models had same arrangement but different number of vetiver tillers per point. M-1 had 3 tillers per point, whereas M-4 had 5. After 1 year, on an average, they had 15 and 29 tillers per point, respectively. However, the canopy cover provided by M-4 was 1.49 m², slightly less than M-1 which can be seen in Figure 4.13. Though negligible, one reason for the lower quantity of erosion of M-4 may be larger number of active tillers which generate greater number of roots and hold the soil firmly.

Also, the clump diameter of M-4 was 15.9 cm which was higher than the clump diameter of M-1 which was 14.6 cm. This may have also helped to provide better reinforcement and bondage between soil particles of M-4.

4.5.2.2 Effect of spacing between vetiver tillers

M-3 has vetiver tillers planted at 23 cm c/c spacing. On the contrary, the c/c spacing between vetiver tillers of M-1 and M-4 was 15 cm. From Figure 4.14, we can observe that M-3 produces erosion load of 0.54 kg, which is respectively 14.3% and 8.5% less than M-1 and M-4.

One probable reason for this may have been the dense and spread-out canopy provided by greater number of tillers. The average number of tillers for M-3 was 31 which was the highest among all five vegetated models. We know that the nutrient content of the soil was low. For this, there may have been a phenomenon of competitive growth between the vetiver plants. Initially M-3 had the lowest number of tillers, only 36, whereas both M-1 and M-4 had 60 tillers in total. Thus more nutrient was available for the growth of the tillers of M-3. As a result, the growth was higher.

The projected area of canopy cover provided by M-3 was 20% greater than M-1 and 22% greater than M-4. This provided more protection to the soil against the impact of rainfall and thus the erosion was reduced. So, the c/c spacing of 23 cm is found to be more effective in reducing soil erosion. However, for validation, the spacing parameters need to be studied further in large scale plantation.

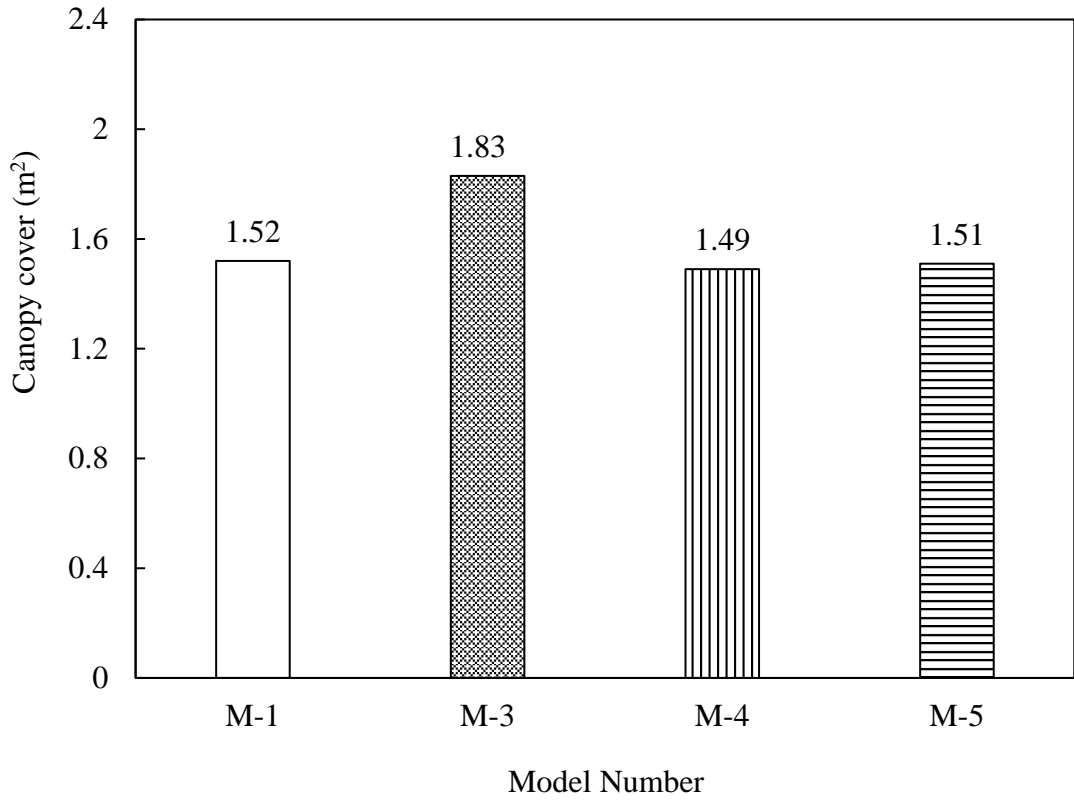


Figure 4.13: Area of canopy covers (m²) for different models

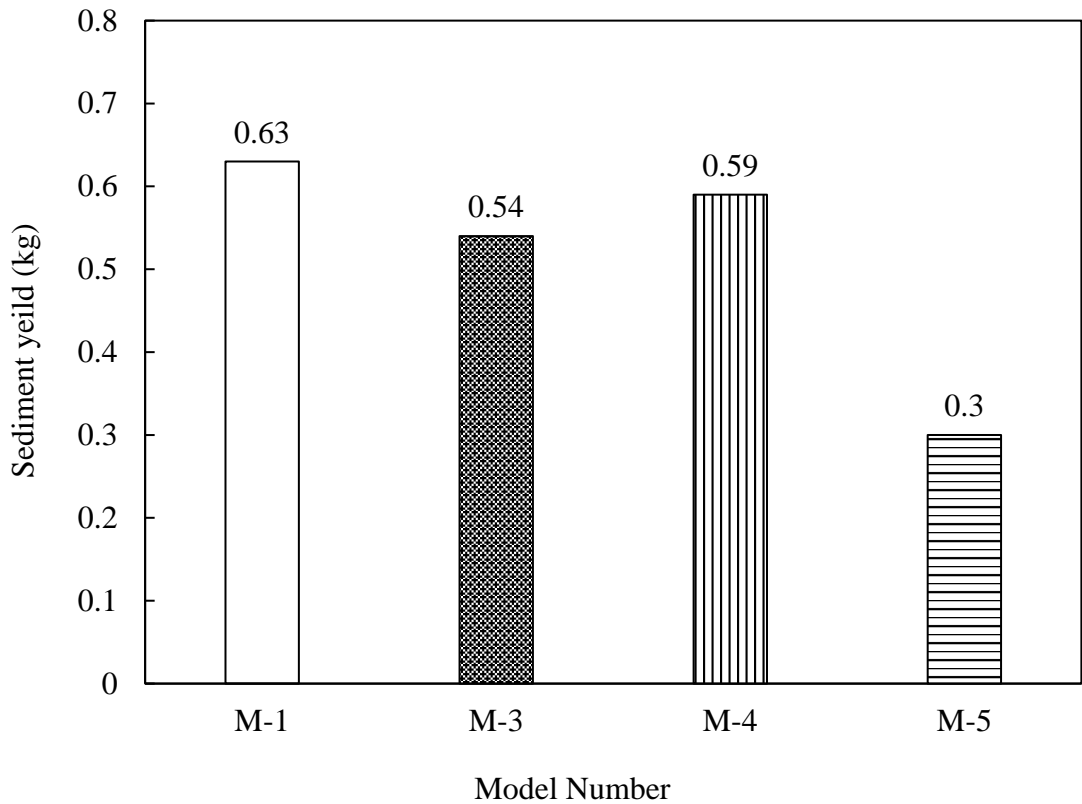


Figure 4.14: Sediment yield (kg) produced by different models after 30 minutes of rainfall with an intensity of 500mm/hr

4.5.3 Effect of jute geo-textile along with vegetation in erosion reduction

M-5 had two protective measures for erosion control: vegetation and jute geo-textile. The model with bare soil, M-6 generated an erosion load of 11.7 kg. Sole use of vetiver reduced this erosion by 94.6%, 94.9% and 95.4 % for M-1, M-4 and M-3, respectively. In M-5, the erosion load is 0.30 kg which is 97.4% lower than M-6. It is also lower than other three vegetated models of S-1 as seen in Figure 4.14. The jute geo-textile (JGT) covered the soil surface and reduced the probability of soil detachment. Moreover, when the eroded soil flows with the runoff water, its motion is impeded by jute geo textile. However, during the test, the JGT was a year old and the roughness had reduced. Thus it can be inferred that its effect could have been much prominent in the initial days. Geo-textile also influences the growth of vegetation positively. As jute geo-textile has a good moisture retention capacity, it creates a moist environment around the soil surface that is conducive to rapid growth of vegetation (Molla, 2014). Due to this combined reinforcing of JGT and vegetation, along with the positive impact on vegetation growth, the erosion was least in M-5 compared to all the other models of S-1.

4.5.4 Effect of vetiver on erosion reduction of different soil type

M-1 and M-2 had vetiver tillers planted in the same pattern but consisted of different soil. When both the models were exposed to same rainfall intensity for thirty minutes, M-1 generated an erosion load of 0.63 kg and M-2 generated an 84.1% lower erosion load of 0.10 kg. Though the vegetation growth in both the models were similar, this significant difference in erosion is observed due to the soil type.

In case of evaluating soil erodibility, the presence of silt is considered as the most important factor. Silt size particles can easily reduce the permeability of the soil due to their small size. As rainwater falls on slopes, a part of it is infiltrated and some flows along the slope as runoff. When silt size particles start to flow with the runoff it easily blocks the pore spaces of the soil. This results in greater runoff along with greater erosion load (Goldman et al., 1986). M-1 is sandy silt which contains 65.64% silt. M-2 is comprised of silty sand, where the main soil type is sandy. Hence, M-1 has greater potential of soil erosion. Considering the dimensions of the glass model and applying Universal Soil Loss Equation (USLE), S-1 and S-2 generate a soil loss of 417.84 ton/ha/yr and 170.8 ton/ha/yr. According to the soil erodibility class, both the soil are

of very high erodibility (Balasubramani et al., 2015). However, we can also observe that the soil loss for S-2 is less than S-1. According to the USLE, the soil loss depends on 5 different factors, among which soil erodibility (K) is one. K is a measure of susceptibility of soil particles to detachment by rainfall and runoff. The value of K has been obtained as $0.071 \text{ t ha h ha}^{-1} \text{ MJ}^{-1} \text{ mm}^{-1}$ for sandy silt. Whereas it is only $0.029 \text{ t ha h ha}^{-1} \text{ MJ}^{-1} \text{ mm}^{-1}$ for soil S-2. Considering all the other 4 factors are same for M-1 and M-2, it is the value of K that causes this difference between eroded sediment yield.

4.6 Effect of Vegetation on Infiltration and Runoff

4.6.1 Comparison between vegetated and bare models for same soil type

Figure 4.15 shows the decrease in volume of infiltration with time for M-1 and M-6. It can be observed that, at a given time, the infiltration volume is higher for M-1 than M-6 and both decrease with time. The cumulative infiltration after 30 minutes of rainfall for M-1 was 0.12 m^3 . For M-6, in the same time span, it was 0.09 m^3 which is 25% lower than M-1.

Infiltration effects the magnitude and timing of the runoff, thus is related to erosion. When under rainfall, as the water retention capacity of soil decreases with time, the infiltration decreases (Meeuwig, 1970). The presence of vetiver effects the infiltration as vetiver cover impedes the motion of runoff allowing more time for the water to infiltrate into soil. As a result, the volume of infiltrated water increases. However, in bare soil, e.g. M-6, there are no barriers to slow down the runoff. This runoff erodes and transports fine particles, which fills the pore spaces and infiltration is further reduced (Horton, 1933). This can also be observed from the Figure 4.15, as the infiltration decreases rapidly in M-6 as compared to M-1. As a result of more infiltration, the runoff generated from vegetated models is lower than bare soil which can be seen from Figure 4.16. It shows the cumulative runoff of four vegetated models (M-1, M-3, M-4 and M-5) and one bare model (M-6) composed of soil S-1.

4.6.2 Comparison between vegetated models of different soil type

Figure 4.17 shows the relationship between infiltration and time for both M-1 and M-2. It can be observed that the decrease rate of infiltration is quite low for M-2, whereas

it is high for M-1. This is due to the difference of permeability between the two types of soil that M-1 and M-2 consists. The soil of M-1, S-1, is sandy silt having a permeability of 4.61×10^{-7} - 1.56×10^{-6} m/s. M-2 is composed of S-2, silty sand, and has a permeability much higher than S-1; 3.71×10^{-5} - 5.30×10^{-5} m/s.

The amount of water infiltrating into slope mainly depends on soil infiltration capacity, which eventually depends on, permeability coefficient (Zhang et al., 2014). As the permeability of S-2 is higher, so is the infiltration capacity. For this, the infiltrated water also gets drained easily through the bottom of the glass model. The total infiltration after 30 minutes of rainfall for, S-2 was 0.155 m^3 which is almost 1.3 times higher than S-1 which had an infiltration of 0.12 m^3 . Observations from the experiment also show that the start of runoff was delayed in M-2 when compared to M-1. As discussed earlier, rainfall causes disintegration of soil particles which flow down with runoff. Once the threshold of infiltration capacity of the soil is reached, runoff starts, and it carries the detached soil particles along with the nutrients of topsoil.

Though the runoff was similar in first few minutes, cumulative runoff of M-2, after thirty minutes of rainfall was 0.025 m^3 . Figure 4.18 shows that M-1 generated a cumulative runoff of 0.06 m^3 which is 2.4 times higher than M-2. The slope with poor permeability and steep slope is conducive to the runoff of rainwater that could not infiltrate into soil in time (Horton, 1933). Similarly, M-1 comprising of low permeability soil S-1, generates more runoff and eventually more eroded soil than M-2 in the same timeframe.

4.7 Change of Slope Angle due to Erosion

Rainfall events effects the slope angles. In this experiment, the initial slope angle for all the models was 37° . The slopes changed due to natural erosion process. The reduced slope angles varied between 29° to 34° , which was due to natural process. Figure 4.19 shows the slope angles of the models before and after the rainfall simulation. It can be observed that for all the vegetated models, e.g. M-1 to M-5, the slopes remained same before and after the test. However, the slope angle changed from 29° to 22° for M-6, which was the bare model without any vegetation. This shows that vetiver has been effective in conserving the slope by reducing the erosion.

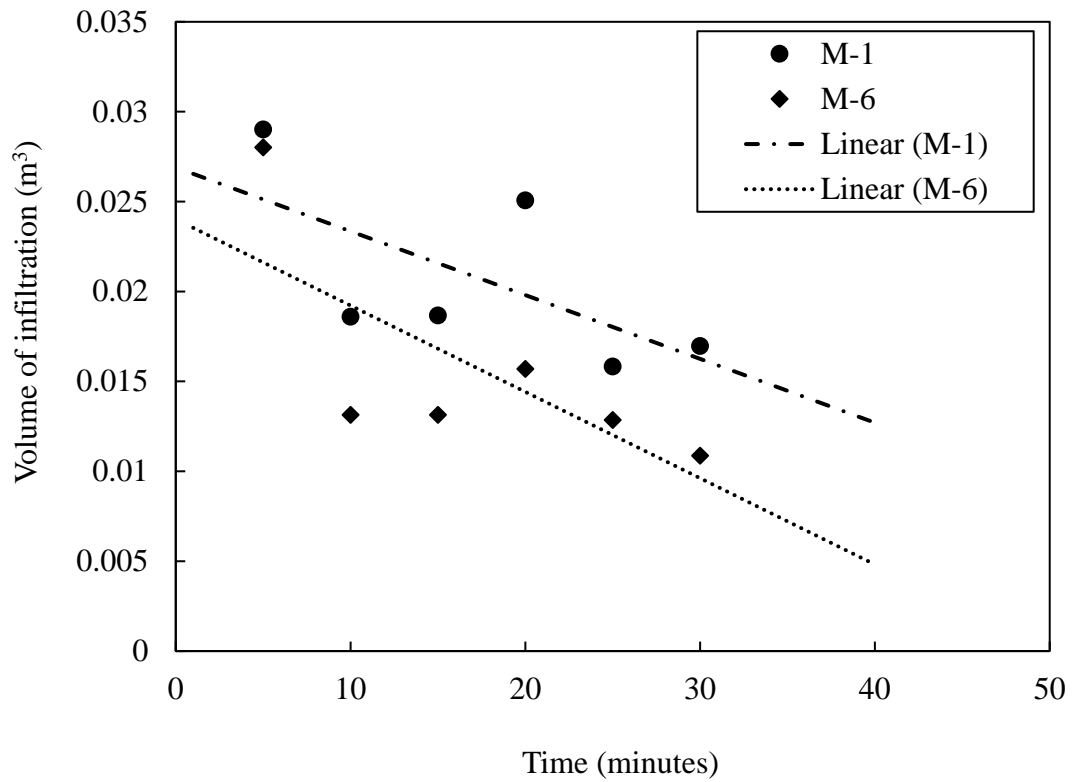


Figure 4.15: Variation of volume of infiltration (m^3) with time (minutes) for M-1 and M-6

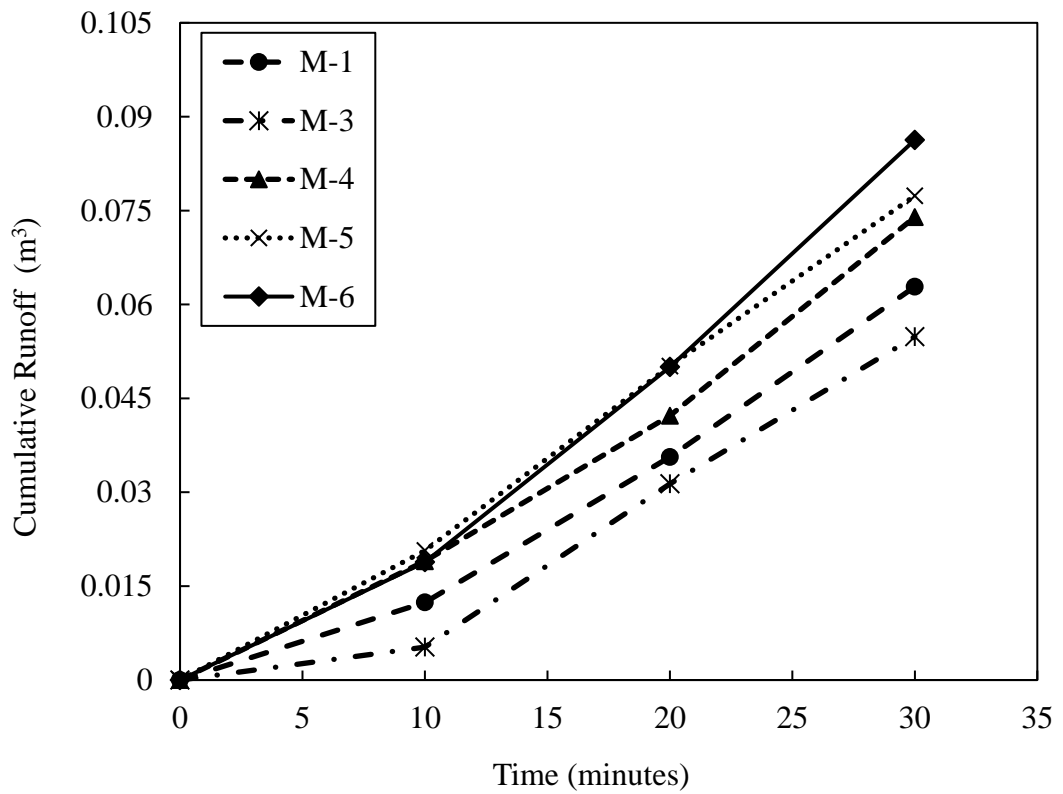


Figure 4.16: Cumulative runoff (m^3) of M-1, M-3, M-4, M-5 and M-6 with time (minutes)

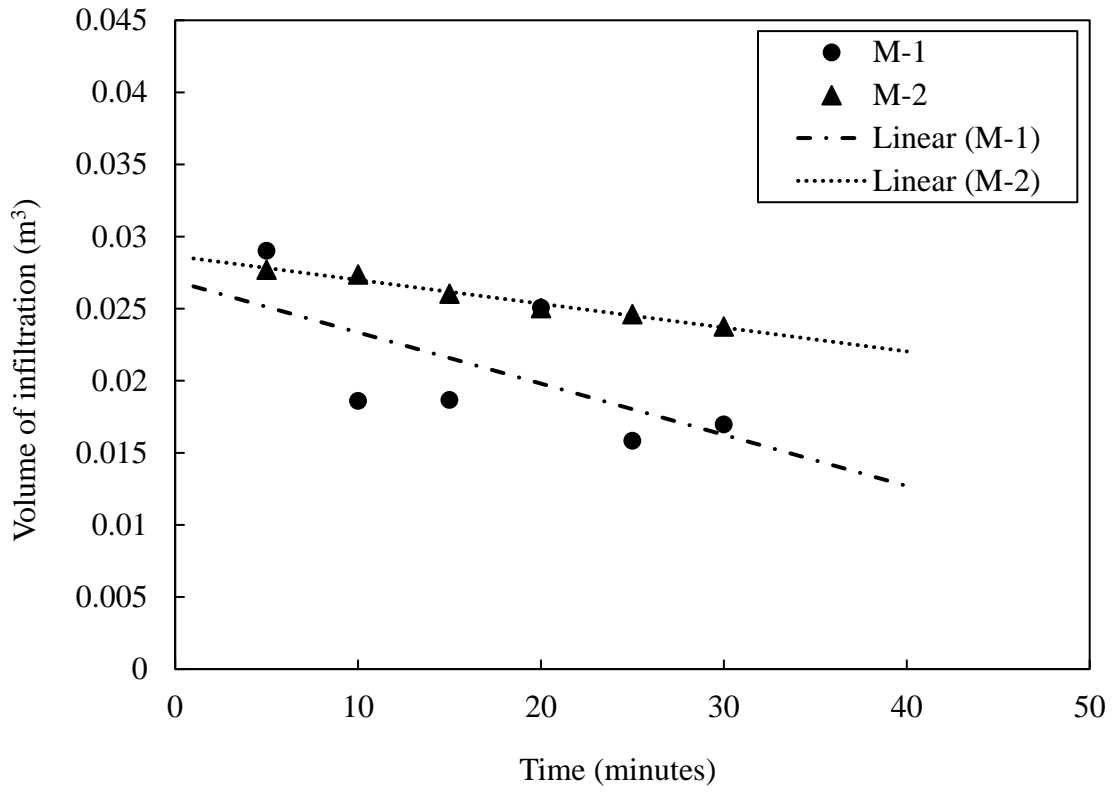


Figure 4.17: Variation of volume of infiltration (m^3) with time (minutes) for M-1 and M-2

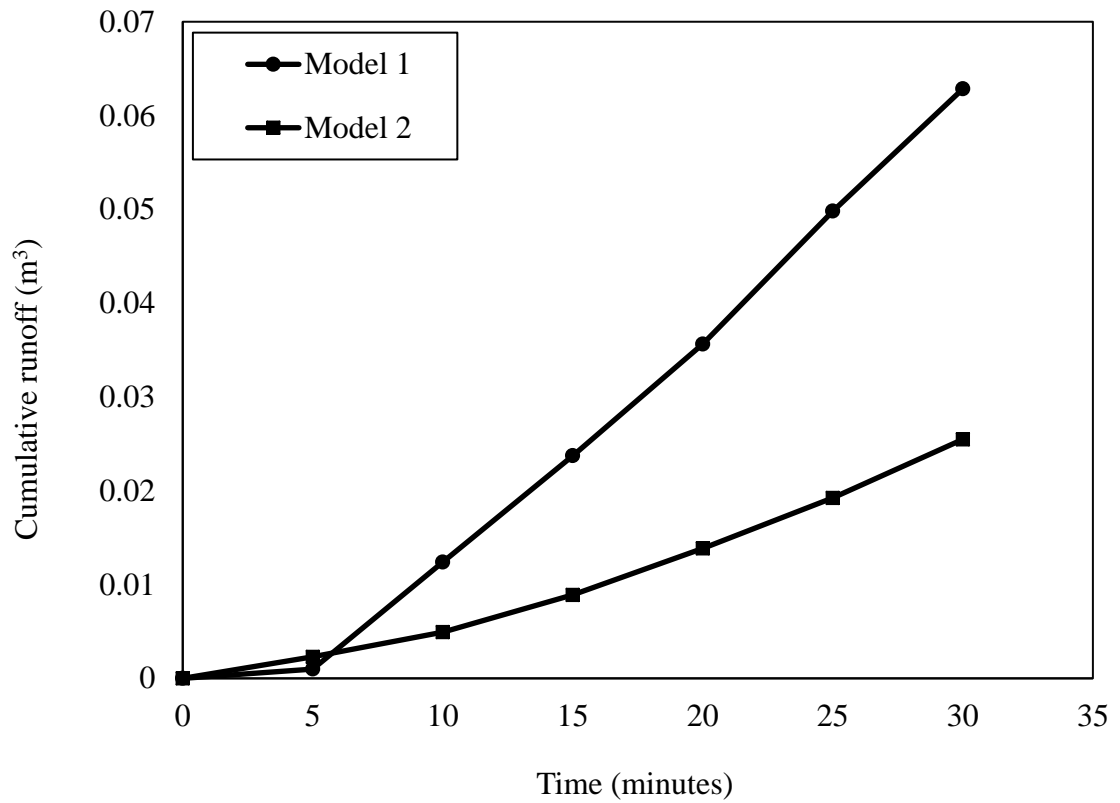


Figure 4.18: Cumulative runoff (m^3) of M-1 and M-2 with time (minutes)

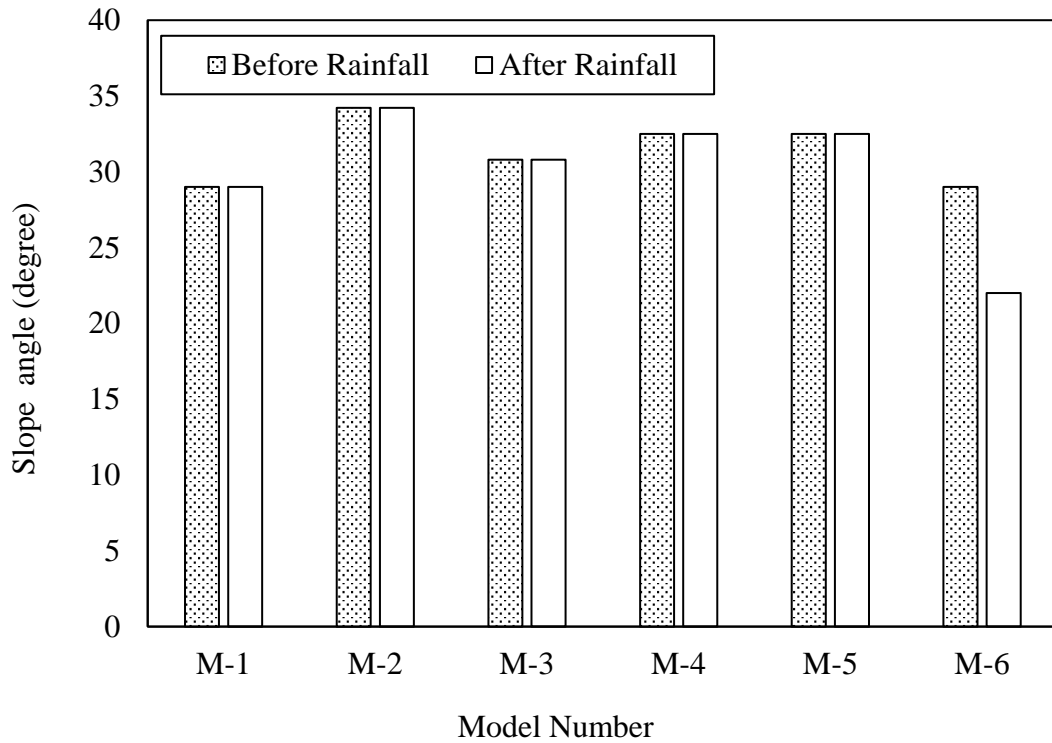


Figure 4.19: Slope angles (degree) for different models before and after rainfall

4.8 Effect of Slope Angle on Soil Erosion

The slope angle has a major role in determining the erosion potential of soil. While applying the USLE, we can observe the effect of slope length and steepness factor (LS) is quite prominent. When the slope gradient was 1V:1.33H, the obtained soil loss for S-1 was 2414.87 ton/ha/yr which drastically increased to 4636.76 ton/ha/yr when the slope gradient was increased to 3V:1H. Similar occurrence were observed for S-2. At lower gradient it produced a soil loss of 986.35 ton/ha/yr which increased to 1893.88 ton/ha/yr as the gradient became steeper. So, the steeper the slope angle, the greater will be the soil erosion. This will eventually lead to instability of the existing slope.

4.9 Results from Numerical Analysis

For the numerical modeling and analysis, the soil properties mentioned in Table 4.1 were used as input parameters. Apart from these, Young's modulus and Poisson ratio were taken from Bowels (2012). According to Bowels (2012), the Young's modulus E , for both the soil, was taken as 15×10^3 kPa and Poisson ratio was considered as $\nu=0.3$. The soil was considered as homogenous.

4.9.1 Stable angle for bare slope

Figure 4.20 shows the relationship of factor of safety with slope angle β for a natural slope with slope height (H) of 15m.

The results depict, as the slope angle is decreased, the factor of safety increases. So, slope angle has a prominent effect on the slope stability and low to moderate slopes are more stable (Chok et al., 2015; Kokutse et al., 2016; Tsige et al., 2020).

For S-1, at 38° , the factor of safety was 1.014. As the slope angle increases to 39° , factor of safety became less than 1.0. For S-2, at 30° the factor of safety was 1.010 and an increased slope angle yielded factor of safety < 1.0. So, these two angles, e.g. 38° for S-1 and 30° for S-2, can be defined as the maximum angles where the slope will be stable under existing condition. As the slope becomes steeper, the tendency of downward movement of materials by gravitational force becomes greater (Biswas et al., 2017). This generates higher shear stresses and results in increased instability. The existing slope angles of Tiger Pass and Berma Haji hill are higher than their respective safe slope angles. Hence, the existing bare hills are unstable, and measures need to be taken towards stabilizing them.

Again at the same slope angle, e.g. 30° , the factor of safety in S-1 was higher than S-2. Hence, we can say that at bare condition, S-1 will be more stable than S-2 at steeper slopes. The higher angle of internal friction of S-1 may be responsible for this because it has higher shear strength than S-2.

4.9.2 Effect of vetiver on slope stability of natural slope

4.9.2.1 Effect of spatial distribution

Vetiver's effect was incorporated in increasing the slope stability at respective safe slope angles of S-1 and S-2 thus at $\beta=38^\circ$ and $\beta=30^\circ$ and till the root zone depth of 0.5m. Vetiver can naturally grow at any part of the hill and hence the effect of its growth on different parts of the slopes had also been investigated. The results are presented in Table 4.4.

From the results, it can be noticed that the maximum increase in factor of safety due to incorporation of vegetation was achieved when the whole slope surface, including top and bottom of the slope, was covered with vetiver. For both the soil types the

increase was nearly same. Hence, the observations conclude that to obtain maximum advantage, the entire slope should be covered with vetiver as suggested by previous studies of Chok et al., (2015) and Tsige et al., (2020).

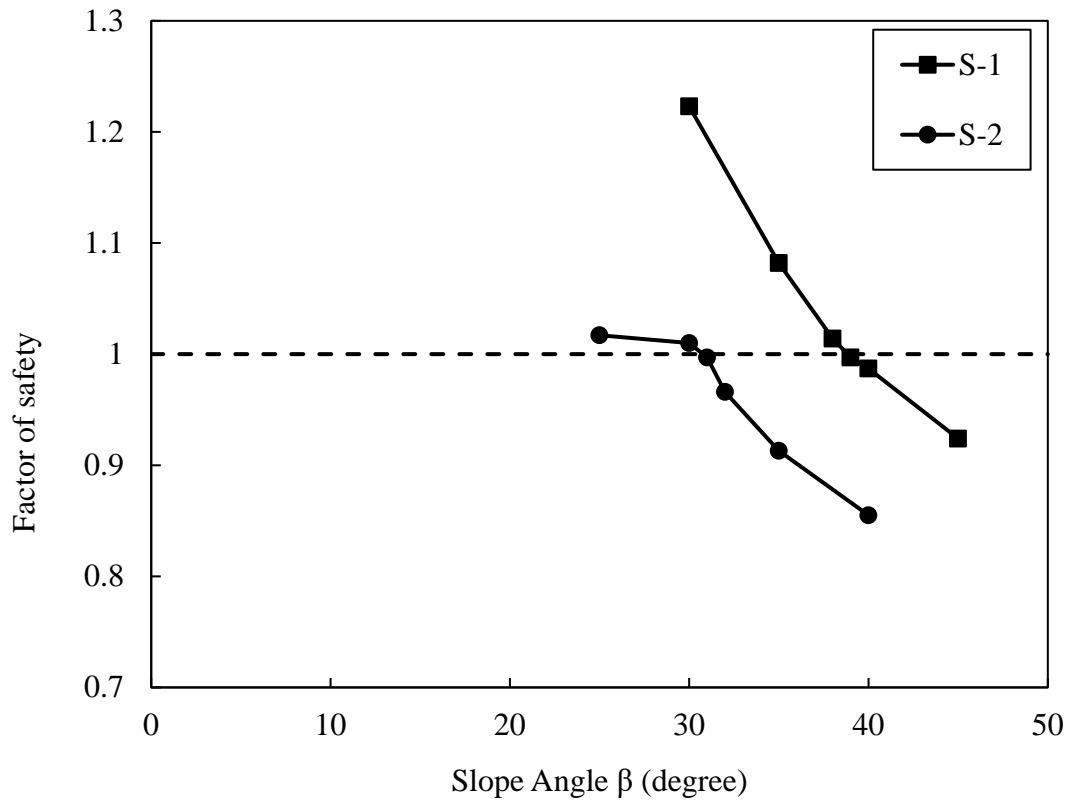


Figure 4.20: Change of factor of safety with slope angle (degree) for natural slope (H=15m)

Table 4.4: Factor of safety of rooted soil

Soil Type	Condition of soil	Bare slope	Vetiver on entire slope (including top and bottom surface)	Vetiver only on inclined surface of slope	Vetiver on top of slope	Vetiver on toe of slope
S-1	Factor of safety	1.014	1.071	1.017	1.032	1.017
	% increase in factor of safety	-	5.6	0.3	1.8	0.3
S-2	Factor of safety	1.010	1.064	1.045	1.024	1.024
	% increase in factor of safety	-	5.4	3.5	1.4	1.4

4.9.2.2 Effect of root zone depth

The factor of safety at different root zone depths (h_r) is presented in Table 4.5. It can be observed from Table 4.5 and Figure 4.21 that with the incorporation of vetiver the factor of safety increases.

Figure 4.22 shows the percent increase in factor of safety with increase of the root zone depth. As vegetation is added to the soil, the thin roots of vetiver, while interacting with soil, provides additional cohesion (Waldron and Dakessian, 1981; Stokes et al., 2009; Teerawattanasuk et al., 2014). When the effective root zone was up to 0.5m, the factor of safety increased about 6% for both the soil types which is quite insignificant. As the depth of root zone increased, factor of safety increased. The incorporation of root also reduced the total displacement as shown in Figure 4.23, Figure 4.24 and in Figure A.1 to Figure A.8 (Appendix-A).

The percent increase in factor of safety became substantial, almost 13% - 16%, once the root zone depth was greater than 2m. Islam et al. (2020) also observed that for silty sand, vetiver roots can increase the factor of safety around 15%. However, the added cohesion of roots alone cannot provide the desired stability if they cannot reach the slip surface. The roots need to intercept the shear surface (Kokutse, 2003; Chok et al., 2004; Kokutse et al., 2016) which may be located up to 2m below the soil surface (Norris et al., 2008). As the roots at greater depth transverse the critical failure, the factor of safety increases due to the mechanical effect of the roots. Thus, the substantial increase in factor of safety after root zone depth reaches 2m and beyond can be justified.

However, the factor of safety here may be underestimated as the aspect of hydrological reinforcement via evapotranspiration and changed hydraulic properties of soil induced though roots have not been taken into consideration. Uptake of water by roots generates suction which increases soil shear strength (Ng and Menzies, 2007). The effect of suction goes beyond root zones and has been reported to be as much as 4 times the root depth (Ng and Shi, 1998; Ng et al., 2013; Ng et al., 2014). Previous study by Ni et al., (2017) suggest that the mechanical effect of roots is important in addressing shallow slope stability problem, and the effect of hydrological reinforcement is pronounced due to higher preserved suction at depths of 1-2m, where critical slip surfaces typically generate.

Another observation that is made, at the same root zone depth the increase in factor of safety is higher for S-1, even though the slope angle is steeper than S-2. The additional cohesion provided by the roots are same for both the soil, however, S-1 has a greater angle of internal friction which results in additional shear strength. Thus even at steeper slope angles, the effect of vetiver is more pronounced for S-1.

Table 4.5: Factor of safety at different root zone depths

Soil Type	Slope angle β	Factor of Safety						
		Bare soil	Root zone depth (h_r) (m)					
			0.5	1.0	1.5	2.0	2.5	3.0
S-1	38°	1.014	1.071	1.097	1.118	1.132	1.152	1.173
S-2	30°	1.010	1.064	1.079	1.081	1.103	1.136	1.171

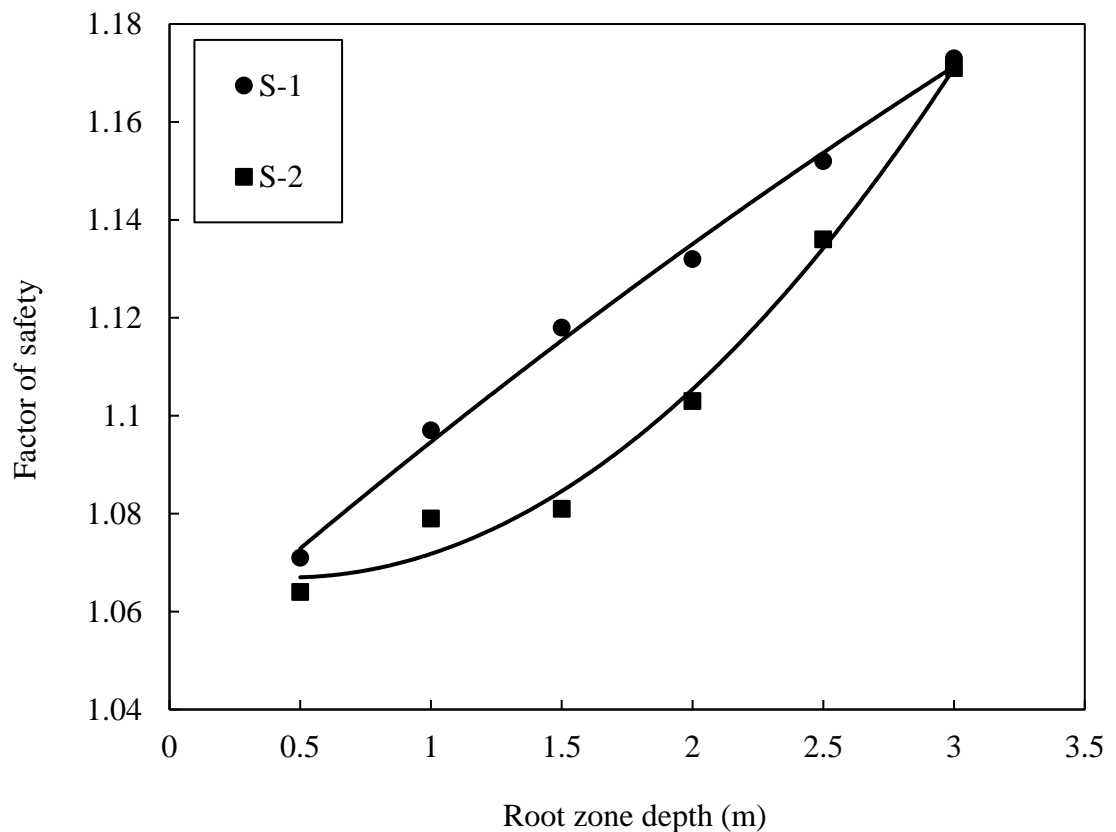


Figure 4.21: Change of factor of safety with root zone depth (m) for S-1 and S-2

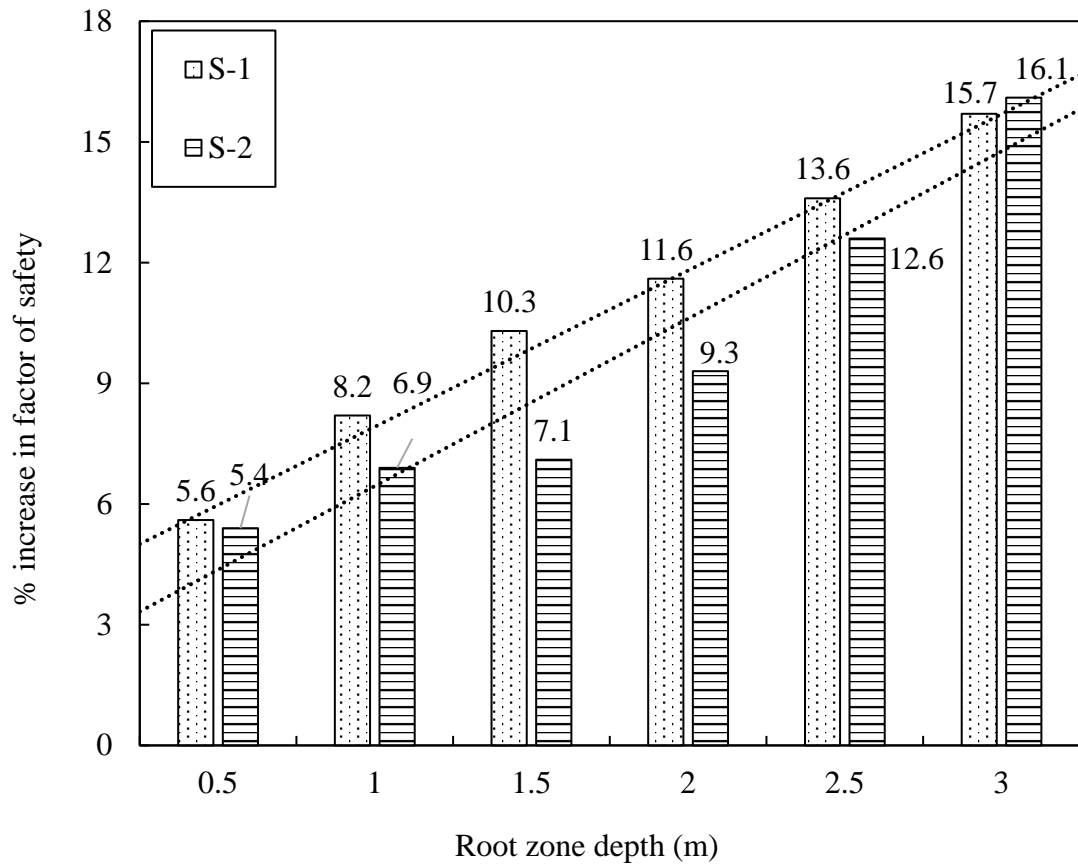


Figure 4.22: Percent increase in factor of safety at different root zone depths (m)

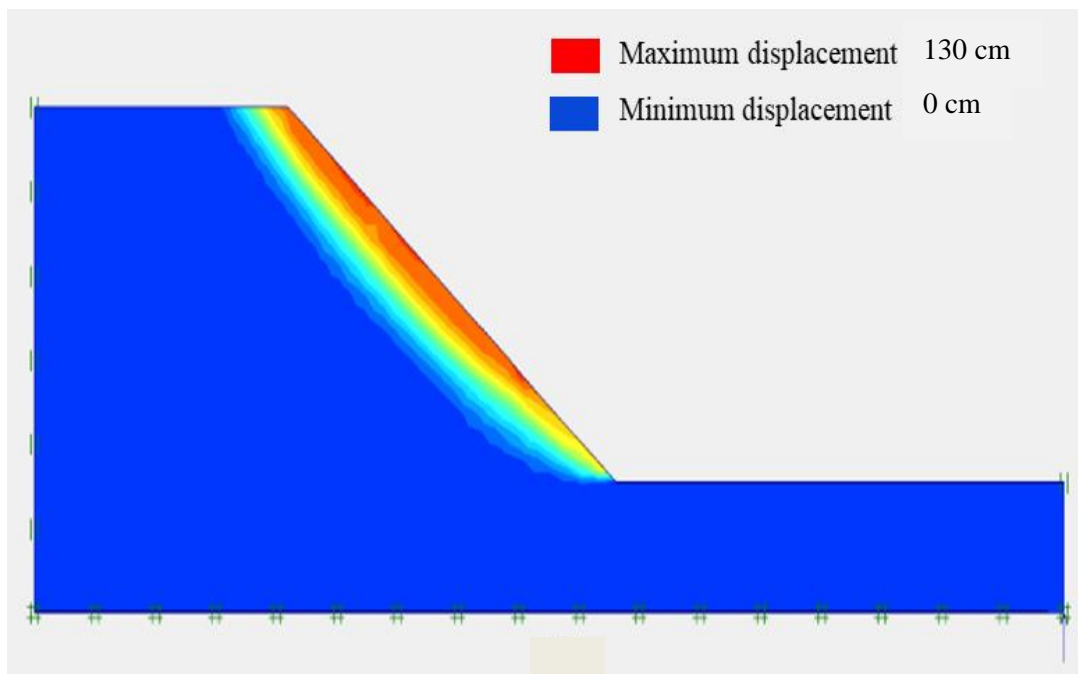


Figure 4.23: Total displacement at bare condition for S-1

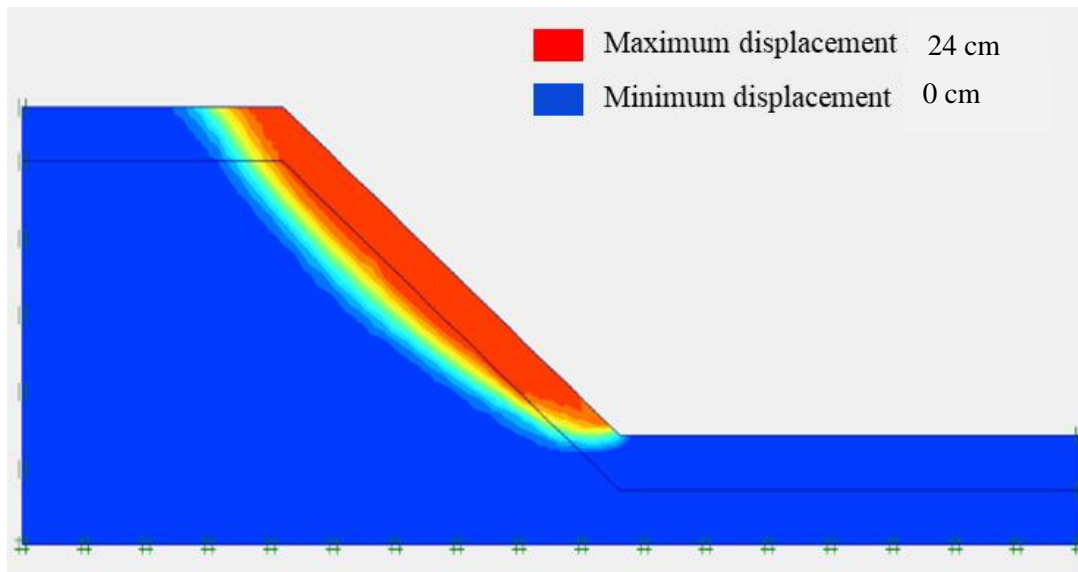


Figure 4.24: Total displacement at rooted condition ($h_r=2m$) for S-1

4.9.3 Threshold angles for stable natural slope with vetiver

Table 4.6 presents the value of the maximum angle (β_{lim}) up to which the reinforcement due to roots of vetiver was effective. The results were obtained by determining the limiting angle for varying root zone depths and taking the mean value along with standard deviations.

The results suggest that vetiver can be effective in providing stability to the natural slope up to a certain slope angle. At β_{lim} the factor of safety is marginal and is around 1.01-1.02. When $\beta > \beta_{lim}$ occurs, the effect of roots mechanical reinforcement is nullified by the steepness of the slope. The observations also show that, the threshold angle for S-1 is much larger than S-2. Thus, vetiver proved to be more effective in case of sandy silts compared to silty sand. In cases, where slope angles are greater than β_{lim} , alternate measures need to be considered for providing sufficient safety to the slopes (changing geometry, using nails etc.)

Table 4.6: Threshold angle for natural slope with $H=15m$

Soil Type	Threshold angle (β_{lim}) ^o	Factor of Safety
S-1	46.33±3.50	1.01±0.01
S-2	33.33±1.97	1.02±0.01

4.9.4 Stability analysis of terraced slopes

As discussed in the previous section, the effect of vetiver is reduced as the slope becomes steep and becomes absent at $\beta > \beta_{lim}$. Apart from slope angle, another aspect of slope geometry plays an important part in ensuring slope stability, e.g. the slope height. Terracing practices for cultivation are common in the hill tracts and terracing can reduce the slope height.

4.9.5 Safe angles for different step heights of terraced slope

The geometry of the slope was changed by terracing the slope in 2 steps (each of 7.5m height) and 3 steps (each of 5m height). Figure 4.25 shows the variation of slope angle with height of each step (H_T). The results show that for S-1, when $H_T = 7.5m$, the safe slope angle increased from 38° to 46° . When H_T was further reduced to 5m the safe slope angle increased to 55° . So, reducing the slope height has a positive impact on slope stability.

This impact was not so prominent in case of S-2. As compared to the natural slope having a height of 15m, when the slope height was reduced to 7.5m and then to 5m by terracing, the increase in stable slope angle was very negligible, 1° and 2° respectively. However, as the number of steps was increased and the slope height was further reduced to 3m, the stable slope angle increased to 45° . The reduced height of the slopes advocate for this advantage gained in case of stable slope angles at fallow condition. This signifies that terracing with a suitable slope height can be adopted as a measure to increase the stability of the barren hills.

4.9.6 Effect of vetiver on terraced slope

Table 4.7 and

Table 4.8 present the factor of safety for different slope heights, thus step heights, for different h_r . From Figure 4.26 it can be seen, even in case of terraced slope, with the increase in root zone depth, the factor of safety increased for both type of soil as observed earlier. However, the increase in factor of safety due to the presence of vetiver roots was much higher for terraced slopes.

For S-1, for natural slope ($H=15\text{m}$) and $\beta=38^\circ$, the maximum factor of safety was 1.173 with $h_r=3\text{m}$. For terraced slope with $H_T=7.5\text{m}$, at $\beta=46^\circ$ the maximum factor of safety was found to be 1.378 with $h_r=3\text{m}$.

As shown in Figure 4.27, in the latter case, the percent increase in factor of safety, from bare to vegetated condition, was 36%, which is greater than the 15.6% increase in the previous case, that too at steeper slope angle. As the step height is reduced to 5m and slope angle was increased to 55° , nearly 54% increase in factor of safety is obtained at $h_r=3\text{m}$ and the factor of safety was 1.598. Similarly for S-2, for $H=15\text{m}$, the maximum increase of factor of safety due to mechanical reinforcement of vetiver was only 16.1% at $\beta=30^\circ$.

On the contrary, even at slightly higher angles viz, 31° and 32° , the terraced slope's factor of safety increased nearly by 42% and 64% at $h_r=3\text{m}$ as shown in Figure 4.28. Hence, it can be inferred that the step height has a prominent effect on slope stability and by reducing it stability of the slope can be ensured and effectiveness of vetiver can be maximized.

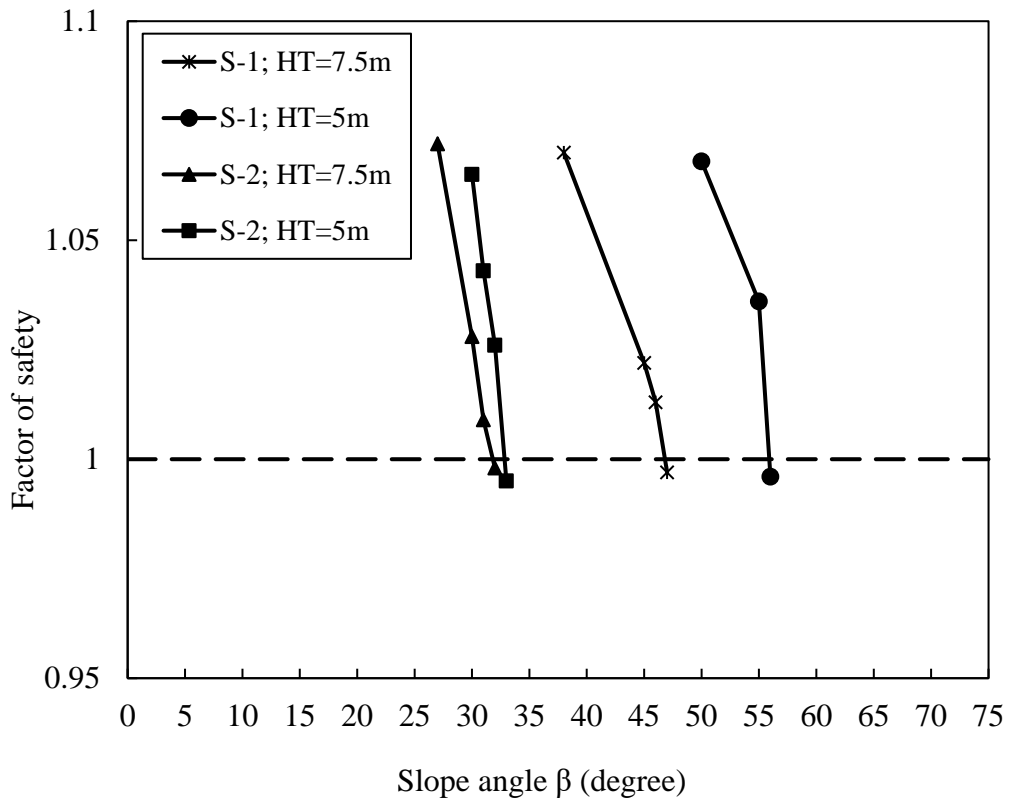


Figure 4.25: Factor of safety for different slope height (m) and slope angles (degree) for terraced slope

Table 4.7: Factor of safety at different root zone depth for terraced slope for S-1

Step height (H _T) (m)	Slope angle β (°)	Factor of Safety						
		Bare soil	Root zone depth (h _r) (m)					
			0.5	1	1.5	2	2.5	3
7.5	46	1.013	1.160	1.228	1.287	1.291	1.327	1.378
5	55	1.036	1.252	1.350	1.389	1.443	1.516	1.598

Table 4.8: Factor of safety at different root zone depth for terraced slope for S-2

Step height (H _T) (m)	Slope angle β (°)	Factor of Safety						
		Bare soil	Root zone depth (h _r) (m)					
			0.5	1	1.5	2	2.5	3
7.5	31	1.009	1.150	1.205	1.247	1.326	1.374	1.432
5	32	1.026	1.211	1.331	1.454	1.515	1.62	1.678

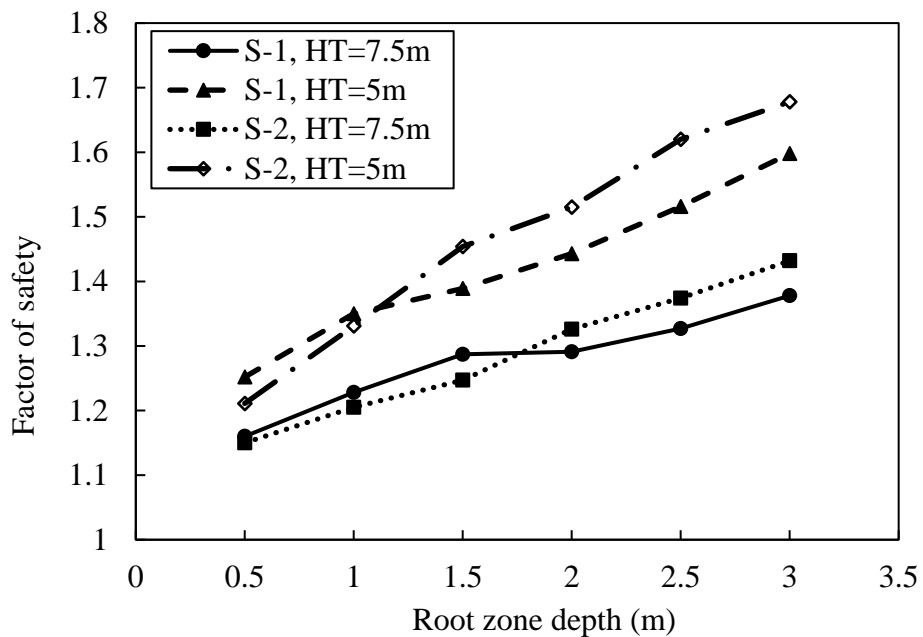


Figure 4.26: Change of factor of safety with increasing root zone depth (m) for terraced slope

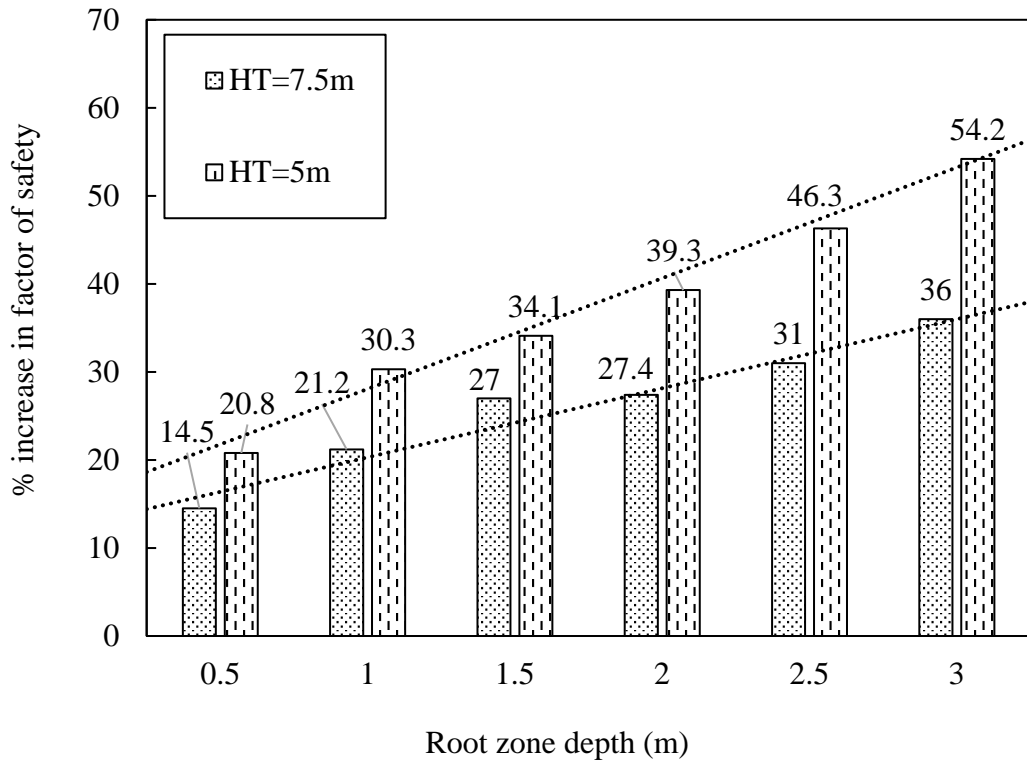


Figure 4.27: Percent increase of factor of safety with varying root zone depth (m) for terraced slope for S-1

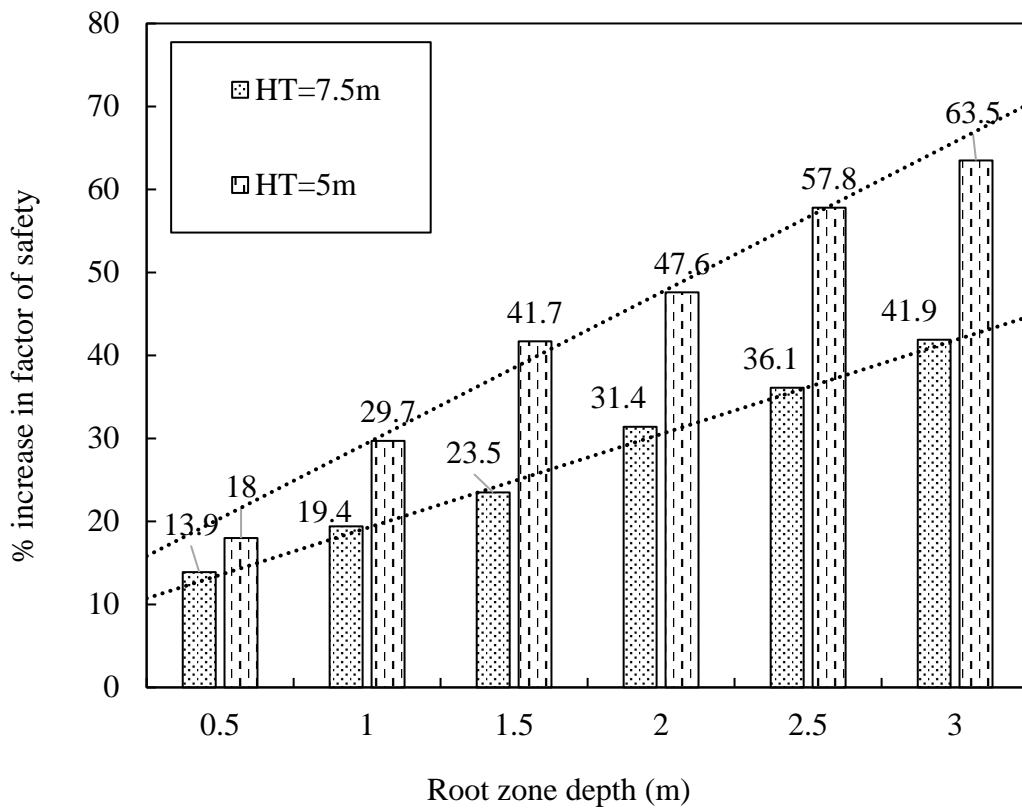


Figure 4.28: Percent increase of factor of safety with varying root zone depth (m) for terraced slope for S-2

4.9.7 Threshold angle for stable terraced slopes with vetiver

As the slope height was reduced by terracing, the threshold angles also increased, and vetiver was effective in increasing factor of safety for higher slope angles. The results of threshold angle of stable terraced slope with vetiver is presented in Table 4.9.

Attempts of stabilizing slopes with vetiver can be successful up to a slope angle of 81.67° by terracing a slope of $H=15\text{m}$ into two steps, each having $H_T=7.5\text{m}$ for soil type S-1. By further reducing the step height to 5m provide a factor of safety of 1.20 ± 0.11 at $\beta=90^\circ$. For S-2, the threshold angle was increased from 33.33° and reached nearly to 71° by making terrace with three steps, each having $H_T=5\text{m}$. However, to stabilize vertical slopes with vetiver, the step heights need to be reduced further. When 5 steps are generated, each with $H_T=3\text{m}$, factor of safety of 1.35 ± 0.12 was obtained at $\beta=90^\circ$.

Hence, for S-1, a step height greater than 5m but less than 7.5m may produce an optimized step height for stabilizing vertical hill cuts with vegetation. For S-2, this range will be within 5m - 3m . Restoration of stable slope following this process of terracing also require lower amount of earthwork compared to that of natural slopes.

Table 4.9: Threshold angle for stable terraced slopes with vetiver for S-1 and S-2

Soil Type	Slope height (H_T) (m)	Threshold angle (β_{lim}) $^\circ$	Factor of Safety
S-1	7.5	81.67 ± 10.33	1.02 ± 0.02
S-2	7.5	47.83 ± 7.57	1.020 ± 0.005
	5	70.33 ± 12.48	1.01 ± 0.008

4.9.8 Parametric study

4.9.8.1 Relation between factor of safety and root zone depth

Figure 4.29 shows the relationship of factor of safety with root zone depth. The values of factor of safety were obtained by taking the average factor of safety for six different root zone depth (h_r) for different slope heights (both single and terraced slope) at

varying slope angles ($\beta=30^\circ, 31^\circ, 32^\circ, 38^\circ, 45^\circ, 46^\circ, 55^\circ$ and 63°). The results show that the relationship of factor of safety with h_r is linearly proportional in this case where the added cohesion remained constant over h_r . The regression analysis shows a positive slope.

4.9.8.2 Relationship between factor of safety and slope angle

Figure 4.30 shows the relationship between different slope angles and factor of safety. The average values of factor of safety for 6 different h_r at a certain slope angle was calculated by varying the slope height. This was done for both type of soil and regression analysis was performed. It shows that the relationship between factor of safety and slope angle is parabolic and negative. This also signifies that decreasing the slope angle stabilizes the slope and increases factor of safety.

4.9.8.3 Relation between factor of safety and height of slope for terraced slope

Figure 4.31 shows how factor of safety changes with slope height for terraced slope. The step height was varied and average values of factor of safety for 6 varying h_r at 4 different slope angles ($\beta= 27^\circ, 32^\circ, 44^\circ$ and 55°) was plotted. The regression lines show that the relationship is linear but negative. This indicates that reducing the slope height will increase the factor of safety of the slope.

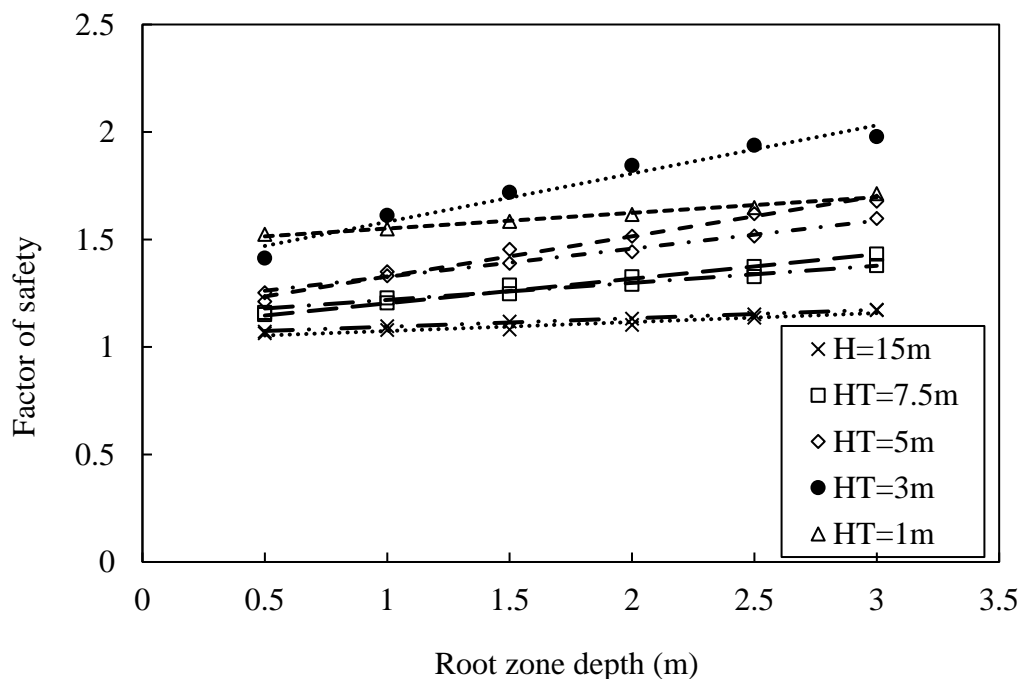


Figure 4.29: Relationship between factor of safety and root zone depth (m) at different step heights

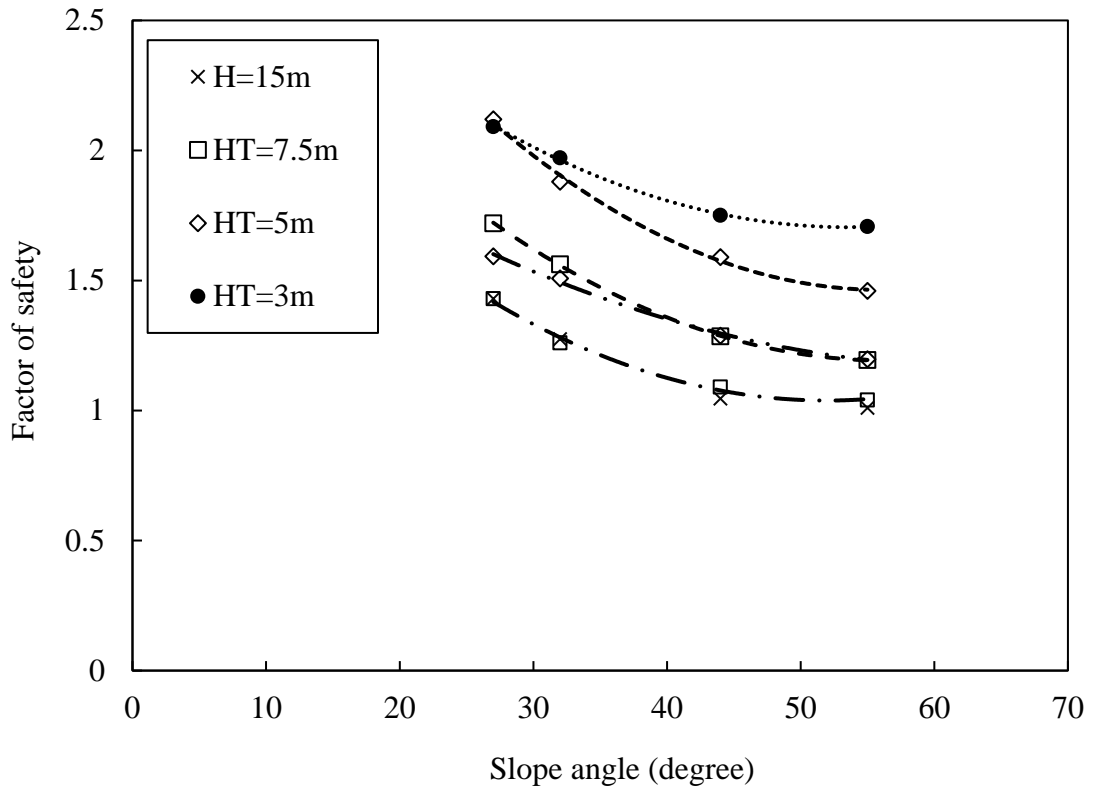


Figure 4.30: Relationship between factor of safety and slope angle (degree) at different slope heights

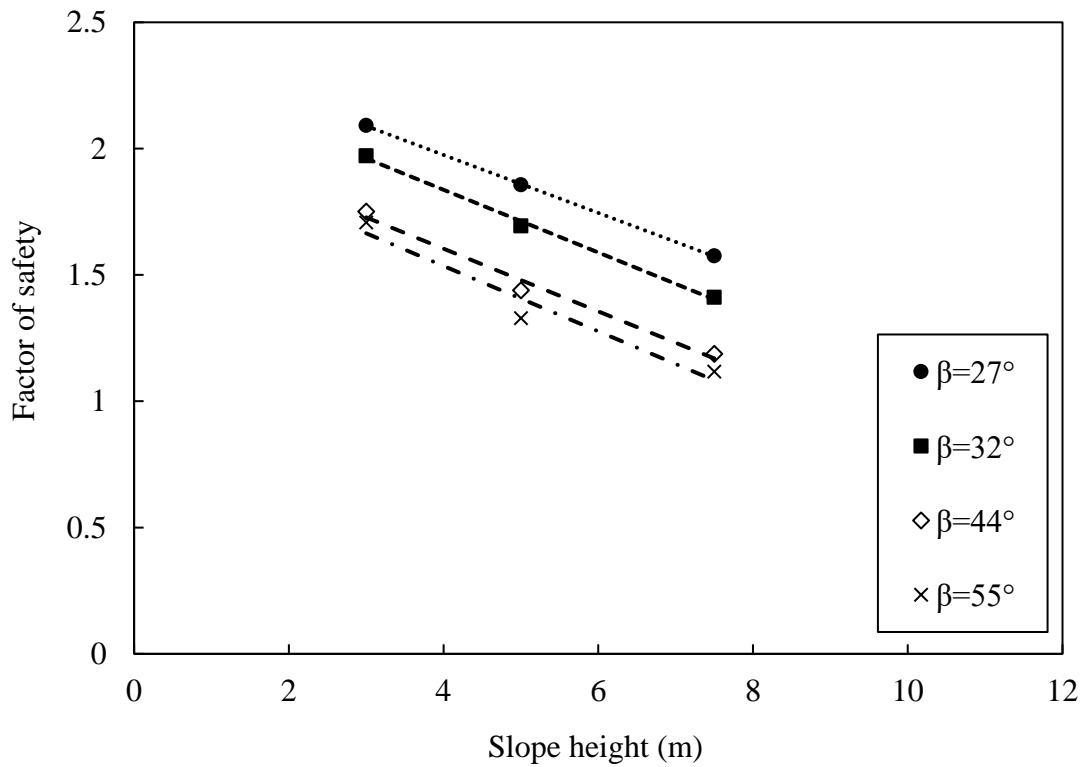


Figure 4.31: Relationship between factor of safety and slope height (m) for terraced slope at different slope angles

4.9.9 Effect of nailing in slope stability

4.9.9.1 Effect of nail length

To see the effect of nailing in increasing slope stability, nails with different lengths (l) was modeled in Plaxis 2D along with varying the slope angle. Table 4.10 and

Table 4.11 show the results obtained from the finite element analysis for S-1 and S-2.

From the results it was observed that inclusion of nails increases the factor of safety in all cases. With the increase in nail length, the maximum factor of safety was achieved when the nail length was $0.9H$.

However, nailing was more effective in case of S-1. The maximum increase in factor of safety obtained for S-1 was 70% whereas, it was only 23.3% for S-2. The angle of internal friction (ϕ) may have a role in this occurrence. Previous study by Elahi (2018) shows that increase in ϕ increases the factor of safety of nailed slope while all other parameters remain same. Here S-1 has a higher ϕ compared to S-2. Thus, the effect of nails was more prominent for S-1 type of soil. Figure 4.32 and Figure 4.33 show the percent increase in factor of safety for different nail lengths for S-1 and S-2, respectively at different slope angles.

For S-1, increasing the nail length from $0.5H$ to $0.9H$ increased the factor of safety by nearly 27% for $\beta=38^\circ$. However, this increase is more prominent in case of steeper slopes. At $\beta=55^\circ$, factor of safety was increased by 70% with a nail length of $0.9H$ which is 37% greater than the one achieved with $0.5H$ nail length.

Similarly for S-2, for $l=0.9H$, 11% increase in factor of safety was achieved at $\beta=38^\circ$ which became 23.3% at $\beta=55^\circ$. These conclude that the effect of increasing the nail length provides more benefit in case of steeper slopes.

This study used horizontal nails with an inclination of 0° . In studies by Fan and Luo (2008) and Rotte et al., (2011), it has been observed that with the increase in slope angle, the optimum nail inclination of nails, to obtain maximum factor of safety, with horizontal decreases. So, as the slope angle β increases, the maximum factor of safety will result when nail inclination will be minimum. This supports the findings of the present study where horizontal nails (inclination 0°) provide maximum increase in factor of safety at steepest slope angle $\beta=55^\circ$ for both the soil types.

Table 4.10: Factor of safety for different nail lengths at different slope angles for S-1

Slope Height H (m)	Slope angle β ($^{\circ}$)	Factor of safety			
		Bare condition	Nailed slope		
			Nail length l (m)		
			0.5H	0.7H	0.9H
15	38	1.014	1.193	1.321	1.469
	46	0.924	1.168	1.321	1.468
	55	0.88	1.171	1.338	1.496

Table 4.11: Factor of safety for different nail lengths at different slope angles for S-2

Slope Height H (m)	Slope angle β ($^{\circ}$)	Factor of safety			
		Bare condition	Nailed slope		
			Nail length l (m)		
			0.5H	0.7H	0.9H
15	38	0.876	0.929	0.958	0.973
	46	0.820	0.956	0.949	0.950
	55	0.811	0.885	0.926	1.000

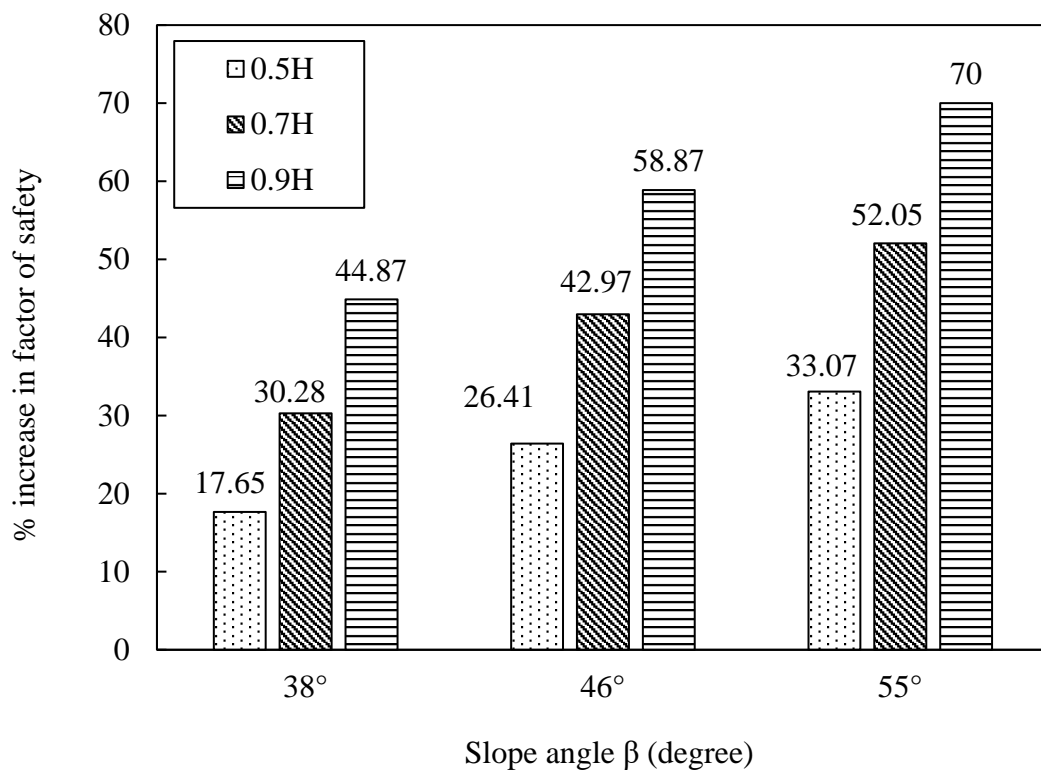


Figure 4.32: Percent increase in factor of safety for different nail length (m) at different slope angle (degree) for S-1

4.9.9.2 Effect of nailing on terraced slope

As the maximum increase in factor of safety was achieved at a nail length of $0.9H$ in the previous section, a nail length of $0.9H$ was used for terraced slope.

In case of S-1, for a terrace having two steps, e.g. height of each slope $H_T=7.5\text{m}$ and nail length $l=6.75\text{m}$, the percent increase in factor of safety for varying slope angles varied between 33-46%. On the other hand, in the previous case, where $H=15\text{m}$, and $l=7.5\text{m}$ the increase in factor of safety varied between 17% to 33%. Hence, the nailing of similar length produced more profound results in case of reduced slope heights. Also, the total displacements were reduced in case of terraced slopes for all three slope angles.

Again, despite using a smaller nail length than that of the natural slope with $H=15\text{m}$, the percent increase in factor of safety was greater for the terraced slope in S-1. So, it can be inferred that for S-1, the reduced height of slope provided more advantage in case of slope stability than compared to the increased nail length. However, for S-2, the reduction of slope height produced very negligible effect in case of increase in factor of safety, as can be seen from Figure 4.34.

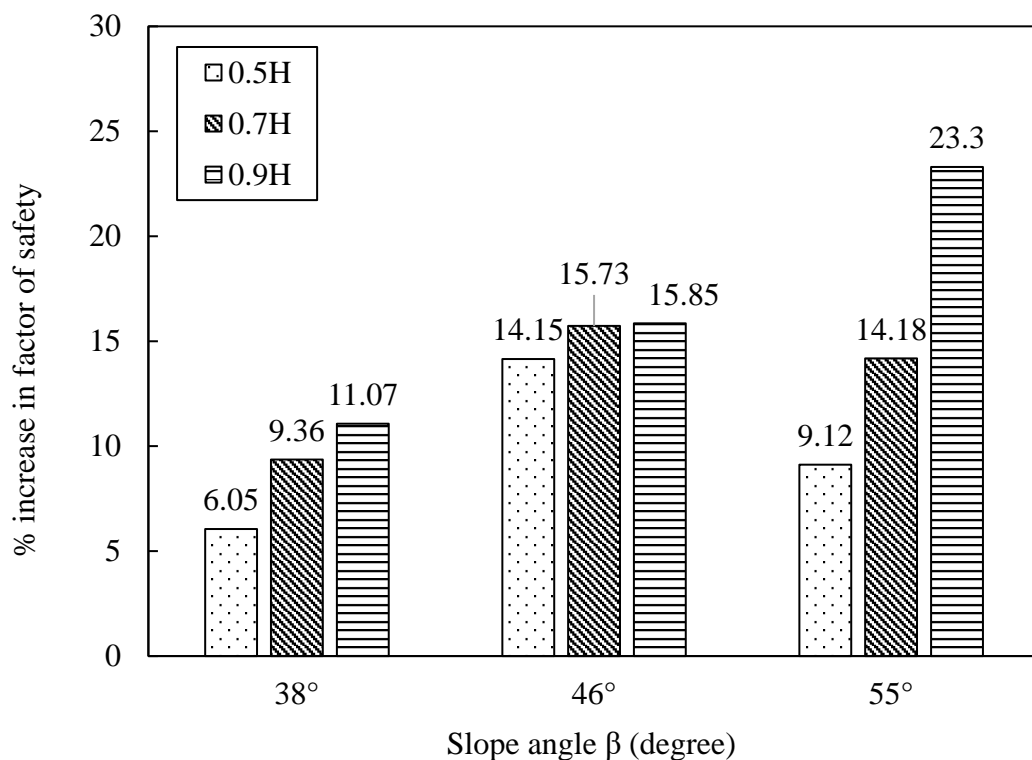


Figure 4.33: Percent increase in factor of safety for different nail length at different slope angle (degree) for S-2

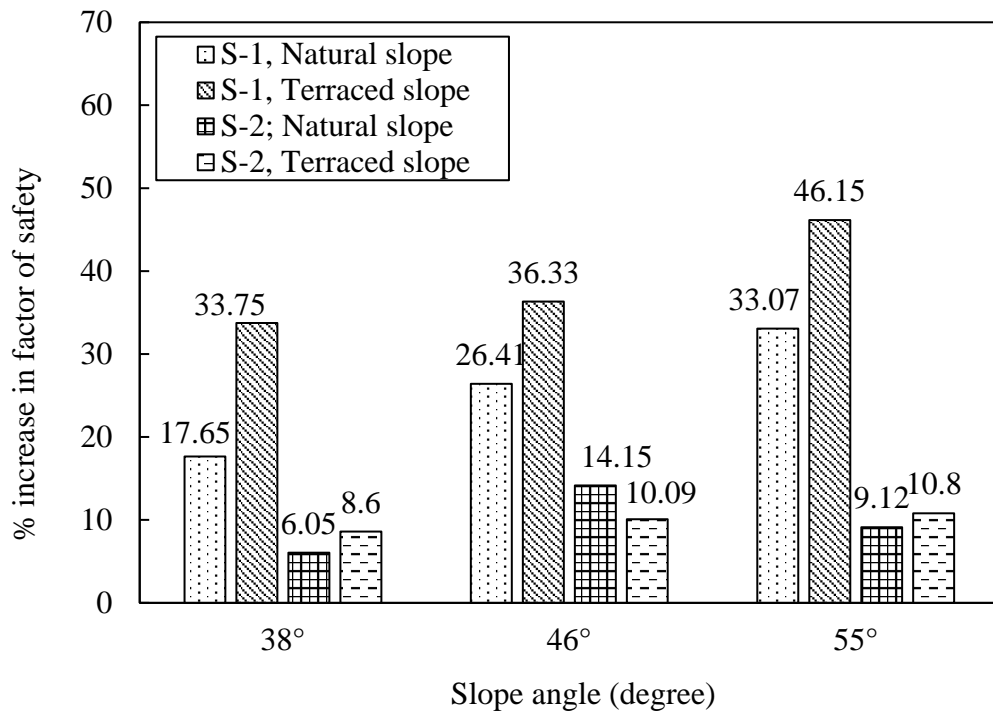


Figure 4.34: Percent increase in factor of safety for natural and terraced slope at different slope angle (degree)

4.10 Findings of the Study

From the results of laboratory experiments along with experiments on small scale glass models, we observed that the hilly soil was nutrient deficient, yet roots of vetiver grew up to 86.4 cm in the soil and had a maximum root diameter of 2.80 mm. It was effective in erosion reduction and generated 94.6%-99% lower eroded soil compared to bare soil. Results from numerical analysis, for natural and terraced slope have also been presented. In natural condition, beyond 38° and 30°, the slopes of S-1 and S-2 were unstable and had a factor of safety less than 1.0. Incorporation of vetiver increased the factor of safety up to 16% for the previous cases. Terraced slopes were found to be stable in steeper angles and here the increase in factor of safety was as high as 54%-60%, and the value varied from 1.150-1.678 for different soil type and step height. But, to obtain the positive impact of vegetation, the slope angles needed to remain within the threshold angles β_{lim} . Ranges of the threshold angles have been determined and reported in this study. Nails with a length of 0.9H were found to be effective in imparting stability to a slope with H=15m and the increase in factor of safety was 70% for S-1. Terracing increased the reinforcing through nails in S-1. However, the effect was not very prominent in case of S-2.

CHAPTER 5

CONCLUSIONS AND RECOMMENDATIONS

5.1 Introduction

In this current study, the effect of vegetation and nailing on slope stability and its prospect in case of landslide risk reduction for Chattogram have been focused. Laboratory tests have been performed to classify the hilly soil and determine their characteristics. Growth of vetiver has been studied for a year in small scale glass model, containing the soil collected from Chattogram hill tracts, upon which experiments have been carried out under artificially simulated rainfall to determine the erosion reduction by vegetation. Then numerical analysis has been performed to determine the effect of both vegetation and nailing on slope stability at different slope geometries. This chapter presents the conclusions derived from this study followed by some recommendations for future work.

5.2 Conclusions

The major findings and conclusions of the research are stated below:

- a) The soil collected from hills of Chattogram were non-plastic and are poor in nutrient contents. However, the *Vetiveria zizanoides* exhibited satisfactory growth in the nutrient deficient soil in terms of root length and tiller numbers.
- b) One major role of vegetation is to reduce the top-soil erosion and runoff. The results from small scale glass model show that in all the vegetated models, both the runoff and eroded soil load (varying between 0.10-0.63 kg) were significantly less than that of bare soil (11.7 kg). The minimum sediment yield (0.10 kg) was obtained for the model made with silty sand. The percent reduction in erosion varied from 94.6% to 99%. Considering the extremely high erodibility of the hills of Chattogram, vegetation can be a suitable solution to reduce the erosion of these hills which in the long term will provide safety against slope failure.
- c) Numerical analysis results represent that at bare condition, the natural hill slope, comprising of sandy silt, is stable till 38° whereas the one with silty sand is stable till 30°. The inclusion of vetiver grass increases the stability and

maximum increase of 16% in factor of safety has been observed for natural slopes, when roots penetrate up to 3m.

The positive effect of vegetation is overruled by the steepness of the natural slope after certain threshold angle. As the natural slope angles go beyond threshold angles; $\beta_{lim}=46.33\pm 3.50^\circ$ for sandy silt and $\beta_{lim}=33.33\pm 1.97^\circ$ for SM, vegetation alone cannot yield a factor of safety >1 . In this case, reducing the slope height by introducing terracing can be a potential option for imparting stability to the slopes.

- d) Terracing the natural slope and reducing the slope height increases the maximum angle for stable slope at bare condition. This increase is more pronounced in sandy silts.

Vegetation at terraced slope, can provide greater safety to the slopes as compared to natural ones with large slope height ($H=15m$), even at steeper slope angles. The maximum increase in factor of safety, as compared to bare condition, due to incorporation of vegetation, can be 54%-60% when the 15m slope is terraced into three steps each having a slope height of 5m. Hence, terracing and use of vegetation is a vital solution for slope stability at steeper slope angles.

At terraced condition, vetiver can provide safety to slopes up to $81.67\pm 10.33^\circ$ and $47.83^\circ\pm 7.57^\circ$ for sandy silt and silty sand for $H_T=7.5m$. As H_T is further reduced to 5m, the threshold angle for SM becomes $70.33^\circ\pm 12.48^\circ$. The slope with silty sand has a factor of safety of 1.35 ± 0.12 for $H_T=3m$ and $\beta=90^\circ$. Whereas for sandy silt, the slope height of 5m generates a factor of safety of 1.20 ± 0.11 at slope angle of 90° . Hence, for sandy silt, step height greater than 5m but less than 7.5m and for silty sand a step height greater than 3m but less than 5m may produce an optimized step height for stabilizing vertical hill cuts with vegetation.

- e) Parametric study reveals that factor of safety has a negative linear relationship with slope height whereas the relation is parabolic with slope angle. Decreasing the slope height and slope angle will stabilize the slope. Also, a positive linear correlation exist between factor of safety and root zone depth.
- f) It can be suggested that, if the existing stepper slopes can be reduced to $46.33\pm 3.50^\circ$ (for sandy silt) and $33.33\pm 1.97^\circ$ (for silty sand) then stability can

be achieved through application of vetiver only. However, this may not be viable owing to requirements of large amount of earthwork. Hence to address the instability of slopes having slope angles greater than mentioned above, alongside vetiver plantation, terracing the slope by reducing the slope height can be a practical option. The obtained threshold angles for various slope heights of terraced slope will offer a guideline for selecting an optimal slope geometry for restoration of slope stability with minimum amount of earthwork.

- g) Nailing can provide sufficient safety to slopes at steeper slope angles where only vegetation is not effective. By increasing the nail length the factor of safety can be further increased for both soil types at different slope geometries.

5.3 Recommendations

During the period of this study, different aspects have come up which may contribute to expand the scope of the study in future and provide more comprehensive results. Some recommendations for future work to make the study more inclusive are provided below:

- a) Existing condition of others hills of Chattogram hill tracts, especially in urbanized Chattogram city can be studied in context to risk of landslide and how sustainable measures like vegetation can reduce this.
- b) The root area ratio (RAR) and tensile strength of vetiver can be measured and used to calculate additional cohesion provided by vetiver. In-situ direct shear tests from the small scale models can be performed to determine actual bearing capacity of vegetated soil and can be utilized in numerical modeling.
- c) Research can be conducted in determining the energy of the rain drops which hit the soil surface. Thus a relationship between drop size, impact energy and erosion potential can be determined.
- d) Three-dimensional numerical analysis can be performed for simulating more realistic conditions from the field. The modeling may also include artificial rainfall simulation for comparison with experimental results.
- e) The applied numerical modeling in this research only considers the mechanical reinforcement of vetiver roots which can be further merged with the considerations of hydraulic reinforcing effects to reflect a more practical process of slope stabilization.

- f) Dynamic analysis can be performed as many landslides are also triggered by earthquakes.
- g) The use of nailing in field can provide knowledge about the constraints and challenges of construction and its implications. The feasibility of combining nailing with vegetation can also be studied followed by a comparative cost estimation.
- h) The best results for this type of studies can be obtained from plantation in the field level. Currently a project is being implemented at Tiger Pass hill to study the growth of vetiver in actual climatic conditions of Chattogram and how it contributes in stabilizing the slope. It may offer a scope to study the relationship between vetiver plantation density and canopy area provided by it while planation is done in larger scale covering a significant area. Comparing the test results of numerical simulation and small scale experiments with the field data can result in a more comprehensive study.

5.4 Summary

Above mentioned criterions are recommended to be investigated further in this topic to overcome the limitations of the present study. The findings of this study, complimented through the future work, will be an informative window which will provide an opportunity for the authorities and policy makers to see the application of vegetation and nailing as an efficient solution for increasing slope stability and thus reducing landslide risks for Chattogram city. This will also promote long term infusion of engineering practices with eco-friendly solutions to address the natural and man-made hazards like landslides in urban areas.

REFERENCES

- Abe, K., and Ziemer, R. R. (1991). Effect of tree roots on a shear zone: modeling reinforced shear stress. *Canadian Journal of Forest Research*, 21(7), 1012-1019.
- Aerts, R., and Chapin III, F. S. (1999). The mineral nutrition of wild plants revisited: a re-evaluation of processes and patterns. In *Advances in ecological research* (Vol. 30, pp. 1-67). Academic Press.
- Ahmed, B. (2014). Landslide susceptibility mapping using multi-criteria evaluation techniques in Chittagong Metropolitan Area, Bangladesh. *Landslides*, 12(6), 1077-1095.
- Ahmed, B. (2017). *Community vulnerability to landslides in Bangladesh* (Doctoral dissertation, UCL (University College London)).
- Ahmed, B., and Dewan, A. (2017). Application of bivariate and multivariate statistical techniques in landslide susceptibility modeling in Chittagong City Corporation, Bangladesh. *Remote Sensing*, 9(4), 304.
- Ahmed, B., Rahman, M. S., Rahman, S., Huq, F. F., and Ara, S. (2014). Landslide inventory report of Chittagong Metropolitan Area, Bangladesh.
- Ahmed, B., Rahman, M., Islam, R., Sammonds, P., Zhou, C., Uddin, K., and Al-Hussaini, T. M. (2018). Developing a dynamic Web-GIS based landslide early warning system for the Chittagong Metropolitan Area, Bangladesh. *ISPRS International Journal of Geo-Information*, 7(12), 485.
- Alam, M. K., Hasan, A. K. M., Khan, M. R., and Whitney, J. W. (1990). Geological map of Bangladesh. Geological Survey of Bangladesh (GSB), Dhaka.
- Alcántara-Ayala, I., Esteban-Chávez, O., and Parrot, J. F. (2006). Landsliding related to land-cover change: A diachronic analysis of hillslope instability distribution in the Sierra Norte, Puebla, Mexico. *Catena*, 65(2), 152-165.
- Ali, R. M. E., Tunbridge, L. W., Bhasin, R. K., Akter, S., Khan, M. M. H., and Uddin, M. Z. (2018). Landslides susceptibility of Chittagong city, Bangladesh and development of landslides early warning system. *Landslide Science for a Safer Geoenvironment*, 423-428.

- Alsubal, S., Harahap, I. S., and Babangida, N. M. (2017). A typical design of soil nailing system for stabilizing a soil slope: Case Study. *Indian Journal of Science and Technology*, 10(4), 1-7.
- Arif, M. Z. U. (2017). *Investigation of vetiver root growth in sandy soil and slope stabilization*. B. Sc. Engg. Thesis, Department of Civil Engineering, Bangladesh University of Engineering and Technology (BUET), Dhaka, Bangladesh.
- Aryal, K. P. (2008). Differences between LE and FE methods used in slope stability evaluations. In *12th International Conference of International Association for Computer Methods and Advances in Geomechanics (IACMAG)*, 1-6.
- ASTM D1556. (2015). Standard test method for density and unit weight of soil in place by sand-cone method. ASTM International, West Conshohocken, PA.
- ASTM D3080. (2011). Standard test method for direct shear test of soils under consolidated drained conditions. ASTM International, West Conshohocken, PA.
- ASTM D442. (2019). Standard test method for particle size analysis of soil. ASTM International, West Conshohocken, PA.
- ASTM D5084. (2016). Standard test methods for measurement of hydraulic conductivity of saturated porous materials using a flexible wall permeameter. ASTM International, West Conshohocken, PA.
- ASTM D854. (2014). Standard test methods for specific gravity of soil solids by water pycnometer. ASTM International, West Conshohocken, PA.
- Aziz, S.A., Islam, M. S., and Ahmed, M. (2020). A model study to quantify soil erosion by artificially simulated rainfall and observe effectiveness of bio-engineering to reduce landslide risk in Chittagong Hill Tracts. In *Proceedings of International Conference on Earth and Environmental Sciences (ICCEST 2020)*, Paper No. ICDRS-O-005, 154-156, Dhaka, Bangladesh.
- Babu, G. S., and Singh, V. P. (2009). Simulation of soil nail structures using Plaxis 2D. *Plaxis Bulletin*, 25, 16-21.
- Balasubramani, K., Veena, M., Kumaraswamy, K., and Saravanabavan, V. (2015). Estimation of soil erosion in a semi-arid watershed of Tamil Nadu (India) using revised universal soil loss equation (rusle) model through GIS. *Modeling Earth Systems and Environment*, 1(3), 10.

- Bangladesh Meteorological Department. (2013). Annual rainfall pattern of Chittagong City.
- Bangladesh Agricultural Research council. (2005). Fertilizer recommendation guide, Dhaka, Bangladesh.
- Bangladesh National Building Code. (2020). Dhaka, Bangladesh.
- Bentley, W. A. (1904). Studies of raindrops and raindrop phenomena. *Mon Weather Rev*, 32, 450-456.
- Biswas, R. N., Islam, M. N., and Islam, M. N. (2017). Modeling on management strategies of slope stability and susceptibility to landslides catastrophe at hilly region in Bangladesh. *Modeling Earth Systems and Environment*, 3(3), 977-998.
- Bourrier, F., Kneib, F., Chareyre, B., and Fourcaud, T. (2013). Discrete modeling of granular soils reinforcement by plant roots. *Ecological Engineering*, 61, 646-657.
- Bowels, E. J. (2012). Foundation analysis and design, 152, *McGraw-Hill Kogakusha Limited*.
- Brand, E. W., Premchitt, J., and Phillipson, H. B. (1984). Relationship between rainfall and landslides in Hong Kong. In *Proceedings of the 4th International Symposium on Landslides* (Vol. 1, 377-384). Toronto: Canadian Geotechnical Society.
- Briggs, K. (2010). Charing embankment: climate change impacts on embankment hydrology. *Ground Engineering*, 43(6).
- Carlin, G. D., Truong, P., Cook, F. J., Thomas, E., Mischke, L., and Mischke, K. (2003). Vetiver grass hedges for control of runoff and drain stabilisation. Pimpama Queensland. *Commonwealth Scientific and Industrial Research Organisation*.
- Chae, B. G., Park, H. J., Catani, F., Simoni, A., and Berti, M. (2017). Landslide prediction, monitoring and early warning: A concise review of state-of-the-art. *Geosciences Journal*, 21(6), 1033-1070.
- Chaipattana Foundation. (1996). What is vetiver grass? Chaipattana Network Webmaster, 1-4.
- Chakrabarti, B., Shivananda, P., and Scholar, P. D. (2017). Two-dimensional slope stability analysis by plaxis-2d. *International Journal for Research in Applied Science and Engineering Technology*, 5, 817-877.
- Chang, K. T., Chiang, S. H., and Lei, F. (2008). Analysing the relationship between typhoon-triggered landslides and critical rainfall conditions. *Earth Surface Processes*

and *Landforms: The Journal of the British Geomorphological Research Group*, 33(8), 1261-1271.

Cheng, Y. M., and Lau, C. K. (2014). *Slope stability analysis and stabilization: new methods and insight*. CRC Press.

Cheng, Y. M., Au, S. K., Pearson, A. M., and Li, N. (2013). An innovative geonail system for soft ground stabilization. *Soils and foundations*, 53(2), 282-298.

Chok, Y. H., Jaksa, M. B., Kaggwa, W. S., and Griffiths, D. V. (2015). Assessing the influence of root reinforcement on slope stability by finite elements. *International Journal of Geo-Engineering*, 6(1), 12.

Chok, Y., Kaggwa, G., Jaksa, M., and Griffiths, D. (2004). Modelling the effects of vegetation on stability of slopes. Australia-New Zealand Conference on Geomechanics; Centre for Continuing Education, Auckland, New Zealand, 391–397.

Chowdhury, M. E., Islam, M. A., Islam, M. S., Shahriar, M. S., and Alam, T. (2017). Design, operation and performance evaluation of a portable perforated steel tray rainfall simulator. In *Proceedings of 14th Global Engineering and Technology Conference*, 29-30.

Chowdhury, S. Q. (2012). Chittagong City. *Banglapedia*, National encyclopedia of Bangladesh (2), Trust, Asiatic Society of Bangladesh, Dhaka, Bangladesh.

Chu, L. M., and Yin, J. H. (2005). A laboratory device to test the pull-out behavior of soil nails. *Geotechnical testing journal*, 28(5), 499-513.

Clarke, M. A., and Walsh, R. P. (2007). A portable rainfall simulator for field assessment of splash and slopewash in remote locations. *Earth Surface Processes and Landforms: The Journal of the British Geomorphological Research Group*, 32(13), 2052-2069.

Comprehensive Disaster Management Programme-II (2012). rainfall triggered landslide hazard zonation in Cox's Bazar and Teknaf municipalities as well as introducing community-based Early Warning System for landslide hazard management; Ministry of Food and Disaster Management (MoFDM): Dhaka, Bangladesh.

Coutts, M. P. (1983). Root architecture and tree stability. *Tree root systems and their mycorrhizas* (pp. 171-188). Springer, Dordrecht.

- Cruden, D. M. (1991). A simple definition of a landslide. *Bulletin of the International Association of Engineering Geology-Bulletin de l'Association Internationale de Géologie de l'Ingénieur*, 43(1), 27-29.
- Cruden, D. M., and Varnes, D. J. (1996). Landslide types and processes. Turner AK, Schuster RL (eds) *Landslides: investigation and mitigation*. Transportation Research Board, Special Report 247. National Academy Press, Washington, 36–75.
- Das, D. K. (1990). Forest types of Bangladesh. *Forest types of Bangladesh*, (6).
- De Baets, S., Poesen, J., Knapen, A., Barberá, G. G., and Navarro, J. A. (2007). Root characteristics of representative Mediterranean plant species and their erosion-reducing potential during concentrated runoff. *Plant and Soil*, 294(1-2), 169-183.
- De Baets, S., Poesen, J., Reubens, B., Wemans, K., De Baerdemaeker, J., and Muys, B. (2008). Root tensile strength and root distribution of typical Mediterranean plant species and their contribution to soil shear strength. *Plant and soil*, 305(1-2), 207-226.
- Dixon, N., Smith, A., Flint, J. A., Khanna, R., Clark, B., and Andjelkovic, M. (2018). An acoustic emission landslide early warning system for communities in low-income and middle-income countries. *Landslides*, 15(8), 1631-1644.
- Duncan, J. M., Wright, S. G., and Brandon, T. L. (2014). *Soil strength and slope stability*. John Wiley and Sons.
- Egeli, I., and Pulat, H. F. (2011). Mechanism and modelling of shallow soil slope stability during high intensity and short duration rainfall. *Scientia Iranica*, 18(6), 1179-1187.
- Egodawatta, P. K. (2007). *Translation of small-plot scale pollutant build-up and wash-off measurements to urban catchment scale* (Doctoral dissertation, Queensland University of Technology).
- Ekanayake, J. C., Marden, M. I. C. H. A. E. L., Watson, A. J., and Rowan, D. O. N. N. A. (1997). Tree roots and slope stability: a comparison between *Pinus radiata* and *kanuka*. *New Zealand Journal of Forestry Science*, 27(2), 216-233.
- Elahi, T. E. (2018). *Effectiveness of nailing and vegetation for protection of landslides in Chittagong Hill Tracts of Bangladesh*, M. Sc. Engg. Thesis, Department of Civil Engineering, Bangladesh University of Engineering and Technology (BUET), Dhaka, Bangladesh.

- Elahi, T. E., Islam, M. A., and Islam, M. S. (2018). Stability analysis of selected hill slopes of Rangamati. In *Proceedings of the 4th International Conference on Advances in Civil Engineering (ICACE 2018)*, Chattogram, Bangladesh.
- Elahi, T. E., Islam, M. A., and Islam, M. S. (2019). Effect of vegetation and nailing for prevention of landslides in Rangamati. In *Proceedings of International Conference on Disaster Risk Management (ICDRM 2019)*, Dhaka, Bangladesh.
- Emran, A., Roy, S., Bagmar, M. S. H., and Mitra, C. (2018). Assessing topographic controls on vegetation characteristics in Chittagong Hill Tracts (CHT) from remotely sensed data. *Remote Sensing Applications: Society and Environment*, 11, 198-208.
- Fan, C. C., and Luo, J. H. (2008). Numerical study on the optimum layout of soil-nailed slopes. *Computers and Geotechnics*, 35(4), 585-599.
- Farid, A. T. M., Iqbal, A., and Karim, Z. (1992). Soil erosion in the Chittagong Hill Tract and its impact on nutrient status of soils [in Bangladesh]. *Bangladesh Journal of Soil Science (Bangladesh)*.
- Gabet, E. J., Burbank, D. W., Putkonen, J. K., Pratt-Sitaula, B. A., and Ojha, T. (2004). Rainfall thresholds for landsliding in the Himalayas of Nepal. *Geomorphology*, 63(3-4), 131-143.
- Gafur, A., Borggaard, O. K., Jensen, J. R., and Petersen, L. (2000). Changes in soil nutrient content under shifting cultivation in the Chittagong Hill Tracts of Bangladesh. *Geografisk Tidsskrift-Danish Journal of Geography*, 100(1), 37-46.
- Geoguide-7. (2008) Guide to soil nail design and construction. Geotechnical Engineering Office, Civil Engineering and Development Department, The Government of the Hong Kong Special Administrative Region.
- Geological Survey of Bangladesh. (2013). Geological map of Chittagong City and Surrounding Areas.
- Goldman, S. J., and Jackson, K. E. (1986). *Erosion and sediment control handbook*.
- Gray, D. H. (1974). Reinforcement and stabilization of soil by vegetation. *Journal of Geotechnical and Geoenvironmental Engineering*, 100.
- Gray, D. H. (1978). Role of woody vegetation in reinforcing soils and stabilizing slopes. In *Proceedings of Symposium of Soil Reinforcing and Stabilising Techniques, Sydney, Australia*, 253-306.

- Gray, D. H., and Barker, D. (2004). Root-soil mechanics and interactions. *Riparian vegetation and fluvial geomorphology*, 8, 113-123.
- Gray, D. H., and Leiser, A. T. (1982). *Biotechnical slope protection and erosion control*. Van Nostrand Reinhold Company Inc.
- Greenwood, J. R. (2006). SLIP4EX—A program for routine slope stability analysis to include the effects of vegetation, reinforcement and hydrological changes. *Geotechnical and Geological Engineering*, 24(3), 449.
- Griffiths, D. V., and Lane, P. A. (1999). Slope stability analysis by finite elements. *Geotechnique*, 49(3), 387-403.
- Guidicini, G., and Iwasa, O. Y. (1977). Tentative correlation between rainfall and landslides in a humid tropical environment. *Bulletin of the International Association of Engineering Geology-Bulletin de l'Association Internationale de Géologie de l'Ingénieur*, 16(1), 13-20.
- Gunawan, I., Surjandari, N. S., and Purwana, Y. M. (2017). The study on length and diameter ratio of nail as preliminary design for slope stabilization. *Journal of Physics: Conference Series*, 909 (1).
- Gupta, V., Bhasin, R. K., Kaynia, A. M., Kumar, V., Saini, A. S., Tandon, R. S., and Pabst, T. (2016). Finite element analysis of failed slope by shear strength reduction technique: a case study for Surabhi Resort Landslide, Mussoorie township, Garhwal Himalaya. *Geomatics, Natural Hazards and Risk*, 7(5), 1677-1690.
- Guzzetti, F., Cardinali, M., Reichenbach, P., Cipolla, F., Sebastiani, C., Galli, M., and Salvati, P. (2004). Landslides triggered by the 23 November 2000 rainfall event in the Imperia Province, Western Liguria, Italy. *Engineering Geology*, 73(3-4), 229-245.
- Guzzetti, F., Mondini, A. C., Cardinali, M., Fiorucci, F., Santangelo, M., and Chang, K. T. (2012). Landslide inventory maps: New tools for an old problem. *Earth-Science Reviews*, 112(1-2), 42-66.
- Guzzetti, F., Peruccacci, S., Rossi, M., and Stark, C. P. (2008). The rainfall intensity–duration control of shallow landslides and debris flows: an update. *Landslides*, 5(1), 3-17.
- Gyssels, G., Poesen, J., Bochet, E., and Li, Y. (2005). Impact of plant roots on the resistance of soils to erosion by water: a review. *Progress in physical geography*, 29(2), 189-217. Hammouri, N.A.

- Hammouri, N. A., Malkawi, A. I. H., and Yamin, M. M. (2008). Stability analysis of slopes using the finite element method and limiting equilibrium approach. *Bulletin of Engineering Geology and the Environment*, 67(4), 471.
- Haneberg, W. C. (1991). Observation and analysis of pore pressure fluctuations in a thin colluvium landslide complex near Cincinnati, Ohio. *Engineering Geology*, 31(2), 159-184.
- Hasan, A. K. M. S. (1981). Slope instability and construction damages at Mercantile Marine Academy, Chittagong District, Bangladesh.
- Hassan, M., Hassan, R., Pia, H. I., Hassan, M. A., Ratna, S. J., and Aktar, M. (2017). Variation of soil fertility with diverse hill soils of Chittagong Hill tracts, Bangladesh. *International Journal of Plant and Soil Science*, 18(1), 1-9.
- Highland, L., and Bobrowsky, P. T. (2008). *The landslide handbook: a guide to understanding landslides*, 129. Reston: US Geological Survey.
- Horton, R. E. (1933). The role of infiltration in the hydrologic cycle. *Eos, Transactions American Geophysical Union*, 14(1), 446-460.
- Hossain, M. I., Kashem, M. A., and Osman, K. T. (2014). Fertility status of some forested soils of Chittagong Hill Tracts, Bangladesh. *International Journal of Latest Research in Science and Technology*, 3, 82-87.
- Huat, B. B., and Mohammed, T. A. (2006). Finite element study using FE code (PLAXIS) on the geotechnical behavior of shell footings. *Journal of Computer Science*, 2(1), 104-108.
- Islam, M. A. (2018) *Measures for landslide prevention in Chittagong Hill Tracts of Bangladesh*. M.Sc. Engg. Thesis, Department of Civil Engineering, Bangladesh University of Engineering and Technology (BUET), Dhaka, Bangladesh.
- Islam, M. A., Islam, M. S., and Elahi, T. E. (2020). Effectiveness of vetiver grass on stabilizing hill slopes: a numerical approach. In *Geo-Congress 2020: Engineering, Monitoring, and Management of Geotechnical Infrastructure*, 106-115, Reston, VA: American Society of Civil Engineers.
- Islam, M. A., Islam, M. S., and Islam, T. (2017). Landslides in Chittagong Hill Tracts and possible measures. In *Proceedings of International Conference on Disaster Risk Mitigation (ICDRM 2017)*, Paper No. CDW154, Dhaka, Bangladesh.

- Islam, M. S. (2013). *Use of vegetation and geo-jute for slope protection*, M. Sc. Engg. Thesis, Department of Civil Engineering, Bangladesh University of Engineering and Technology (BUET), Dhaka, Bangladesh.
- Islam, M. S., and Badhon, F. F. (2020). A mathematical model for shear strength prediction of vetiver rooted soil. In *Geo-Congress 2020: Engineering, Monitoring, and Management of Geotechnical Infrastructure*, 96-105. Reston, VA: American Society of Civil Engineers.
- Islam, M. S., and Shahin, H. M. (2013). Reinforcing effect of vetiver (*Vetiveria zizanioides*) root in geotechnical structures-experiments and analyses. *Geomechanics and Engineering*, 5(4), 313-329.
- Iverson, R. M. (2000). Landslide triggering by rain infiltration. *Water resources research*, 36(7), 1897-1910.
- Islam, M. S., Arif, M. Z. U., Badhon, F. F., Mallik, S., and Islam, T. (2016). Investigation of vetiver root growth in sandy soil. In *Proceedings of BUET-ANWAR ISPAT 1st Bangladesh Civil Eng. SUMMIT*, Dhaka, Bangladesh, GE62-GE69.
- Islam, M. S., Hoque, M. S., Mallick, S., Parshi, F. N., and Islam, T. (2017). Performance evaluation of bio-engineering in slope protection of different soils. In *Proceedings of the International Conference on Disaster Risk Mitigation (ICDRM 2017)*, Paper No. CDW157, Dhaka, Bangladesh.
- Islam, M. S., Khan, A. J., Siddique. A., Saleh, A. M. and Nasrin, S. (2014). Control of erosion of hill slope top soil using geojute and vegetation. *National Seminar on Jute Geotextiles*, Dhaka, Bangladesh.
- Islam, M. S., Shahriar, B. A. M., and Shahin, H. M. (2013). Study on growth of vetiver grass in tropical region for slope protection. *International Journal of GEOMATE*, 5(2), 729-734.
- Islam, M., Arifuzzaman, N., and Nasrin, S. (2010). In-situ shear strength of vetiver grass rooted soil. In *Bangladesh Geo. Conf.: Natural Hazards and Counter Measures in Geotechnical Engg*, Dhaka, Bangladesh, 274-279.
- Islam, M.S. and Arifuzzaman (2010). Performance of vetiver grass in protecting embankments on the Bangladesh coast against cyclonic tidal surge. In *5th National Conference on Coastal and Estuarine Habitat Restoration*, USA.

- Janbu, N. (1957). Earth pressure and bearing capacity calculations by generalized procedure of slices. In *Proceedings of 4th International Conference on Soil Mechanics and Foundation Engineering, London, 1957*.
- Jayanandan, M., and Chandrakaran, S. (2015). Numerical simulation of soil nailed structures. *Int J Eng Res Technol*, 4(8), 525-530.
- Karim, M. F., Ahmed, S., and Olsen, H. W. (1990). Engineering geology of Chittagong City Bangladesh. Geological Survey of Bangladesh and U.S. Geological Survey.
- Kelman, I., Ahmed, B., Esraz-Ul-Zannat, M., Saroar, M. M., Fordham, M., and Shamsudduha, M. (2018). Warning systems as social processes for Bangladesh cyclones. *Disaster Prevention and Management: An International Journal*.
- Kelman, I., and Glantz, M. H. (2014). Early warning systems defined. In *Reducing disaster: Early warning systems for climate change*, 89-108. Springer, Dordrecht.
- Khan Y. A., and Chang, C. (2006). Landslide potentialities in low hills in Chittagong, Bangladesh. In *Proceedings of Korean Society of Engineering Geology Conference*, Daejeon, South Korea, 79–88.
- Khan, Y. A., and Chang, C. (2008). Landslide hazard mapping of Chittagong City Area, Bangladesh. *J Eng Geol Indian Soc Eng Geol* 35(1–4), 303–311.
- Khan, Y. A., Lateh, H., Baten, M. A., and Kamil, A. A. (2012). Critical antecedent rainfall conditions for shallow landslides in Chittagong City of Bangladesh. *Environmental Earth Sciences*, 67(1), 97-106.
- Kirschbaum, D. B., Adler, R., Hong, Y., Hill, S., and Lerner-Lam, A. (2010). A global landslide catalog for hazard applications: method, results, and limitations. *Natural Hazards*, 52(3), 561-575.
- Kokutse, N. K. (2003). Analyse numérique de L'effet mécanique de la végétation Sur la Stabilité des Sols en Pente. *Université de Lomé, Togo*, 59.
- Kokutse, N. K., Temgoua, A. G. T., and Kavazović, Z. (2016). Slope stability and vegetation: Conceptual and numerical investigation of mechanical effects. *Ecological Engineering*, 86, 146-153.
- Krishnan, M. S. (1982). Geology of India and Burma (6th edn). *Delhi: CBS Pubs. and Distributors*, 536.
- Lavania, S. (2003). Vetiver root system: search for the ideotype. In *Proceedings of the 3rd International Conference on Vetiver and Exhibition, Guangzhou, China*, 526-530.

- Laws, J. O., and Parsons, D. A. (1943). The relation of raindrop-size to intensity. *Eos, Transactions American Geophysical Union*, 24(2), 452-460.
- Leung, A. K., and Ng, C. W. W. (2013). Analyses of groundwater flow and plant evapotranspiration in a vegetated soil slope. *Canadian Geotechnical Journal*, 50(12), 1204-1218.
- Lin, D. G., Huang, B. S., and Lin, S. H. (2010). 3-D numerical investigations into the shear strength of the soil–root system of Makino bamboo and its effect on slope stability. *Ecological Engineering*, 36(8), 992-1006.
- Machado, L., Holanda, F. S. R., da Silva, V. S., Maranduba, A. I. A., and Lino, J. B. (2015). Contribution of the root system of vetiver grass towards slope stabilization of the Sao Francisco River. *Semina: Ciências Agrárias*, 36(4), 2453-2463.
- Mangiza, N. D. M., Arimah, B. C., Jensen, I., Yemeru, E. A., and Kinyanjui, M. K. (2011). Cities and climate change: global report on human settlements, United Nations Human Settlements Programme (UN-Habitat), Nairobi, Kenya.
- Manschadi, A. M., Sauerborn, J., Stützel, H., Göbel, W., and Saxena, M. C. (1998). Simulation of faba bean (*Vicia faba L.*) root system development under Mediterranean conditions. *European Journal of Agronomy*, 9(4), 259- 272.
- Marques, R., Zêzere, J., Trigo, R., Gaspar, J., and Trigo, I. (2008). Rainfall patterns and critical values associated with landslides in Povoação County (São Miguel Island, Azores): relationships with the North Atlantic Oscillation. *Hydrological Processes: An International Journal*, 22(4), 478-494.
- Maula, B. H., and Zhang, L. (2011). Assessment of embankment factor safety using two commercially available programs in slope stability analysis. *Procedia engineering*, 14, 559-566.
- Meeuwig, R. O. (1970). Infiltration and soil erosion as influenced by vegetation and soil in northern Utah. *Rangeland Ecology and Management/Journal of Range Management Archives*, 23(3), 185-188.
- Mickovski, S. B., Stokes, A., Van Beek, R., Ghestem, M., and Fourcaud, T. (2011). Simulation of direct shear tests on rooted and non-rooted soil using finite element analysis. *Ecological Engineering*, 37(10), 1523-1532.
- Miguntanna, N. P. (2009). *Nutrients build-up and wash-off processes in urban land uses* (Doctoral dissertation, Queensland University of Technology).

- Molla, M. D. H. (2014). Performance of Jute Geo Textile (JGT) for soil erosion control and management of slope land in Bangladesh, Dhaka, Bangladesh.
- Moriwaki, R., and Kanda, M. (2004). Seasonal and diurnal fluxes of radiation, heat, water vapor, and carbon dioxide over a suburban area. *Journal of Applied Meteorology*, 43(11), 1700-1710.
- Muminullah, M. (1978). *Geology of the northern part of Chittagong district, Bangladesh*. Geological Survey of Bangladesh, Government of the People's Republic of Bangladesh.
- Nasrin, S. (2013). *Erosion control and slope stabilization of embankments using vetiver system*, M.Sc. Engg. Thesis, Department of Civil Engineering, Bangladesh University of Engineering and Technology (BUET), Dhaka, Bangladesh.
- Nasrin, S. and Islam, M. S. (2018). A model study on erosion control of embankment by vegetation. *Fareast Int. University Journal*, 1(1), 60-71.
- Navas, A., Alberto, F., Machín, J., and Galán, A. (1990). Design and operation of a rainfall simulator for field studies of runoff and soil erosion. *Soil Technology*, 3(4), 385-397.
- Neves, M., Cavaleiro, V., and Pinto, A. (2016). Slope stability assessment and evaluation of remedial measures using limit equilibrium and finite element approaches. *Procedia engineering*, 143, 717-725.
- Ng, C. W. W., and Menzies, B. (2007). *Advanced unsaturated soil mechanics and engineering*. Taylor and Francis. *New York*.
- Ng, C. W. W., and Shi, Q. (1998). Influence of rainfall intensity and duration on slope stability in unsaturated soils. *Quarterly Journal of Engineering Geology and Hydrogeology*, 31(2), 105-113.
- Ng, C. W. W., Leung, A. K., and Woon, K. X. (2014). Effects of soil density on grass-induced suction distributions in compacted soil subjected to rainfall. *Canadian Geotechnical Journal*, 51(3), 311-321.
- Ng, C. W. W., Woon, K. X., Leung, A. K., and Chu, L. M. (2013). Experimental investigation of induced suction distribution in a grass-covered soil. *Ecological Engineering*, 52, 219-223.

- Ni, J. J., Leung, A. K., Ng, C. W. W., and Shao, W. (2017). Modelling hydro-mechanical reinforcements of plants to slope stability. *Computers and Geotechnics*, 95, 99-109.
- Nilsen, T. H., Taylor, F. A., and Brabb, E. E. (1976). *Recent landslides in Alameda County, California (1940-71): An estimate of economic losses and correlations with slope, rainfall, and ancient landslide deposits, 1398*. US Government Printing Office.
- Norris, J. E., Stokes, A., Mickovski, S. B., Cammeraat, E., Van Beek, R., Nicoll, B. C., and Achim, A. (Eds.). (2008). *Slope stability and erosion control: ecotechnological solutions*. Springer Science and Business Media.
- Oberste-Lehn, D. (1976). *Slope stability of the Lomerias Muertas area, San Benito County, California* (Doctoral dissertation, Stanford University, California, USA).
- Onodera, T., Yoshinaka, R., and Kazama, H. (1974). Slope failures caused by heavy rainfall in Japan. *Journal of the Japan Society of Engineering Geology*, 15(4), 191-200.
- Osmany, S. H. (2014). Chittagong City. *Banglapedia-the National encyclopedia of Bangladesh*.
- Parshi, F. N. (2015). *Strength-deformation characteristics of rooted soil*. M. Sc. Engg. Thesis, Department of Civil Engineering, Bangladesh University of Engineering and Technology (BUET), Dhaka, Bangladesh.
- Persits, F. M., Wandrey, C. J., Milici, R. C., and Manwar, A. (2001). digital geologic and geophysical data of Bangladesh. The U.S. Geological Survey.
- Plaxis 2D Reference Manual CONNECT Edition V20 (2019), Bentley.
- Pollen, N., and Simon, A. (2005). Estimating the mechanical effects of riparian vegetation on stream bank stability using a fiber bundle model. *Water Resources Research*, 41(7).
- Prasannakumar, V., Vijith, H., Abinod, S., and Geetha, N. J. G. F. (2012). Estimation of soil erosion risk within a small mountainous sub-watershed in Kerala, India, using revised universal soil loss equation (rusle) and geo-information technology. *Geoscience Frontiers*, 3(2), 209-215.
- Rabby, Y. W., and Li, Y. (2020). Landslide inventory (2001–2017) of Chittagong hilly areas, Bangladesh. *Data*, 5(1), 4.

- Rahman, T. (2012). *Landslide risk reduction of the informal foothill settlements of Chittagong city through strategic design measure*, M. Sc. Engg. Thesis, BRAC University, Dhaka, Bangladesh.
- Rotte, V., Viswanadham, B., and Chourasia, D. (2011). Influence of slope geometry and nail parameters on the stability of soil-nailed slopes. *International Journal of Geotechnical Engineering*, 5(3), 267-281.
- Samiezadeh, S., Avval, P. T., Fawaz, Z., and Bougherara, H. (2014). Biomechanical assessment of composite versus metallic intramedullary nailing system in femoral shaft fractures: A finite element study. *Clinical Biomechanics*, 29(7), 803-810.
- Sarker, A. A., and Rashid, A. M. (2013). Landslide and flashflood in Bangladesh. In *Disaster risk reduction approaches in Bangladesh*, 165-189. Springer, Tokyo.
- Schwarz, M., Cohen, D., and Or, D. (2010). Root-soil mechanical interactions during pullout and failure of root bundles. *Journal of Geophysical Research: Earth Surface*, 115(F4).
- Sharma, P., Rawat, S., and Gupta, A. K. (2019). Study and remedy of Kotropi landslide in Himachal Pradesh, India. *Indian Geotechnical Journal*, 49(6), 603-619.
- Shiu, Y. K., and Chang, G. W. K. (2006). *Effects of inclination, length pattern and bending stiffness of soil nails on behavior of nailed structures*. Geotechnical Engineering Office, Civil Engineering and Development Department.
- Shrestha, S., Kang, T. S., and Suwal, M. K. (2017). An ensemble model for co-seismic landslide susceptibility using GIS and random forest method. *ISPRS International Journal of Geo-Information*, 6(11), 365.
- Simon, A., Pollen, N., and Langendoen, E. (2006). Influence of two woody riparian species on critical conditions for streambank stability: Upper Truckee River, California. *Jawra Journal of the American Water Resources Association*, 42(1), 99-113.
- Singh, V. P., and Babu, G. S. (2010). 2D numerical simulations of soil nail walls. *Geotechnical and Geological Engineering*, 28(4), 299-309.
- Smith, G. D., and Srivastava, K. L. (1989). ICRISAT Annual Report, Andhra Pradesh, India.

- Soga, K., Alonso, E., Yerro, A., Kumar, K., and Bandara, S. (2016). Trends in large-deformation analysis of landslide mass movements with particular emphasis on the material point method. *Géotechnique*, 66(3), 248-273.
- Stokes, A., Atger, C., Bengough, A. G., Fourcaud, T., and Sidle, R. C. (2009). Desirable plant root traits for protecting natural and engineered slopes against landslides. *Plant and soil*, 324(1-2), 1-30.
- Talukdar, P., Bora, R., and Dey, A. (2018). Numerical investigation of hill slope instability due to seepage and anthropogenic activities. *Indian Geotechnical Journal*, 48(3), 585-594.
- Tang, O. L., and Jiang, Q. M. (2015). Stability analysis of slope under different soil nailing parameters based on the Geostudio. *International Journal of Georesources and Environment-IJGE (formerly Int'l J of Geohazards and Environment)*, 1(2), 88-92.
- Teerawattanasuk, C., Maneecharoen, J., Bergado, D. T., Voottipruex, P., and Le, G. L. (2014). Root strength measurements of vetiver and ruzi grasses. *Lowland Technology International*, 16(2), 71-80.
- Temgoua, A. G. T., Kokutse, N. K., Kavazović, Z., and Richard, M. (2017). A 3D model applied to analyze the mechanical stability of real-world forested hillslopes prone to landslides. *Ecological Engineering*, 106, 609-619.
- The U.S. Geological Survey (2004). Landslide types and processes, U.S. Department of the Interior, Fact Sheet 2004-3072.
- Tirkey, A. S., Pandey, A. C., and Nathawat, M. S. (2013). Use of satellite data, GIS and RUSLE for estimation of average annual soil loss in Daltonganj watershed of Jharkhand (India). *Journal of Remote Sensing Technology*, 1(1), 20-30.
- Truong, P. N. (2002). Vetiver grass technology. In 'Vetiveria'. (Ed. M Maffei), 114–132.
- Truong, P., and Baker, D. (1998). *Vetiver grass system for environmental protection*. Pacific Rim Vetiver Network, Office of the Royal Development Projects Board.
- Truong, P., and Loch, R. (2004). Vetiver system for erosion and sediment control. In *Proceeding of 13th international soil conservation organization conference*, 1-6.
- Truong, P., Baker, D. E., and Christiansen, I. (1995). Stiffgrass barrier with vetiver grass: a new approach to erosion and sediment control. In *Proceedings of the Downstream Effects of Land Use Conference, Chiang Rai, Thailand*.

- Truong, P., Van, T. T., and Pinners, E. (2008). Vetiver system applications technical reference manual. *The Vetiver Network International*, 89.
- Tschuchnigg, F., Schweiger, H. F., and Sloan, S. W. (2015). Slope stability analysis by means of finite element limit analysis and finite element strength reduction techniques. Part I: Numerical studies considering non-associated plasticity. *Computers and Geotechnics*, 70, 169-177.
- Tsige, D., Senadheera, S., and Talema, A. (2020). Stability analysis of plant-root-reinforced shallow slopes along mountainous road corridors based on numerical modeling. *Geosciences*, 10(1), 19.
- Van Westen, C. J., Quan Luna, B., Vargas Franco, R., Malet, J. P., Jaboyedoff, M., Horton, P., and Kappes, M. (2010). Development of training materials on the use of geo-information for multi-hazard risk assessment in a mountainous environment. In *Proceedings of the Mountain Risks International Conference, Firenze, Italy*, 24-26.
- Varnes, D. J. (1978). Slope movement types and processes. *Special report*, 176, 11-33.
- Voottipruex, P., Bergado, D. T., Mairaeng, W., Chucheepsakul, S., and Modmoltin, C. (2008). Soil reinforcement with combination roots system: A case study of Vetiver grass and Acacia Mangium willd. *Lowland Technology International*, 10(2, Dec), 56-67.
- Waldron, L. J., and Dakessian, S. (1981). Soil reinforcement by roots: calculation of increased soil shear resistance from root properties. *Soil science*, 132(6), 427-435.
- Weaver J. E., and Clements, F. E. (1938). *Plant ecology*. McGraw-Hill, New York.
- Wu, C. (2017). Comparison and evolution of extreme rainfall-induced landslides in Taiwan. *ISPRS International Journal of Geo-Information*, 6(11), 367.
- Wu, T. H. (1976). Investigation of landslides on Prince of Wales Island, Alaska. *Geotechnical Engineering Report 5*, Department of Civil Engineering, Ohio State University, Columbia, Ohio.
- Wu, T. H., McKinnell III, W. P., and Swanston, D. N. (1979). Strength of tree roots and landslides on Prince of Wales Island, Alaska. *Canadian Geotechnical Journal*, 16(1), 19-33.
- Xie, M., Esaki, T., and Cai, M. (2004). A time-space based approach for mapping rainfall-induced shallow landslide hazard. *Environmental Geology*, 46(6-7), 840-850.

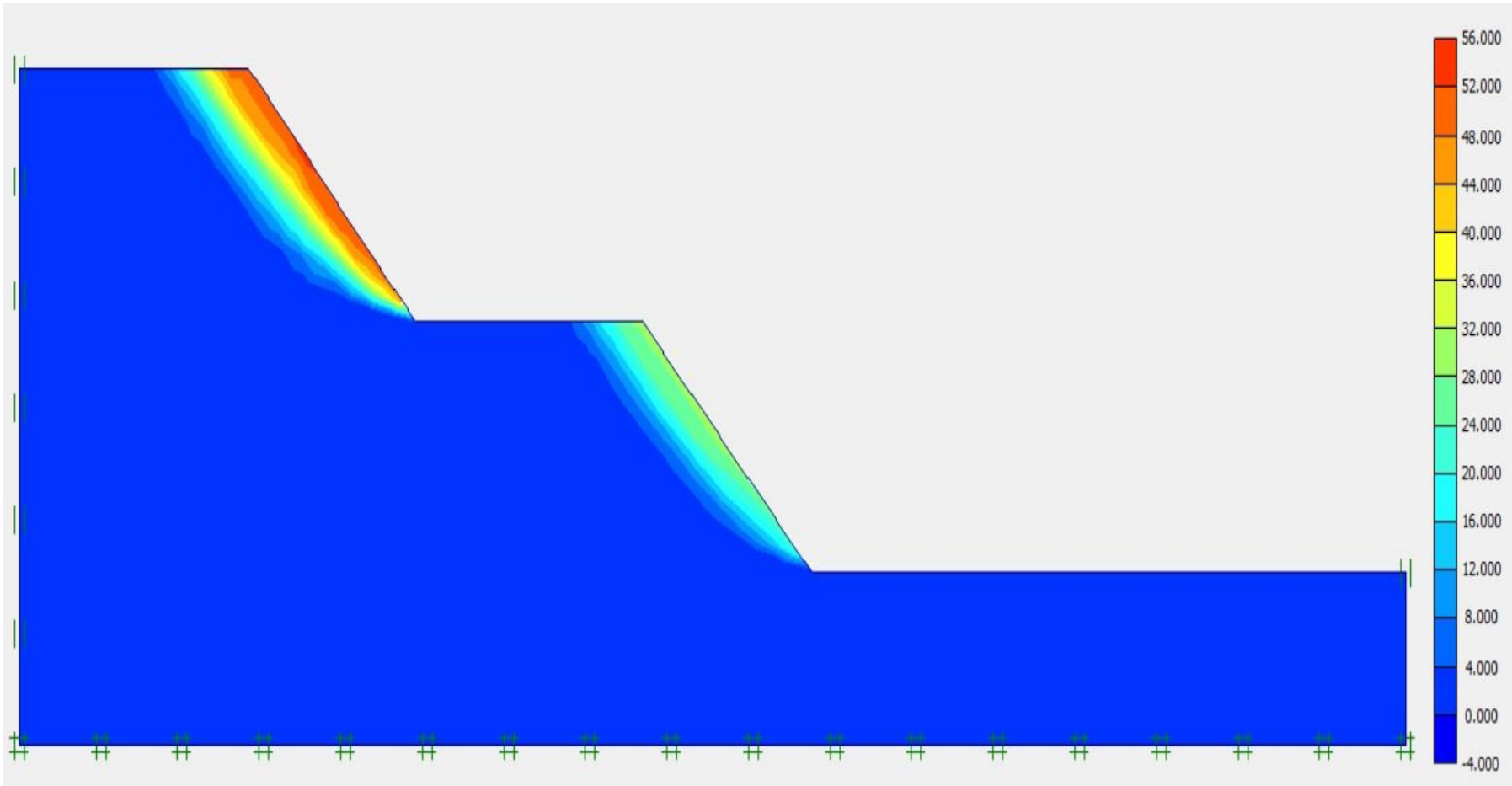
Xuan, T. (2014). Vetiver system for infrastructure protection in Vietnam: A review after fifteen years of application on the Ho Chi Minh highway.

Yang, M. Z., and Drumm, E. C. (2000). Numerical analysis of the load transfer and deformation in a soil nailed slope. In *Numerical Methods in Geotechnical Engineering* (pp. 102-115).

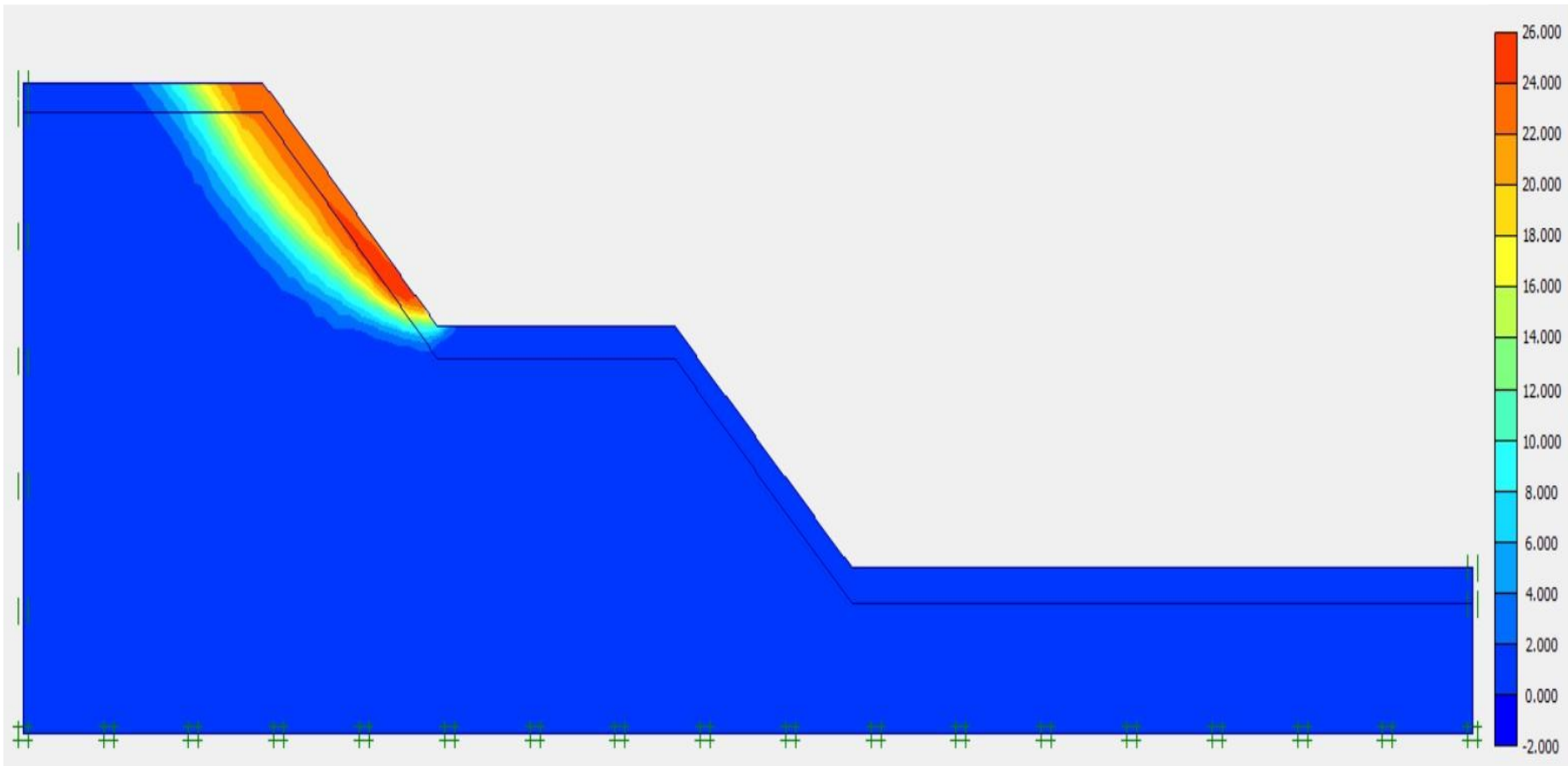
Zhang, G. R., Qian, Y. J., Wang, Z. C., and Zhao, B. (2014). Analysis of rainfall infiltration law in unsaturated soil slope. *The Scientific World Journal*.

APPENDIX A

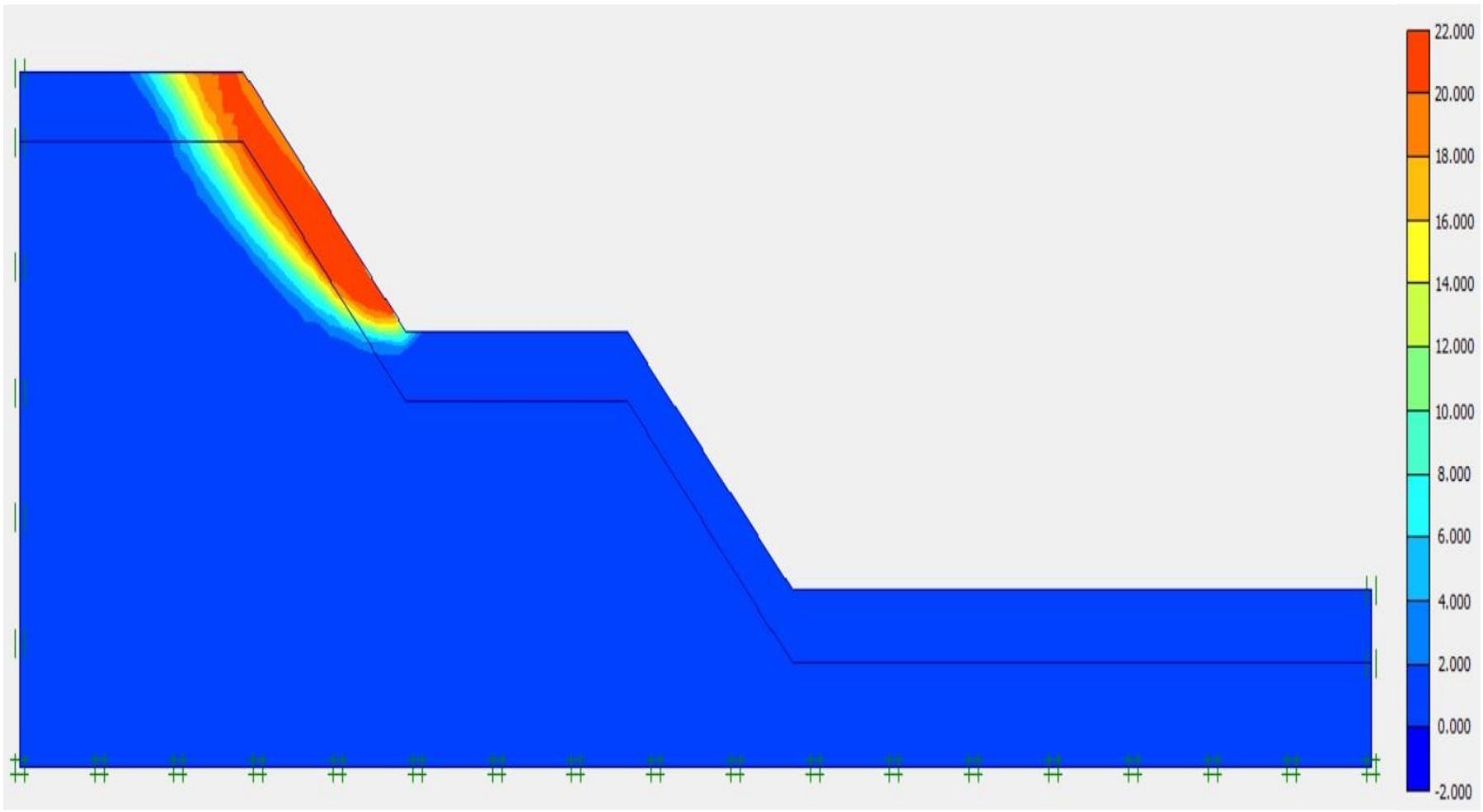
**TOTAL DISPLACEMENT OF BARE, ROOTED AND NAILED
SOIL**



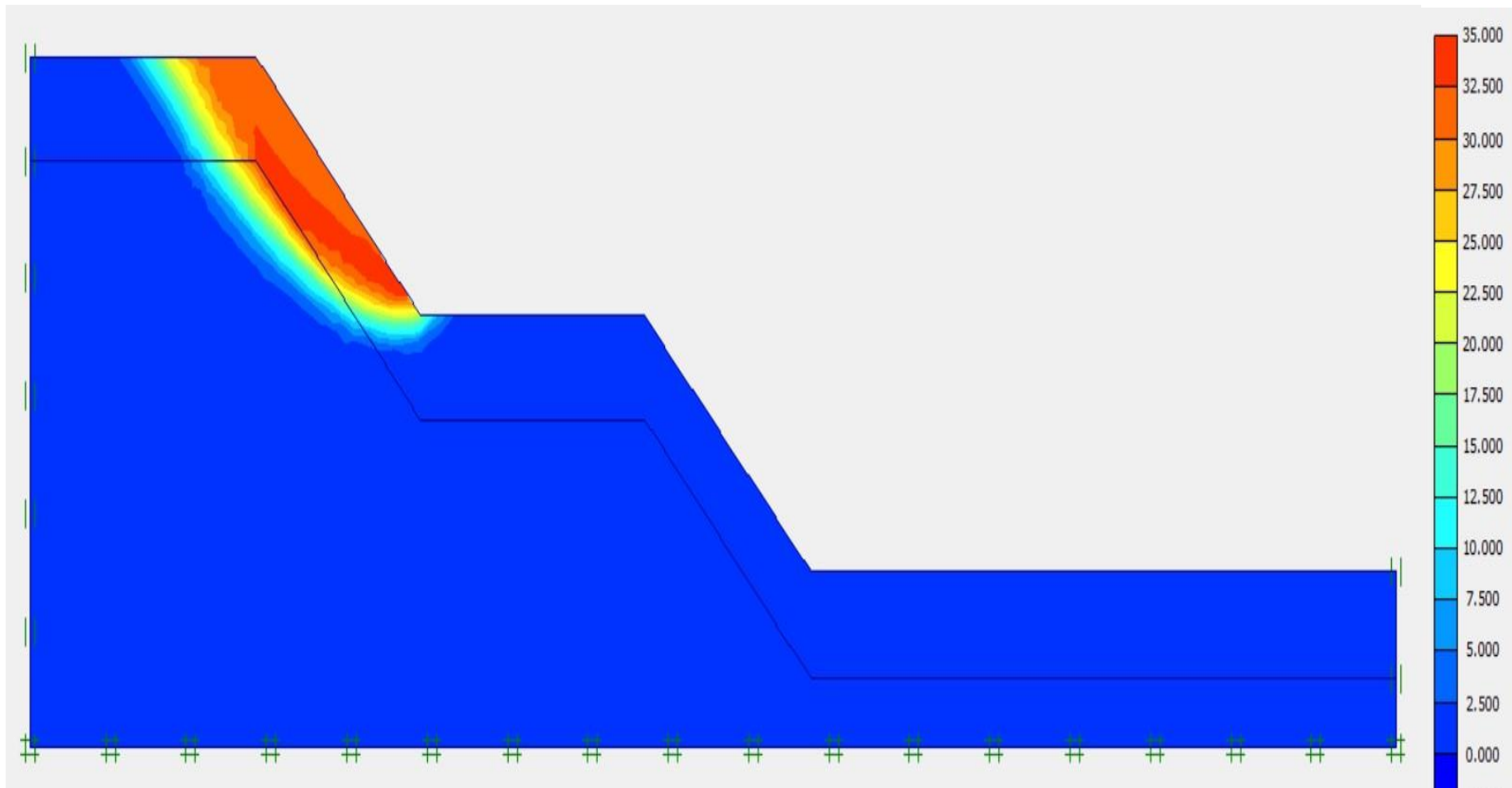
(a)



(b)

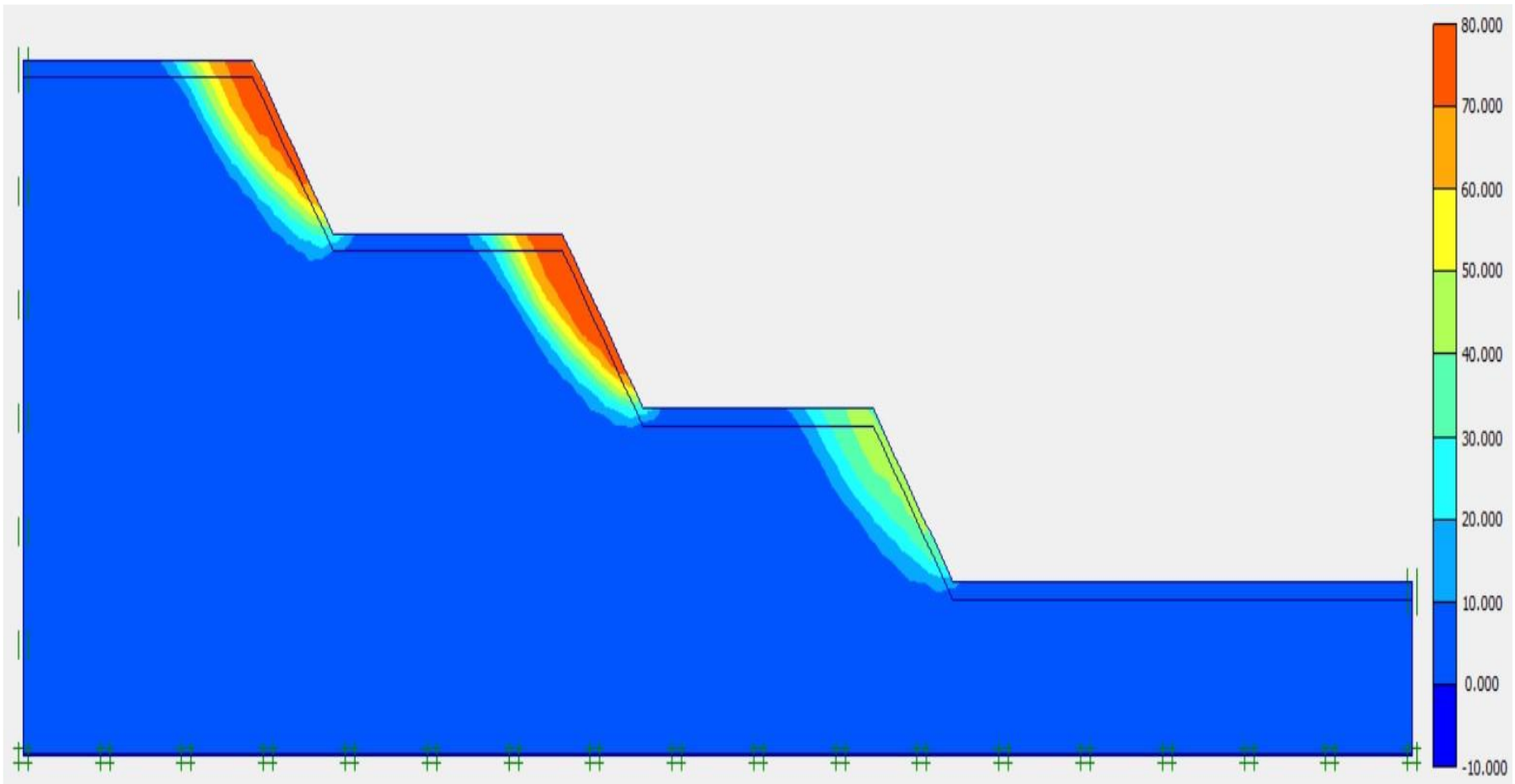


(c)

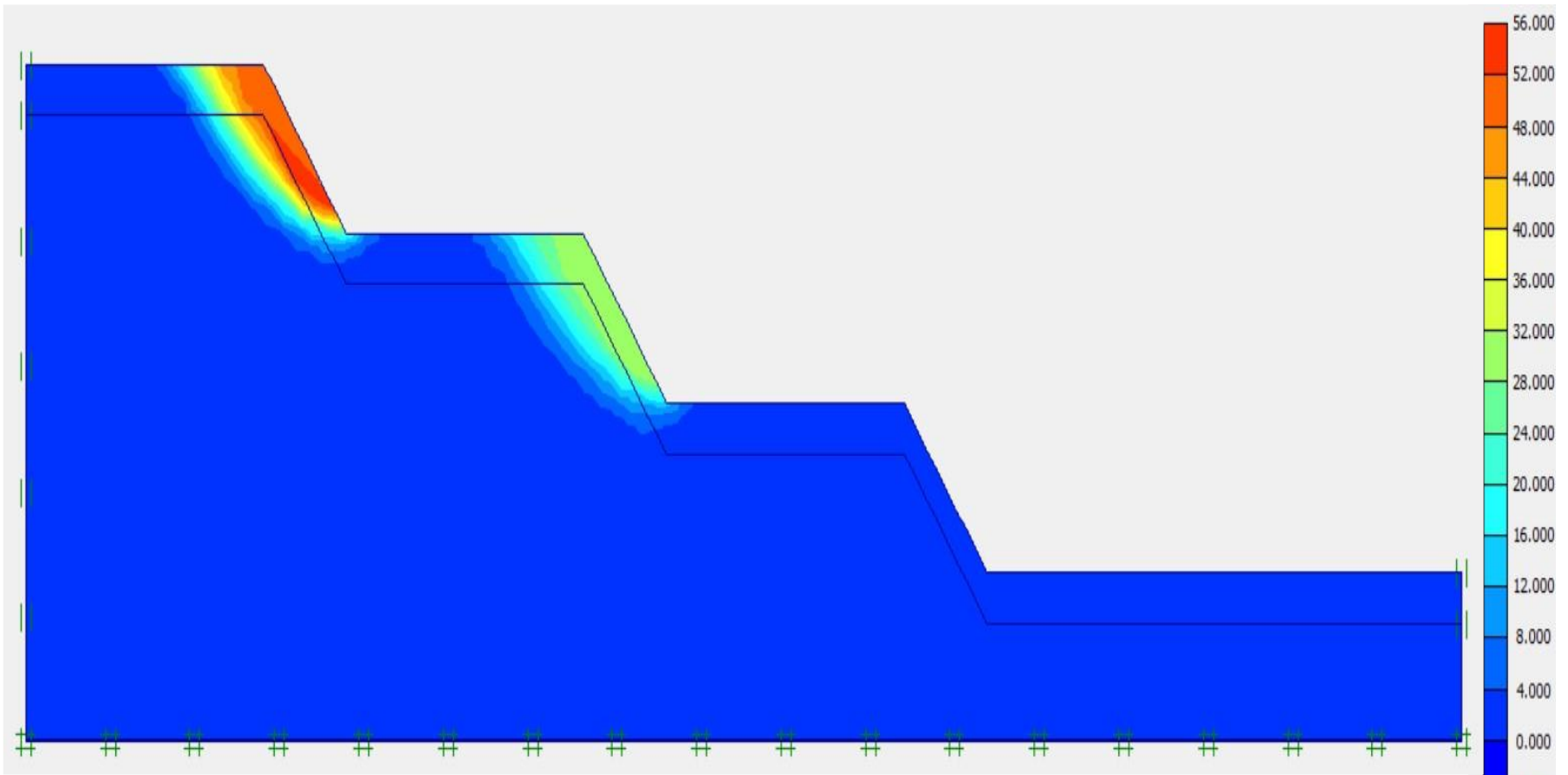


(d)

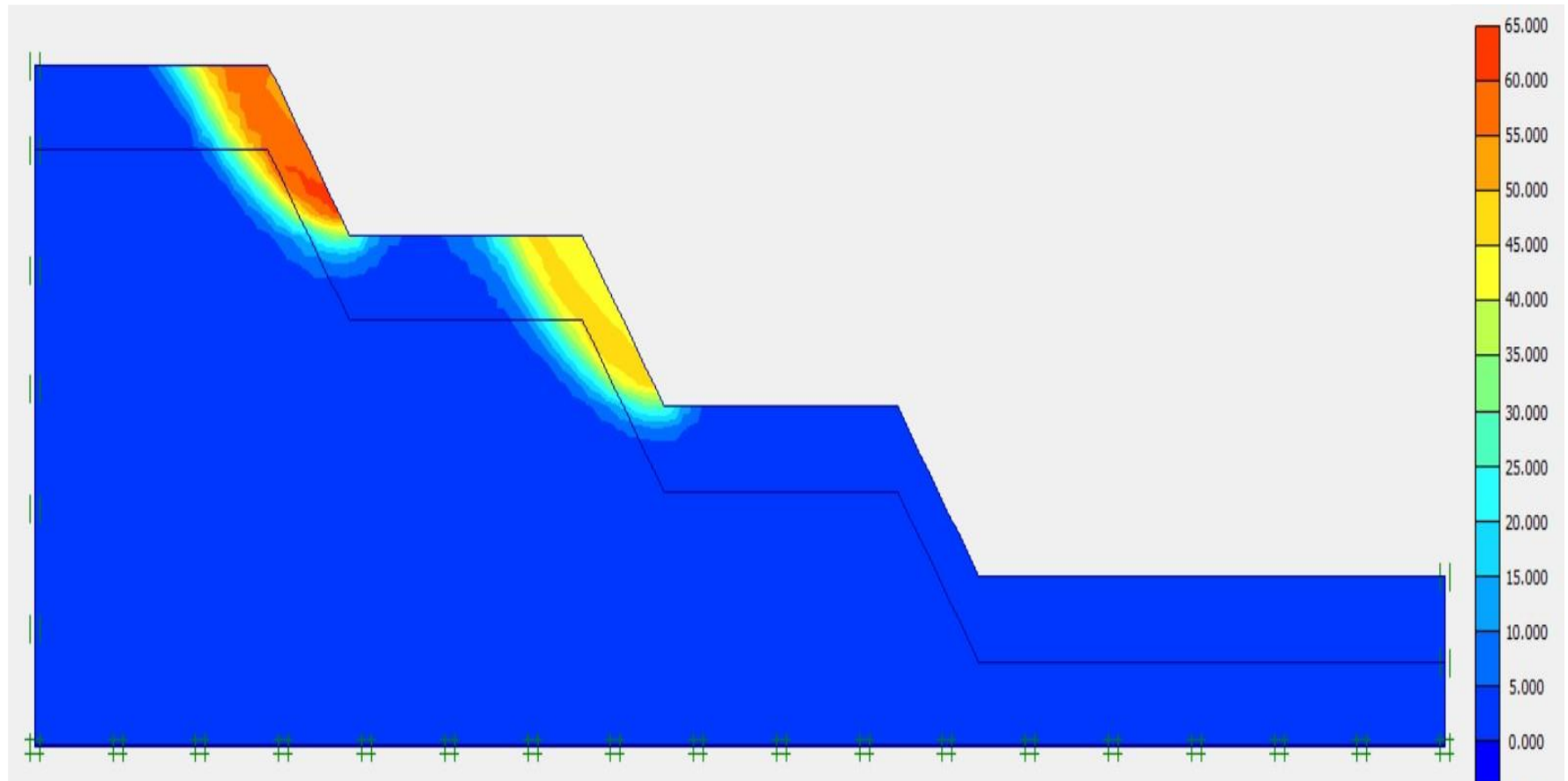
Figure A.1: Potential failure surface and total displacement (cm) of soil S-1 for terraced slope ($H_T=7.5$ m, $\beta=46^\circ$); (a) Bare condition; (b)-
 (d) Rooted condition where h_r is respectively 1.0 m, 2.0 m, 3.0 m



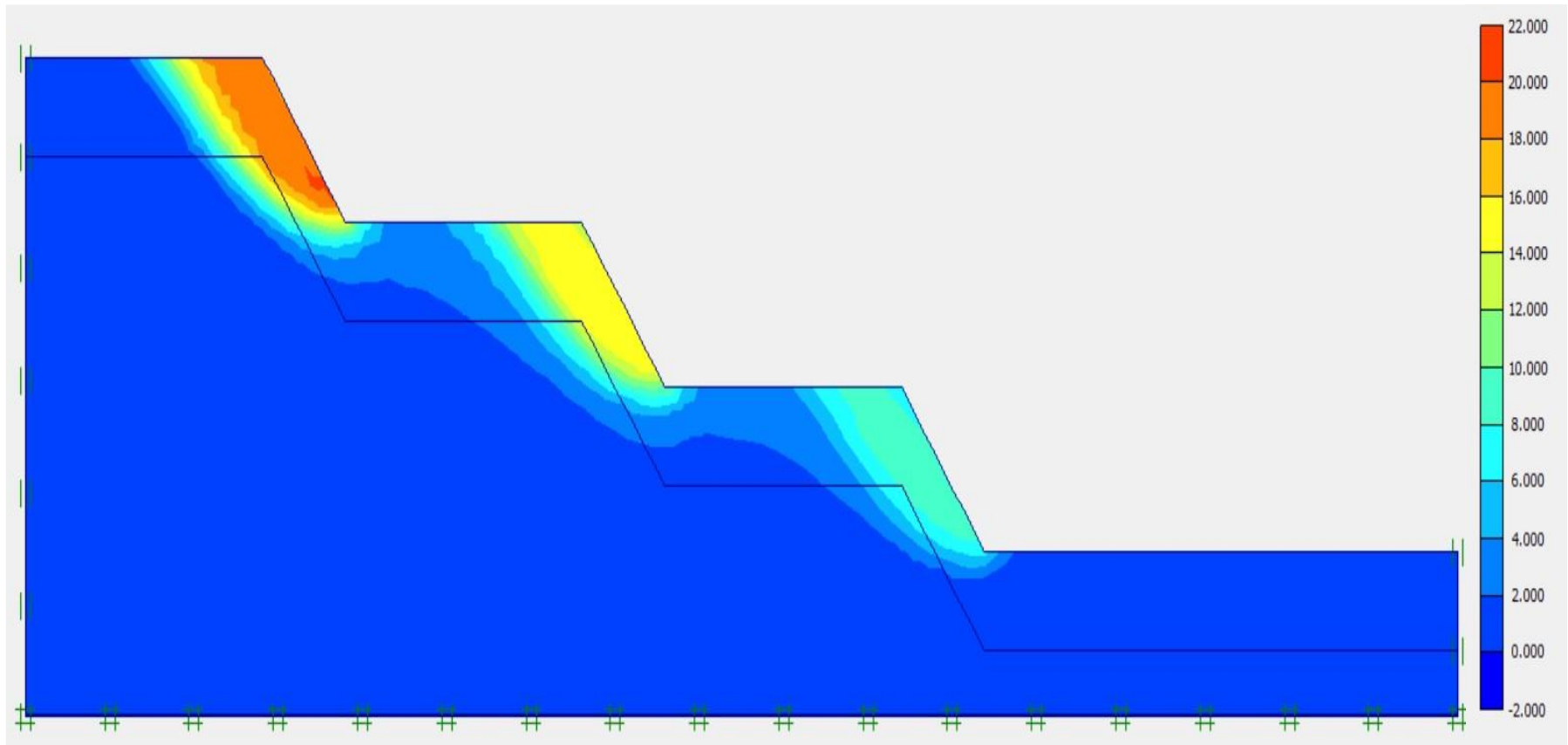
(a)



(b)



(c)



(d)

Figure A.2: Potential failure surface and total displacement (cm) of soil S-1 for terraced slope ($H_T=5$ m, $\beta=55^\circ$); (a)-(d) Rooted condition where h_r is respectively 0.5 m, 1.5 m, 2.5 m, 3.0 m

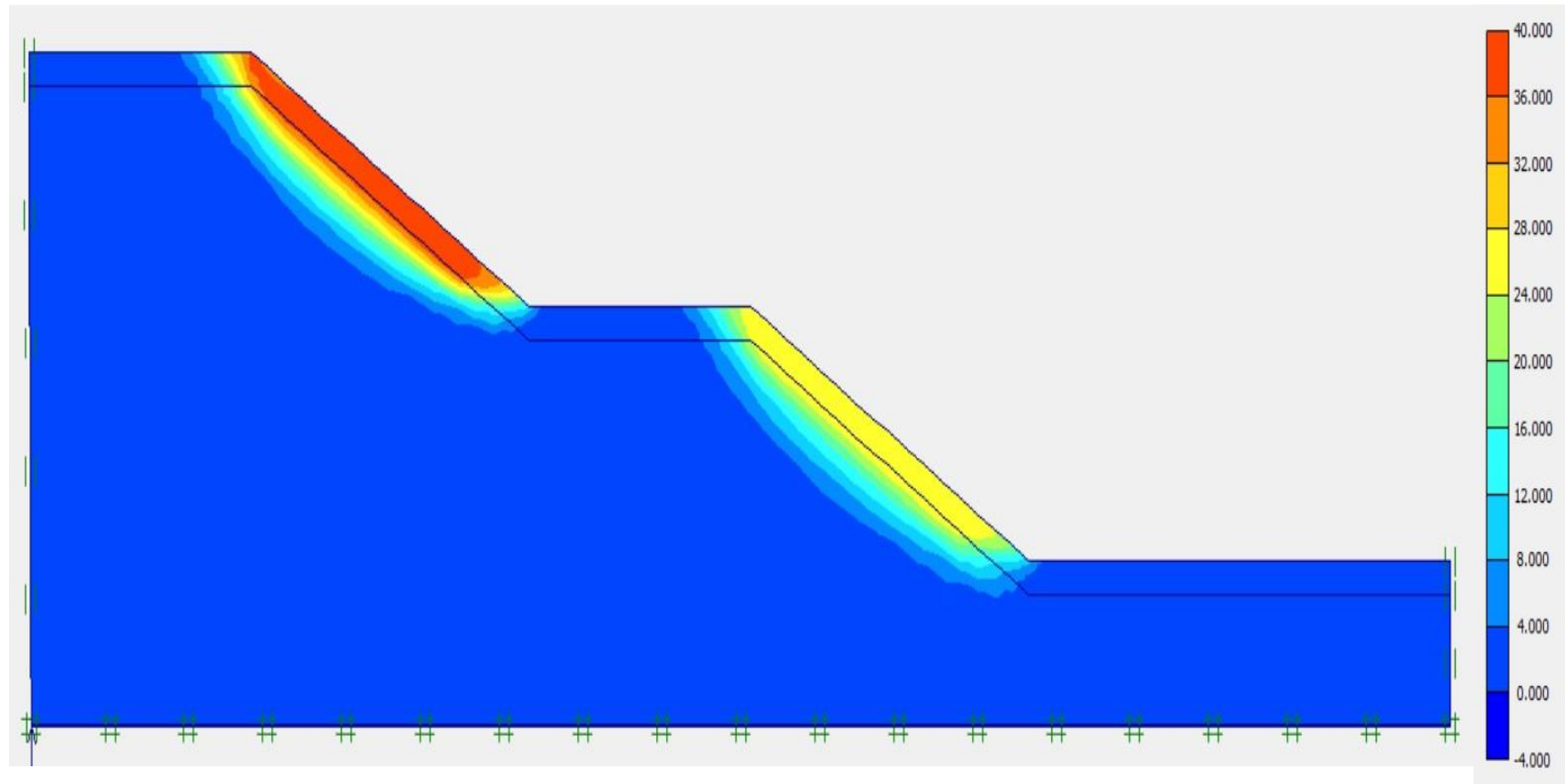
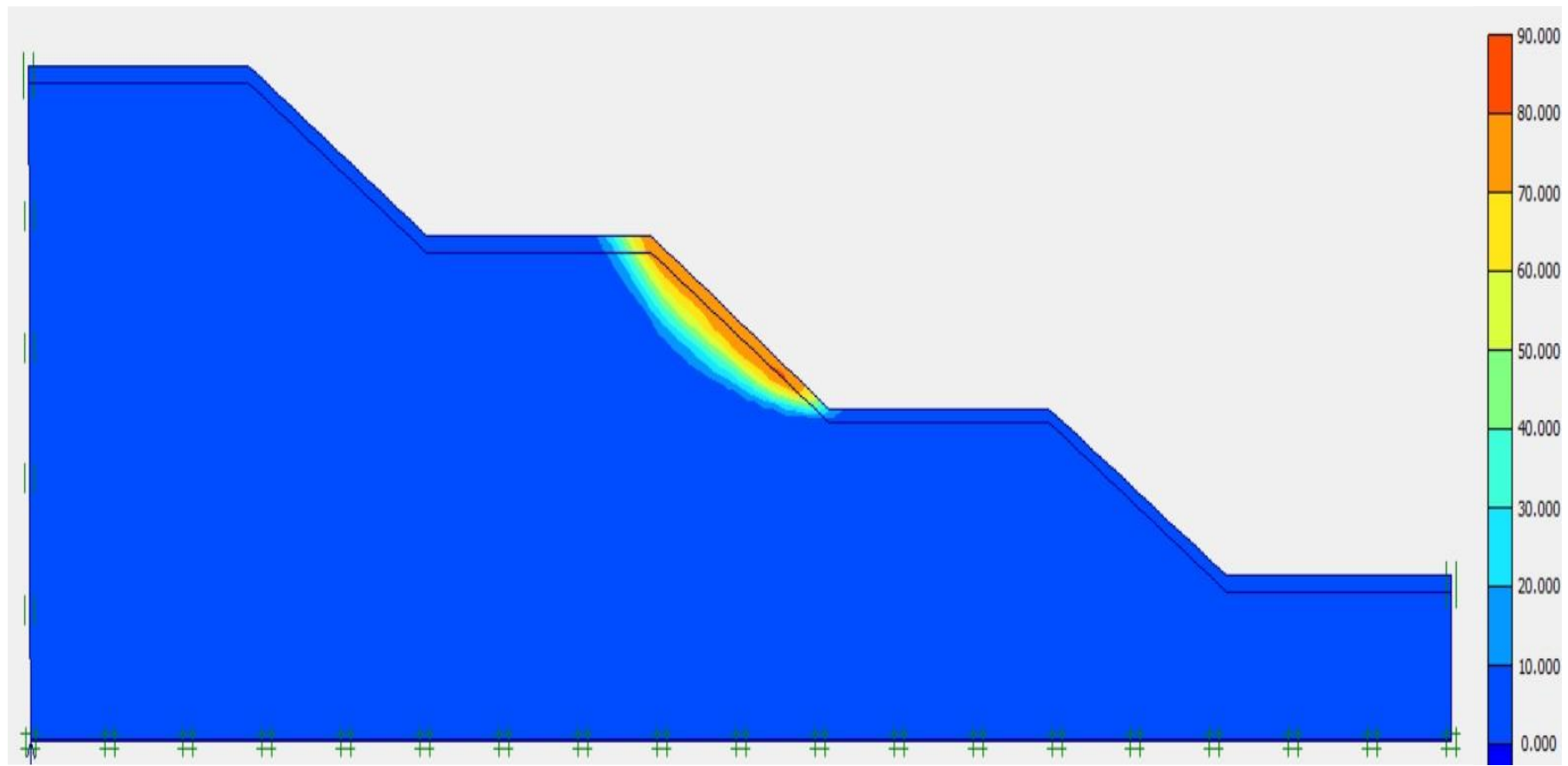
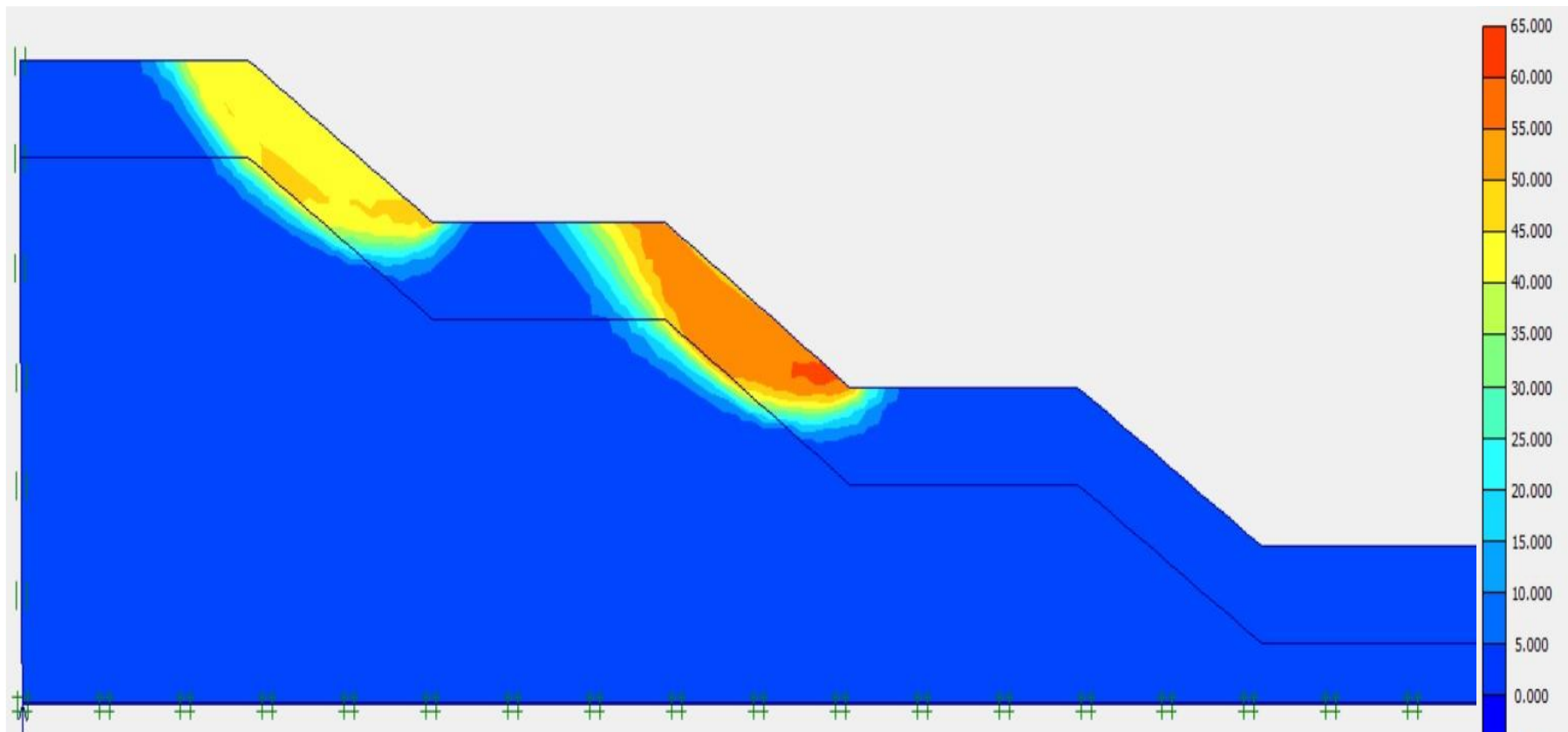


Figure A.3: Potential failure surface and total displacement (cm) of soil S-2 for terraced slope ($H_r=7.5$ m, $\beta=31^\circ$) in rooted condition where h_r is 1.5 m

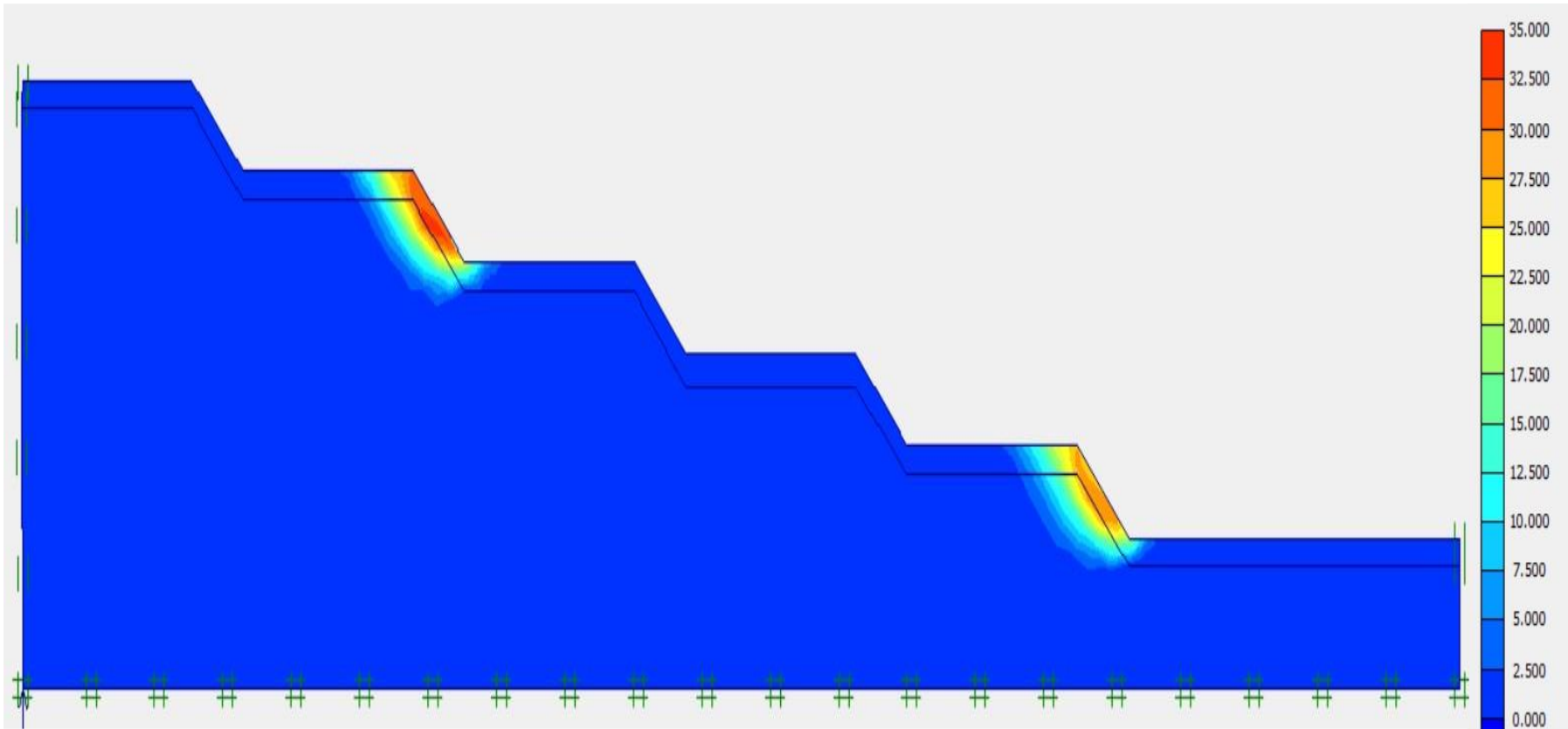


(a)

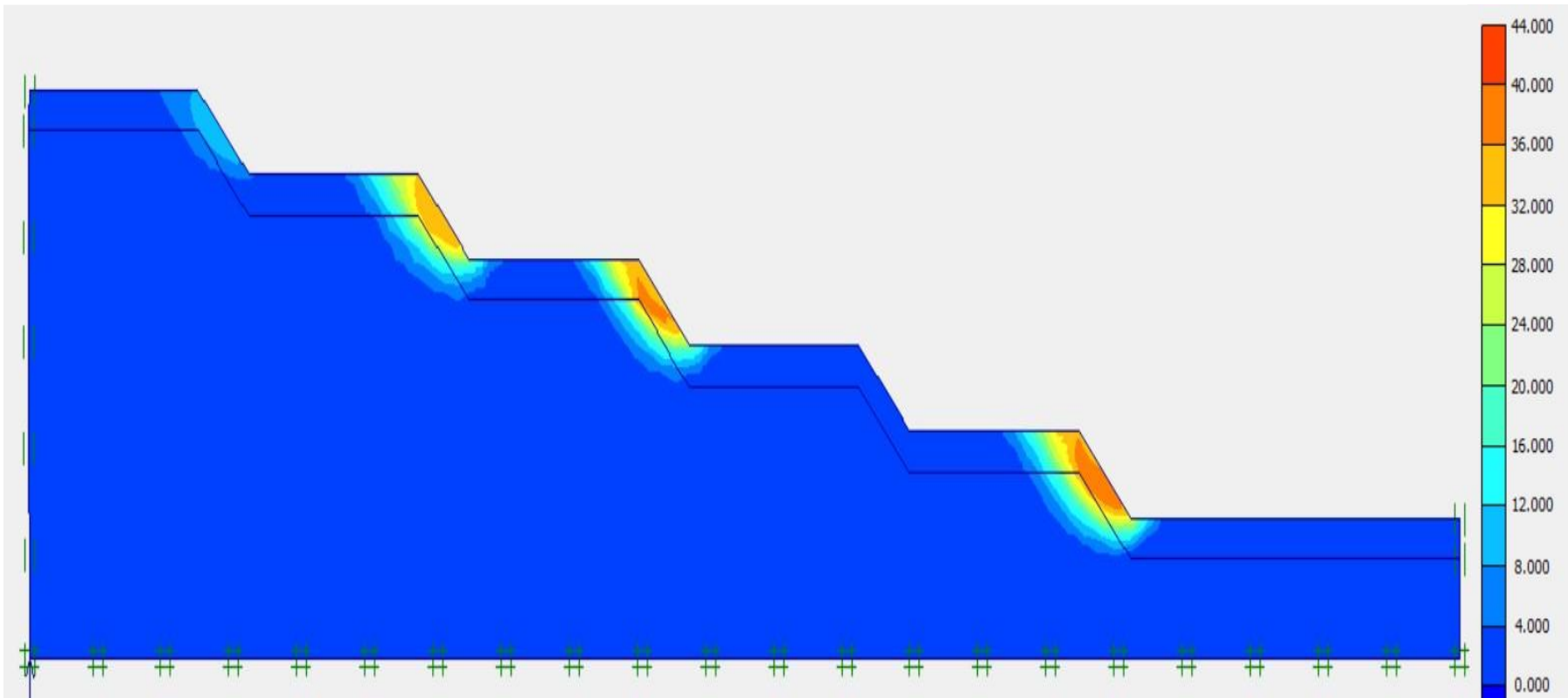


(b)

Figure A.4: Potential failure surface and total displacement (cm) of soil S-2 for terraced slope ($H_T=5$ m, $\beta=32^\circ$); (a) Rooted condition where h_r is 0.5m; (b) Rooted condition where h_r is 3.0 m

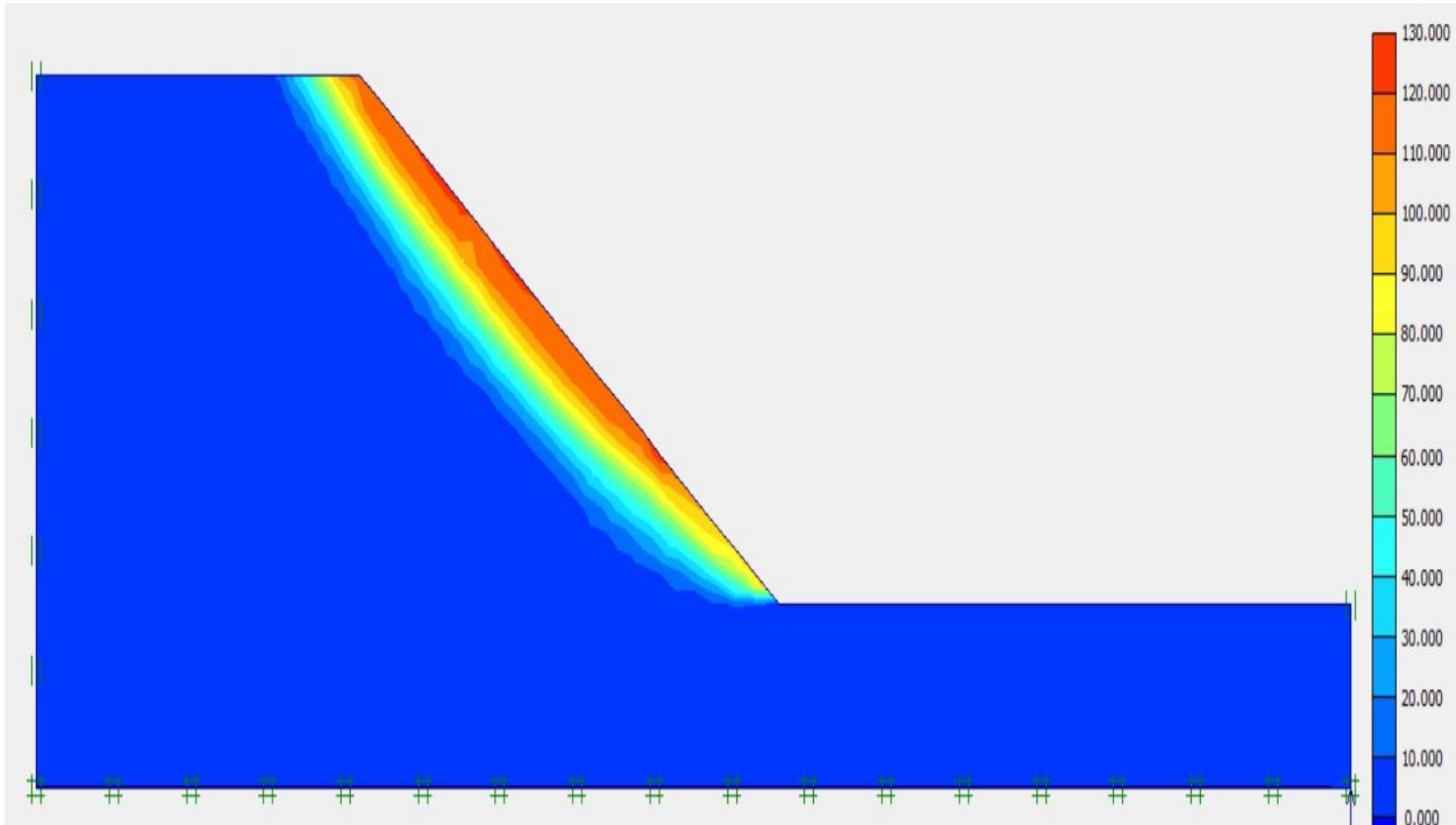


(a)

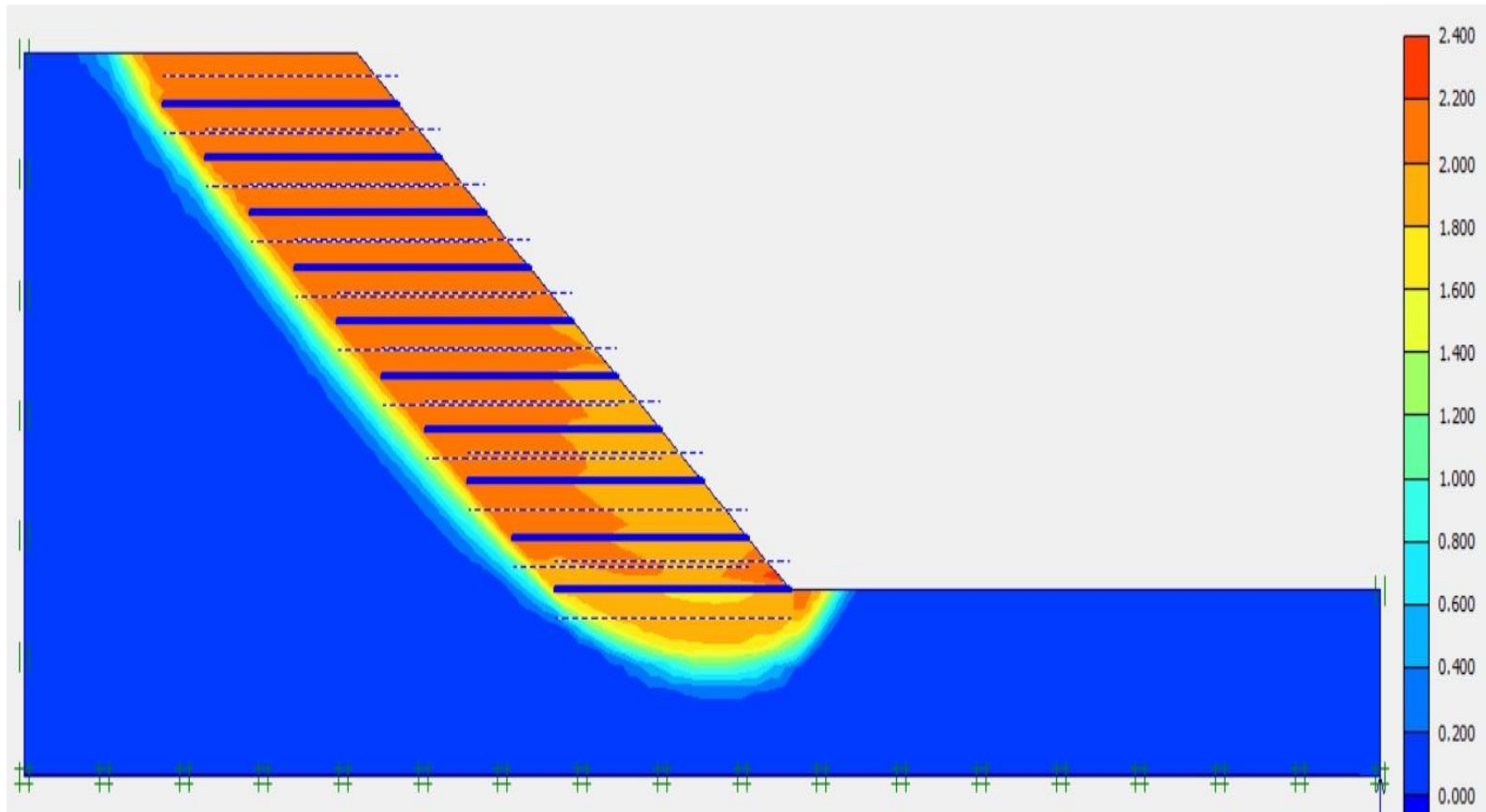


(b)

Figure A.5: Potential failure surface and total displacement (cm) of soil S-2 for terraced slope ($H_r=3$ m, $\beta=45^\circ$); (a) Rooted condition where h_r is 1.0 m; (b) Rooted condition where h_r is 1.5 m

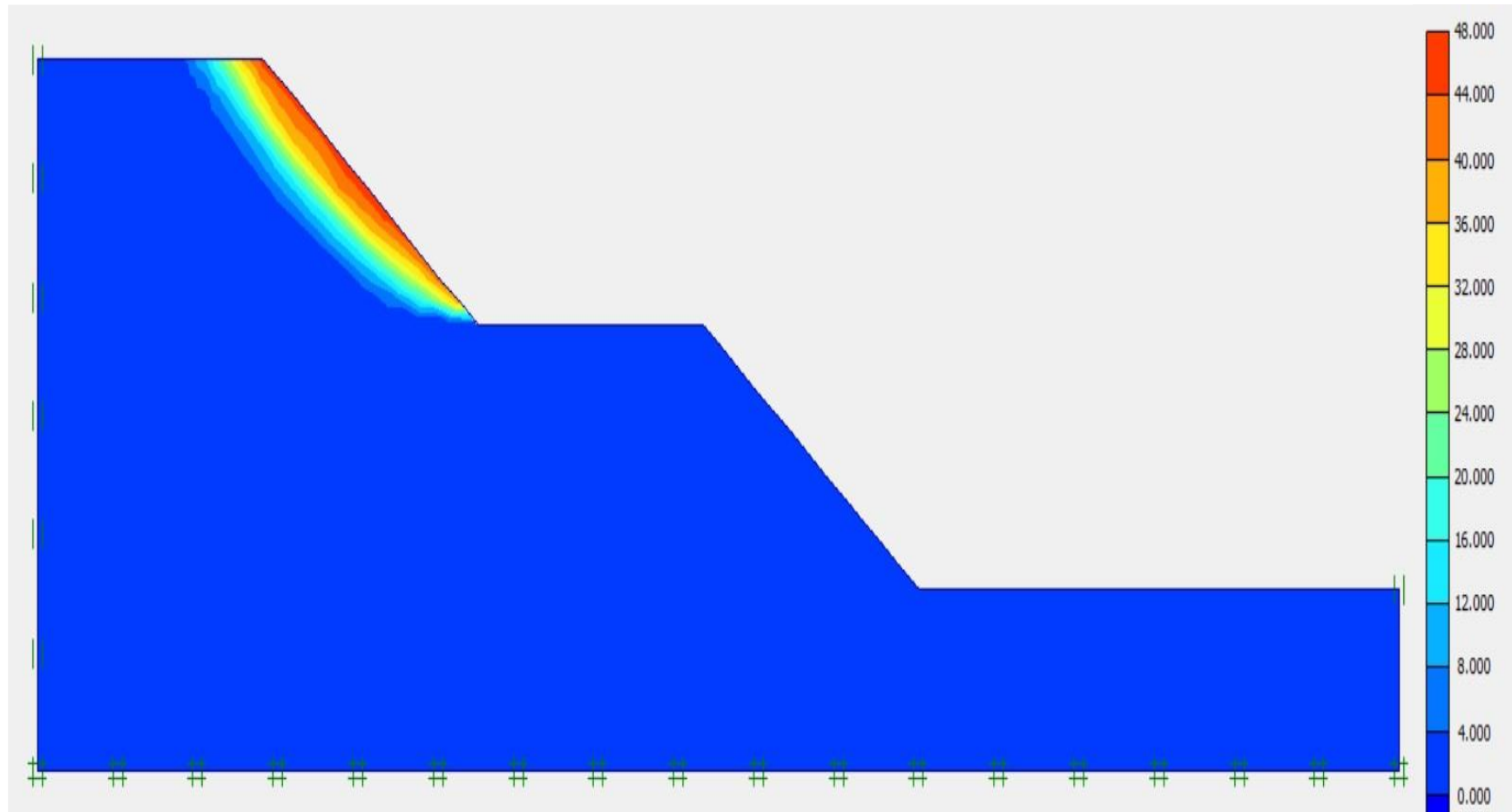


(a)

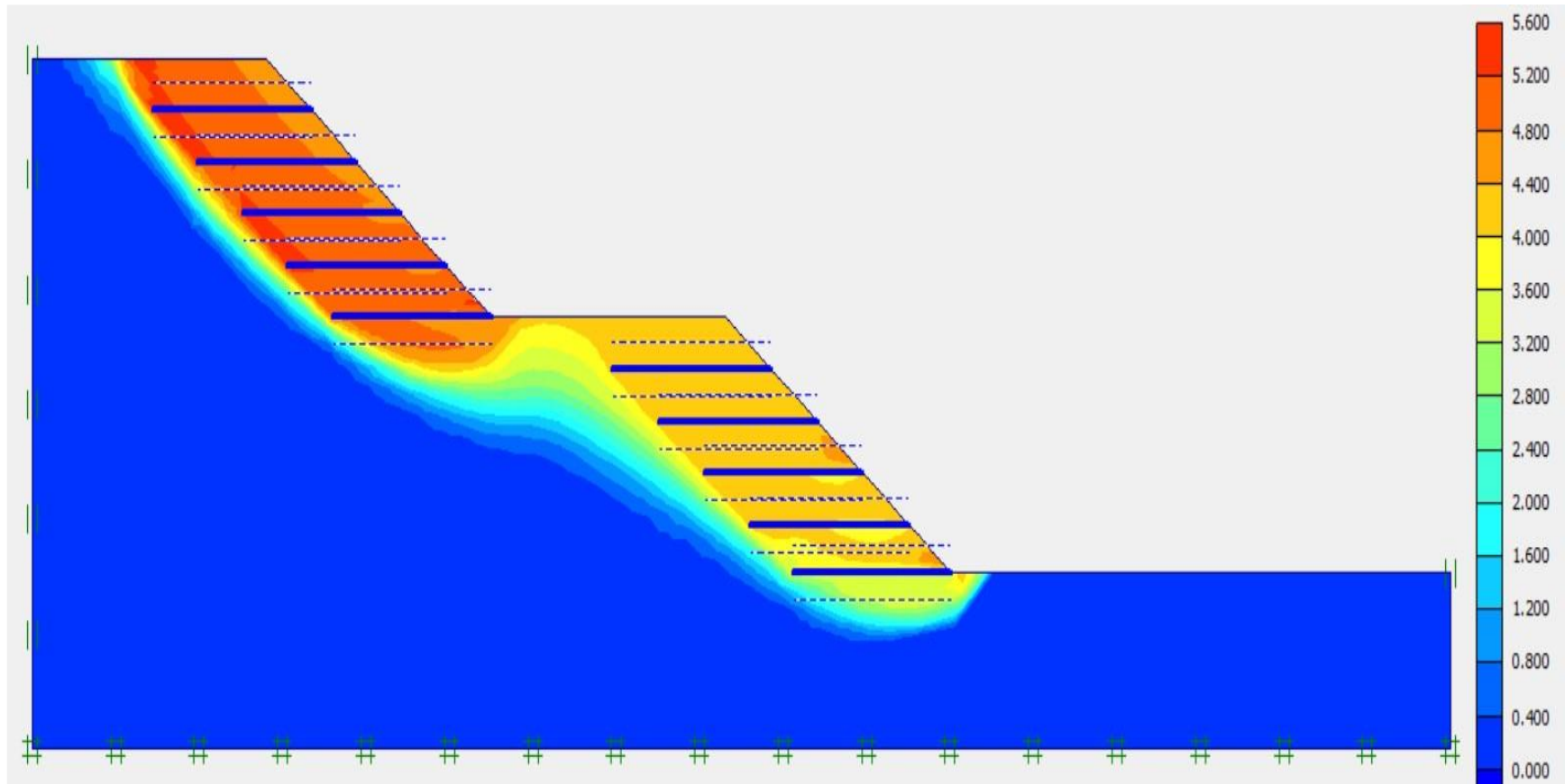


(b)

Figure A.6: Potential failure surface and total displacement (cm) of soil S-1 for natural slope ($H=15$ m, $\beta=38^\circ$); (a) Bare condition; (b) Nailed condition where nail length (l) is 10.5 m ($0.7H$)

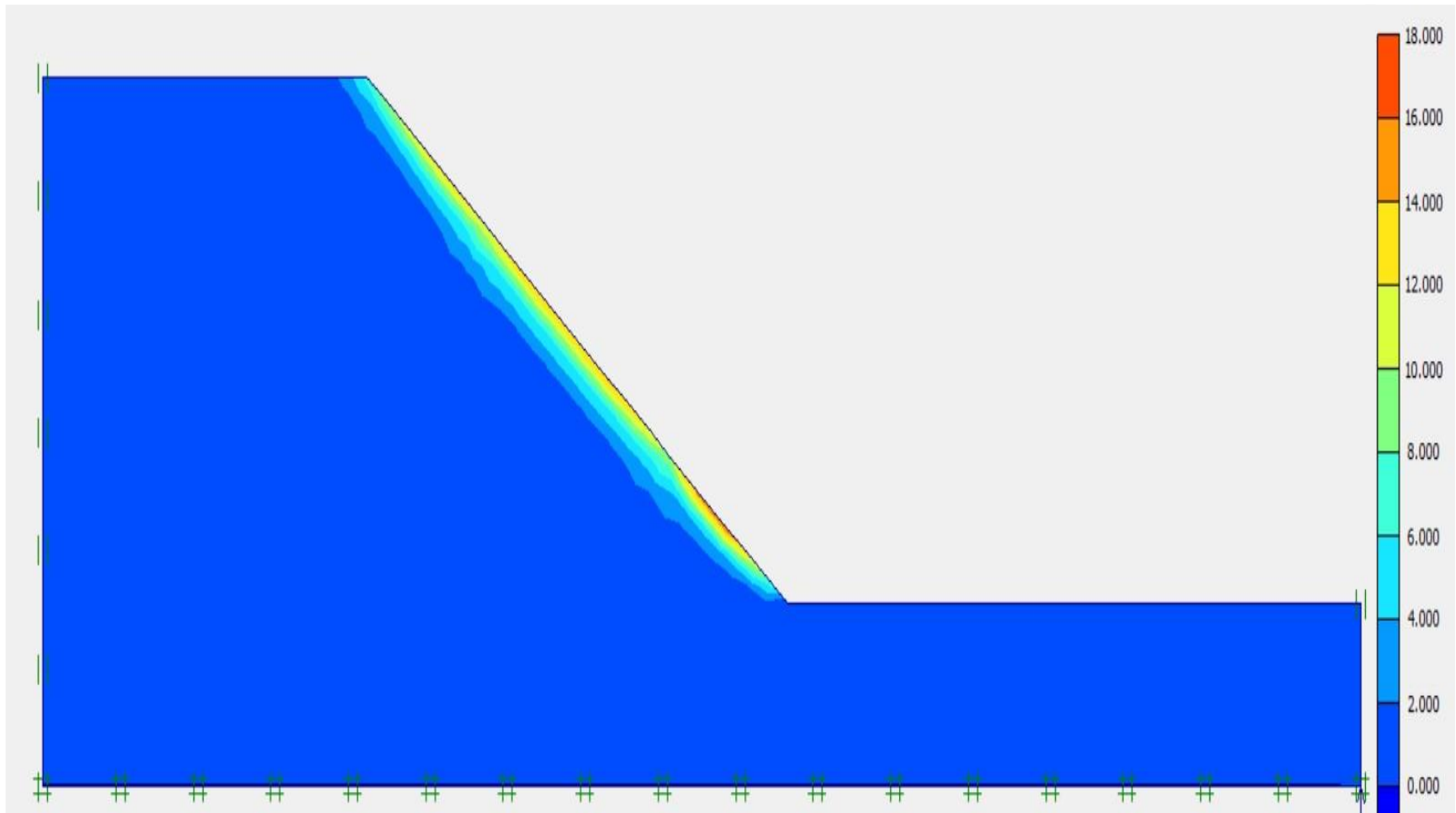


(a)

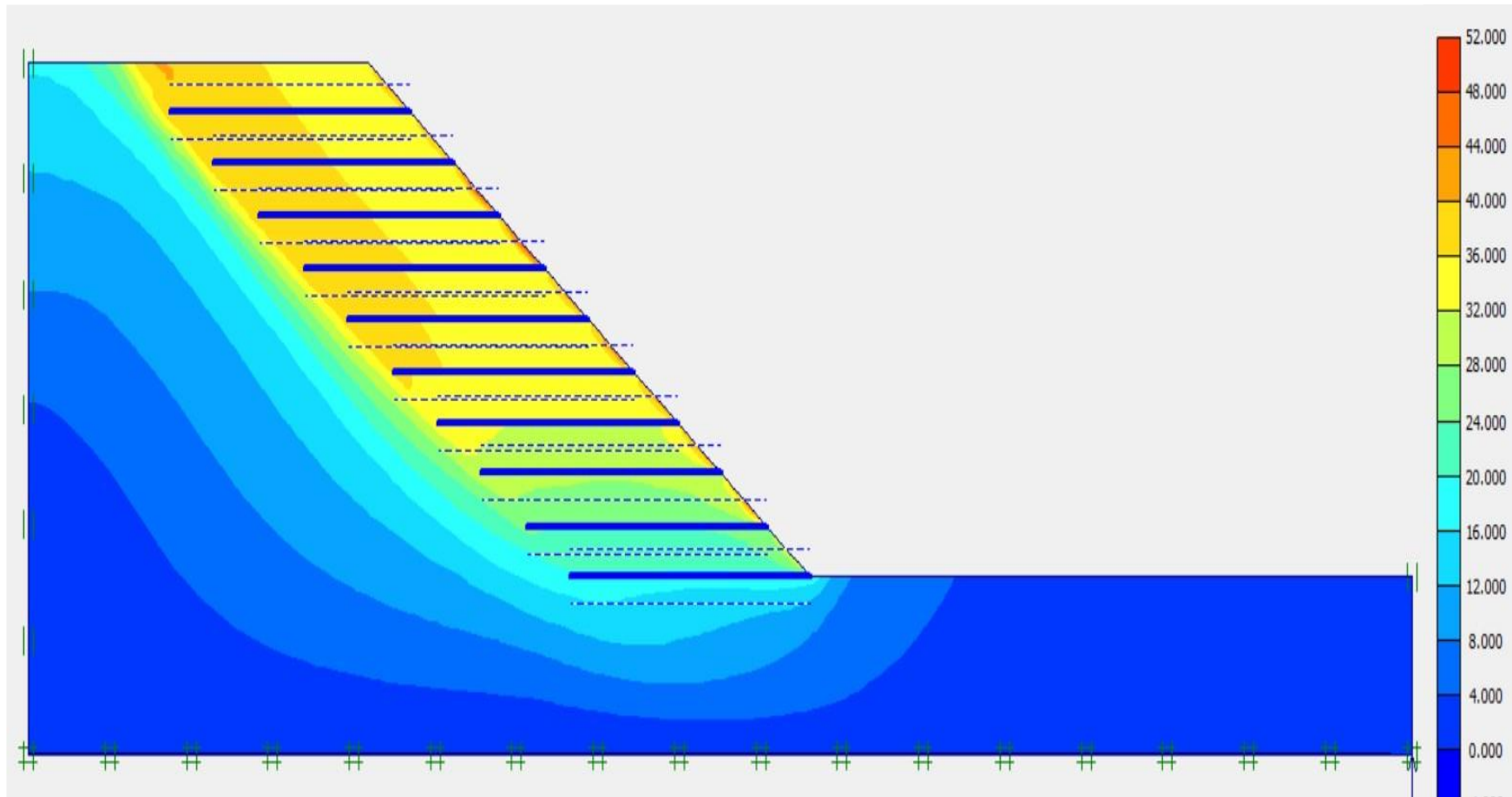


(b)

Figure A.7: Potential failure surface and total displacement (cm) of soil S-1 for terraced slope ($H_T=7.5$ m, $\beta=38^\circ$); (a) Bare condition; (b) Nailed condition where nail length (l) is 6.75 m ($0.9H_T$)



(a)



(b)

Figure A.8: Potential failure surface and total displacement (cm) of soil S-2 for natural slope ($H=15$ m, $\beta=38^\circ$); (a) Bare condition; (b) Nailed condition where nail length (l) is 10.5 m ($0.7H$)

